Regulatory interactions of enzymes of the citric acid cycle in *Bacillus subtilis*

Dissertation

for the award of the degree

“Doctor rerum naturalium”

Division of Mathematics and Natural Sciences

of the Georg-August-Universität Göttingen

submitted by

Frederik Meyer

from Gehrden

Göttingen 2012

Members of the Thesis Committee:

Prof. Dr. Jörg Stülke (Supervisor and 1st Reviewer)
(Institute for Microbiology and Genetics, Department of General Microbiology, University of Göttingen)

Prof. Dr. Kai Tittmann (2nd Reviewer)
(Albrecht-von-Haller-Institute for Plant Science, Department of Bioanalytics, University of Göttingen)

Prof. Dr. Holger Stark
(Max Planck Institute for Biophysical Chemistry Göttingen)

Date of oral examination: 21.01.2013

I hereby declare that the doctoral thesis entitled, “Regulatory interactions of enzymes of the citric acid cycle in *Bacillus subtilis*” has been written independently and with no other sources and aids than quoted.

Frederik Meyer

Danksagung

An erster Stelle möchte ich mich ganz herzlich bei Prof. Dr. Jörg Stülke für die hervorragende Betreuung meiner Doktorarbeit bedanken. Vielen Dank für das außergewöhnliche Engagement an dieser Arbeit und die konstante fachliche als auch persönliche Unterstützung.

Prof. Dr. Kai Tittmann gilt mein Dank für die Übernahme des Korreferates. Ihm und Prof. Dr. Holger Stark möchte ich auch für die Teilnahme an meinem Thesis Committee danken. Des Weiteren danke ich Prof. Dr. Christiane Gatz, Prof. Dr. Ralf Ficner und Dr. Fabian Commichau für ihre Teilnahme an meiner Prüfungskommission.

Prof. Dr. Sonenshein und seiner Arbeitsgruppe gilt ein besonderes Dankeschön für die freundliche Zusammenarbeit und die vorübergehende Aufnahme in die Arbeitsgruppe. Der Forschungsaufenthalt in den USA war für mich ein besonderer Abschnitt meiner Doktorarbeit. Ebenso möchte ich mich bei Prof. Dr. Uwe Völker und Dr. Elke Hammer von der Universität Greifswald für die Kooperation im Rahmen dieser Arbeit bedanken.

Julia Busse danke ich sehr herzlich für ihre tatkräftige Unterstützung im Labor, die viel zum Gelingen meiner Arbeit beigetragen hat.

Des Weiteren möchte ich mich bei allen Mitgliedern der Abteilung für ihre Hilfsbereitschaft und das äußerst angenehme Arbeitsklima bedanken. Meinen Bürokollegen Martin Lehnik-Habrink und Fabian Rothe danke ich für viele hilfreiche Gespräche und für die stets fröhliche Büroatmosphäre. Christina Herzberg und Katrin Gunka danke ich sehr für ihre guten fachlichen Ratschläge und ihre Unterstützung bei den alltäglichen Problemen im Labor. Auch Christine Diethmaier, Jan Gerwig, Felix Mehne, Arne Schmeisky und Christopher Zschiedrich gilt Dank für ihre Unterstützung. Ebenso möchte ich mich für die Hilfe durch meine zahlreichen Praktikanten, Bachelor- und Masterstudenten und ihr Interesse an meiner Arbeit bedanken. Ein großes Dankeschön gebührt außerdem Bärbel Herbst, deren Hilfe die tägliche Arbeit im Labor sehr erleichtert.

Zum Schluss möchte ich mich bei meiner Familie und meinen Freunden bedanken, die mich während meines Studiums stets ermutigt und gefördert haben. Ganz besonders gilt dieser Dank meinen Eltern. Vielen Dank für eure Unterstützung.

Table of content

List of publication

Meyer, F. M., Gerwig, J., Hammer, E., Herzberg, C., Commichau, F. M., Völker, U. & Stülke, J. (2011). Physical interactions between tricarboxylic acid cycle enzymes in *Bacillus subtilis*: Evidence for a metabolon. *Metab. Eng*. 13, 18-27.

Meyer, F. M., Jules, M., Mehne, F. M., Le Coq, D., Landmann, J. J., Görke, B., Aymerich, S. & Stülke, J. (2011). Malate-mediated carbon catabolite repression in *Bacillus subtilis* involves the HPrK/CcpA pathway. *J. Bacteriol*. 193, 6939-6949

Meyer, F. M. & Stülke, J. (2012). Malate metabolism in *Bacillus subtilis*: Distinct roles for three classes of malate-oxidizing enzymes. *FEMS Microbiol. Lett*. *in press.*

Pechter, K. B., **Meyer, F. M.**, Serio, A. W., Stülke, J. & Sonenshein, A. L. (2012). Two roles for aconitase in the regulation of tricarboxylic acid branch gene expression in *Bacillus subtilis*. *J. Bacteriol*. *in revision.*

List of abbreviations

% (vol/vol)	% (volume/volume)
% (wt/vol)	% (weight/volume)
ADP	adenosine diphosphate
Amp	ampicillin
AP	alkaline phospatase
ATP	adenosine triphosphate
B.	*Bacillus*/*Bordetella*
B2H / BACTH	bacterial two-hybrid
bp	base pair
CAA	Casamino acids
CDP*	disodium 2-chloro-5-(4-methoxyspiro {1,2-dioxetane-3,2'-(5'-chloro) tricyclo[3.3.1.13,7]decan}-4-yl) phenyl phosphate
Cm	chloramphenicol
DNA	deoxyribonucleic acid
E.	*Escherichia*
E	glutamate
EDTA	ethylenediaminetetraacetic acid
Em	erythromycin
et al.	*Et altera*
FA	formaldehyde
Fig.	figure
fwd	forward
Glc	glucose
LB	Luria Bertani (medium)
LFH-PCR	Long Flanking Homology PCR
Lin	Lincomycin
mRNA	messenger RNA
NAD^+	Nicotinamide adenine dinucleotide
NADH	Nicotinamide adenine dinucleotide (reduced form)
$NADP^+$	Nicotinamide adenine dinucleotide phosphate
NADPH	Nicotinamide adenine dinucleotide phosphate (reduced form)
OD_x	optical density , measured at the wavelength λ = x nm
ONPG	ortho-Nitrophenyl-β-galactoside
ori	origin of replication
P	promoter
PAGE	polyacrylamide gel electrophoresis
PCR	polymerase chain reaction
pH	power of hydrogen
PVDF	polyvinylidene difluoride
rev	reverse
RNA	ribonucleic acid
S.	*Saccharomyces*
S	succinate
SD	Shine-Dalgarno
SDS	sodium dodecyl sulfate
SP	sporulation medium
Spc	Spectinomycin

SPINE	Strep-protein interaction experiment
Tab.	Table
Tris	tris(hydroxymethyl)aminomethane
U	units
UTR	untranslated regions
WT	wild type
X-Gal	5-bromo-4-chloro-3-indolyl-ß-D-galactopyranoside

Units

A	Ampere	k	kilo	10^{3}
bp	Base pair	m	milli	10^{-3}
°C	Grad Celsius	µ	micro	10^{-6}
Da	Dalton	n	nano	10^{-9}
g	Gramm			
h	Hour	**Nucleotides**		
l	Liter			
m	Meter	A	Adenine	
M	molar (mol/l)	C	Cytosine	
min	Minute	G	Guanine	
sec	Second	T	Thymine	
V	Volt	U	Uracil	
W	Watt			

Amino acids

A	Ala	Alanine	M	Met	Methionine
C	Cys	Cysteine	N	Asn	Asparagine
D	Asp	Aspartate	P	Pro	Proline
E	Glu	Glutamate	Q	Gln	Glutamine
F	Phe	Phenylalanine	R	Arg	Arginine
G	Gly	Glycine	S	Ser	Serine
H	His	Histidine	T	Thr	Threonine
I	Ile	Isoleucine	V	Val	Valine
K	Lys	Lysine	W	Trp	Tryptophan
L	Leu	Leucine	Y	Tyr	Tyrosine

Summary

In most organisms the tricarboxylic acid (TCA) cycle is a fundamental hub in metabolism. The TCA cycle is the origin and the endpoint of a broad spectrum of intermediates and provides the cell with energy and cellular building blocks. Especially in bacteria the pathway importantly contributes to their broad metabolic abilities.

In this work it is shown that the majority of the TCA cycle enzymes in *Bacillus subtilis* interact with each other via protein-protein interactions and a model for a TCA cycle metabolon is established. The assembly in complexes seems to be a common feature of metabolic enzymes like the enzymes of the TCA cycle. A complex of enzymes might lead to higher local substrate concentrations and might enhance metabolic fluxes by substrate channeling. Furthermore, interactions between enzymes of the TCA cycle and enzymes of connected metabolic pathways, like gluconeogenesis or nitrogen metabolism, are identified. Consequently, it can be assumed that the connection of the pathways via protein-protein interactions might directly trigger the flux through the different pathways.

Another aim of this work was to elucidate the mechanism of malate-mediated carbon catabolite repression (CCR) and to analyze the role of the *B. subtilis* malate dehydrogenases in malate metabolism. For malate-mediated CCR an unknown mechanism was supposed to be active in *B. subtilis*. However, in this work it is demonstrated that malate-mediated repression is achieved by the global mechanism of CCR via the CcpA/HPrK pathway and that malate triggers the formation of ATP and fructose 1,6-bisphosphate levels sufficient for CcpA/HPrK pathway activation. Malate is a preferred carbon source of *B. subtilis* and for an efficient utilization *B. subtilis* relies on a number of specific transporters and enzymes. Here, the essential role of the malate dehydrogenase and the phosphoenolpyruvate carboxykinase in malate utilization and the role of the malic enzymes of *B. subtilis* to supply the cell with NADPH, NADH and ATP are demonstrated.

Finally a novel mechanism of TCA cycle branch control is identified. In *B. subtilis,* the regulation of the TCA cycle is mainly exerted at the transcriptional level. Especially the expression of the first two enzymes, citrate synthase and aconitase, is controlled by a complex interplay of several transcription factors. In this work it is demonstrated that the iron regulatory protein aconitase is able to bind the mRNA of citrate synthase under high intracellular citrate concentrations and thus to destabilize its transcript to reduce the level of citrate synthase protein in the cell.

1. Introduction

1.1. The tricarboxylic acid cycle

Central carbon metabolism

A living organism (a cell) can be considered as a chemical factory with thousands of different reactions. The metabolism (from the Greek word “metabole”, change) is the sum of all these reactions. Metabolic reactions are organized in a huge network of different pathways, in which every step is catalyzed by a specific enzyme. Furthermore, all these reactions as well as all metabolic pathways can be divided into two classes of reactions: anabolic and catabolic reactions. Catabolic reactions are used for the production of energy and anabolic reactions are used for the production of complex molecules from less complex precursors. Also the central carbon metabolism can be divided into these two classes. On the one hand the central carbon metabolism is needed for the production of energy and on the other hand it provides the cell with important building blocks for the production of complex molecules. As the central carbon metabolism is the central part of a huge network of metabolic reactions, it is connected to many other pathways. In many organisms the central carbon metabolism is presented by glycolysis, the pentose phosphate pathway and the tricarboxylic acid (TCA) cycle.

The tricarboxylic acid cycle

The tricarboxylic acid (TCA) cycle plays a central role in the metabolism of many organisms (for an overview see Fig. 1.1). The TCA cycle is the endpoint of numerous intermediates (carbohydrates, fatty acids and amino acids) which are used for the production of energy through the complete oxidation to carbon dioxide. On the other hand the TCA cycle is the origin for the production of various metabolic intermediates. Due to its central role in catabolism and anabolism the cycle is highly connected in a network of metabolic pathways. Through the pyruvate dehydrogenase complex the TCA cycle is connected with glycolysis and through the enzymes of the phosphoenolpyruvate-pyruvate-oxaloacetate node to gluconeogenesis. During glycolysis glucose is metabolized to pyruvate while producing energy (ATP) by substrate-level phosphorylation and reducing power in the form of NADH. Pyruvate is then a target of the pyruvate dehydrogenase complex that converts pyruvate to acetyl-CoA.

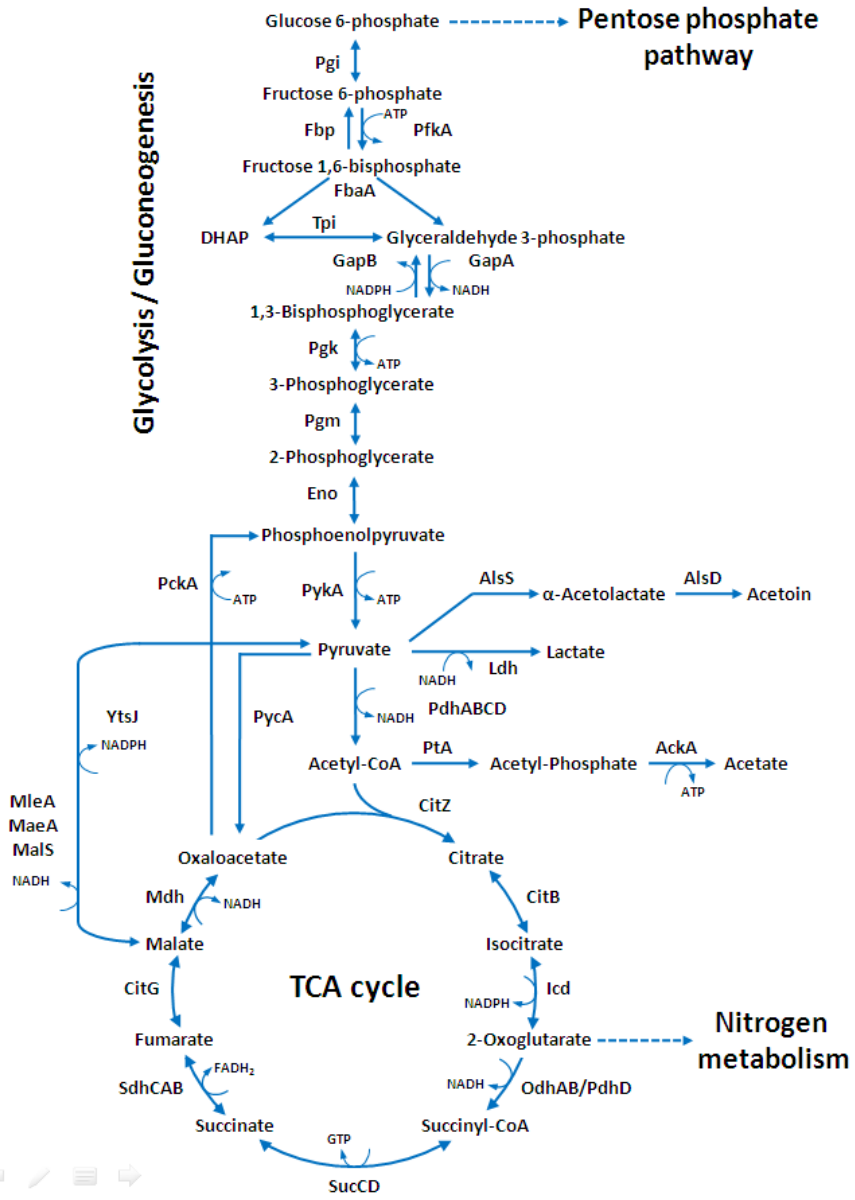

Fig. 1.1. Overview about the central carbon metabolism in *B. subtilis*. Abbreviations used in this figure: AckA, acetate kinase; AlsS, acetolactate synthase; AlsD, acetolactate decarboxylase; CitB, aconitase; CitG, fumarase; CitZ, citrate synthase; Eno, enolase; FbaA, fructose 1,6-bisphosphate aldolase; Fbp, fructose 1,6-bisphosphatase; GapA, Glyceraldehyde 3-phosphate dehydrogenase; GapB, Glyceraldehyde 3-phosphate dehydrogenase; Icd, isocitrate dehydrogenase; Ldh, lactate dehydrogenase; MaeA, malic enzyme; MalS, malic enzyme; Mdh, malate dehydrogenase; MleA, malic enzyme; PdhABCD, pyruvate dehydrogenase; OdhAB/PdhD, 2-oxoglutarate dehydrogenase; PckA, phosphoenolpyruvate carboxykinase; PfkA, phosphofructokinase; Pgi, glucose 6-phosphate isomerase; Pgk, phosphoglycerate kinase; Pgm, phosphoglycerate mutase; PtA, phosphotransacetylase; SdhCAB, succinate dehydrogenase; SucCD, succinyl-CoA synthetase; Tpi, triose phosphate isomerase; PycA, pyruvate carboxylase; PykA, pyruvate kinase; YtsJ, malic enzyme.

Afterwards acetyl-CoA enters the TCA cycle and forms together with oxaloacetate the first intermediate of the TCA cycle (citrate). Otherwise glucose can be generated from non-carbohydrate carbon sources through gluconeogenesis. For this purpose, the TCA cycle intermediate oxaloacetate is decarboxylated by the phosphoenolpyruvate carboxykinase and converted to phosphoenolpyruvate. In addition to its connection to glycolysis or gluconeogenesis the TCA cycle is directly connected with the nitrogen metabolism through the TCA cycle intermediates 2-oxoglutarate and oxaloacetate. Both intermediates are precursors of several amino acids. Moreover, 2-oxoglutarate and oxaloacetate are important for the synthesis of DNA and RNA via the assembly of pyrimidine and purine bases. The first intermediate of the TCA cycle (citrate) is necessary for the synthesis of fatty acids and sterols. Moreover, succinyl-CoA is a precursor of porphyrins.

Variations of the TCA cycle

Not every organism possesses a complete TCA cycle as shown in Fig. 1.1 for *B. subtilis*. Several variations of the TCA cycle are known and reflect the adaptation of diverse organisms to their specific lifestyles. Some organisms encode additional enzymes which complement the TCA cycle with further functions or that are necessary to bypass some reactions. An example for a bypass is the glyoxylate cycle. During the reaction sequence of the TCA cycle two carbon atoms are lost as carbon dioxide. Therefore, many organisms are not able to use acetate as a sole carbon source because they cannot synthesize essential carbohydrates from acetate. However, certain bacteria, plants, fungi and invertebrates encode additional enzymes (isocitrate lyase and malate synthase) and are as a result able to circumvent this problem. With these two enzymes a part of the TCA cycle can be bypassed and thus it is possible to synthesize carbohydrates from acetate. Isocitrate lyase catalyses the cleavage of isocitrate to glyoxylate and succinate. As a result, the two steps in the TCA cycle in which carbon is lost are bypassed. Malate synthase then catalyses the condensation of glyoxylate and acetyl-CoA to produce malate and CoA-SH. The glyoxylate cycle is essential to use lipids or acetate as single carbon sources. Another example for a variation of the TCA cycle is the reverse TCA cycle that is used by green sulfur bacteria and some archaea (Avans *et al*., 1966; Buchanan & Arnon, 1990). The reverse TCA cycle can be used for auxotrophic carbon fixation as the oxidative steps of the TCA cycle are reversed and carbon dioxide can be fixed. The irreversible reactions of the TCA cycle (see Fig. 1.1) are avoided by the use of 2-oxoglutarate synthase and citrate lyase. Furthermore, a fumarate reductase is used

instead of succinate dehydrogenase. Beside organisms which encode additional enzymes, there are others which do not possess a complete TCA cycle. *Listeria monocytogenes* for example, a Gram-positive bacterium closely related to *B. subtilis,* possesses an incomplete TCA cycle and lacks oxoglutarate dehydrogenase, succinyl-CoA synthetase and succinate dehydrogenase (Kim *et al*., 2006; Trivett & Meyer, 1971). Some organisms completely miss the TCA cycle. One example is *Mycoplasma pneumonia*, an organism with a highly reduced genome size due to its pathogenic life style (Manolukas *et al*., 1988).

1.2. *Bacillus subtilis*

Although microorganisms are rather inconspicuous, they represent the most abundant and most multifarious life form on earth. Especially because of their simplicity but also their ability to adapt to various habitats and to live even under extreme environmental conditions, they are of great importance for science. One example is the ubiquitous soil bacterium *Bacillus subtilis* which became the model organism for Gram-positive bacteria. *B. subtilis* is a non-pathogenic bacterium with closely related pathogenic organisms, it is naturally competent and its genome was one of the first to be sequenced (Barbe *et al*., 2009; Kunst *et al*., 1997). The formation of endospores by *B. subtilis* is a basic mechanism of cell differentiation and enables this organism to outlast extremely long periods of time (Gest & Mandelstam, 1987; Piggot & Hilbert, 2004). For these reasons and due to the fact that *B. subtilis* can be used for the production of antibiotics, vitamins and enzymes this organism is an interesting tool for science and industry (Craig *et al*., 1949; Bacher *et al*., 2000; Pierce *et al*., 1992). *B. subtilis* is a heterotrophic organism with various metabolic abilities. These abilities enable *B. subtilis* to adapt to a fast changing habitat and to compete with other organisms. Especially the TCA cycle allows *B. subtilis* to metabolize many organic acids (intermediates of the TCA cycle). In nature organic acids are commonly available and are therefore an important carbon source.

The TCA cycle of *B. subtilis*

In *B. subtilis* the first reaction of the TCA cycle is catalyzed by the citrate synthase (CitZ) which catalyzes the condensation reaction of acetyl-CoA and oxaloactate to citrate. The second step in the cycle is catalyzed by aconitase (CitB). CitB is a large protein, containing an iron-sulfur cluster which directly modulates the enzymatic activity of this enzyme. In the enzymatic active

state CitB catalyzes the isomerization of citrate to isocitrate via the unstable intermediate cis-aconitate. Under iron-limiting conditions one iron atom of the iron-sulfur cluster of CitB can leave the cluster and causes a conformational change of the protein. Under these conditions the protein acts not longer as an active enzyme in the TCA cycle, but is instead active as a RNA-binding iron-regulatory protein (Alén & Sonenshein, 1999; Volz, 2008).

After the formation of isocitrate this intermediate is converted to 2-oxoglutarate by the isocitrate dehydrogenase (Icd). During the Icd-mediated oxidative decarboxylation of isocitrate NADPH is produced. Thus, this reaction is an important source of this coenzyme which is essential for many anabolic reactions. 2-Oxoglutarate is then again oxidized to succinyl-CoA by the 2-oxoglutarate dehydrogenase complex (OdhAB/PdhD), a protein complex consisting of three subunits. In addition to the oxidation of 2-oxoglutarate by OdhAB/PdhD this intermediate directly connects the TCA cycle with the nitrogen metabolism. 2-Oxoglutarate can be used by the GS-GOGAT cycle to synthesize glutamate (Gunka & Commichau, 2012). The GS-GOGAT cycle combines the reactions of glutamine synthetase (GS) and glutamate synthase (GOGAT). Through this cycle two molecules of glutamate are produced by transferring the amide group from glutamine to 2-oxoglutarate. *B. subtilis* assimilates ammonium only through the GS-GOGAT cycle, thus the connection of the TCA cycle with nitrogen metabolism via 2-oxoglutarate plays an essential role in ammonium assimilation. Glutamate is the most abundant metabolite in the cell and an essential donor of amino groups during biosynthesis of proteins (Bennett *et al*., 2009).

The next step in the TCA cycle is the hydrolysis of succinyl-CoA to succinate by the succinyl-CoA synthetase (SucCD) coupled to the production of GTP. Succinate is then oxidized by the membrane-bound succinate dehydrogenase (SdhCAB). SdhCAB forms a complex within the respiratory chain of *B. subtilis* (Hederstedt & Rutberg, 1983). After that fumarase (CitG) catalyzes the hydration of fumarate to malate. Finally the oxidation of malate to oxaloacetate by the malate dehydrogenase (Mdh) completes the sequential reactions of the cycle. The reaction equation of the TCA cycle of *B. subtilis* can thus be summarized to:

$$\text{Acetyl-CoA} + \text{NADP}^+ + 2\ \text{NAD}^+ + \text{FAD} + \text{GDP} + \text{P}_i + 2\ \text{H}_2\text{O} \rightarrow 2\ \text{CO}_2 + \text{NADPH} + \text{H}^+ + 2\ \text{NADH} + \text{H}^+ + \text{FADH}_2 + \text{GTP} + \text{CoA-SH}$$

In addition to the production of NADPH, two molecules NADH are produced by OdhAB/PdhD and Mdh and one molecule $FADH_2$ is produced by SdhCAB. The produced NADH and $FADH_2$ can finally be used for the generation of ATP through the respiratory chain.

1.3. The phosphoenolpyruvate-pyruvate-oxaloacetate node

The phosphoenolpyruvate-pyruvate-oxaloacetate node (or the anaplerotic node) connects the major pathways of carbon metabolism. It connects glycolysis with the TCA cycle or the TCA cycle with gluconeogenesis. Especially in bacteria which can use a broad range of carbon sources for growth this node is an important control point of carbon fluxes. Depending on the available carbon source the flux switches between glycolysis and gluconeogenesis (Sauer & Eikmann, 2005).

During glycolysis, glucose is degraded to pyruvate and enters the TCA cycle after the conversion to acetyl-CoA. In addition, pyruvate can directly enter the TCA cycle via carboxylation to oxaloacetate by pyruvate carboxylase. As several intermediates of the cycle are needed for anabolic reactions and therefore leave the cycle, the TCA cycle would simply stall without the anaplerotic reaction of pyruvate carboxylase. Thus, this enzyme is needed to replenish the cycle and to keep it running during growth with sugars as single carbon sources.

During growth on intermediates of the TCA cycle or carbon sources which are metabolized via acetyl-CoA (such as fatty acids and acetate) the phosphoenolpyruvate-pyruvate-oxaloacetate node is needed to build up glycolytic intermediates from malate or oxaloacetate. While the reactions of glycolysis and the TCA cycle are quite similar in most organisms, the phosphoenolpyruvate-pyruvate-oxaloacetate node is rather diverse (Sauer & Eikmann, 2005).

The phosphoenolpyruvate-pyruvate-oxaloacetate node of *B. subtilis*

In *B. subtilis* the phosphoenolpyruvate-pyruvate-oxaloacetate node is presented by pyruvate carboxylase (PycA), phosphoenolpyruvate carboxykinase (PckA) and four malic enzymes (MaeA, MalS, MleA and YtsJ) (see Fig. 1.1). The pyruvate carboxylase catalyses the carboxylation of pyruvate to oxaloacetate and so replenishes the TCA cycle with oxaloacetate. The phosphoenolpyruvate carboxykinase converts oxaloacetate to phosphoenolpyruvate and is in *B. subtilis* the essential reaction to connect the TCA cycle with gluconeogenesis (Tännler *et al.*, 2008). Through this connection *B. subtilis* is able to build up glucose from intermediates of the TCA cycle and is so able to use organic acids as carbon sources. Finally the malic enzymes connect the two pathways by oxidative decarboxylation of malate to pyruvate.

The available carbon source has a great impact on the phosphoenolpyruvate-pyruvate-oxaloacetate node. During growth with glucose a high metabolic flux through glycolysis and the

TCA cycle can be detected (Kleijn *et al.*, 2010). In consequence, a high flux through PycA is necessary to replenish the TCA cycle under these conditions. On the other hand the activity of PckA and the malic enzymes is not needed in glucose grown cells. Therefore, the expression of PckA is repressed to avoid the loss of energy trough futile cycles (Servant *et al.*, 2005; Tännler *et al*., 2008). During growth with malate (an organic acid and an intermediate of the TCA cycle) a high flux through PckA and the malic enzymes occurs (Kleijn *et al.*, 2010). Now the anapleroctic reaction of PycA is not longer needed as in the presence of glucose, because the TCA cycle is directly replenished by the used carbon source. Interestingly, the flux through the TCA cycle is much lower during the use of malate than in the presence of glucose. In addition, the production of overflow products varies between glycolytic and gluconeogenic growth conditions. With glucose the main overflow product is acetate, whereas in the presence of malate beside acetate also pyruvate is produced in substantial amounts (Kleijn *et al.*, 2010).

Malate: Another preferred carbon source of *B. subtilis*

Like many other heterotrophic bacteria, *Bacillus subtilis* can utilize a wide range of carbon and energy sources such as several sugars, complex carbohydrates and organic acids. For a long time glucose was considered as the preferred carbon source for *B. subtilis*. However, recent findings demonstrate that *B. subtilis* prefers the organic acid malate in addition to glucose (Kleijn *et al.*, 2010). In comparison with other heterotrophic bacteria *B. subtilis* thus represents an exception, as most of these organisms prefer just on carbon source (glucose) (Görke & Stülke, 2008; Singh *et al*., 2008). In the habitat of *B. subtilis* (the soil and plant surfaces) malate is commonly available (Bais *et al.*, 2006; Barbe *et al*., 2009; Deng *et al.*, 2011; Rudrappa *et al*., 2008). Malate is the primary product of carbon dioxide fixation in a large group of plants and accumulates in unripe fruits. Furthermore, several carboxylic acids, among them malate, are secreted by plant roots into the rhizosphere. The secretion of carboxylic acids recruits beneficial bacteria that help to reduce susceptibility to plant pathogens (Bais *et al.*, 2006; Weisskopf *et al*., 2008). Thus, the preference for malate as a second carbon source in addition to glucose is not surprising. Moreover, *B. subtilis* can adapt its metabolism more quickly to malate utilization than to glucose utilization. During a shift to malate utilization malate causes a fast response which mainly occurs on the posttranscriptional level. On the other hand, a shift to glucose utilization requires a major reprogramming of transcription (Buescher *et al.*, 2012; Nicolas *et al.*, 2012).

Many bacteria which can use C_4-dicarboxylates (like succinate, fumarate, malate and oxaloacetate) and citrate for growth possess specific transporters for the uptake of these carbon sources. *E. coli* for example codes for at least six different C_4-dicarboxylate transporters. However, the expression of these transporters is only activated in the presence of organic acids by two-component sensor regulators (Janausch *et al*., 2002).

C_4-dicarboxylates can be used as carbon and energy sources and can be oxidized in the TCA cycle to carbon dioxide. To metabolize malate, *B. subtilis* can rely on a number of transporters and enzymes. However, the precise roles of all these proteins are not fully understood. *B. subtilis* encodes five potential transporters for malate, two of which (MaeN and YflS) are specifically induced in the presence of malate (Groeneveld *et al*., 2010; Krom *et al*., 2001; Tanaka *et al*., 2003; Wei *et al*., 2000). Malate is sensed by the two-component system MalKR which induces the expression of the *maeN* and *yflS* transporter genes and additionally the *maeA-ywkB* operon encoding a malic enzyme and a protein of unknown function (Doan *et al*., 2003; Tanaka *et al*., 2003). However, the analysis of *maeN* and *yflS* mutants revealed that MaeN is the only malate transporter and that YflS is not involved in the uptake of malate (Tanaka *et al*., 2003). In addition to MaeN and YflS, *B. subtilis* encodes the presumptive malate transporters CimH, DctP and MleN. CimH has been annotated as a transporter for citrate and malate. However, inhibition assays suggest that citrate but not malate is the physiological substrate (Krom *et al*., 2001). DctP is described as a transporter for succinate, fumurate, malate and oxaloacetate, but lack of impact of a *dctP* inactivation on malate utilization and the failure of a *maeN* mutant to grow with malate suggests that DctP does not play a role in malate transport (Asai *et al*., 2000; Groeneveld *et al*., 2010; Tanaka *et al*., 2003). Finally, MleN is a malate/lactate antiporter that does not contribute to malate assimilation as a carbon source (Wei *et al*., 2000). In the presence of preferred carbon sources (glucose and malate), the expression of a broad range of transporters and enzymes for the uptake and consumption of secondary carbon sources is repressed by the global transcription regulator CcpA in *B. subtilis* (Kleijn *et al*., 2010; Meyer *et al*., 2011b). As *cimH*, *dctP* and *mleN* are all targets of catabolite repression via CcpA it seems unlikely that they play a role in malate metabolism (Asai *et al*., 2000; Marciniak *et al*., 2012; Yamamoto *et al*., 2000). Thus, only the malate symporter MaeN is essential for malate uptake in *B. subtilis* (Tanaka *et al*., 2003). After malate is taken up it enters the TCA cycle at the phosphoenolpyruvate-pyruvate-oxaloacetate node.

Under anaerobic conditions the cells lack a functional TCA cycle thus C_4-dicarboxylates are used for fermentation (e. g. fumarate respiration, citrate fermentation, etc.). Especially

malate can be used for malolactic fermentation by many lactic acid bacteria (e. g. *Oenococcus oeni*, *Lactobacilli*, *Pediococci*) and also eukaryotic organisms like *Saccharomyces cerevisiae*. During the malolactic fermentation process in lactic acid bacteria malate is decarboxylated to lactate coupled with the consumption of a cytoplasmic proton. In consequence the energy of this exergonic reaction is conserved in form of PMF (proton motive force). In addition, the malolactic fermentation process is combined with a specific transport system for the uptake of malate and the export of lactate (Dimroth & Schink, 1998; Poolman *et al*.,1991). *B. subtilis* as well encodes a malate/lactate antiporter (MleN) which enhances growth under certain growth conditions (Wei *et al*., 2000).

1.4. Carbon catabolite repression

All living cells possess a basic setup of constitutively expressed genes (housekeeping genes) for the maintenance of essential cellular functions. In addition to the housekeeping genes the cells possess further genes with additional functions which are not needed every time but enable the cell to adapt to various environmental influences in their habitat. Changing nutrient supply or even stress conditions (like heat stress, salt stress, etc.) can have a great impact on gene expression.

Carbon catabolite repression (also referred to as the glucose effect) is a regulatory mechanism that allows the cells to quickly adapt to a preferred carbon and energy source. It enables the cells to make a choice among several available carbon sources and to use the best carbon source first. The paradigm for carbon catabolite repression is the diauxic growth of *E. coli* discovered by Jacques Monod (Monod, 1942). In the presence of a mixture of carbon sources (for example glucose and lactose) the preferred carbon source of *E. coli* (glucose) is metabolized first, leading to a diauxic growth curve with an additional short lag phase. This additional lag phase reflects the switch from preferred (and now exhausted) to less preferred carbon source.

In many bacteria carbon catabolite repression is one of the most important regulatory mechanisms and controls 5-10% of all genes (Görke & Stülke, 2008). Moreover, CCR does not strictly control just catabolic genes. CCR also plays an important role in the expression of virulence genes in pathogenic organisms. However, virulence of pathogens is primarily a further strategy to get access to nutrients and not just to harm the host.

On the one hand carbon catabolite repression (CCR) controls the gene expression and prevents the transcription of catabolic genes and on the other hand it controls the activity of

proteins to prevent the uptake or formation of the specific inducers of catabolic operons (inducer exclusion) (Deutscher, 2008). In many organisms the control of catabolic genes by CCR is accomplished by a combination of a global mechanism and of operon specific mechanisms. In the model organisms *E. coli* and *B. subtilis* CCR was intensively studied. In both organisms the outcome of the global mechanism of carbon catabolite repression is similar. However, the mechanisms are completely different. In *E. coli* the activation of transcription of catabolic genes is prevented in the presence of glucose. On the contrary in *B. subtilis* the expression of these genes is controlled by a repressor (Görke & Stülke, 2008).

These two examples already demonstrate the diversity of the mechanisms of carbon catabolite repression. In other organism yet different mechanisms were discovered and in some cases the hierarchy of the preferred carbon sources is completely different. In *Pseudomonas* for example, glucose plays only a minor role. These organisms prefer organic acids and amino acids instead of glucose (Collier *et al*., 1996; Rojo, 2010).

Carbon catabolite repression in *B. subtilis*

In *B. subtilis* and most other Firmicutes carbon catabolite repression is controlled by the pleiotropic transcription factor CcpA (catabolite control protein A) which is a member of the LacI/GalR family of transcriptional regulators (Henkin *et al*., 1991).

In *B. subtilis* the key player in CCR is the histidine protein (HPr). HPr is a general component of the phosphoenolpyruvate-carbohydrate phosphotransferase system (PTS), a multiprotein system involved in the uptake and simultaneous phosphorylation of specific carbohydrates (Postma *et al*., 1993). The PTS consists of at least three phosphocarrier proteins: enzyme I (EI), HPr and the sugar-specific permease enzyme II (EII). During sugar transport via the PTS the phoshporyl group of phosphoenolpyruvate is transferred to EI, then from EI to HPr (phosphorylated at residue His15), and finally to EII, which transfers the phosphate to the carbohydrate. The phosphorylation state of the PTS components is dependent on PEP availability and the transport activity of the PTS. PTS sugars, which are taken up via the PTS, lead to the dephosphorylation of HPr (His15) and enzyme II. In contrast, in the absence of PTS sugars the level of HPr(His-P) and phosphorylated enzyme II is high. Thus, the phosphorylation state of HPr at His15 is a sensor for sugar availability. In addition to the phosphorylation during phosphate transfer in the PTS, HPr can be phosphorylated at a regulatory site (Ser46) by the HPr kinase/phosphorylase (HPrK) (Deutscher *et al*., 2006; Nessler *et al*., 2003). The activity of HPrK

and thus the phosphorylation of HPr through HPrK is controlled by the intracellular pools of fructose 1,6-bisphosphate (FBP), ATP and P_i. FBP is an effector of HPrK and activates HPrK by allosteric binding (Galinier *et al*., 1998; Hanson *et al.*, 2002; Jault *et al*., 2000; Saier *et al*., 1989). In the presence of a preferred carbon source like glucose the FBP levels in the cell are high, HPrK is active and phosphorylates HPr. After phosphorylation HPr(Ser-P) is not longer active in the PTS but serves as a cofactor for the transcription factor CcpA (Deutscher *et al*., 1995). The binding of HPr(Ser-P) to CcpA induces a conformational change of CcpA and enables it to bind to DNA (Schumacher *et al.*, 2007). The interaction between HPr(Ser-P) and CcpA is enhanced by FBP and glucose-6-phosphate (Schumacher *et al.*, 2007). As a consequence of the activation of CcpA by HPr(Ser-P) about 300 genes of *B. subtilis* are repressed, while a few genes involved in overflow metabolism and the biosynthesis of amino acids are induced (Fujita, 2009; Görke & Stülke, 2008). The genes which are regulated by CcpA are characterized by specific palindromic operator sequences in their promoter region which are called catabolite responsive elements (*cre*). CcpA binding sites (*cre*-sites) in the promoter regions of a gene lead to the repression of transcription. In contrast, binding to upstream regions of the promoter can activate the transcription (Fujita, 2009; Görke & Stülke, 2008). Only His15 unphosphorylated HPr is able to bind to CcpA (Reizer *et al*., 1996). The termination of CCR is thus caused by the stop of sugar uptake through the PTS and low FBP levels which stop the activity of HPrK. Furthermore, low FBP levels enhance the phosphorylase activity of HPrK and HPr(Ser-P) is actively dephosphorylated (Mijakovic *et al*., 2002; Monedero *et al*., 2001). In addition to the key protein in CCR (HPr) *B. subtilis* possesses an additional protein (Crh) which is a homolog of HPr. This carbon-flux-regulating protein (Crh) shares over 40% sequence identity with HPr (Galinier *et al*., 1997; Landmann *et al*., 2012). Crh is not involved in sugar uptake through the PTS, due to the missing His15 phosphorylation site. Nevertheless, Crh contains the Ser46 phosphorylation site and can partially complement the functions of HPr in carbon catabolite repression (Singh *et al*., 2008). However, the intracellular concentrations of Crh are much lower as compared to HPr and Crh has a lower binding affinity for CcpA (Görke *et al*., 2004; Seidel *et al*., 2005). In addition to the back-up function of Crh in CCR it was recently discovered that Crh plays an important role in the control of a glycolytic bypass in *B. subtilis* (Landmann *et al*., 2011).

1.5. Regulation of central metabolic pathways in *B. subtilis*

The adaptation to various environmental influences is of large importance for the cell. In particular the regulation of the metabolism is triggered by the different needs of the organism and the nutritional supply. As a major regulatory mechanism carbon catabolite repression has a great impact on metabolism (see chapter 1.4). However, certain additional control mechanisms are needed for appropriate control. The control of metabolic pathways at the level of gene expression (transcriptional and translational control) is only the first level of control, as the control of gene expression in bacteria takes minutes. In addition to gene expression control the activity of proteins can be directly controlled by allosteric regulation or posttranslational mechanisms (e. g. phosphorylation, adenylation, etc.). The control of enzyme activities can occur in seconds and is thus rather important for the fine-tuning of metabolic pathways. In this paragraph the regulation of the metabolic pathways glycolysis, the pentose phosphate pathway and the tricarboxylic acid (TCA) cycle in *B. subtilis* will be discussed.

Regulation of the glycolysis/gluconeogenesis and the pentose phosphate pathway

The genes of glycolysis are either expressed constitutively or are induced in the presence of glucose (Blencke *et al*., 2003; Ludwig *et al*., 2001). *pgi* and *fbaA* are expressed constitutively, whereas *pfkA* and *pykA* and the genes encoded in the hexacistronic *gapA* operon are induced by glucose (Ludwig *et al*., 2001). The expression of the *gapA* operon is repressed by the transcriptional regulator CggR (Fillinger *et al*., 2000; Ludwig *et al*., 2001). However, fructose 1,6-bisphosphate acts as inhibitor of CggR activity (Doan & Aymerich, 2003). Thus, in the presence of glucose the repression by CggR is lost due to high intracellular FBP levels.

Especially the switch between glycolytic to gluconeogenic growth conditions is strictly regulated by the transcription factor CcpN, which represses the expression of gluconeogenic genes (*gapB* and *pckA*) and the regulatory RNA SR1 (Servant *et al*., 2005; Licht *et al*., 2005). Thus, in the presence of glycolytic substrates, the flux through the letter enzymes is prevented. As described before, PckA is an essential to connect the TCA cycle with gluconeogenesis. However, it can lead to futile reactions under glycolytic growth. Similarly GapB is necessary to bypass the irreversible reaction of GapA in glycolysis. Nevertheless, a simultaneous expression of *gapA* and *gapB* in the presence of glycolytic substrates would as well lead to futile reactions.

The control by CcpN is thus highly important to maintain efficient carbon fluxes in *B. subtilis* (Tännler *et al*., 2008).

In *B. subtilis* and also many other bacteria not much is known about the regulation of the pentose phosphate pathway. In *B. subtilis* the genes of the pentose phosphate pathway are expressed constitutively (Blencke *et al*., 2003; Nicolas *et al*., 2012). Less control of this central pathway probably reflects the continuous need of NADPH and precursors for nucleotide biosynthesis under any growth condition. However, the carbon flux through the pentose phosphate pathway is enhanced in the presence of organic acids by a yet unknown mechanism (Schilling *et al*., 2007).

Regulation of the TCA cycle

The TCA cycle is a central platform in carbon metabolism and is connected to several other metabolic pathways. Therefore, a tight control of the TCA cycle is crucial for *B. subtilis*. Especially the entrance into the TCA (the first enzymes) is highly regulated. In *B. subtilis* the primary control of the TCA cycle occurs at the level of gene expression, whereas regulation at the level of enzyme activity (e. g. allosteric regulation and regulation by phosphorylation) plays only a minor role.

First of all the TCA cycle is subject to carbon catabolite repression and several genes are target of the transcription regulator CcpA (Blencke *et al*., 2006; Miwa *et al*., 2000). In addition to CcpA this pathway is controlled by a TCA cycle specific regulator CcpC (catabolite control protein C), a regulator of the LysR family (Jourlin-Castelli *et al*., 2000).

As already described, the entrance into the TCA cycle is catalyzed by citrate synthase (CitZ). The gene for *citZ* is encoded in an operon together with isocitrate dehydrogenase and malate dehydrogenase (*citZ icd mdh*) (see chapter 5). The expression of the operon is controlled by three different promoters (Jin & Sonenshein, 1994b; Jin & Sonenshein, 1996). In front of the *citZ* gene a promoter is located which is controlled by CcpA and CcpC. In the presence of a preferred carbon source such as glucose or malate the expression is repressed by CcpA. In the presence of glucose and glutamate (a good nitrogen source) the expression is additionally repressed by CcpC (Kim *et al*., 2002; Jourlin-Castelli *et al*., 2000). As *citZ*, *icd* and *mdh* form an operon the regulatory control influences the expression of the whole operon. Nevertheless, the additional promoters in front of *icd* and in front of *mdh* are constitutive.

The expression of the second enzyme of the TCA cycle (CitB) is also strictly controlled. *citB* is monocitronically transcribed and the expression of the gene is first of all controlled by CcpA and CcpC (in the presence of glucose and a good nitrogen source) (Blencke *et al*., 2003; Jourlin-Castelli *et al*., 2000). In the presence of branched-chained amino acids the expression of *citB* is additionally repressed by the pleiotropic transcriptional repressor CodY (Kim *et al*., 2002). Under iron limiting conditions CitB acts as a trigger enzyme involved in iron homeostasis (see chapter 1.1). Under these conditions expression of *citB* is then additionally regulated at the RNA-level. The small RNA FsrA inhibits *citB* translation through the binding of its mRNA (Gaballa *et al*., 2008). Moreover, during the transition from growth to stationary phase the expression of *citB* is enhanced by the transcriptional regulator AbrB, due to the involvement of CitB in sporulation (Kim *et al.,* 2003a). CitB stabilizes the mRNA of the transcriptional regulator GerE (Serio *et al*., 2006). Beside the complex regulation of *citZ* (*citZ icd mdh* operon) and *citB* the two operons *odhAB* and *sucCD* are targets of CcpA-mediated carbon catabolite repression (Blencke *et al*., 2003). Interestingly, recent analyses of the binding affinities of CcpA to its TCA cycle targets revealed a strong affinity to the *cre*-sites of *sucC* and only a weak affinity to the *cre*-sites of *citZ* and *odhA* (Marciniak *et al*., 2012). *sdhCAB* and *citG* are constitutively expressed.

The connection between carbon and nitrogen metabolism in *B. subtilis*

Due to the essential role of glutamate and glutamine in the cell (serving as the major amino group donors), the control of the intersection between carbon and nitrogen metabolism plays a crucial role in the metabolism of *B. subtilis*. As described above (see chapter 1.1), glutamate is synthesized in *B. subtilis* exclusively by the GS-GOGAT cycle using the TCA cycle intermediate 2-oxoglutarate (Gunka & Commichau, 2012). However, the branch to the GS-GOGAT cycle is only active when no preferred nitrogen source (glutamine) is available. In the presence of glutamine the expression of the glutamine synthetase (GS, encoded by *glnA*) is repressed by the transcriptional repressor GlnR (Schreier *et al*., 1989). The expression of glutamate synthase (GOGAT, encoded by *gltAB*) is controlled by the transcription activator GltC and the global regulator protein of nitrogen metabolism TnrA (Gunka & Commichau, 2012). In the presence of glucose GltC activates the expression of *gltAB*, whereas in the absence of glucose and presence of glutamate GltC is inactive and does not activate transcription (Belitsky & Sonenshein, 2004; Commichau *et al*., 2007a; Wacker *et al*., 2003). In the absence of glutamine the expression of *gltAB* is repressed by TnrA (Belitsky & Sonenshein, 2004). TnrA binds to the

promoter of *gltAB* and thereby prevents the activation via GltC. If glutamine is missing the expression of *gltAB* is not required.

B. subtilis encodes two glutamate dehydrogenases (RocG and GudB) which are strictly catabolically active. In the presence of arginine or of a nitrogen source that can be degraded to glutamate the transcription of *rocG* is activated by the transcription factors AhrC and RocR (Belitsky & Sonenshein, 1998; Commichau *et al*., 2007b). In contrast, in the presence of glucose the expression is repressed by the transcription factor CcpA (Belitsky & Sonenshein, 2004; Choi & Saier, 2005). In the *B. subtilis* laboratory strain 168 the *gudB* gene is cryptic. The enzyme is not active because of direct repeat of 9 bp in the *gudB* gene (Zeigler *et al*., 2008). Interestingly, in a *rocG* mutant the cryptic *gudB* gene is activated and the active glutamate dehydrogenases (GudB1) can replace RocG (Gunka *et al*., 2012).

1.6. Protein interactions

Every living cell is composed of four classes of macromolecules (lipids, polysaccharides, nucleic acids and proteins). Among these macromolecules, proteins are the main components of cells. In *E. coli* for example, the total concentration of protein and RNA amounts to about 340 g/l (Zimmerman & Minton, 1993). Proteins are structurally highly developed molecules and are involved in numerous cellular functions. They are active as catalytic proteins (enzymes), are involved in regulatory processes and are essential for the structure of a cell (structural proteins). The interplay between proteins as well as between proteins and nucleic acids (RNA and DNA) is a fundamental aspect of cellular activity in living cell.

Protein-protein interactions

The majority of biological functions is accomplished by proteins which are active in complexes rather than in an isolated way. The individual proteins of such complexes interact mostly via non-covalent bonds (van der Waals force and hydrogen bonds) and are so kept together. Especially the shape of the protein and the distribution of charges on its surface are crucial for complex formation. Numerous well established complexes are known which are formed by protein-protein interactions. For example the replication machinery, the RNA polymerase or the ribosomes (a protein/RNA complex) form large protein complexes. However, not only these sophisticated machineries of the cell form large complexes, also enzymes

involved in metabolism like the pyruvate dehydrogenase form large complexes and are even visible under a microscope. Beside well established complexes several recent proteome-wide interactome studies have suggested that interactions between proteins are very common (Hu *et al*., 2009; Menon *et al*., 2009; Kühner *et al*., 2009). Nevertheless, it remains still a challenge to discover all protein complexes due to the fact that not all protein complexes are stable (transient complexes) and proteins often interact with several other proteins (Williamson & Sutcliffe, 2010). An example for such a transient complex is the eukaryotic purinosome (An *et al*., 2008). The enzymes involved in *de novo* purine biosynthesis only interact under purine-depleted condition whereas under purine-rich conditions no interaction is detectable. It is assumed that the interaction between the single proteins of this pathway is necessary for a direct transfer of the intermediates (substrate channeling) and that it in addition regulates the purine synthesis (An *et al*., 2008). The direct transfer of intermediates between enzymes which catalyse sequential reactions seems to be a common feature of many metabolic pathways. Especially reactions with volatile intermediates which can simply leave the cell through the membrane or intermediates which are toxic for the cell require the direct transfer from enzyme to enzyme. A well-known example is tryptophan biosynthesis. By an interaction the intermediate indole is directly transferred via an interconnecting tunnel from one enzyme to the other and is thus hindered to leave the cell (Dunn *et al*., 2008). Also for enzymes involved in central carbon metabolism several studies detected interactions between enzymes of these pathways. In prokaryotes (among them *B. subtilis*) and in eukaryotes interactions between glycolytic enzymes and enzymes of the TCA cycle were already found (Barnes & Weitzman, 1986; Campanella *et al*., 2005; Commichau *et. al*., 2009; Grandier-Menon *et al*., 2009; Mitchell, 1996; Mowbray & Moses, 1976).

Protein-RNA and protein-DNA interactions

The interaction of proteins with DNA or RNA is in addition to protein-protein interactions crucial for cellular life. Proteins or protein complexes, which interact with DNA or RNA, can be divided into two classes: enzymatically active proteins (e. g. the replication machinery, the RNA polymerase or the ribosome) and regulatory proteins. The contact of protein and nucleic acid is carried out by an interaction via the amino acids of the protein and the nucleobases and the backbone of DNA/RNA. Furthermore, the interaction happens either in an unspecific way (e. g. eukaryotic histones) or in a sequence specific manner. Beside DNA and RNA replication or

translation especially the control of gene expression is controlled by interactions between proteins and DNA or RNA. These proteins mostly interact via specific protein motifs with DNA and can activate or repress the expression of genes. Typically motifs of these proteins are helix turn helix or zinc finger motifs. The already described transcription regulator CcpA of *B. subtilis*, which is a member of the LacI/GalR family of transcriptional regulators, interacts with the DNA via a helix turn helix motif (Henkin *et al*., 1991).

Another example is the regulatory function of the TCA cycle enzyme aconitase which is involved in the control of iron homeostasis. Under iron-limiting conditions the aconitase is not longer an active enzyme in the TCA cycle but active as an iron regulatory protein (IRP) (Alén & Sonenshein, 1999; Volz, 2008). The IRP is then able to bind to specific motifs in the 5´UTR or the 3´UTR of specific mRNAs (so called iron responsive elements [IREs]). The binding of the IRP to the RNA can either stabilize or destabilize the mRNA or can prevent translation.

2. Physical interactions between TCA cycle enzymes in *Bacillus subtilis*

The results described in this chapter were published in:

Meyer, F. M., Gerwig, J., Hammer, E., Herzberg, C., Commichau, F. M., Völker, U. & Stülke, J. (2011). Physical interactions between tricarboxylic acid cycle enzymes in *Bacillus subtilis*: Evidence for a metabolon. *Metab. Eng*. 13, 18-27.

Author's contribution:

The study was designed and interpreted by FMM, FMC and JS. The *in vivo* pull down experiments were done by FMM, JG and CH. The bacterial two-hybrid analysis was performed by FMM and JG. The Protein identification by mass spectrometry was done by EH. The paper was written by FMM and JS.

Abstract

The majority of all proteins of a living cell is active in complexes rather than in an isolated way. These protein-protein interactions are of high relevance for many biological functions. In addition to many well established protein complexes an increasing number of protein-protein interactions, which form rather transient complexes has recently been discovered. The formation of such complexes seems to be a common feature especially for metabolic pathways. In the Gram-positive model organism *Bacillus subtilis*, we identified a protein complex of three citric acid cycle enzymes. This complex consists of the citrate synthase, the isocitrate dehydrogenase, and the malate dehydrogenase. Moreover, fumarase and aconitase interact with malate dehydrogenase and with each other. These five enzymes catalyze sequential reaction of the TCA cycle. Thus, this interaction might be important for a direct transfer of intermediates of the TCA cycle and thus for elevated metabolic fluxes via substrate channeling. In addition, we discovered a link between the TCA cycle and gluconeogenesis through a flexible interaction of two proteins: the association between the malate dehydrogenase and phosphoenolpyruvate carboxykinase is directly controlled by the metabolic flux. The phosphoenolpyruvate carboxykinase links the TCA cycle with gluconeogenesis and is essential for *B. subtilis* growing on gluconeogenic carbon sources. Only under gluconeogenic growth conditions an interaction of these two proteins is detectable and disappears under glycolytic growth conditions.

Introduction

With the availability of more and more genome sequences, we now know basically all the components of living cells. However, the genome is just a blueprint, and processes of life depend on the actual presence of the components and their interactions. The analysis of gene expression patterns to elucidate the presence of specific gene products (usually proteins) has been extensively applied at the level of complete transcriptomes or proteomes for many years. In contrast, the analysis of the interactions between cellular components is only emerging to be recognized as equally important. Recently, several proteome-wide studies suggested that interaction between different proteins are very common and that some proteins may even contribute to multiple interactions (Hu *et al*., 2009; Menon *et al*., 2009; Kühner *et al*., 2009).

For a long time and until very recently, bacteria were thought to be poorly internally organized reaction vessels in which all the biochemical reactions take place in an unorganized way. However, the concentration of macromolecules in a bacterial cell is very high. In *Escherichia coli*, the total concentration of protein and RNA amounts to about 340 g/l (Zimmerman and Minton, 1993). This would make any effective metabolism difficult if the enzymes would just be expressed and localized without any organization. Indeed, a first level of such organization was discovered with the detection of co-ordinated expression of the genes encoding the enzymes of one specific pathway. While this has long been realized for specific biosynthetic or degradative pathways, the regulation of the central metabolic pathways such as glycolysis and the tricarboxylic acid (TCA) cycle has become a subject of intensive investigation only in the last few years. Similarly, early studies suggested that enzymes of specific pathways might form complexes (termed metabolon) in which the substrates and intermediates escape free diffusion resulting in higher efficiency of the pathways (Srere, 1987). Such complexes were observed or suggested for tryptophan biosynthesis in *E. coli* and for glycolysis in *E. coli*, *Bacillus subtilis* and eukaryotic cells (Yanofsky and Rachmeler, 1958; Mowbray and Moses, 1976; Commichau *et al*., 2009; Campanella *et al*., 2005). However, the relevance of the formation of such complexes was shown only recently for purine biosynthesis and branched-chain amino acid catabolism in human cells (An *et al*., 2008; Islam *et al*., 2007). Moreover, a recent in silico study supports the idea that glycolytic flux is much more efficient if the enzymes form a complex as compared to free floating enzymes (Amar *et al*., 2008). Unfortunately, these metabolons tend to escape their discovery in high-throughput analyses; because of their fragility (Williamson and Sutcliffe, 2010).

We are interested in basic metabolism and its control in the Gram-positive model bacterium *B. subtilis*. These bacteria are of great importance for a variety of biotechnological applications including the technical production of vitamins and of enzymes for laundry detergents. *B. subtilis* uses glucose and malate as the preferred sources of carbon and energy (Stülke and Hillen, 2000; Kleijn *et al*., 2010). Glucose is metabolized via glycolysis, the pentose phosphate pathway and the TCA cycle, and malate is directly introduced into the TCA cycle and glucose is synthesized via gluconeogenesis.

As most glycolytic enzymes are also required for gluconeogenesis, these enzymes must be constitutively synthesized. Indeed, only the genes for those enzymes that catalyze irreversible glycolytic reactions are specifically induced in the presence of glycolytically catabolized sugars in *B. subtilis* (Fillinger *et al*., 2000; Ludwig *et al*., 2001). On the other hand,

the gluconeogenic enzymes phosphoenolpyruvate (PEP) carboxykinase and the NADP-dependent glyceraldehyde-3-phosphate dehydrogenase encoded by the pckA and gapB genes, respectively, are repressed by glucose and are only expressed if TCA cycle intermediates serve as the only carbon source (Blencke *et al*., 2003; Servant *et al*., 2005). The genes for the pentose phosphate pathway are constitutively expressed (Blencke *et al*., 2003).

The TCA cycle is the central hub in metabolism in most heterotrophic organisms from bacteria such as *B. subtilis* and *E. coli* to eukaryotes such as yeast and man. It serves to generate reducing power for respiration and for the supply of precursors for many important metabolites including amino acids and vitamins. In *B. subtilis*, the expression of the initial enzymes of the cycle, citrate synthase and aconitase encoded by *citZ* and *citB*, respectively, is synergistically repressed by glucose and glutamate (Jourlin-Castelli *et al*., 2000). The other enzymes are required under all conditions for anabolic purposes and are therefore always expressed (Sonenshein, 2007). In addition to regulation at the level of gene expression, many TCA cycle enzymes are subject to post-translational modification by protein phosphorylation (Macek *et al*., 2007; Eymann *et al*., 2007).

The possible interactions between metabolic enzymes in *B. subtilis* have so far only poorly been studied. Recently, interactions among glycolytic enzymes were detected (Commichau *et al*., 2009). In this study, we addressed the possible interactions between enzymes of the TCA cycle in *B. subtilis*. These protein-protein interactions were detected by the purification of cross-linked protein complexes and by an unbiased bacterial two-hybrid system. The use of a cross-linker in the purification of proteins facilitates the isolation of fragile complexes that are otherwise difficult to detect (Williamson and Sutcliffe, 2010). Our results suggest the formation of a complex of TCA cycle enzymes, the TCA cycle metabolon. Moreover, we demonstrate that in vivo interactions between enzymes are controlled by the metabolic flux.

Materials and methods

Bacterial strains and growth conditions - All *B. subtilis* strains are listed in Table 8.3. They are derived from the laboratory wild type strain 168. Deletion of the *mdh* and *citG* genes was achieved by transformation with PCR products constructed using oligonucleotides to amplify DNA fragments flanking the target genes and an intervening spectinomycin resistance cassette from plasmid pDG1726 (Guérout-Fleury *et al*., 1995) as described previously (Wach, 1996). *E. coli* DH5a, XL1-Blue and BTH101 (Sambrook *et al*., 1989; Karimova *et al*., 1998) were used for

cloning experiments and bacterial two-hybrid (B2H) analyses, respectively. *B. subtilis* was grown in C minimal medium containing ammonium as basic source of nitrogen (Blencke *et al*., 2006). C-malate is C medium containing malate (0.5%, w/v) as the carbon source. The medium was supplemented with auxotrophic requirements (at 50 mg/l). *E. coli* was grown in LB medium. LB, SP and C medium plates were prepared by the addition of 17 g Bacto agar/l (Difco) to LB, SP or C medium, respectively.

DNA manipulation and transformation - Transformation of *E. coli* and plasmid DNA extraction were performed using standard procedures and transformants were selected on LB plates containing ampicillin (100 mg/ml) or kanamycin (50 mg/ml) (Sambrook *et al*., 1989). Restriction enzymes, T4 DNA ligase and DNA polymerases were used as recommended by the manufacturers. DNA fragments were purified from agarose gels using the QIAquick PCR purification kit (Qiagen, Germany). Phusion DNA polymerase was used for the polymerase chain reaction as recommended by the manufacturer. All primer sequences are provided as supplementary material (Table 8.1). DNA sequences were determined using the dideoxy chain termination method (Sambrook *et al*., 1989). All plasmid inserts derived from PCR products were verified by DNA sequencing. Chromosomal DNA of *B. subtilis* was isolated as described (Kunst and Rapoport, 1995).

B. subtilis was transformed with plasmid or chromosomal DNA according to the two-step protocol described previously (Kunst and Rapoport, 1995). Transformants were selected on SP plates containing chloramphenicol (Cm 5 mg/ml), kanamycin (Km 10 mg/ml), spectinomycin (Spc 150 mg/ml), or erythromycin plus lincomycin (Em 2 mg/ml and Lin 10 mg/ml).

Western blotting - For Western blot analysis, proteins were separated by 12.5% SDS-PAGE and transferred onto polyvinylidene difluoride (PVDF) membranes (Bio-Rad) by electroblotting. Rabbit anti-FLAG polyclonal antibodies (Sigma-Aldrich; 1:10,000), anti-CitZ (1:4000) (Jin and Sonenshein, 1996), and anti-CitB (1:1000) (Nakano *et al*., 1998), anti-Icd (1:10,000) (Nakano *et al*., 1998), anti-HPr (1:10,000) (Monedero *et al*., 2001) served as primary antibodies. The antibodies were visualized by using anti-rabbit immunoglobulin G-alkaline phosphatase secondary antibodies (Promega) and the CDP-Star detection system (Roche Diagnostics), as described previously (Commichau *et al*., 2007b).

B2H assay - Primary protein-protein interactions were identified by bacterial two-hybrid (B2H) analysis (Karimova *et al*., 1998). The B2H system is based on the interaction-mediated reconstruction of adenylate cyclase (CyaA) activity from *Bordetella pertussis* in *E. coli*. The CyaA enzyme consists of two complementary fragments T18 and T25 that are not active when

physically separated. Fusion of these fragments to interacting proteins results in functional complementation between the T18 and T25 fragments and the synthesis of cAMP. cAMP production can be monitored by measuring the β-galactosidase activity of the cAMP-CAP dependent promoter of the *E. coli lac* operon. Thus, a high β-galactosidase activity reflects the interaction between the hybrid proteins. Plasmids pUT18 and p25-N allow the expression of proteins fused to the N-terminus of the T18 and T25 fragments of the CyaA protein, respectively, and the plasmids pUT18C and pKT25 allow the expression of proteins fused to the C-terminus of the T18 and T25 fragments of the CyaA protein, respectively (Karimova *et al*., 1998; Claessen *et al*., 2008). The plasmids pKT25-zip and pUT18C-zip served as positive controls for complementation. These plasmids express T18-zip and T25-zip fusion proteins that can associate due to the leucine zipper motifs resulting in an active CyaA enzyme and a high β-galactosidase activity. DNA fragments corresponding to the TCA cycle genes were obtained by PCR (for primers, see Table 8.1). The PCR products were cloned into the four vectors of the two-hybrid system. The resulting plasmids (Table 8.2) were used for cotransformations of *E. coli* BTH101 and the protein-protein interactions were then analyzed by plating the cells on LB plates containing ampicillin (100 mg/ml), kanamycin (50 mg/ml), X-Gal (40 mg/ml) (5-bromo-4-chloro-3-indolyl-b-D-galactopyranoside) and IPTG (0.5mM) (isopropyl-b-D-thiogalactopyranoside), respectively. The plates were incubated for a maximum of 48 h at 30°C.

In vivo detection of protein-protein interactions - The isolation of protein complexes from *B. subtilis* cells was performed by the SPINE technology (Herzberg *et al*., 2007). To express enzymes of the TCA cycle fused to a N-terminal Strep-tag, they were amplified (for primers see Table 8.1) and the resulting PCR products cloned into the expression vector pGP380. The PCR products were digested with *Bam*HI and *Sal*I and ligated to vector pGP380 (Herzberg *et al*., 2007). The resulting plasmids are pGP1119 (*gltB*), pGP1120 (*citZ*), pGP1121 (*icd*), pGP122 (*citG*), pGP1123 (*mdh*), pGP1145 (*odhB*), and pGP1753 (*pckA*) (for details see Table 8.2).

To facilitate the detection of Mdh, PckA and YtsJ by Western blot analysis, we fused these proteins to a C-terminal triple FLAG-tag using plasmid pGP1331 (Lehnik-Habrink *et al*., 2010). Briefly, fragments of the *mdh*, *pckA* and *ytsJ* genes were amplified by PCR (for primers see Table 8.1) and cloned into pGP1331. The resulting plasmids were pGP1751 (*pckA*), pGP1752 (*mdh*) and pGP1758 (*ytsJ*) (for details see Table 8.2). These plasmids were used to transform *B. subtilis* 168 in order to introduce the fusions into the chromosome. The designations of the resulting strains are listed in Table 8.3.

For cultivation one liter culture was inoculated to an OD_{600} of 0.1 with an overnight culture. This culture was grown at 37°C until OD_{600} 0.9-1.0 and divided. One half was harvested immediately, and the other was treated with formaldehyde (0.6% w/v, 20 min) to facilitate the cross-linking (Herzberg *et al*., 2007). After cross-linking, the cells were also harvested and washed with a buffer containing 50 mM Tris-HCl (pH 7.5) and 200 mM NaCl. The pellets were lysed using a French press (20,000 p.s.i., 138,000 kPa; Spectronic Instruments, UK). After lysis the crude extracts were centrifuged at 100,000g for 1 h. For purification of the Strep-tagged proteins the resulting supernatants were passed over a Streptactin column (IBA, Göttingen, Germany) (0.5 ml bed volume). The recombinant proteins were eluted with desthiobiotin (IBA, Göttingen, Germany, final concentration 2.5 mM). Aliquots of the different fractions were subjected to SDS-PAGE. Prior to electrophoresis, the protein samples were boiled for 20 min in Laemmli buffer to reverse the cross-links. As a control, the *B. subtilis* strain carrying the empty vector pGP380 was used.

Protein identification by mass spectrometry - Silver nitrate stained gel slices were destained by incubation in 30 mM $K_3[Fe(CN)_6]$/100 mM $Na_2S_2O_3$ until colorless and washed three times in water before processing of gel slices as previously described Commichau *et al*., 2009. Briefly, gel pieces were washed twice with 200 ml 20 mM NH_4HCO_3/50% (v/v) acetonitrile (ACN) for 30 min, at 37°C and dried by adding 200 ml ACN two times for 15 min. Trypsin solution (10 ng/ml trypsin in 20 mM ammonium bicarbonate) was added until gel pieces stopped swelling and digestion was allowed to proceed for 16-18 h at 37°C. Peptides were extracted from gel pieces by incubation in an ultrasonic bath for 30 min in 40 ml 0.1% (v/v) acetic acid followed by a second extraction with 40 ml 50% ACN in 0.05% acetic acid. The supernatants containing peptides were collected, combined, ACN depleted by evaporation, and transferred into microvials for mass spectrometric analysis. Peptides were separated by a nonlinear water-acetonitrile gradient in 0.1% acetic acid on a PepMap reverse phase column (75-µm I.D. x 150 mm, LC Packings, Idstein, Germany) with a MDLC nano-HPLC (GE Healthcare, Freiburg, Germany) coupled on-line with a LTQ-Orbitrap mass spectrometer (Thermo Electron, Bremen) operated in data-dependent MS/MS mode. Proteins were identified by searching all MS/MS spectra in .dta format against a *B. subtilis* protein database (4106 entries, extracted from SubtiList (genolist.pasteur.fr/SubtiList/) using SEQUEST (Bioworks 3.2/Sequest v. 2.7 rev. 11, Thermo Electron) on an IBM cluster with eight dual nodes. Initial mass tolerance for peptide identification on MS and MS/MS peaks were 10 ppm and 1 Da, respectively. Up to two missed tryptic cleavages were allowed. Methionine oxidation (+15.99492 Da) and propionamide

modification on cysteine (+71.037109 Da) were set as variable modifications. Protein identification results were evaluated by determination of probability for peptide and protein assignments provided by PeptideProphet and ProteinProphet (ISI Seattle, WA, USA) incorporated in the Scaffold software package rel. 2.01 (Proteome Software, Portland, OR, USA). Proteins were identified by at least two peptides with peptide probability >90% reflecting protein probability of >99%. Annotation information was derived from the SubtiWiki web server (Lammers *et al*., 2010).

Assay of isocitrate dehydrogenase activity - For the determination of plasmid-borne isocitrate dehydrogenase activity, *B. subtilis* 168 carrying plasmid pGP1121 was grown in C-malate medium, and the Strep-tagged enzyme was purified as described above. The isocitrate dehydrogenase activity was determined by a photometric assay of $NADPH_2$ formation in assay buffer (200 mM Tris-Cl (pH 8.5), 1 mM $MgCl_2$, 144 µM $NADP^+$, and 230 µM isocitrate).

Results

Expression and functional analysis of TCA cycle enzymes carrying a N-terminal Strep-tag - In order to identify potential interactions between the enzymes of the TCA cycle and of closely related pathways (gluconeogenesis and glutamate synthesis), we attempted to use the SPINE technology, i.e. purification of proteins of interest cross-linked to their interaction partners (Herzberg *et al*., 2007). This requires cloning of the bait proteins to allow their expression with a Strep-tag. We chose to perform this experiment with citrate synthase (encoded by *citZ*), isocitrate dehydrogenase (*icd*), the E2 subunit of 2-oxoglutarate dehydrogenase (*odhB*), fumarase (*citG*), and malate dehydrogenase (*mdh*). These enzymes represent the different parts of the TCA cycle and they are in a size range that allows easy purification. In addition, we used the small subunit of the glutamate synthase, *GltB*. This enzyme provides the major link between carbon catabolism and anabolism in *B. subtilis* (Commichau *et al*., 2006), and it uses the TCA cycle intermediate 2-oxoglutarate as the substrate.

The genes encoding the enzymes mentioned above were all cloned into the expression vector pGP380 thereby creating proteins fused to a N-terminal Strep-tag. The functional activity of these fusion proteins was tested for GltB, CitG, Mdh and Icd. The activity of Strep-GltB (encoded on plasmid pGP1119) was assayed by complementation of the glutamate auxotrophy of the gltB mutant strain GP717. The activities of Strep-CitG and Strep-Mdh (pGP1122 and pGP1123) were tested by complementation of the growth defect of the corresponding *citG* and

mdh mutant strains (GP718 and GP719, respectively) on C minimal medium with glucose as the single carbon source. A complementation test was not possible for the isocitrate dehydrogenase since *icd* mutants tend to accumulate secondary *citZ* mutations (Matsuno *et al*., 1999). Therefore, the Strep-tagged enzyme was purified from *B. subtilis* 168/ pGP1121, and its biochemical activity verified (data not shown).

Purification of complexes of TCA cycle enzymes with their potential interaction partners - The purification of protein complexes is only possible if the cells are grown under conditions that allow expression of the candidate proteins. As we expected interactions of TCA cycle enzymes with other enzymes of the cycle, the SPINE experiments had to be performed under conditions that allow maximal expression of these enzymes. The expression of the genes coding for the initial enzymes of the TCA cycle (*citZ*, *citB*) is synergistically repressed by glucose and glutamate (Jourlin-Castelli *et al*., 2000). To identify suitable conditions, we determined the activity of the *citB* promoter in the presence of different TCA cycle substrates with or without glucose. For this purpose, we studied the β-galactosidase activity driven by a fusion of the *citB* promoter to a promoterless *lacZ* gene present in *B. subtilis* GP205. Our results indicate that C medium with malate and ammonium as the single carbon and nitrogen sources, respectively, allows both rapid growth of the bacteria and a high expression of the *citB* gene (data not shown). Therefore, this medium was chosen for the SPINE experiments.

To obtain a snapshot of in vivo interactions, protein complexes were cross-linked by formaldehyde, purified by affinity chromatography and the cross-links were broken. Finally, the proteins were analyzed by SDS-PAGE and the interaction partners were identified by mass spectrometry. Those potential interaction partners that were detected with ten or more peptides or with at least 25% sequence coverage were regarded as significant in this study.

This procedure was performed for the five selected TCA cycle enzymes and for the small subunit of the glutamate synthase. As an example, Fig. 2.1 shows the purification of isocitrate dehydrogenase (Icd) with its potential interaction partners. As can be seen, the application of the purification scheme to a control strain carrying the empty vector pGP380 revealed appreciable purification of one protein, which was identified as pyruvate carboxylase (PycA), a biotin-containing protein that has an intrinsic affinity to the Streptactin purification matrix. In contrast, several distinct bands in addition to the bait protein (Strep-Icd) and PycA were observed in the strain carrying the expression vector pGP1121. These bands were identified as Icd, citrate synthase (CitZ), and a subunit of the succinyl-CoA synthetase (SucC).

For citrate synthase (CitZ) we identified 114 proteins that were cross-linked and co-purified with the bait. However, many of these potential interaction partners were identified only with a few peptides. 20 potential interaction partners, among them isocitrate dehydrogenase exceeded the threshold of ten peptides (see Table 2.1). For isocitrate dehydrogenase (Icd), 34 proteins were co-purified with the bait, and nine of these proteins, among them CitZ and a subunit of the succinyl-CoA synthetase (SucC) (see Fig. 2.1), were above the threshold. For the E2 subunit of 2-oxoglutarate dehydrogenase (OdhB), 33 potentially interacting proteins were identified, and seven of these proteins exceeded the cut-off. As expected, the E1 subunit of 2-oxoglutarate dehydrogenase (OdhA) and the shared E3 subunit of the pyruvate/2-oxoglutarate dehydrogenase (PdhD) were among the prominent interaction partners, however PdhD was slightly below the threshold (seven peptides/20.6% sequence coverage). 56 proteins that were co-purified with fumarase (CitG) were identified. Eight of these proteins including citrate synthase (CitZ), aconitase (CitB), and isocitrate dehydrogenase (Icd) were present in sufficient amounts to exceed the cut-off. Finally, 152 different proteins were co-purified with malate dehydrogenase (Mdh). It has been observed in a previous study that some proteins such as enolase and phosphoglycerate kinase tend to interact with a huge number of other proteins (Commichau *et al*., 2009). Mdh seems to be a member of this group. Applying the threshold of ten identified peptides or 25% sequence coverage, Mdh does still interact with 31 proteins. These include isocitrate dehydrogenase, the beta subunit of the succinyl-CoA synthetase (SucC), the gluconeogenic enzyme PEP carboxykinase (see below), and an uncharacterized putative beta-hydroxyacid dehydrogenase (YkwC). For the small subunit of glutamate synthase (GltB), 57 potential partners were identified, six of which met the criterion of being significant. As expected, GltB interacts with its corresponding large subunit, GltA, and in addition, interaction with malate dehydrogenase was observed.

The protein identification of the SPINE experiments was based on the determination of the specific proteins in excised bands. It is, however, possible, that some interaction partners were not present in prominent bands and did therefore escape our analysis. To address this problem, the SPINE experiments were repeated and the presence of citrate synthase, aconitase and isocitrate dehydrogenase was assayed using monoclonal antibodies specific for these proteins. The results of these experiments are shown in Fig. 2.2. They are in perfect agreement with the original SPINE results. The interactions of isocitrate dehydrogenase with citrate synthase, fumarase and malate dehydrogenase as well as that between citrate synthase and fumarase were detected both in the unbiased protein identification and in the Western blot

analysis. Moreover, the Western blot experiments revealed interactions of malate dehydrogenase with citrate synthase and aconitase and of isocitrate dehydrogenase with OdhB and GltB (see Fig. 2.2).

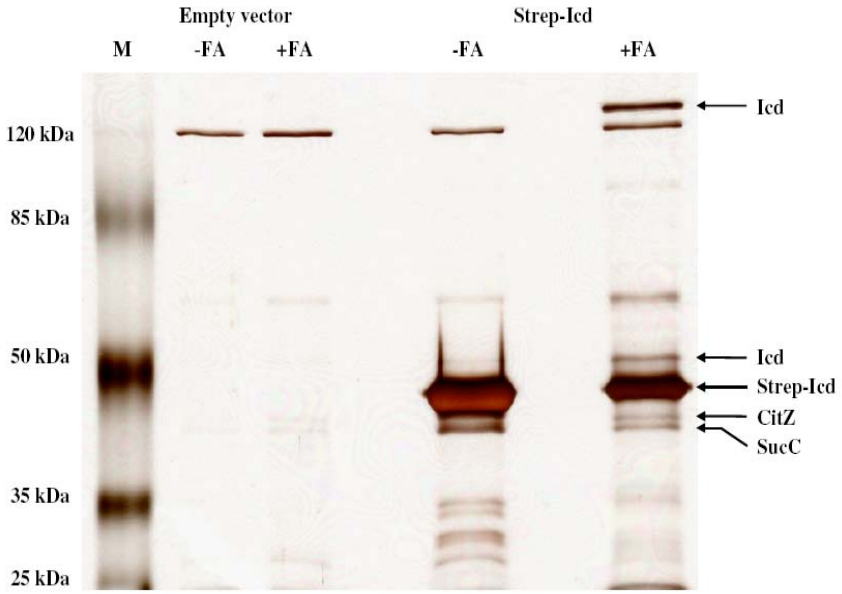

Fig. 2.1. Identification of potential interaction partners of isocitrate dehydrogenase. The protein complex was isolated from *B. subtilis* carrying either pGP380 (empty vector) or pGP1121 (expressing Icd). All strains were grown in C-malate medium. 15 ml of the elution fractions from each purification without (-FA) or with (+FA) cross-linking by formaldehyde were analyzed by 12.5% SDS-PAGE. Protein bands were visualized by silver staining. M, protein molecular mass marker (Fermentas).

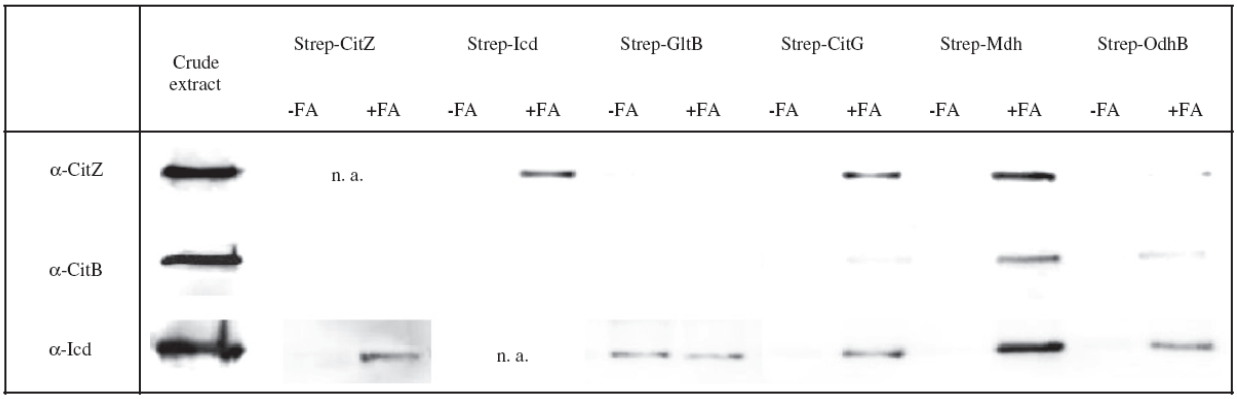

Fig. 2.2. Detection of in vivo interactions between TCA cycle enzymes by Western blot analysis. The protein complexes were isolated from *B. subtilis* 168 carrying expression plasmids for the respective Strep-tagged TCA cycle enzyme. All strains were grown in C-malate medium. 15 ml of the elution fractions from each purification without (-FA) or with (+FA) cross-linking by formaldehyde were analyzed by 12.5% SDS-PAGE. After electrophoresis and blotting onto a PVDF membrane, interaction partners were detected by antibodies raised against CitZ, CitB and Icd. n.a., not analyzed.

Table 2.1. Interaction partners of TCA cycle enzymes.

Bait	Interaction partner	Function	No. of peptides	SC (%)
CitZ	CitZ	Citrate synthase	21	48.90
	Icd	Isocitrate dehydrogenase	16	46.30
	FbaA	Fructose-1,6-bisphosphate aldolase	9	33.00
	Eno	Enolase	6	28.80
Icd	Icd	Isocitrate dehydrogenase	36	66.40
	SucC	Succinyl-CoA synthetase (beta subunit)	14	39.20
	CitZ	Citrate synthase	8	27.40
	PdhA[a]	Pyruvate dehydrogenase (E1 alpha subunit)	8	22.90
OdhB	OdhA	2-Oxoglutarate dehydrogenase (E1 subunit)	33	38.20
	PdhB	Pyruvate dehydrogenase (E1 beta subunit)	12	50.20
	PdhD[a]	Pyruvate / 2-Oxoglutarate dehydrogenase (E3 subunit)	7	20.60
	Pyk[a]	Pyruvate kinase	5	21.50
	Icd	Isocitrate dehydrogenase	Western blot	
CitG	Icd	Isocitrate dehydrogenase	24	58.20
	CitG	Fumarate hydratase	23	41.80
	CitB	Aconitate hydratase	22	30.60
	SucC[a]	Succinyl-CoA synthetase (beta subunit)	8	22.30
	CitZ	Citrate synthase	7	29.60
	AspB	Aspartate aminotransferase	7	26.70
Mdh	Mdh	Malate dehydrogenase	22	61.50
	Icd	Isocitrate dehydrogenase	15	39.50
	PckA	Phosphoenolpyruvate carboxykinase	11	23.10
	SucC	Succinyl-CoA synthetase (beta subunit)	9	27.80
	Pgi	Glucose-6-phosphate isomerase	9	28.40
	FbaA	Fructose-1,6-bisphosphate aldolase	9	30.90
	Ndh[a]	NADH dehydrogenase	7	22.70
	YkwC	Putative beta-hydroxyacid dehydrogenase	5	25.70
	CitZ	Citrate synthase	Western blot	
	CitB	Aconitase	Western blot	
GltB	GltA	Glutamate synthase (large subunit)	23	18.40
	Mdh	Malate dehydrogenase	14	52.90
	SucC[a]	Succinyl-CoA synthetase (beta subunit)	9	21.80
	Ndh[a]	NADH dehydrogenase	7	21.70
	Icd	Isocitrate dehydrogenase	Western blot	

[a] These proteins did not meet the cut-off criterion used in this study (>10 peptides identified or >25% sequence coverage). However, they are part of the TCA cycle or closely related and they were identified with sequence coverage of at least 20%. Therefore they might be relevant.

Interestingly, isocitrate dehydrogenase was co-purified with the small subunit of glutamate synthase even in the absence of the cross-linker suggesting a strong interaction. Thus, both the biased and the unbiased SPINE experiments are in good support of the idea of interactions between the enzymes of the TCA cycle and the adjacent reactions such as glutamate biosynthesis or phosphoenolpyruvate replenishment.

Analysis of binary interactions between all enzymes of the TCA cycle - The SPINE approach is highly efficient to isolate protein complexes but it does not allow determining the primary interactions in a protein complex that is composed of more than two partners. Moreover, it is well established that each individual method to study protein-protein interactions can detect only about one third of the actual interactions (Braun *et al*., 2009). Therefore, an alternative screen for interactions between the enzymes of the TCA cycle was required. For this purpose, we used the bacterial two-hybrid (B2H) system to exhaustively analyze the primary protein-protein interactions among the TCA cycle enzymes. In the B2H system, the T25 and the T18 fragments of the catalytic domain of the *B. pertussis* adenylate cyclase were fused to full-length copies of all enzymes of the TCA cycle and adjacent reactions. The leucine zipper of the yeast GCN4 transcription factor served as a control (Karimova *et al*., 1998). As an example, selected results of the B2H analysis are shown in Fig. 2.3.

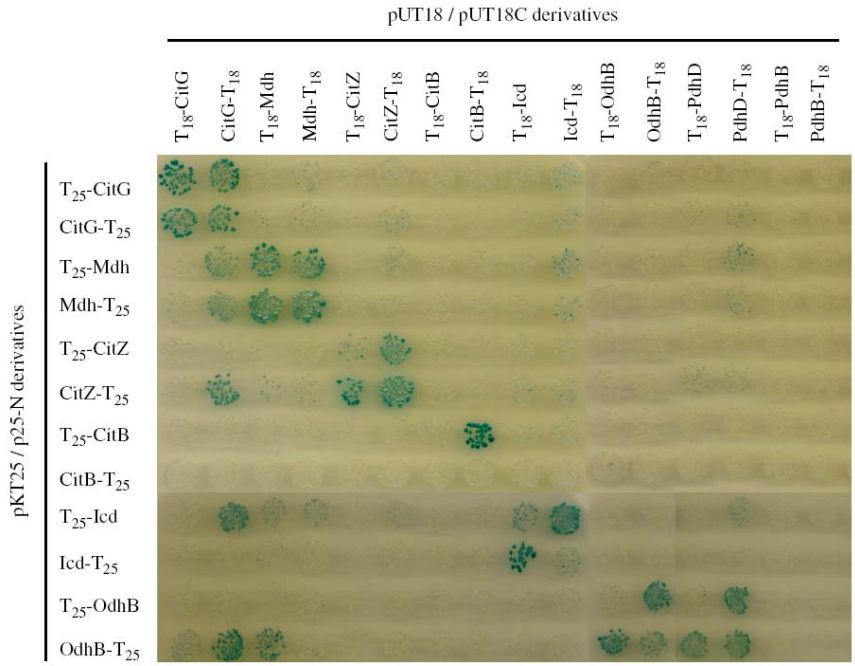

Fig. 2.3. Bacterial two-hybrid analysis to identify primary interactions among the enzymes of the TCA cycle of *B. subtilis*. All genes were cloned into the plasmids pUT18, pUT18C, p25-N and pKT25. Plasmids pUT18 and pUT18C allow the expression of the selected enzymes fused either to the N- or C-terminus of the T18 domain of the *B. pertussis* adenylate cyclase, respectively. Plasmids p25-N and pKT25 allow the expression of the selected enzymes fused either to the N- or C-terminus of the T25 domain of the adenylate cyclase, respectively. The *E. coli* transformants were incubated for 48 h at 30°C. Degradation of X-Gal (blue color) indicates the presence of a functional adenylate cyclase owing to the interaction of the two proteins of interest. CitG, fumarase; Mdh, malate dehydrogenase; CitZ, citrate synthase; CitB, aconitase; Icd, isocitrate dehydrogenase; OdhB, E2 subunit of 2-oxoglutarate dehydrogenase.

The results are summarized in Table 2.2. As expected, the leucine zipper of GCN4 showed strong self-interaction (data not shown). Many enzymes gave positive signals for self-interaction. This observation corresponds to the formation of dimers (or larger oligomers) and is in excellent agreement with the results of the SPINE assay: Self-interactions were detected for CitZ, Icd, CitG and Mdh with both methods whereas neither method revealed indications for self-interaction of OdhB and GltB. Similarly, the B2H analysis confirmed the interactions between citrate synthase and fumarase, between isocitrate dehydrogenase and fumarase, between the E2 subunit of 2-oxoglutarate dehydrogenase and the corresponding E1 subunit (OdhA) and the common E3 subunit of pyruvate/2-oxoglutarate dehydrogenase (PdhD), and between the beta subunit of succinyl-CoA synthetase and malate dehydrogenase (see Fig. 2. 3, Table 2.2).

Table 2.2. Binary interactions of TCA cycle enzymes based on the bacterial two-hybrid system analysis.

Protein	Self-interaction	Interaction partners
CitZ	CitZ	CitG
CitB	CitB	-
Icd	Icd	CitG
OdhA	-	OdhB
OdhB	OdhB	OdhA, CitG, PdhD
PdhD	PdhD	OdhB, PdhC
SucC	SucC	SucD, Mdh
SucD	-	SucC
SdhA	-	-
SdhB	SdhB	-
SdhC	-	-
CitG	CitG	CitZ, Icd, OdhB, Mdh, PckA
Mdh	Mdh	SucC, CitG,
PckA	PckA	CitG
PdhA	PdhA	PdhB
PdhB	PdhB	PdhA
PdhC	-	PdhD
GltA	-	-
GltB	-	-

All these interactions were also detected by the SPINE analysis. In addition, the two-hybrid assays revealed the potential of several other pairs of TCA cycle enzymes to interact physically (see Table 2.2). These include known interactions as those among the subunits of the pyruvate and 2-oxoglutarate dehydrogenases or the succinyl-CoA synthetase. Moreover, previously undetected interactions were observed in the two-hybrid screens such as the interaction between fumarase and malate dehydrogenase that catalyze sequential reactions.

Taken together, the B2H experiments confirm the ability of the TCA cycle enzymes to interact physically observed by the SPINE approach.

A core complex of the TCA cycle metabolon - The data presented above suggest that the three enzymes citrate synthase, isocitrate dehydrogenase and malate dehydrogenase might form the core of the TCA cycle metabolon (Fig. 2.4A). However, each experiment did only detect binary interactions. Thus, the question whether all three proteins interact simultaneously required an answer. For this purpose, we performed SPINE experiments using either of the three enzymes as the bait. Then, the co-purification of the other two proteins was assayed by Western blot analyses using the antibodies directed against citrate synthase or isocitrate dehydrogenase. To detect the malate dehydrogenase we constructed a strain (GP1130) that expressed Mdh fused to a C-terminal triple FLAG-tag. This experimental setup allowed us to express and purify one enzyme carrying a Strep-tag, and to assay the presence of the two other proteins in the eluate. As shown in Fig. 2.5, each of the three proteins was co-purified with both partners simultaneously. The constitutively expressed HPr protein of the phosphotransferase system served as a control. This protein was present in the crude extract in each experiment, however, it was never co-purified with one of the three enzymes of the TCA cycle metabolon. Thus, the detected interactions are specific. For the SPINE experiment with Mdh, we did also perform a Western blot of the eluate with the antibodies raised against citrate synthase and isocitrate dehydrogenase at the same time. As shown in Fig. 2.5C, both proteins were detected. Taken together, the results provide strong evidence for the formation of a complex between citrate synthase, isocitrate dehydrogenase and malate dehydrogenase.

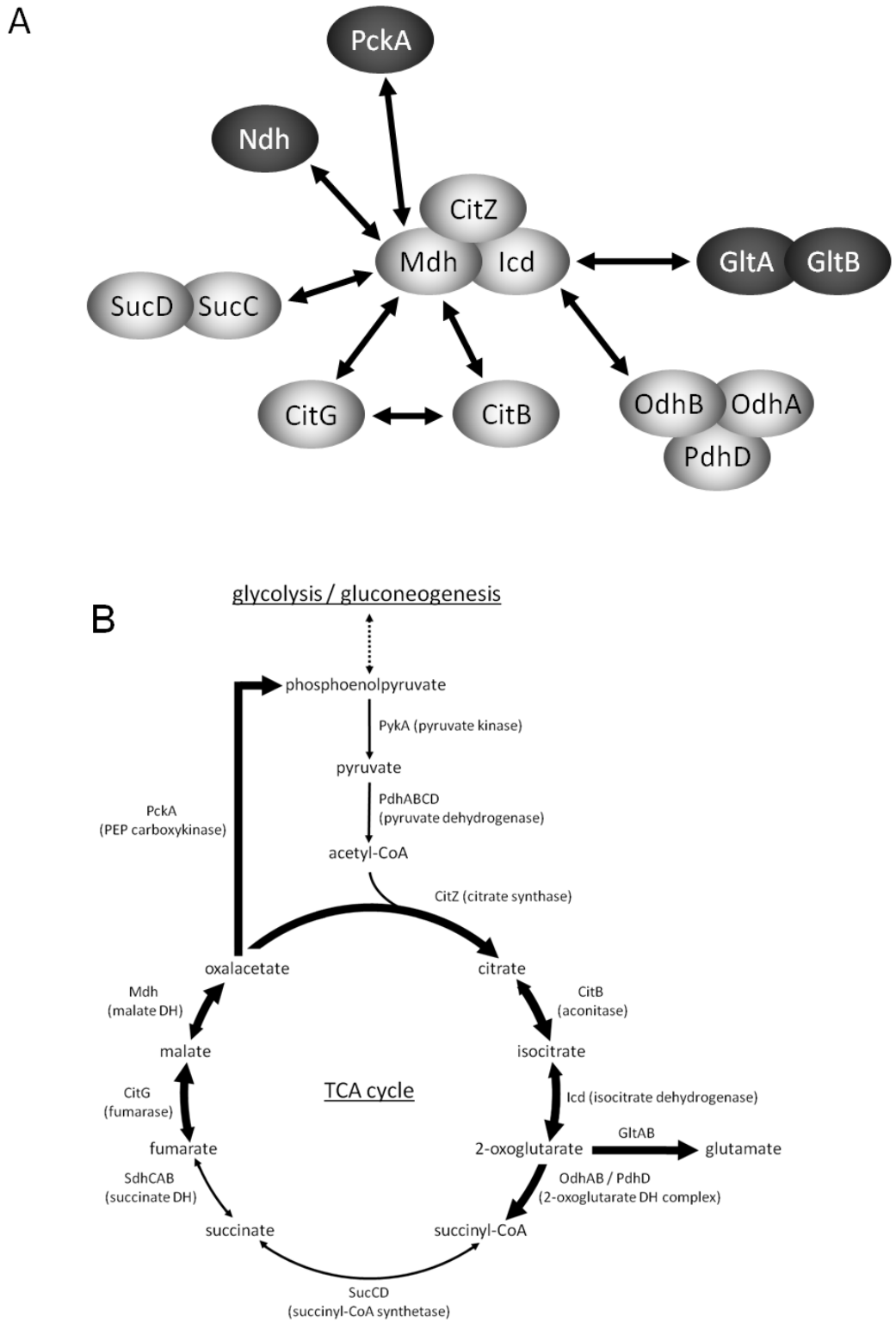

Fig. 2.4. Interactions between TCA cycle enzymes and their potential impact on the metabolic flux. (A) Summary of the observed interactions between enzymes of the TCA cycle (light gray symbols) and enzymes of associated pathways (dark gray symbols). (B) The TCA cycle and associated pathways in *B. subtilis*. Reactions that might profit from the observed protein-protein interactions are labeled by bold arrows. GltAB: glutamate synthase; DH: dehydrogenase.

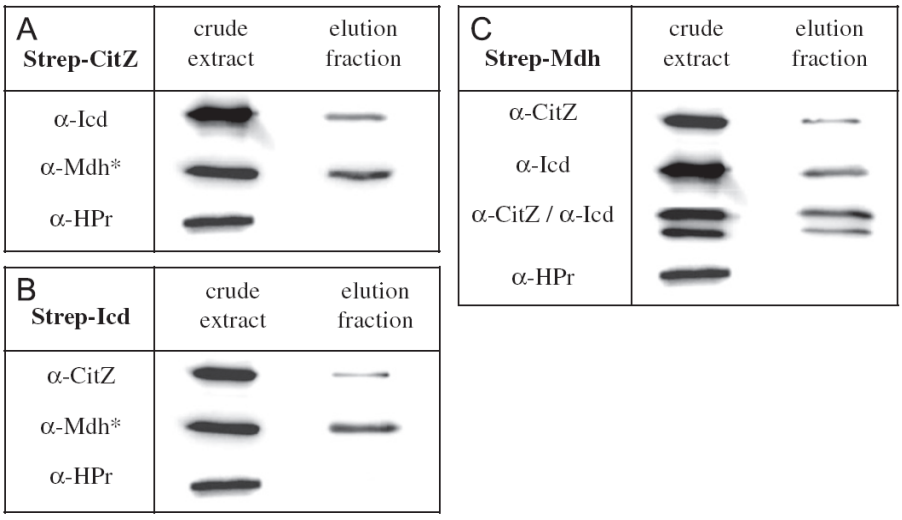

Fig. 2.5. Evidence for a complex of citrate synthase, isocitrate dehydrogenase and malate dehydrogenase. The protein complex was isolated after cross-linking with formaldehyde from *B. subtilis* GP1130 carrying pGP1120 (expressing Strep-CitZ; A) or carrying pGP1121 (expressing Strep-Icd; B) and from *B. subtilis* 168 carrying pGP1123 (expressing Strep-Mdh; C). All strains were grown in C-malate medium. In total 15 ml of the elution fractions of each purification were analyzed by 12.5% SDS-PAGE. After electrophoresis and blotting onto a PVDF membrane, interaction partners were detected in the crude extracts and in the protein eluates by antibodies raised against citrate synthase, isocitrate dehydrogenase and malate dehydrogenase * (*antibody raised against the FLAG-tag). HPr served as a negative control.

The interaction between malate dehydrogenase and phosphoenolpyruvate carboxykinase - All SPINE experiments described so far were performed under gluconeogenic conditions in medium with malate as the single carbon source. Growth with malate as the only carbon source requires a strong flux of carbon via malate dehydrogenase and phosphoenolpyruvate (PEP) carboxykinase (PckA) to feed the gluconeogenesis (Kleijn *et al*., 2010). Therefore, the observed interaction between Mdh and PckA might be relevant to achieve an efficient metabolism under these conditions.

To facilitate the detection of the interaction between these proteins, we used strains that expressed Mdh and PckA fused to a C-terminal triple FLAG-tag. These strains, GP1129 and GP1130 were transformed with plasmids expressing the Strep-tagged variant of the presumptive interaction partner. GP1131 that expressed the malic enzyme YtsJ fused to a triple FLAG-tag served as control. These strains were grown in C minimal medium with malate as the only carbon source and the respective Strep-tagged proteins were purified with their interaction partners. As shown in Fig. 2.6, the FLAG-tagged proteins were expressed under our

experimental conditions as judged from the Western blot signals obtained with the crude extracts. In excellent agreement with the original SPINE experiment, a reciprocal interaction between Mdh and PckA was detected; i.e. the interacting protein was present both with Mdh or PckA as the bait in the experiment. In contrast, neither protein interacted with the FLAG-tagged malic enzyme YtsJ (see Fig. 2.6). Thus the assay was specific and the interaction signals did not result from an artificial binding to the FLAG-tag. Next, we asked whether Mdh and PckA would also interact under glycolytic conditions, i.e. upon reversal of the carbon flow. Since the chromosomal copy of pckA is not transcribed under such conditions (Blencke *et al*., 2003; Servant *et al*., 2005), we addressed this question using plasmid-borne PckA-Strep in a strain expressing the malate dehydrogenase fused to a triple FLAG-tag (GP1130) from its own constitutive promoter (Jin and Sonenshein, 1994). As shown in Fig. 2.7, Mdh was present in similar amounts in the crude extract both under gluconeogenic and under glycolytic conditions. As observed before, FLAG-tagged Mdh was co-purified with PckA from cells grown in the absence of glucose. This interaction seems to be rather strong since its detection did not require cross-linking of interacting proteins. Under glycolytic conditions, PckA was purified and Mdh was present in the bacteria, however, no interaction between the two proteins was detectable even after the addition of formaldehyde to stabilize weak interactions. This observation strongly suggests that the interaction between malate dehydrogenase and PEP carboxykinase takes place only under gluconeogenic conditions when the sequential activity of the two proteins is required.

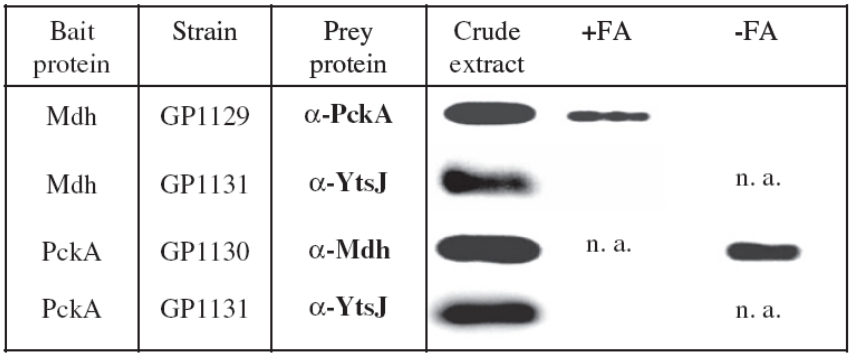

Fig. 2.6. Confirmation of the *in vivo* interaction between malate dehydrogenase and phosphoenolpyruvate carboxykinase. Strains expressing the prey proteins fused to a C-terminal triple FLAG-tag (to facilitate detection of the proteins) were transformed with plasmids expressing the Strep-tagged bait proteins Mdh or PckA (to facilitate complex purification). FLAG-tagged YtsJ served as a negative control. Bacteria were grown in C-malate medium. In total 15 ml of the elution fractions from each purification with (+FA) or without (-FA) cross-linking by formaldehyde were analyzed by 12.5% SDS-PAGE. After electrophoresis and blotting onto a

PVDF membrane, interaction partners were detected in the crude extracts and in the protein eluates by antibodies raised against the FLAG-tag. n.a., not analyzed.

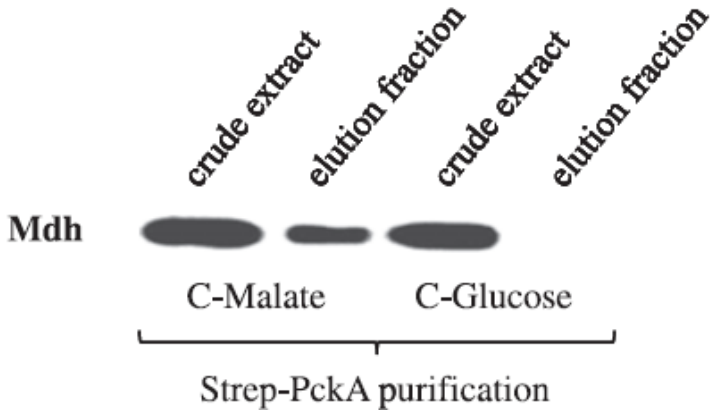

Fig. 2.7. Control of the interaction between malate dehydrogenase and phosphoenolpyruvate carboxykinase by the metabolic flux. *B. subtilis* GP1130 expressing FLAG-tagged Mdh was transformed with pGP1753 that allows expression of Strep-tagged PckA. The bacteria were grown in C-malate or C-glucose medium. In total 15 ml of the elution fractions from each purification without cross-linking by formaldehyde were analyzed by 12.5% SDS-PAGE. After electrophoresis and blotting onto a PVDF membrane, FLAG-Mdh was detected in the crude extracts and in the protein eluates by antibodies raised against the FLAG-tag.

Discussion

The TCA cycle is one of the most important metabolic intersections in all heterotrophic bacteria: It provides the cell with reducing power for respiration and it generates many of the precursors for anabolic pathways. Thus, the efficient flow of metabolites through the cycle is of primary importance for the cell. This can be achieved in four different ways: (i) the expression of the TCA cycle genes is controlled to ensure that the required enzymes are present under the given condition; (ii) the kinetic parameters of the enzymes are optimized with respect to the availability of the substrates in the environment of any given species; (iii) the activity of the enzymes can be fine-tuned by post-translational modification; and (iv) the interaction between the enzymes may optimize the flux through the TCA cycle. In *B. subtilis*, the expression of citrate synthase and aconitase is synergistically repressed by glucose and glutamate, i.e. if the cycle is required neither for energy production nor supply of 2-oxoglutarate, the glutamate precursor (Flechtner and Hanson, 1969; Jourlin-Castelli *et al*., 2000). Moreover, citrate synthase, the initial enzyme of the cycle is inhibited by ATP resulting in a reduced flux if the cell has sufficient energy available (Flechtner and Hanson, 1969; Jin and Sonenshein, 1996). Post-translational

modifications have been detected for most of the TCA cycle enzymes in *B. subtilis*, including citrate synthase, isocitrate dehydrogenase and malate dehydrogenase, however, the impact of these phosphorylation events on the TCA cycle flux has not yet been determined (Macek *et al*., 2007; Eymann *et al*., 2007). In this work, we provide evidence for the presence of a TCA cycle metabolon, i.e. a complex of enzymes of this pathway.

As shown in Fig. 2.4A, the three enzymes citrate synthase, isocitrate dehydrogenase and malate dehydrogenase form the core of the TCA cycle metabolon. In addition, the isocitrate and malate dehydrogenases interact with further TCA cycle enzymes and with enzymes of associated pathways. As a result of these interactions, intermediates can be easily transferred among most of the enzymes. Under the standard growth conditions used here (malate as the only carbon source), the cells need the TCA cycle for the generation of reducing power, for glutamate biosynthesis and to initiate gluconeogenesis. Indeed, our experiments revealed interactions between core components of the metabolon and these associated reactions: malate dehydrogenase interacts with NADH dehydrogenase and with PEP carboxykinase, the first enzyme of gluconeogenesis; and isocitrate dehydrogenase associates with glutamate synthase. Thus, 2-oxoglutarate, the product of the former enzyme might directly serve as the substrate for the latter enzyme. As a result of the protein-protein interactions in the TCA cycle metabolon, those reactions of the cycle that are required under the physiological conditions may proceed with high efficiency (see Fig. 2.4B).

An interesting result of this study is the interaction among the core enzymes of the TCA cycle metabolon. These enzymes, citrate synthase, isocitrate dehydrogenase and malate dehydrogenase, are encoded in the *citZ icd mdh* operon (Jin and Sonenshein, 1994). This operon organization is conserved in bacilli. In the related genera *Listeria*, *Staphylococcus* and *Streptococcus*, the *citZ* and *icd* genes are colocalized. It has been suggested that a conserved clustering of genes is a strong indication for physical interaction of the encoded proteins (Dandekar *et al*., 1998). Indeed, recent studies revealed physical interactions between glycolytic enzymes (GapA-Pgk and Tpi-Pgm) that are encoded by conserved gene clusters in *B. subtilis* and *Mycoplasma pneumoniae* (Commichau *et al.*, 2009; Stülke, J. 2010a; Kühner *et al*., 2009). The conservation of the *citZ icd mdh* cluster suggests that the formation of the core TCA cycle metabolon is not specific to *B. subtilis*. Indeed, an interaction between these enzymes (citrate synthase, isocitrate dehydrogenase and malate dehydrogenase) was also detected in *E. coli*, *Pseudomonas aeruginosa* and in mitochondria. As observed here for *B. subtilis*, this core metabolon interacts with fumarase and aconitase in these species as well (Barnes and

Weitzman, 1986; Mitchell, 1996; Robinson and Srere, 1985). Moreover, the physical association of citrate synthase and isocitrate dehydrogenase was also observed during non-denaturing fractionation of the complete proteome of the archaeon *Pyrococcus furiosus* (Menon *et al*., 2009).

Our experiments were performed during growth with malate and ammonium as the single sources of carbon and nitrogen, respectively. Thus, it is not surprising that glutamate synthase and PEP carboxykinase physically interact with the core TCA cycle metabolon under these conditions. The interaction between malate dehydrogenase and PEP carboxykinase is particularly strong since it is detectable even in the absence of a cross-linker. The interaction between these enzymes that catalyze consecutive reactions may be very valuable for the cell under conditions of gluconeogenesis. However, the metabolite flow from malate to phosphoenolpyruvate is not required if glucose is available. Using a strain that constitutively expresses PEP carboxykinase, we could demonstrate that the two enzymes do not interact under conditions of a metabolic ‘‘counter-flow’’. Regulation of the formation of a metabolon by the metabolic conditions was also observed for the glycolytic enzymes of Arabidopsis thaliana (Graham *et al*., 2007). Unfortunately, it is unknown how the metabolic flux controls the association between malate dehydrogenase and PEP carboxykinase. The interaction might be controlled by direct binding of a metabolite or by covalent modification of one of the partners. Indeed, malate dehydrogenase can be phosphorylated in vivo, but the actual stimulus and mechanism of this modification is unknown (Macek *et al*., 2007).

In this work, we have provided evidence for the existence of a TCA cycle metabolon in *B. subtilis*. This finding immediately raises the next questions: What are the kinetic and physiological consequences of these interactions? Which mechanisms link the metabolic fluxes to the physical association of proteins? Does the formation of the core of the TCA cycle metabolon also depend on the physiological conditions? And ultimately: What is the structure of the metabolon? Our future work is aimed at finding answers to these questions.

Acknowledgments

We are grateful to Linc Sonenshein for the generous gift of antibodies. Martin Lehnik-Habrink is acknowledged for helpful discussions on the identification of interaction partners. This work was supported by grants of Max-Buchner Forschungsstiftung, the Deutsche

Forschungsgemeinschaft and the Federal Ministry of Education and Research SYSMO network (PtJ-BIO/0313978D and 0313978A) to J.S. and U.V.

3. Malate-mediated carbon catabolite repression in *Bacillus subtilis*

The results described in this chapter were published in:

Meyer, F. M., Jules, M., Mehne, F. M., Le Coq, D., Landmann, J. J., Görke, B., Aymerich, S. & Stülke, J. (2011). Malate-mediated carbon catabolite repression in *Bacillus subtilis* involves the HPrK/CcpA pathway. *J. Bacteriol*. 193, 6939-6949.

Author's contribution:

The study was designed and interpreted by FMM, FMPM, MJ, SA and JS. The enzyme activity of *xynB* was measured by FMM. The *in vivo* pull down experiment was done by FMPM. The analysis of the phosphorylation state of HPr was done by JJL. The fructose 1,6-bisphosphate and ATP measurements were done by FMM and FMPM. The analysis of fluorescence in the LCA was done by MJ and DC. The determination of promoter activity was performed by MJ and DC. The paper was written by FMM, FMPM, SA and JS.

Abstract

Most organisms can choose their preferred carbon source from a mixture of nutrients. This process is called carbon catabolite repression. The Gram-positive bacterium *Bacillus subtilis* uses glucose as the preferred source of carbon and energy. Glucose-mediated catabolite repression is caused by binding of the CcpA transcription factor to the promoter regions of catabolic operons. CcpA binds DNA upon interaction with its cofactors HPr(Ser-P) and Crh(Ser-P). The formation of the cofactors is catalyzed by the metabolite-activated HPr kinase/phosphorylase. Recently, it has been shown that malate is a second preferred carbon source for *B. subtilis* that also causes catabolite repression. In this work, we addressed the mechanism by which malate causes catabolite repression. Genetic analyses revealed that malate-dependent catabolite repression requires CcpA and its cofactors. Moreover, we demonstrate that HPr(Ser-P) is present in malate-grown cells and that CcpA and HPr interact *in vivo* in the presence of glucose or malate but not in the absence of a repressing carbon source. The formation of the cofactor HPr(Ser-P) could be attributed to the concentrations of ATP and fructose 1,6-bisphosphate in cells growing with malate. Both metabolites are available at concentrations that are sufficient to stimulate HPr kinase activity. The adaptation of cells to environmental changes requires dynamic metabolic and regulatory adjustments. The repression strength of target promoters was similar to that observed in steady-state growth conditions, although it took somewhat longer to reach the second steady-state of expression when cells were shifted to malate.

Introduction

Like many other heterotrophic bacteria, the Gram-positive soil bacterium *Bacillus subtilis* can utilize a wide range of sugars, organic acids, and other organic compounds as sources of carbon and energy. Traditionally, glucose was regarded as the preferred carbon source for *B. subtilis*; this view is supported by the rapid growth and by the strong repression of genes encoding the enzymes for the utilization of alternative carbon sources in the presence of glucose (Fujita, 2009, Stülke & Hillen, 2000). Recently, it was discovered that malate serves as a second preferred carbon source for *B. subtilis*; its utilization occurs in parallel with that of glucose, and as observed for glucose, malate causes a strong catabolite repression of transporters for alternative carbon sources (Kleijn *et al*., 2010).

Catabolite repression is the regulatory mechanism that allows the cells to choose among several available carbon sources. Usually, it involves regulation at the level of gene expression to prevent transcription of catabolic genes and operons (catabolite repression in a strict sense) as well as regulation at the level of protein activity to prevent uptake or formation of the specific inducers of catabolic operons (inducer exclusion) (Deutscher, 2008; Görke & Stülke, 2008). Repression of the *Escherichia coli* lactose operon by glucose was the first example of gene regulation understood at the molecular level, and it is still the paradigm for carbon catabolite repression. However, the molecular mechanisms by which catabolite repression is achieved differ strongly between the different bacteria. In *E. coli*, inducer exclusion and transcription activation of catabolic genes by the complex of the Crp protein with cyclic AMP are crucial (Crasnier, 1996; Saier, 1989). In contrast, in *B. subtilis* and most other Gram-positive bacteria, catabolite repression is exerted by the CcpA repressor protein (Fujita, 2009; Warner & Lolkema, 2003).

In many bacteria, glucose and other sugars are transported and concomitantly phosphorylated by the phosphotransferase system (PTS). This system is composed of two soluble general phosphotransferases, enzyme I and HPr, and of a set of sugar-specific multidomain permeases. The domains of the permeases may be present in one protein, or they may exist as individual polypeptides (Deutscher *et al*., 2006). In *B. subtilis* and most other Gram-positive bacteria, HPr is a key player in the regulation of carbon metabolism: this protein can become phosphorylated by enzyme I on His-15 to be active in sugar transfer in the PTS, and in addition it is subject to a regulatory phosphorylation on Ser-46 (Deutscher *et al*., 2006). The phosphorylation of HPr on Ser-46 is catalyzed by the metabolite-sensitive HPr kinase/phosphorylase HPrK (Nessler *et al*., 2003). The latter phosphorylation has several consequences: (i) the protein is not longer active in glucose transport, since it is a very poor substrate for enzyme I (Deutscher *et al*., 1984); (ii) HPr loses the ability to phosphorylate and thus to activate the PRD-type transcription regulators that are required for the expression of specific catabolic operons (Lindner *et al*., 2002); and (iii) HPr(Ser-P) serves as a cofactor for the transcription factor CcpA (Deutscher *et al*., 1995). In the complex with HPr(Ser-P), CcpA is able to bind specific target sites (catabolite-responsive element, or *cre*, sites) in the control region of its target genes (Jones *et al*., 1997). This binding results in the repression of a large set of about 300 genes (Fujita, 2009). Moreover, transcription of some genes involved in overflow metabolism and amino acid biosynthesis is activated by the CcpA-HPr(Ser-P) complex (Grundy *et al*., 1993; Ludwig *et al*., 2002a; Nessler *et al*., 2003). Thus, the activity of the HPr

kinase/phosphorylase is crucial not only for the phosphorylation state of HPr but also for the regulatory output of CcpA. The HPrK is a bifunctional enzyme; its kinase activity is allosterically activated by ATP and fructose 1,6-bisphosphate (FBP), i.e., under conditions of good nutrient supply (Jault *et al*., 2000). Under starvation conditions, or when less favorable carbon sources are present, the HPrK has no kinase activity, nor does it even dephosphorylate HPr(Ser-P) if the pool of inorganic phosphate is high (Mijakovic *et al*., 2002; Monedero *et al*., 2001). Thus, the HPr kinase couples the nutrient state of the cell to the regulatory outcome that is directly governed by CcpA.

B. subtilis is able to use many intermediates of the citric acid cycle as single carbon sources. However, malate seems to have a special position, since it is the only known substrate that can be cometabolized with glucose (Kleijn *et al*., 2010). In order to utilize malate, the bacteria need a functional citric acid cycle and a link to gluconeogenesis. The citric acid cycle and gluconeogenesis are sufficient to provide the cell with all precursors for anabolic reactions. In *B. subtilis*, malate is linked to gluconeogenesis by the activities of malate dehydrogenase and phosphoenolpyruvate carboxykinase. Moreover, four malic enzymes that catalyze the oxidative decarboxylation of malate with the formation of pyruvate are present in *B. subtilis* (Doan *et al*., 2003). The mechanisms of malate utilization have not yet been elucidated in detail, but the malate dehydrogenase Mdh and the NADP-dependent malic enzyme YtsJ seem to be very important, since corresponding mutant strains exhibit impaired growth with malate as the only carbon source (Lerondel *et al*., 2006). While the expression of Mdh and YtsJ is constitutive, the phosphoenolpyruvate carboxykinase (PckA) is expressed only when the bacteria grow in the absence of glucose, since the corresponding *pckA* gene is subject to repression by the transcription factor CcpN (Servant *et al*., 2005). Once phosphoenolpyruvate is formed, the glycolytic enzymes that catalyze the reversible reactions, the anabolic glyceraldehydes 3-phosphate dehydrogenase GapB (Fillinger *et al*., 2000) and the fructose 1,6-bisphosphatase, lead to the synthesis of glucose 6-phosphate. While malate was shown to exert efficient catabolite repression of several nutrient transporters, the mechanism(s) involved in this repression has so far remained unknown. It was proposed that the mechanism may differ from the canonical CcpA-HPr(Ser-P) repression pathway, since the concentration of the metabolite that triggers the activity of the HPrK might be too low in the presence of malate as the only carbon source (Kleijn *et al*., 2010). In this work, we demonstrate that the repression by malate is also exerted by the CcpA-HPr(Ser-P) complex. We demonstrate that the complex malate

metabolism allows the accumulation of the regulatory metabolites ATP and FBP that are sufficient to trigger the HPrK kinase activity and thus carbon catabolite repression.

Materials and methods

Bacterial strains and growth conditions - The *B. subtilis* strains used in this study are listed in Table 8.3. The presence of the *ptsH1* mutation was verified by sequencing of chromosomal DNA of the relevant strains. *E. coli* DH5α and *E. coli* TG1 (Sambrook & Russell, 2001) were used for plasmid constructions and transformation using standard techniques (Sambrook & Russell, 2001). Luria-Bertani (LB) broth was used to grow *E. coli* and *B. subtilis*. When required, media were supplemented with antibiotics at the following concentrations: ampicillin, 100 μg ml^{-1}; spectinomycin, 150 μg ml^{-1} (for *E. coli*); spectinomycin, 100 μg ml^{-1}; kanamycin, 7.5 μg ml^{-1}; chloramphenicol, 5 μg ml^{-1} (for *B. subtilis*). *B. subtilis* was grown in C minimal medium supplemented with carbon sources and auxotrophic requirements (at 50 mg $liter^{-1}$) as indicated (Wacker *et al*., 2003). Potentially repressing carbon sources were used at a concentration of 0.5% (wt/vol) unless stated otherwise. SP plates were prepared by the addition of 17 g $liter^{-1}$ Bacto agar (Difco) to sporulation medium.

Transformation and enzyme assays - Chromosomal DNA of *B. subtilis* was isolated using the DNeasy tissue kit (Qiagen) according to the supplier's protocol. *B. subtilis* was transformed with plasmids and chromosomal DNA according to the two-step protocol (Anagnostopoulos & Spizizen, 1961; Kunst & Rapoport, 1995.). Transformants were selected on SP plates containing antibiotics as indicated above or erythromycin plus lincomycin (2 and 25 μg ml^{-1}, respectively). For enzyme assays, cells were harvested in exponential growth phase at an optical density at 600 nm (OD_{600}) of 0.6 to 0.8. β-Xylosidase activities were determined in cell extracts using *p*-nitrophenyl xyloside as the substrate (Lindner *et al*., 1994).

In vivo detection of protein-protein interactions - The isolation of protein complexes from *B. subtilis* cells was performed by the SPINE technology (Herzberg *et al*., 2007) using a chromosomally encoded CcpA protein carrying a C-terminal Strep tag. For the construction of this strain, GP1303, we made use of the cloning vector pGP1389, which allows easy integration of the constructs into the chromosome (Lehnik-Habrink *et al*., 2011). The *ccpA* gene was amplified (for primers, see Table 8.1), and the PCR product was cloned between the *Bam*HI and *Sal*I sites of pGP1389, giving pGP1952. This plasmid was used to construct *B. subtilis* GP1303 expressing the Strep-tagged CcpA. For the purification of CcpA with its interaction partners,

growing cultures of *B. subtilis* were treated with formaldehyde (0.6% [wt/vol], 20 min) to facilitate cross-linking of interacting proteins (Herzberg *et al*., 2007). The Strep-tagged CcpA and its potential interaction partners were then purified from crude extracts using a Strep-Tactin column (IBA, Göttingen, Germany) and desthiobiotin as the eluent. HPr was identified by Western blot analysis.

Analysis of the phosphorylation state of HPr in vivo - HPr phosphorylation was assayed *in vivo* by Western blot analysis as follows. Bacteria were grown in C minimal medium with succinate and glutamate (CSE) in the presence of the indicated carbon sources to an OD_{600} of 0.6. Cells were disrupted using a French press, and crude extracts were prepared as described previously (Ludwig *et al*., 2002b). Proteins (3.5 µg of each sample) were separated on nondenaturing 12% polyacrylamide gels. On these gels, phosphorylated HPr migrates faster than the nonphosphorylated protein. HPr(His-P) was dephosphorylated by incubation of the crude extract for 10 min at 70°C. After electrophoresis, the proteins were blotted to a polyvinylidene difluoride (PVDF) membrane. The different forms of HPr were detected using antibodies directed against *B. subtilis* HPr (Monedero *et al*., 2001). The antibodies were visualized by using anti-rabbit IgG-AP secondary antibodies (Chemikon International, Temecula, CA) and the CDP* detection system (Roche Diagnostics).

Determination of FBP concentrations - Protein-free cell extracts for the determination of fructose 1,6-bisphosphate (FBP) concentrations in *B. subtilis* were prepared as described previously (Mijakovic *et al*., 2002; Singh *et al*., 2008). Briefly, cells of the *B. subtilis* wild-type strain 168 were grown in 50 ml CSE medium in the presence of the indicated carbon sources. For each growth condition, at least three independent experiments were carried out. Cultures were harvested by centrifugation, and pellets were frozen in liquid nitrogen. The pellets were resuspended in 0.6 M cold perchloric acid and subsequently incubated on ice for 20 min. The precipitated proteins and cell debris were removed by centrifugation. The pH in the supernatant was adjusted to 7.4 with a solution of cold 0.6 M KOH in 100 mM Tris-HCl (pH 7.4). The precipitated $KClO_4$ was removed by centrifugation. The FBP concentrations were determined in the supernatants as described previously (Mijakovic *et al*., 2002).

Determination of ATP concentrations - Intracellular ATP levels were determined as described previously (Ludwig *et al*., 2002b). Exponentially growing cultures were quenched at an OD_{600} of 0.5 by mixing with dimethyl sulfoxide (DMSO), which released the adenine nucleotides from the cells. ATP levels were measured using an ATP bioluminescence assay kit (CLSII; Roche Diagnostics) and a microplate fluorescence reader (FLUOstar Omega; BMG Labtech). For

calculating the concentrations of intracellular ATP, we used the previously reported aqueous cell volume of 0.85 µl of a culture of 1 ml at an OD_{600} of 1 (Fujita & Freese, 1979).

Plasmid constructions for transcriptional fusions - Fragments corresponding to the promoter regions of *araA*, *araE*, *bglP*, *fruR*, *glpF*, *gntR*, and *sacP*, or to a region in the 3' part of *fruA*, were amplified by PCR from genomic DNA using the appropriate pairs of primers listed in the supplemental material. PCR products were purified after electrophoresis from agarose gel using the Wizard SV gel and PCR clean-up system (Promega, Madison, WI). For *bglP*, *sacP*, *glpF*, and *gntR*, two types of fragments were synthesized: for the first three, the expression of which is inducible through an antitermination mechanism, the target region of the antiterminator was either included or omitted, and for *gntR*, in the open reading frame (ORF) of which a second *cre* site is present, fragments including or not including this site were obtained. Ligation-independent cloning of each fragment in the pBaSysBioII plasmid was performed as described previously (Botella *et al*., 2010). The resulting plasmids were extracted from *E. coli* and, after verification of the correct sequence of constructions, used to transform *B. subtilis*. Integration of each plasmid through single recombination allowed the generation of a transcriptional *gfpmut3* fusion with the corresponding promoter, either directly downstream of it (*araA*, *araE*, *bglP*, *fruR*, *glpF*, *gntR*, and *sacP*) or placed downstream from the last gene of the operon (*fruA*).

Analysis of fluorescence in the LCA - In order to optimize monitoring of fluorescence and to avoid as much as possible any interference linked to the culture medium, live cell array (LCA) experiments were performed as previously set up (Botella *et al*., 2010). A modified M9 medium was used (Harwood & Cutting, 1990) supplemented with isoleucine (25 mg $liter^{-1}$), leucine (50 mg $liter^{-1}$), valine (40 mg $liter^{-1}$), and methionine (20 mg $liter^{-1}$) (Blencke *et al*., 2003). For these experiments, we used strains derived from BSB168, a trp^+ derivative of *B. subtilis* 168, to avoid the intrinsic fluorescence of tryptophan. If not stated otherwise, the primary carbon source was succinate + glutamate (SE) (0.5% each). When necessary for induction, the suitable carbon source (L-arabinose, D-gluconate, D-fructose, glycerol, D-salicin, or D-sucrose) was added at 0.5%. Steady-state and dynamic experiments were performed as previously described (Botella *et al*., 2010). Cells were grown in 100 µl of medium in a 96-well cell culture plate (Cellstar; Greiner Bio-One) and incubated at 37°C under constant shaking in a Synergy II microplate reader (Biotek) for 20 h. The OD_{600} and fluorescence (excitation, 485/20 nm; emission, 528/20 nm) were measured every 10 min (Botella *et al*., 2010). Absorbencies at 900 nm and 977 nm (*A*900 and *A*977, respectively) were read once at the beginning of each experiment in order to correct the OD_{600} to an optical path length of 1 cm. The carbon source shift was carried out by injection

of either glucose to a final concentration of 0.3% or malate to a final concentration of 0.5%, when cells reached an OD_{600} of about 0.3. Fluorescein was present on the microtiter plate at two different concentrations (1 and 10 nM) in duplicate. Each culture was performed in triplicate.

Promoter activity and GFP concentration determination - Green fluorescent protein (GFP) accumulation of the GFPmut3 stable variant was obtained as previously described for *B. subtilis* (Botella *et al*., 2010). Polynomial and exponential functions were used to fit the experimental data sets of GFP and biomass, respectively, and to deduce the rates of biomass and GFP production along the growth. GFP concentration was estimated as GFP per OD_{600} (GFP/OD) at each time point. Promoter activities were calculated taking the derivative of the fluorescence divided by the OD_{600} ([(dGFP/dt)/OD]) at each time point (Ronen *et al*., 2002; Zaslaver *et al*., 2006). Under steady-state growth conditions (μ = constant), both GFP/OD and (dGFP/ dt)/OD are constant. GFP concentration was expressed as units per OD_{600} (1 unit being equivalent to 1 pM fluorescein) and promoter activity as units per hour per OD_{600} unit.

Results

Malate represses transcription of several uptake systems of alternative carbon sources - It was recently shown that malate represses the coutilization of alternative substrates in *B. subtilis* (Kleijn *et al*., 2010). In order to further detail the underlying mechanism, we investigated transcription of the genes coding for uptake systems of several different carbon sources (from C_3 to C_{13}) in the presence/absence of malate. We constructed *gfp* transcriptional fusions reporting promoter activities of transporters, either PTS or not, for fructose (FruA), sucrose (SacP), β-glucosides (BglP), arabinose (AraE), gluconate (GntP), and glycerol (GlpF). Strains were first cultivated in batch culture on M9 minimal medium with either succinate/glutamate (M9SE) as the sole carbon source or on M9SE plus the suitable inducer. For all the fusions, *gfp* expression was barely detectable without the suitable inducer and at least 10 times higher in its presence (Table 3.1). Gfp expression in all reporter strains was then measured in the presence of the suitable inducer and either glucose or malate. Glucose elicited a repression over 70% (Table 3.1), except for gluconate and fructose uptake genes, for which the repression was moderate (about 45%). In agreement with the hierarchy in carbon catabolite repression (CCR) of carbon sources (Singh *et al*., 2008), expression of the transporter of fructose, which is high in the hierarchy, is the least repressed by glucose. Conversely, expression of the transporter of

arabinose which is low in the hierarchy, is the most repressed (Table 3.1). Similarly, in all but one case (P_{sacP}-*gfp*), malate triggered repression of the reporter fusions, although at a lower level than that exerted by glucose (Table 3.1). The weaker repression level together with the absence of measurable repression of the *sacP* promoter may result either from a second, distinct repression mechanism based on the mode of action of the inducer or from an intermediate activation of the HPrK/CcpA CCR pathway.

Table 3.1. Expression levels of genes coding for transporters and/or assimilation pathways of several alternative substrates in the absence and presence of malate and glucose

Strain, fusion[b]	Expression level[a]		
	M9SE*c*	+ Glucose	+ Malate
BBA0223, P_{bglP}-*gfp*	<5[d]	16	31
BBA0359, P_{sacP}-*gfp*	<5[d]	31	>90[e]
BBA0121, P_{glpF}-*gfp*	ND	17	59
BBA0028, P_{gntR}-*gfp*	5	55	60
GM3005, *fruA*-*gfp*	<5[d]	60	86
BBA0118, P_{fruR}-*gfp*	10	>90[e]	90
GM3008, P_{araE}-*gfp*	9	<5[d]	16
GM3001, P_{araA}-*gfp*	<5[d]	8	20

[a] Expression levels are given as a percentage of the expression in the presence of the suitable inducer. Mean values of results from three independent experiments with standard deviations of <±10% are presented. ND, not determined.
[b] The inducer was D-gluconate for the P_{gntR}-*gfp* strain, D-fructose for the *fruA*-*gfp* and P_{fruR}-*gfp* strains, glycerol for the P_{glpF}-*gfp* strain, salicin for the P_{bglP}-*gfp* strains, sucrose for the P_{sacP}-*gfp* strain, and L-arabinose for the P_{araE}-*gfp* and P_{araA}-*gfp* derivative strains.
[c] M9 minimal medium with succinate and glutamate (see Materials and Methods).
[d] Expression level was below 5% or negligible.
[e] Expression level was between 90 and 100% and was not distinguishable from the induced condition with this assay.

Malate repression is independent from the induction mechanism and dependent upon CcpA - To know whether the catabolite repression by malate depends on the induction mechanism of the different uptake systems, we constructed another set of reporter fusions in which the target sequences of the induction mechanism have been precisely deleted (see Materials and Methods). The resulting constitutive expression of the $P_{bglP\Delta RAT\text{-}term}$-*gfp*, $P_{sacP\Delta RAT\text{-}term}$-*gfp*, and $P_{glpF\Delta term}$-*gfp* transcriptional fusions was even higher than the induced expression of the corresponding inducible fusion (data not shown). The addition of glucose, malate, or the cognate inducer to the three modified reporter systems triggered a strong repression of *gfp* expression (80%, 60%, and 70%, respectively) (Fig. 3.1A).

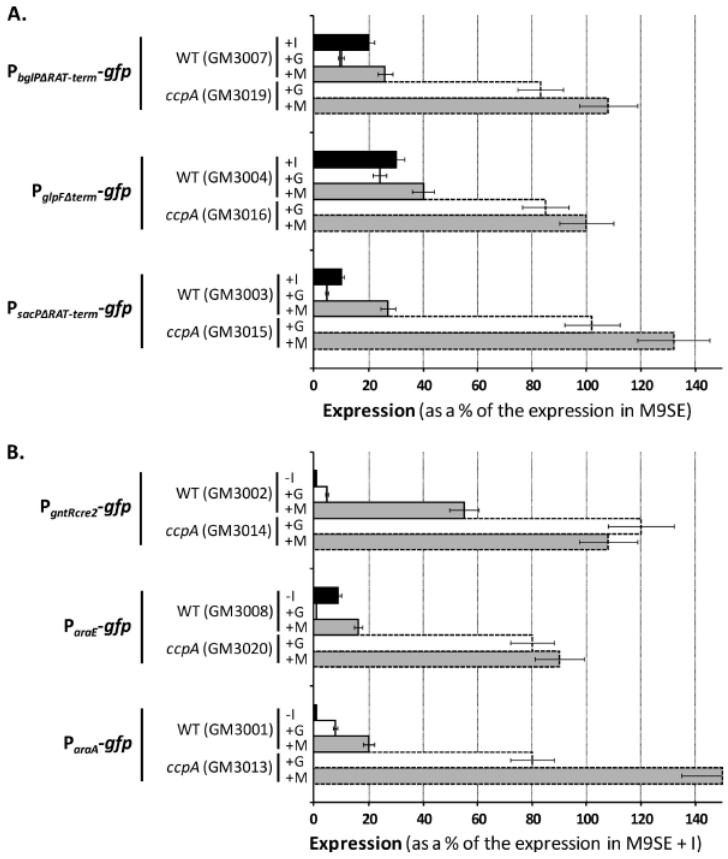

Fig. 3.1. Carbon catabolite repression in the presence of glucose (+G) or malate (+M). (A) Effect of the *ccpA* inactivation on constitutive fusions. (B) Effect of the *ccpA* inactivation on inducible fusions. Expression levels are given as a percentage of the expression in the presence of the suitable inducer (+I) for fusions requiring induction and of the expression in M9SE for constitutive fusions (-I). Mean values of three independent experiments with standard deviations are presented.

These results indicate that malate catabolite repression is independent from the induction mechanisms of these uptake systems. They also confirm that glycolytic carbon sources other than glucose can trigger catabolite repression, most probably through the HPrK/CcpA pathway (Singh *et al*., 2008). We then addressed the question of whether malate hijacks the HPrK/CcpA CCR regulatory pathway by determining *gfp* expression of the previous reporter strains in a *ccpA* mutant genetic context. Figure 3.1A shows that the *ccpA* knockout fully relieved the repression of the $P_{bglP\Delta RAT\text{-}term}$-*gfp*, $P_{sacP\Delta RAT\text{-}term}$*gfp*, and $P_{glpF\Delta term}$-*gfp* reporter fusions. This demonstrated that malate-mediated repression is exerted via the CcpA repressor on these target genes. We also investigated the effect of *ccpA* knockout on the repression of the $P_{gntRcre2}$-*gfp*, *fruA-gfp*, P_{araE}-*gfp*, and P_{araA}-*gfp* reporter fusions, inducible by their cognate inducer. In the absence of inducer, levels of expression were barely detectable (Fig. 3.1B). In the presence of the cognate inducer, the addition of glucose or malate did not trigger repression anymore, except for the *fruA-gfp*

fusion (data not shown), thus confirming the essential role of CcpA for malate catabolite repression. It is worth noting that the repression exerted by glucose on the $P_{gntRcre2}$-*gfp* fusion was stronger than that exerted on the P_{gntR}-*gfp* fusion, in which the second *cre* site located within the *gntR* coding sequence is absent (Fujita, 2009). In order to further investigate the different factors possibly involved in the malate repression, we then focused on the expression of *xynB*, a well-established model system to study the CCR (Singh *et al*., 2008).

Roles of factors involved in glucose repression in the repression by malate - To gain further insights into catabolite repression by malate, we analyzed the effect of malate on the synthesis of β-xylosidase, encoded by the *xynB* gene. This gene is subject to a very strong repression by glucose, and in a strain devoid of the xylose repressor XylR, this repression depends exclusively on a functional CcpA regulatory pathway (Singh *et al*., 2008). Therefore, we studied the synthesis of β-xylosidase in the *xylR* mutant strain GP270 after growth in minimal medium without any added carbon source and in the presence of glucose or malate. As shown in Table 3.2, glucose caused an approximate 25-fold repression of β-xylosidase synthesis. This is in excellent agreement with previous observations (Lindner *et al*., 1994; Singh *et al*., 2008). In the presence of malate, a 9-fold repression was observed, which led us to address the role of CcpA in malate-mediated repression. As reported previously (Singh *et al*., 2008), repression by glucose was nearly completely lost upon inactivation of CcpA. Similarly, repression by malate was strongly reduced in the *ccpA* mutant; however, the β-xylosidase activity in the presence of malate reached only 55% of that observed in CSE medium. This result indicates that CcpA is the major factor causing catabolite repression of β-xylosidase synthesis by malate. It is well established that CcpA efficiently binds its target sites *in vivo* only if it forms a complex with either of its cofactors, HPr(Ser-P) or Crh(Ser-P). For glucose-mediated catabolite repression of β-xylosidase, the two cofactors can replace each other (Galinier *et al*., 1997; Galinier *et al*., 1999). The formation of these cofactors requires the metabolite-activated HPr kinase, and it was proposed that the concentration of the HPr kinase effector fructose 1,6-bisphosphate (FBP) in malate-grown cells would be too low to allow HPr phosphorylation (Kleijn *et al*., 2010). To address these obvious contradictions, we determined the repression by malate in mutants affected in the formation of the cofactors for CcpA. As observed previously, individual mutations of either HPr (the *ptsH1* mutation results in a loss of the phosphorylation site Ser-46) or Crh did not result in significant changes in repression of β-xylosidase synthesis compared to the use of an isogenic wild-type strain (compare GP270 to GP284 and GP297 in Table 3.2). As observed for repression of *xynB* expression by glucose, the combination of the *ptsH1* and *crh* mutations

resulted in a substantial loss of malate-mediated repression and had essentially the same effect as the *ccpA* mutation (GP287 and GP853 in Table 3.2). This finding supports the idea that HPr(Ser-P) and Crh(Ser-P) can functionally replace each other as cofactors of CcpA to cause catabolite repression of *xynB* expression. Finally, we tested the effect of a *hprK* mutation. The corresponding mutant strain, GP289, lacks the HPr kinase, and therefore neither HPr nor Crh can be phosphorylated on Ser-46. As expected, both glucose and malate repression of β-xylosidase synthesis were essentially lost, similar to the observations for the *ccpA* and *ptsH1 crh* mutant strains. May Crh-CcpA and HPr-CcpA complexes have different affinities for the same particular *cre* box and therefore favor the binding of either complex to specific *cre* sequences? In the case of *xynB* repression, HPr and Crh replace each other to exert a similar repression. To test whether this is true for other targets of CcpA, we inserted a *crh* or a *ptsH1* mutation in the *gfp* reporter strains described above. As for the β-xylosidase synthesis, the single *ptsH1* mutation weakly altered the level of repression exerted by either glucose or malate, whereas the *crh* mutation did not show any significant phenotype (Table 3.3). Taken together, these data unequivocally establish that malate-mediated repression is caused by CcpA in a complex with either of its two cofactors, HPr(Ser-P) or Crh(Ser-P).

Table 3.2. Catabolite repression of β-xylosidase by different carbon sources in various mutants

Carbon source[a]	Enzyme activity[b] in U/mg of protein					
	GP270 *ΔxylR*	GP853 *ΔxylR ΔccpA*	GP284 *ΔxylR ptsH1*	GP297 *ΔxylR Δcrh*	GP289 *ΔxylR ΔhprK*	GP287 *ΔxylR Δcrh ptsH1*
None (CSE)	1535 (204)	2548 (179)	1535 (91)	2609 (413)	2414 (445)	2644 (321)
Glucose	59 (2)	2074 (43)	154 (29)	75 (16)	2036 (209)	2385 (48)
Malate	170 (27)	1388 (49)	176 (28)	370 (35)	1579 (231)	1598 (95)

[a] Added to CSE medium.
[b] All measurements were performed at least in triplicate. Values in parentheses indicate the standard deviations.

In vivo interaction of CcpA with HPr during growth with malate - The results described above provide genetic evidence that the interaction of CcpA with HPr(Ser-P) causes catabolite repression of β-xylosidase synthesis during growth with malate. In order to demonstrate this interaction more directly, we attempted to purify CcpA with its interaction partners from cells grown in minimal medium without any additional carbon source and in the presence of glucose or malate. For this purpose, we constructed *B. subtilis* GP1303, which expresses CcpA carrying a

C-terminal Strep tag under the control of its native promoter in the chromosome. CcpA was cross-linked *in vivo* to its interaction partners as described in Materials and Methods and purified by affinity chromatography using a Strep-Tactin matrix. The presence of HPr was assayed by Western blot analysis. As shown in Fig. 3.2, no HPr was detectable when CcpA was purified from CSE-grown cultures. In contrast, HPr was efficiently cross-linked to CcpA when the bacteria were cultivated in the presence of glucose. Similarly, HPr was copurified with CcpA from malate-grown cells. These data demonstrate that the presence of malate is sufficient to trigger the *in vivo* interaction between CcpA and its cofactor, HPr.

Table 3.3. Repression by malate or glucose in the *ptsH1* and Δ*crh* single mutants

Fusion	*ptsH1* genetic context			Δ*crh* genetic context		
	Strain	Expression level[a]		Strain	Expression level[a]	
		+ Glucose	+ Malate		+ Glucose	+ Malate
$P_{bglP\Delta RAT\text{-}term}$-*gfp*	GM3043	26	27	GM3033	8	30
$P_{sacP\Delta RAT\text{-}term}$-*gfp*	GM3079	20	35	GM3067	4	32
$P_{gntRcre2}$-*gfp*	GM3037	27	65	GM3029	9	55
$P_{glpF\Delta term}$-*gfp*	GM3069	45	50	GM3057	20	40
fruA-gfp	GM3071	72	82	GM3059	55	84
P_{fruR}-*gfp*	GM3073	80	90	GM3061	>90[b]	87
P_{araE}-*gfp*	GM3075	26	9	GM3063	14	20
P_{araA}-*gfp*	GM3077	39	43	GM3065	5	19

[a] Expression level is given as a percentage of the expression in the presence of the suitable inducer for fusions requiring induction and of the expression in M9SE for constitutive fusions. Mean values of three independent experiments with standard deviations of <±10% are presented.

[b] Expression level comprised between 90 and 100% and was not distinguishable from the induced condition with this assay.

Effect of malate on the ATP-dependent phosphorylation of HPr and on the metabolites that control the HPrK activity - Binding of HPr to CcpA requires its prior phosphorylation by the HPr kinase at the regulatory site, Ser-46. As shown above, the *hprK* mutant exhibited a strongly reduced repression of β-xylosidase synthesis by malate, suggesting that HPr phosphorylation on Ser-46 is also essential for catabolite repression by malate. To obtain *in vivo* evidence for the hypothesis that HPr is phosphorylated on Ser-46 in malate-grown cells, we determined the phosphorylation pattern of HPr in cells grown in a nonrepressing minimal medium and in the presence of glucose or malate. For this purpose we made use of the different migrations of the

HPr forms in native gels. As shown in Fig. 3.3 (lower panel), the amounts of HPr were similar under all three tested conditions. This is in good agreement with previous observations of the constitutively high expression of HPr (Görke *et al*., 2004; Singh *et al*., 2008). In *B. subtilis* grown in CSE medium, HPr was present mainly in the nonphosphorylated form. In addition, a band corresponding to monophosphorylated HPr was visible. This band disappeared after incubation of the cell extract at 70°C. This heat lability is indicative for a phosphorylation on a histidine residue, i.e., His-15 of HPr (Monedero *et al*., 2001). In the presence of glucose, a large portion of HPr was phosphorylated, and this phosphorylation was heat stable. This indicates that phosphorylation had occurred on Ser-46 and is in perfect agreement with results of previous investigations (Ludwig *et al*., 2002b; Monedero *et al*., 2001; Singh *et al*., 2008). In the malate-grown cells, we also detected that a major fraction of HPr was phosphorylated on Ser-46. Thus, in the presence of malate, HPr is available as HPr(Ser-P) that is competent for the productive interaction with CcpA that we have observed to take place *in vivo*.

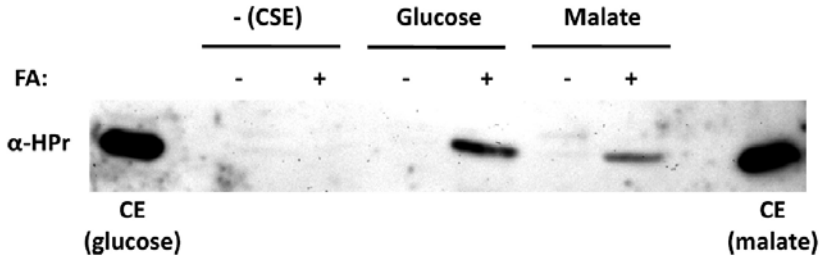

Fig. 3.2. Detection of *in vivo* interactions between CcpA and HPr by Western blot analysis. The protein complexes were isolated from *B. subtilis* GP1303 with a chromosomally encoded CcpA protein carrying a C-terminal Strep tag. The cells were grown in minimal medium without any repressing carbon source (CSE) or in minimal medium supplemented with glucose or malate. Then, 28 µl of the elution fractions from each purification without (-FA) or with (+FA) crosslinking by formaldehyde was analyzed by 15% SDS-PAGE. After electrophoresis and blotting onto a PVDF membrane, interaction partners were detected by an antibody raised against HPr. As a control, 3 µg of the crude extract (CE) from glucose- or malate-grown cells was used.

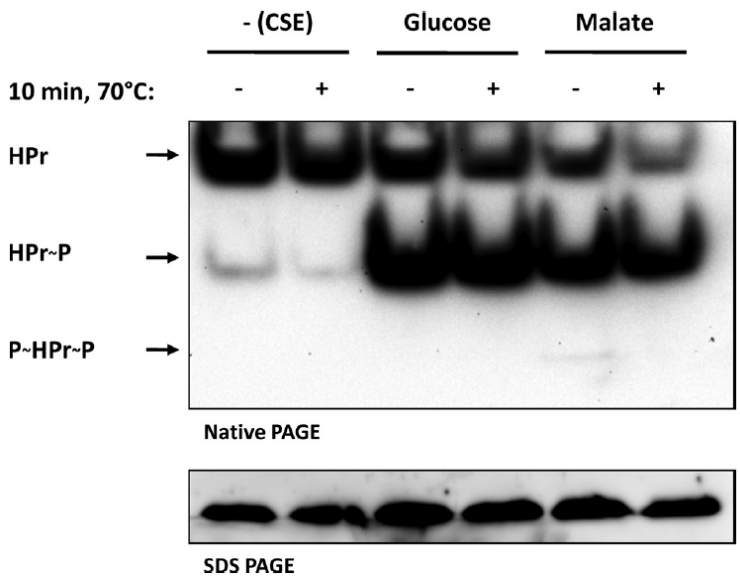

FIG. 3.3. Determination of the phosphorylation state of HPr in the presence of malate. The wild-type strain 168 was grown in CSE medium or in CSE medium supplemented with glucose or malate. Protein extracts were prepared and separated on native 12% polyacrylamide (PAA) gels (top panel). HPr was subsequently detected by Western blotting. To discriminate between HPr(Ser-P) and HPr(His-P), an aliquot of each cell extract was heated (70°C, 10 min) prior to loading. This causes a loss of the phosphohistidine bonds. The lysis buffer used affected the reliability of the Bradford assay for determination of protein concentrations. To account for the differences in the protein estimation and sample loading, 2 µg of each protein extract (as determined by the Bradford assay) was separated in parallel by SDS-PAGE, and total HPr was detected by Western blot analysis (bottom panel).

HPr(Ser-P) is synthesized by the metabolite-activated HPr kinase HPrK. The activity of this protein is known to be triggered by FBP and ATP (Galinier *et al*., 1998; Hanson *et al*., 2002; Jault *et al*., 2000; Reizer *et al*., 1998). However, it was suggested that the concentrations of these metabolites might not reach the critical concentration when *B. subtilis* grows in the presence of malate (Kleijn *et al*., 2010). To clarify this issue, we determined the intracellular concentrations of FBP and ATP. In cells cultivated in CSE minimal medium, the concentration of FBP was 2.3 mM. In contrast, the FBP concentration was significantly increased in glucose-grown cells (12.7 mM). These results are in good agreement with those of previous studies (Mijakovic *et al*., 2002; Singh *et al*., 2008). For malate-grown cells, an intermediate concentration of FBP (5.4 mM) was determined (Table 3.4). This is in the range detected for other repressing carbon sources (Singh *et al*., 2008). In contrast to the FBP concentrations, which were quite variable depending on the carbon source, there were only minor differences in the ATP concentrations under the three conditions tested (Table 3.4). Again, this is in agreement with previous

observations for *B. subtilis* (Ludwig *et al*., 2002b; Voelker *et al*., 1995) and with the idea that the ATP concentrations are generally kept constant in bacterial cells (Koebmann *et al*., 2002).

Table 3.4. Effect of the carbon source on the pools of fructose 1,6-bisphosphate and ATP in *B. subtilis*[b]

Carbon source[a]	Fructose 1,6-bisphosphate, mM	ATP, µM
None (CSE)	2.3 (0.17)	42.6 (4.96)
Glucose	12.7 (0.57)	59.5 (7.52)
Malate	5.4 (0.45)	47.3 (5.14)

[a] Added to CSE medium.
[b] All measurements were performed at least in triplicate. Values in parentheses indicate the standard deviations.

Dynamic transcriptional response after malate or glucose addition - Although we showed that the level of HPr(Ser-P) was high enough during steady-state growth in the presence of malate to trigger catabolite repression, the FBP level was twofold lower than in the presence of glucose. The lower level of FBP observed in malate-grown cells could explain the weaker repression exerted by malate compared to that by glucose. This weaker FBP concentration may lead to not only lower but also slower dynamics of adaptation to a pulse of malate leading to a slower large-scale reorganization of the regulatory network. We therefore designed shift experiments in which cells were first grown on M9SE before the addition of glucose or malate. Time course measurement of the expression of the $P_{bglP\Delta RAT\text{-}term}$-*gfp* reporter fusion during a transition from M9SE to M9SE plus glucose showed that the promoter was fully repressed approximately 40 min after the shift (Fig. 3.4A). In the following 20 min, the repression was slightly relieved and the promoter activity reached a new plateau corresponding to about 5 to 10% of its level before glucose addition. It is worth noting that the final repression level is similar to that observed under steady-state growth conditions in the presence of glucose (Table 3.1). As shown in Fig. 3.4B, the sudden addition of malate elicited a slightly slower repression than that of glucose (maximal repression reached approximately 50 min after the shift). Afterward, the $P_{bglP\Delta RAT\text{-}term}$-*gfp* promoter activity reached equilibrium at about 25% of the activity prior to malate addition, very similar to that estimated in the malate coutilization steadystate experiments (Table 3.1). The $P_{sacP\Delta RAT\text{-}term}$-*gfp* promoter activity behaved dynamically exactly as the $P_{bglP\Delta RAT\text{-}term}$-*gfp* promoter activity did (data not shown), providing further evidence for the involvement of the identical mechanism in malate catabolite repression of both fusions.

Very similar dynamic expression profiles to those of the previous strains were also observed with the $P_{glpF\Delta term}$-*gfp* reporter strain (Fig. 3.4C and D). Again the stable expression level reached 2 h after the shift was very close to that measured under steady-state growth conditions (Table 3.1). However, a transient "overrepression" after glucose addition before reaching a stable level of transcription was even more pronounced with the $P_{glpF\Delta term}$-*gfp* reporter strain (Fig. 3.4C) than with the $P_{bglP\Delta RAT\text{-}term}$-*gfp* one (Fig. 3.4A). Transient accumulation of FBP caused by high glucose influx but slower reorganization of the entire central metabolism could provoke this transient overrepression of the reporter fusions.

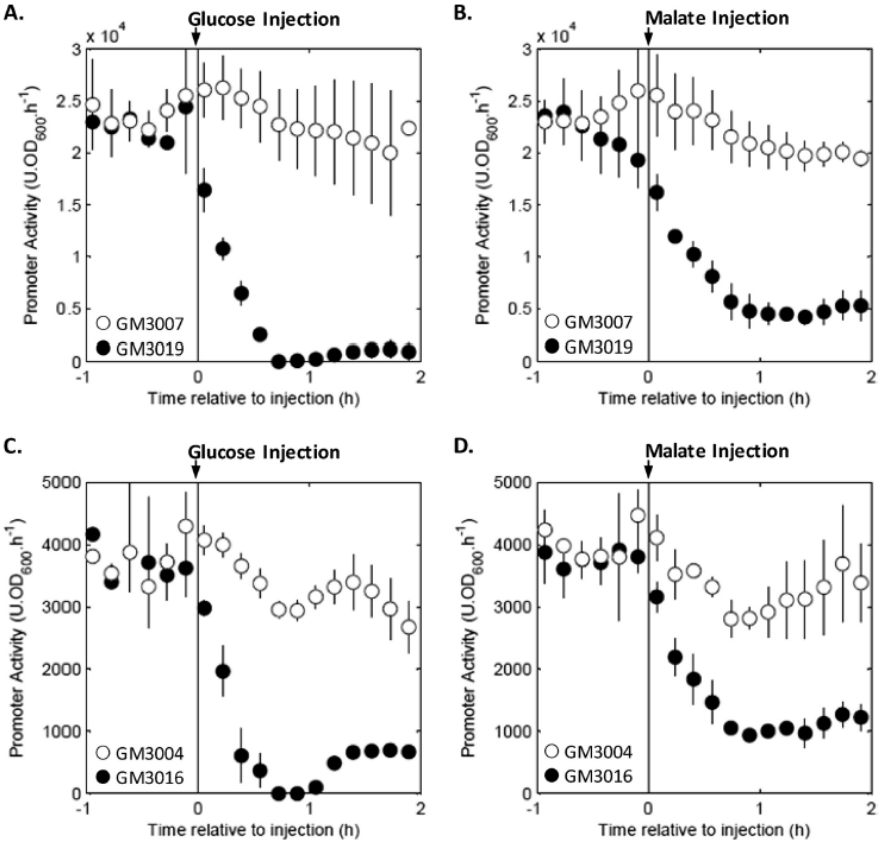

Fig. 3.4. Carbon catabolite repression upon glucose or malate addition to cells grown under gluconeogenic conditions. Wild-type (black circles) and *ccpA* mutant (white circles) strains were grown on succinate as the sole carbon source until the second substrate addition. The glucose (left panels)- or malate (right panels)-mediated repression was followed using strains bearing the transcriptional fusions $P_{bglP\Delta RAT\text{-}term}$-*gfp* (strains GM3007 and GM3019; panels A and B) and $P_{glpF\Delta term}$-*gfp* (strains GM3004 and GM3016; panels C and D). Repression reached its maximum about 40 min and 50 min after the glucose or malate addition, respectively. Promoter activities are the average results for three replicates, and error bars represent standard deviations.

To determine whether CcpA is also the key element involved in the initial response to glucose or malate addition, we investigated the effect of a *ccpA* knockout on the expression of

the reporter fusions during either shifts. As shown in Fig. 3.4, in such a *ccpA* mutant context, promoter activities of $P_{bglP\Delta RAT\text{-}term}$-*gfp* and $P_{glpF\Delta term}$-*gfp* are no more repressed and remained roughly constant upon glucose or malate addition. The same observation was made with the $P_{sacP\Delta RAT\text{-}term}$-*gfp* promoter (not shown). Interestingly, both injections onto the *ccpA* mutant-derived strains led to increasing noise and variations in *gfp* expression that may be due to the particular stress caused by a nutritional perturbation in this particular mutant background. Conversely, the *crh* and *ptsH1* single mutants did not show any particular phenotype compared to the wild type (data not shown), suggesting that, as in steady-state growth conditions, Crh and HPr can replace each other. Altogether, these results demonstrated that the HPrK/CcpA pathway transduces the repression signal immediately after malate addition, as for glucose addition. They also revealed that malate catabolite repression is not only weaker but also slightly slower than glucose catabolite repression, although both malate and glucose maximal repressions were reached in less than a doubling time (see Table 8.5.1 in the supplemental material).

Discussion

This work shows that malate causes carbon catabolite repression in *B. subtilis* by employing the general CcpA-dependent mechanism of repression. This underlines the specific role of malate in the physiology of *B. subtilis*. Malate is the primary product of carbon dioxide fixation in a large group of plants, the so-called C_4 plants, as well as in the crassulacean acid metabolism plants. Moreover, malate accumulates in unripe fruits. Thus, malate is commonly available in soil and on plants, the preferred habitats of *B. subtilis*. Indeed, *B. subtilis* has recently been suggested to be an epiphyte (Barbe *et al*., 2009; Deng *et al*., 2011). Moreover, several carboxylic acids, in particular malate, are substantially secreted by plant roots into the rhizosphere (Bais *et al*., 2006), which enables recruiting beneficial bacteria that help to reduce susceptibility to plant pathogen attack (Weisskopf *et al*., 2008). The plant pathogen *Pseudomonas syringae* pv. tomato elicits the secretion of malate in *Arabdopsis thaliana.* This malate secretion selectively recruits the beneficial rhizobacterium *B. subtilis* FB17 in a dose-dependent manner (Rudrappa *et al*., 2008). With this as the case and with malate as a key nutrient for the bacteria, one would also expect sophisticated mechanisms for malate utilization.

B. subtilis produces five malate dehydrogenases, the canonical Mdh of the citric acid cycle, and four decarboxylating malate dehydrogenases, the so-called malic enzymes. Among the malic enzymes, YtsJ reduces $NADP^+$, whereas the three other enzymes reduce NAD^+ (Deutscher *et al*., 1984; Lerondel *et al*., 2006). In addition to the Mdh/PckA-dependent conversion of malate to phosphoenolpyruvate, the entry point of gluconeogenesis, the bacteria require a functional *ytsJ* gene for efficient malate utilization (Lerondel *et al*., 2006). Under gluconeogenic conditions (i.e., with malate as the only carbon source), the cells do not have the possibility to produce NADPH by the pentose phosphate pathway. Under glycolytic conditions, about 40 to 50% of the glucose enters this pathway (Sauer *et al*., 1997; Schilling *et al*., 2007), which yields two molecules of NADPH per molecule of glucose. This represents about 50% of the NADPH formation in the cell and is important to provide reducing power for all biosynthetic reactions in the cell. Thus, the conversion of malate to pyruvate using the NADPH-forming malic enzyme YtsJ may be important to balance the redox pool of the cell and to allow efficient anabolic reactions.

The identification of malate as a carbon source that causes catabolite repression immediately raised the question of how this repression might be achieved. In a previous study, a mechanism independent of CcpA/HPr(Ser-P) was postulated based on the presumptive low concentration of fructose 1,6-bisphosphate (Kleijn *et al*., 2010). Here, we provide unequivocal evidence that catabolite repression by malate involves all factors that also play a role in sugar-mediated catabolite transcriptional repression, i.e., CcpA, HPr, Crh, and HPrK. We demonstrate that these factors are required for malate-mediated catabolite repression and that their interactions occur as in the presence of glucose. These interactions include the phosphorylation of HPr by the HPr kinase (as assayed by the *in vivo* HPr phosphorylation state) and the binding of HPr to CcpA in the presence of glucose or malate. The activity of HPr kinase is the key to carbon catabolite repression in *B. subtilis*, and this activity is mainly controlled by the ATP and the FBP concentrations. At very high ATP concentrations, the enzyme shows kinase activity even in the absence of FBP, but at physiological ATP concentrations FBP acts as an allosteric effector that stimulates kinase activity (Jault *et al*., 2000). Both the genetic and the biochemical evidence presented in this work strongly suggested that HPr kinase is active in the presence of malate as the only carbon source. Indeed, the analysis of the ATP and FBP concentrations was in excellent agreement with this idea. It had been shown before that the ATP pool is quite constant in *B. subtilis* even under conditions of different carbon supply (Ludwig *et al*., 2002b). In contrast, the FBP concentrations are quite low in media that do not contain repressing carbon sources and

are higher in the presence of glucose and other well-metabolizable sugars (Mijakovic *et al*., 2002; Singh *et al*., 2008). Here, we demonstrate that an intermediate FBP concentration is present if the bacteria utilize malate. Similar FBP concentrations were observed for sorbitol-, glycerol- or mannitol-grown *B. subtilis* cells. Strikingly, the strength of *xynB* repression exerted by these sugar alcohols is similar to that observed with malate (Table 3.2) (Singh *et al*., 2008). Our results also are in perfect agreement with *in vitro* studies on the activity of HPrK: at an ATP concentration of 25 µM (i.e., less than detected *in vivo*), 3 mM FBP is sufficient to trigger full HPr kinase activity (Jault *et al*., 2000).

In *B. subtilis*, several *cre* boxes were identified either experimentally (about 50) or on the basis of their strong similarity to the consensus sequence (about 100) (Fujita, 2009). Repression strength is expected to depend on the affinity of the CcpA-HPr(Ser-P) complex for a particular *cre* box. Repression of *sacP* expression was strong in the presence of either glucose or malate when the sequence involved in the induction mechanism (RAT/terminator) was absent of the reporter fusion (i.e., $P_{sacP\Delta RAT\text{-}term}$). This is consistent with the fact that the probable *cre* sequence (TGAAAGCGTATTCT) is highly similar to the consensus (Fujita, 2009). However, our results showed no significant repression by malate of *sacP* expression when the reporter fusion contained the full-length wild-type leader region (i.e., P*sacP*). Besides, repression by glucose of *sacP* expression was also much weaker than that of the constitutive reporter fusion. In addition, the very similar β-glucoside-inducible *bglP* system was more repressed. This suggests that the sucrose-dependent induction mechanism either is strong enough to compensate for the CcpA-mediated catabolite repression or impairs binding of the CcpA-HPr(Ser-P) complex.

Our results indicate that malate is efficiently metabolized and this metabolism generates levels of key intermediates that control catabolite repression similar to those obtained when sugars are utilized. This raises the question how the observed pool of FBP can be reached. The complex pathways of malate metabolism may provide an answer to this question: the Mdh/ PckA pathway, which actually forms a physical complex *in vivo* during growth on malate (Meyer *et al*., 2011), provides the phosphoenolpyruvate that serves as the starting point for gluconeogenesis. In parallel, YtsJ uses malate to generate NADPH. This in turn, is required for the reduction of 1,3-bisphosphoglycerate by the gluconeogenic glyceraldehyde 3-phosphate dehydrogenase GapB. The other gluconeogenic reactions that give rise to FBP all follow Michaelis-Menten kinetics and the corresponding genes are constitutively expressed (Ludwig *et al*., 2001). In contrast, the *pckA* and *gapB* genes are induced under gluconeogenic conditions (Fillinger *et al*., 2000; Servant *et al*., 2005). In addition, the NAD^+-dependent malic enzymes

might serve for the generation of NADH that can drive oxidative ATP synthesis to provide the cell with energy. Thus, once a sufficient amount of malate becomes available, the concerted activity of the different malate dehydrogenases allows the cell to meet the requirements for precursors, reducing power for anabolism, and energy. Thus, the genetic equipment of *B. subtilis* with enzymes active in malate metabolism reflects the important role of this substrate for the organism and provides a possible explanation of how malate causes carbon catabolite repression.

Acknowledgments

We thank Bernard Freytag for his contribution to the initial phase of this project and Sabine Lentes for technical assistance. We are grateful to Heinz Neumann for providing access to the FLUOstar Omega fluorescence reader.

This work was supported by grants from the Federal Ministry of Education and Research SYSMO network (PtJ-BIO/0313978D) and the DFG (Hi 291/131) to J.S. as well as by French public funds from the Centre National de la Recherche Scientifique and the Institut National de la Recherche Agronomique and by a grant from the European Community BaSysBio Programme (LSHG-CT-2006-037469) to S.A.

4. Malate metabolism in *Bacillus subtilis*

The results described in this chapter were published in:

Meyer, F. M. & Stülke, J. (2012). Malate metabolism in *Bacillus subtilis*: distinct roles for three classes of malate-oxidizing enzymes. *FEMS Microbiol Lett*. *in press.*

Author's contribution:

The study was designed and interpreted by FMM and JS. The experiments were done by FMM. The paper was written by FMM and JS.

Abstract

The Gram-positive soil bacterium *Bacillus subtilis* uses glucose and malate as the preferred carbon sources. In the presence of either glucose or malate, the expression of genes and operons for the utilization of secondary carbon sources is subject to carbon catabolite repression. While glucose is a preferred substrate in many organisms from bacteria to man, the factors that contribute to the preference for malate have so far remained elusive. In this work, we have studied the contribution of the different malate-metabolizing enzymes in *B. subtilis*, and we have elucidated their distinct functions. The malate dehydrogenase and the phosphoenolpyruvate carboxykinase are both essential for malate utilization; they introduce malate into gluconeogenesis. The NADPH-generating malic enzyme YtsJ is important to establish the cellular pools of NADPH for anabolic reactions. Finally, the NADH-generating malic enzymes MaeA, MalS and MleA are involved in keeping the ATP levels high. Together, this unique array of distinct activities makes malate a preferred carbon source for *B. subtilis*.

Introduction

The Gram-positive soil bacterium *Bacillus subtilis* can utilize a wide range of carbon sources such as several sugars, complex carbohydrates and organic acids. Among them glucose and malate are the two preferred carbon sources (Kleijn *et al*., 2010). This is an exceptional situation as compared with other heterotrophic bacteria which mostly prefer just one carbon source (glucose) (Görke & Stülke, 2008; Singh *et al*., 2008). If one considers the habitat of *B. subtilis*, the preference for glucose and especially malate is not surprising. In contrast to glucose, malate is commonly available in the soil and on plant surfaces (Bais *et al*., 2006; Rudrappa *et al*., 2008). The unique role of malate in the metabolic network of *B. subtilis* is also underlined by the rapid adaptation to malate. This adaptation occurs mainly at the posttranscriptional level i. e., it is based on already available mRNAs. In contrast, the adaptation from malate to glucose utilization requires a massive reprogramming of transcription (Buescher *et al*., 2012; Nicolas *et al*., 2012). Moreover, malate triggers biofilm formation in *B. subtilis* (Chen *et al*., 2012).

After malate is taken up it enters the TCA cycle at the PEP-pyruvate-oxaloacetate node which connects the TCA cycle with glycolysis/gluconeogenesis (see Fig. 4.1). Here malate can be oxidized either by the malate dehydrogenase (Mdh) to oxaloacetate or by one of four malic enzymes (MaeA, MalS, MleA or YtsJ) to pyruvate through oxidative decarboxylation. After the

oxidation of malate to oxaloacetate by Mdh, oxaloacetate can then be used for gluconeogenesis (phosphoenolpyruvate carboxykinase, PckA), for the synthesis of amino acids (aspartate and asparagine) or can serve as substrate to replenish the TCA cycle (citrate synthase, CitZ).

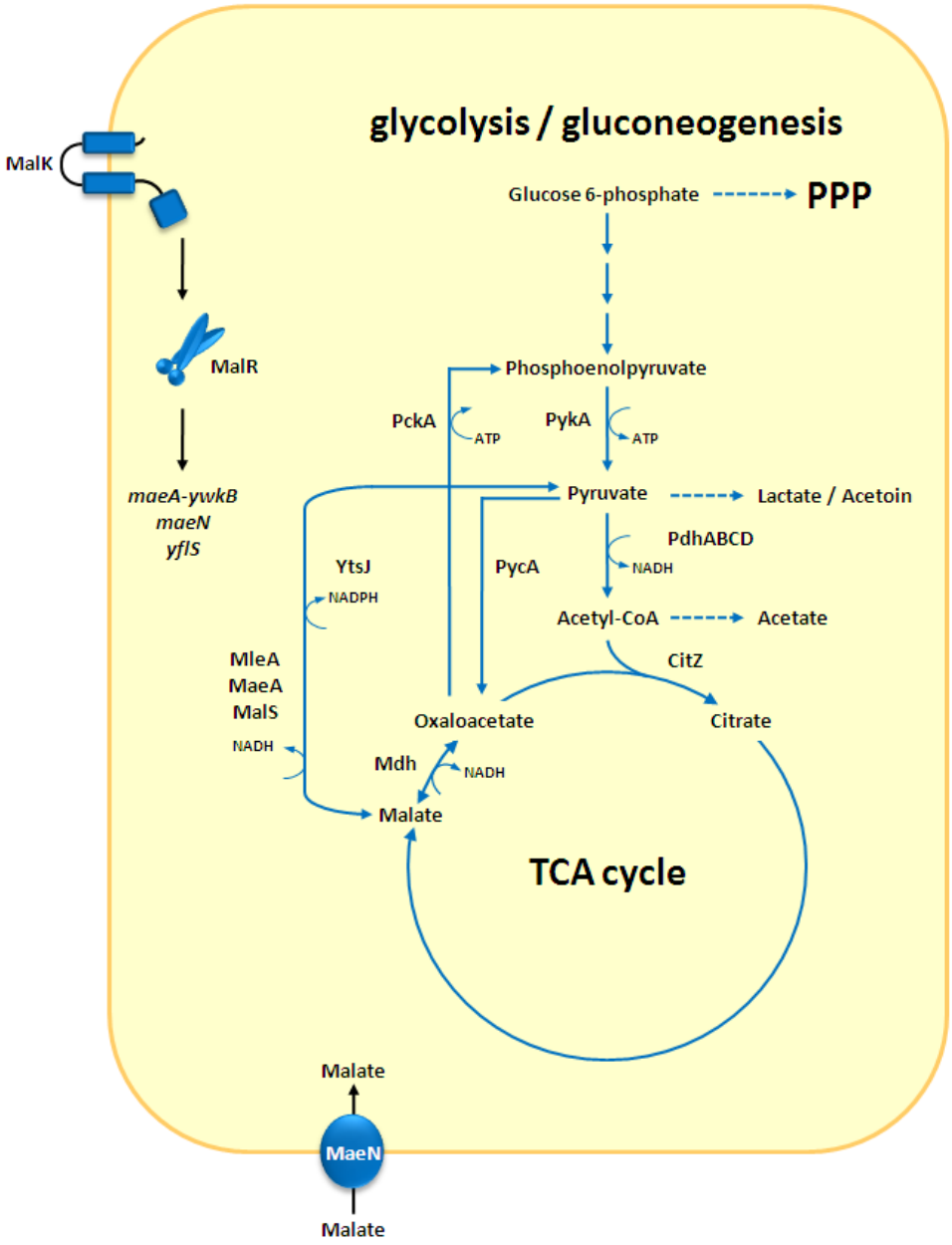

Fig. 4.1. Overview about the PEP-pyruvate-oxaloacetate node, the malate transport and the MalKR two-component system in *B. subtilis*. Abbreviations used in this figure: CitZ, citrate synthase; MaeA, malic enzyme; MaeN, Na+/malate symporter; MalK, two-component sensor kinase; MalR, two-component response regulator; MalS, malic enzyme; Mdh, malate dehydrogenase; MleA, malic enzyme; PdhABCD, pyruvate dehydrogenase; PckA, phosphoenolpyruvate carboxykinase; PPP, pentose phosphate pathway; PycA, pyruvate carboxylase; PykA, pyruvate kinase; *yflS*, malate transporter; YtsJ, malic enzyme; *ywkB*, unknown.

In contrast to the Mdh-PckA pathway the conversion to pyruvate catalyzed by the malic enzymes mainly ends in the production of acetyl coenzyme A or in the production of the overflow metabolites lactate and acetate (Kleijn *et al*., 2010). A recent metabolic flux analysis of *B. subtilis* cells grown in a medium with malate as the single carbon source demonstrated that only 10% of the malate is oxidized in the TCA cycle to CO_2. In contrast, approximately 90% of the malate is oxidized through the Mdh-PckA or malic enzyme pathways. Interestingly both oxidation routes, through the malic enzymes or through Mdh, are almost equally used (Kleijn *et al*., 2010). Nevertheless not much is known about the precise role of the malic enzymes in *B. subtilis*. *B. subtilis* codes for three NAD-dependent malic enzymes (MaeA, MalS and MleA) and one NADP-dependent malic enzyme (YtsJ) (Lerondel *et al*., 2006). Malic enzymes are widely distributed in eukaryotes as well as in prokaryotes. The majority of the sequenced bacterial genomes encode at least one putative malic enzyme, in most cases a YtsJ-like NADP-dependent malic enzyme. The existence of four paralogous isoforms in one species is rather uncommon (Lerondel *et al*., 2006). In *B. subtilis*, YtsJ was already described to play the major physiological role while the functions of the NAD-dependent malic enzymes have remained elusive (Lerondel *et al*., 2006).

In this work we demonstrate the essential role of the Mdh-PckA pathway of *B. subtilis* for the utilization of malate. Furthermore we show that the loss of the NAD-dependent malic enzymes (MaeA, MalS and MleA) but also the loss of the NADP-dependent malic enzyme YtsJ leads to reduced intracellular ATP levels.

Materials and Methods

Bacterial strains and growth conditions - The *B. subtilis* strains used in this study are listed in Table 8.3. *B. subtilis* was grown in C minimal medium supplemented with carbon sources and auxotrophic requirements (at 50 mg l^{-1}) as indicated (Commichau *et al*., 2007b). Carbon sources were used at a concentration of 0.5% (w/v). SP plates were prepared by the addition of 17 g l^{-1} Bacto agar (Difco) to the medium.

Construction of mutants affected in malate metabolism - Deletion of the *mleA* gene was achieved by transformation with PCR products constructed using oligonucleotides (available upon request) to amplify DNA fragments flanking the *mleA* gene and an intervening chloramphenicol resistance cassette (Guérot-Fleury *et al*., 1995) as described previously (Wach,

1996). The *ytsJ* mutant was obtained by a transposon mutagenesis with pIC333 (Steinmetz & Richter, 1994).

Transformation of B. subtilis - Chromosomal DNA of *B. subtilis* was isolated using the DNeasy Tissue Kit (Quiagen) according to the supplier's protocol. *B. subtilis* was transformed with plasmids and chromosomal DNA according to the two-step protocol (Kunst & Rapoport, 1995). Transformants were selected on SP plates containing spectinomycin (150 µg ml^{-1}), chloramphenicol (5 µg ml^{-1}), or kanamycin (10 µg ml^{-1}).

Determination of ATP concentrations - Intracellular ATP levels were determined as described previously (Ludwig *et al*., 2002). Exponentially growing cultures were quenched at an OD_{600} of 0.5 by mixing with dimethyl sulfoxide (DMSO) which released the adenine nucleotides from the cells. ATP levels were measured using an ATP bioluminescence assay kit (CLSII, Roche Diagnostics) and a microplate fluorescence reader (FLUOstar Omega, BMG Labtech). For calculating the concentrations of intracellular ATP we used the previously reported aqueous cell volume of 0.85 µl of a culture of 1 ml at an OD_{600} of 1 (Fujita and Freese, 1979).

Results

Impact of different enzymes on the utilization of malate as a single carbon source - The precise contributions of *B. subtilis* malate dehydrogenases to the utilization of malate as a single carbon source are unknown, although Mdh and YtsJ were described to be the major players in malate utilization (Lerondel *et al*., 2006). To address this issue further, we cultivated deletion mutants of each of the enzymes in minimal medium with glucose or malate as the single carbon source. All strains grew similarly with glucose as the only carbon source (see Fig. 4.2). In contrast, the *mdh* mutant was unable to grow with malate as the only source of carbon and energy. In agreement with previous observations (Lerondel *et al*., 2006), the *ytsJ* mutant affecting the NADP-dependent malic enzyme exhibited a reduced growth with malate whereas the mutants defective in the NAD-dependent malic enzymes were not affected (see Fig. 4.2). These results suggest unique roles for the tricarboxylic cycle enzyme Mdh and the NADP-dependent malic enzyme YtsJ: While Mdh seems to be essential for malate utilization; YtsJ may have a distinct function, most likely in the production of NADPH for biosynthetic purposes.

If the oxidation of malate to oxaloacetate was the major pathway for malate utilization, one would expect that a *pckA* mutant that is unable to convert oxaloacetate to the glycolytic intermediate phosphoenolpyruvate is also impaired in the utilization of malate. However, if the

generation of oxaloacetate as precursor for aspartate was the major role of Mdh, then a *pckA* mutant would be expected to have a minor impact on malate utilization. To distinguish between these alternatives, we assayed the growth of the *B. subtilis* wild type strain 168 and the isogenic *pckA* mutant GP1147 in minimal medium with glucose or malate. As shown in Fig. 4.2, the *pckA* deletion did not affect glucose utilization. This observation is in agreement with previous observations (Tännler *et al*., 2008). With malate as the only carbon source, the *pckA* mutant did not grow at all, and was in this respect indistinguishable from the *mdh* mutant (see Fig. 4.2). These data support the idea that the Mdh-PckA route is the essential pathway for the utilization of malate in *B. subtilis*. However, the different pathways of malate utilization are likely to run in parallel.

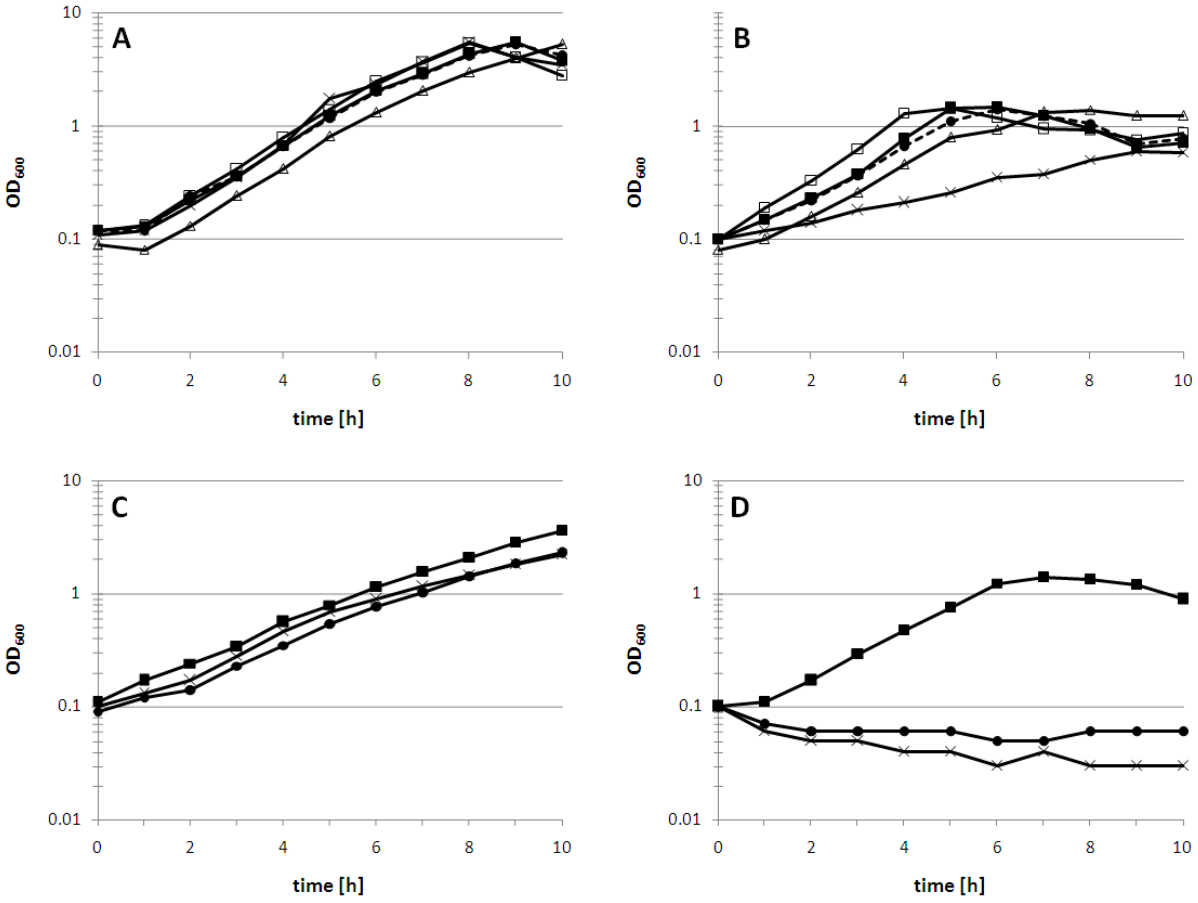

Fig. 4.2. Growth of various *B. subtilis* mutants involved in malate metabolism in minimal medium with glucose (A and C) and minimal medium with malate (B and D). *B. subtilis* strains (A and B): wild type (168), ■; Δ*mleA* (GP1136), □; Δ*malS* (GP1142), ●; Δ*maeA* (GP1141), Δ; Δ*ytsJ* (GP1143), x. *B. subtilis* strains (C and D): wild type (168), ■; Δ*pckA* (GP1147), x; Δ*mdh* (GP1150), ●.

The role of the malic enzymes in the ATP supply of B. subtilis - Malate is one of the preferred carbon sources that triggers carbon catabolite repression in *B. subtilis*. The signal for catabolite repression is generated by the HPr kinase that responds to the cellular ATP and fructose-1.6-bisphosphate pools (Singh *et al*., 2008). Surprisingly, these pools are sufficient to activate the HPr kinase during growth with malate (Meyer *et al*., 2011b). To further elucidate the role of the malic enzymes in the metabolism of *B. subtilis* we determined the contribution of the different enzymes to the ATP levels of the cell. ATP can be produced either by substrate-level phosphorylation or by the use of the respiratory chain. Especially the production of NADH by the NADH-forming malic enzymes, which then can be used for the production of ATP through the respiratory chain of the cell, might be an important contribution of these enzymes.

Thus we determined the intracellular ATP concentrations in wild type and in malic enzyme mutants grown in minimal medium with glucose or with malate. As shown in Table 4.1, the intracellular ATP concentration in wild type cells grown in minimal medium with glucose was 83.10 µM. The ATP concentrations in the various malic enzyme mutants grown in the same medium was similar to the wild type level and fluctuated in a range of about 80 µM. When we analyzed the ATP level of wild type cells grown in malate minimal medium we determined an ATP concentration of 76.17 µM, a slightly lower ATP concentration as compared to the values of glucose-grown cells. A somewhat lower concentration (73.15 µM) was detected for the *mleA* mutant. In contrast to the *mleA* mutant the ATP concentration in the *maeA* and the *malS* mutants was decreased by about 10 % (*maeA*, 67.74 µM; *malS*, 69.97 µM).

Next we analyzed the ATP concentration in a *maeA malS* double mutant and in a triple mutant lacking all three NADH-forming malic enzymes (Δ*maeA* Δ*malS* Δ*mleA*) grown in minimal medium with malate. As described above, all single mutants of the NADH-forming malic enzymes did not show a growth defect in minimal medium with malate. The growth rate of the double mutant (Δ*maeA* Δ*malS*) was as well comparable with the wild type whereas the triple mutant showed a moderate growth defect. This observation is in agreement with previous observations (Lerondel *et al*., 2006). In the double mutant we detected an ATP level reduction of about 10%, a similar ATP concentration compared to the single mutants (see Table 4.1). When we analyzed a mutant lacking all three NADH-forming malic enzymes the reduction had accumulated to about 20% (60.70 µM). To determine whether these changes are significant, we performed a Student's test. The p-values were found to be 0.018 and 0.002 for the double and triple mutant, respectively, indicating that the reduction of the ATP pool was statistically significant.

Finally we analyzed the ATP concentration of the mutant of the NADPH-forming malic enzyme *ytsJ*. Interestingly the ATP concentration in the *ytsJ*-mutant was decreased by about 20% and thus comparable with the triple mutant of the NADH-forming malic enzymes. For the *ytsJ* mutant the p-value was 0.001 indicating that the reduction was significant.

Table 5.1. Impact of different malic enzymes mutants on the pool of ATP in *B. subtilis*

	ATP, µM[1]	
Strain	**C-Glucose**	**C-Malate**
168	83.10 (4.78)	76.17 (3.65)
GP1136 (*ΔmleA*)	84.95 (3.19)	73.15 (4.79)
GP1141 (*ΔmaeA*)	79.48 (2.32)	67.74 (1.73) *****
GP1142 (*ΔmalS*)	78.77 (4.87)	69.97 (5.11)
GP1143 (*ΔytsJ*)	80.41 (2.82)	59.53 (3.46) *****
GP1446 (*ΔmaeA ΔmalS*)	82.03 (3.90)	68.50 (2.50) *****
GP1448 (*ΔmaeA ΔmalS ΔmleA*)	78.18 (2.67)	60.70 (1.98) *****

[1] All measurements were performed at least in triplicate. Values in parentheses indicate the standard deviations

***** *P*-values versus WT (*****$P < 0.05$)

Discussion

B. subtilis produces five malate dehydrogenases, the canonical Mdh of the citric acid cycle, and four decarboxylating malate dehydrogenases, the so-called malic enzymes. Among the malic enzymes, YtsJ reduces $NADP^+$, whereas the three other enzymes reduce NAD^+ (Doan *et al*., 2003, Lerondel *et al*., 2006). Our analysis of the mutants affected in malate metabolism revealed that malate dehydrogenase (Mdh) and the subsequent enzyme, PEP carboxykinase (PckA), are both essential for the utilization of malate as the only carbon source. This common function of the two enzymes is in good agreement with their recently observed physical interaction (Meyer *et al*., 2011a). In addition to the Mdh/PckA-dependent conversion of malate to phosphoenolpyruvate, the entry point of gluconeogenesis, the bacteria require a functional *ytsJ* gene for efficient malate utilization. Under gluconeogenic conditions (i. e. with malate as the only carbon source) the cells do not have the possibility to produce sufficient NADPH by the pentose phosphate pathway. Under glycolytic conditions, about 40 to 50% of the glucose enters this pathway (Sauer *et al*., 1997, Schilling *et al*., 2007) that yields two molecules of NADPH per molecule of glucose. This represents about 50% of the NADPH formation in the cell and is important to provide reducing power for all biosynthetic reactions in the cell. Thus, the conversion of malate to pyruvate using the NADPH-forming malic enzyme YtsJ may be important

to balance the redox pool of the cell and to allow efficient anabolic reactions (Kleijn *et al*., 2010). Interestingly, malic enzyme deletion mutants exhibit increased fluxes through the pentose phosphate pathway (Lerondel *et al*., 2006). However, a gluconeogenic flux to the pentose phosphate pathway requires ATP and might explain the low ATP levels especially in the *ytsJ* mutant. In contrast, none of the NADH-forming malic enzymes seems to be important for malate utilization. This result is quite surprising since the expression of one of the corresponding genes, *maeA*, is strongly induced by malate (Doan *et al*., 2003). The findings reported in this work suggest that the malic enzymes MaeA and MalS contribute to the ATP pool of the cells by providing $NADH^+$.

The unique arrangement of redundant yet functionally specialized enzymes that allows efficient introduction of malate into gluconeogenesis and the TCA cycle, and that provides the cell with high $NADPH^+$ and ATP pools may make malate the second preferred carbon source of *B. subtilis* in addition to glucose.

Acknowledgements

We are grateful to Aneta Żelazo for the help with some experiments and to Heinz Neumann for providing access to the FLUOstar Omega fluorescence reader. This work was supported by a grant of the Federal Ministry of Education and Research SYSMO network (PtJ-BIO/0313978D) to J. S.

5. TCA branch gene expression in *Bacillus subtilis*

The results described in this chapter are to be published in:

Pechter, K. B., **Meyer, F. M.**, Serio, A. W., Stülke, J. & Sonenshein, A. L. (2012). Two roles for aconitase in the regulation of tricarboxylic acid branch gene expression in *Bacillus subtilis*. *J. Bacteriol*. *in revision.*

Author's contribution:

The study was designed and interpreted by KBP, ALS, FMM and JS. Construction of the mutants was done by KBP and ALS. Enzyme assays and western blot analysis were performed by KBP. Northern blot analysis and gel mobility shift assays were done by FMM. Filter binding assays were performed by KBP. The paper was written by KBP and ALS.

Abstract

Previously, it was shown that an aconitase (*citB*) null mutation results in a vast over accumulation of citrate in the culture fluid of growing *Bacillus subtilis* cells, a phenotype that causes secondary effects, including the hyperexpression of the *citB* promoter. *B. subtilis* aconitase is a bifunctional protein; to determine if either or both activities of aconitase were responsible for this phenotype, two point mutants were constructed, one designed to be an enzymatically inactive (C450S; *citB2*) and a second mutant designed to be defective in RNA binding (R741E; *citB7*). The *citB2* mutant was a glutamate auxotroph and accumulated citrate, while the *citB7* mutant was a glutamate prototroph. Unexpectedly, the *citB7* strain also accumulated citrate. Both mutant strains exhibited overexpression of the *citB* promoter and accumulated high levels of aconitase protein. These strains and the *citB* null mutant also exhibited increased levels of citrate synthase protein and enzyme activity in cell extracts, and the major citrate synthase (*citZ*) transcript was present at higher-than-normal levels in the *citB* null mutant, due at least in part to a more than three-fold increase in the stability of the *citZ* transcript compared to wild-type. Purified *B. subtilis* aconitase bound to the *citZ* 5' leader RNA *in vitro*, but the mutant proteins did not. Together these data suggest that wild-type aconitase binds to and destabilizes the *citZ* transcript in order to maintain proper cell homeostasis by preventing the over-accumulation of citrate.

Introduction

Elimination of any one of the three enzymes of the tricarboxylic acid (TCA) branch of the Krebs cycle (citrate synthase, aconitase, and isocitrate dehydrogenase) results in glutamate auxotrophy and a significant defect in spore formation in *B. subtilis* (Craig *et al*., 2007; Jin *et al*., 1997; Jin & Sonenshein, 1994; Matsuno *et al*., 1999). In particular, a null mutation in the aconitase (*citB*) gene causes a dramatic increase in the concentration of citrate in the culture fluid of growing cells (Craig *et al*., 2007). This accumulation of citrate prevents sporulation due to chelation by citrate of divalent cations required for proper functioning of the Spo0A initiated phosphorelay (Craig *et al*., 2007; Matsuno *et al*., 1999).

We had assumed that *citB* null cells accumulate citrate simply because of the lack of aconitase enzyme activity present in this strain. As *B. subtilis* lacks a citrate lyase enzyme, *citB* null cells have no way of enzymatically removing the citrate once it is formed; thus, the citrate

accumulation phenotype has been solely attributed to this metabolic roadblock. However, in this report we present data suggesting that the actual mechanism is more complex.

B. subtilis expresses one aconitase and two citrate synthase enzymes (Dingman & Sonenshein, 1987; Jin & Sonenshein, 1994a). Aconitase is encoded by the *citB* gene in a single-gene transcription unit (Dingman & Sonenshein, 1987). The gene for the major citrate synthase, *citZ*, is the first gene in an operon that also includes the genes for isocitrate dehydrogenase (*icd* or *citC*) and malate dehydrogenase (*mdh* or *citH*). The gene for the minor citrate synthase, *citA*, is present at a separate locus and is expressed as a monocistronic RNA (Jin & Sonenshein, 1994a, Jin & Sonenshein, 1994b). The coordinated expression of *citZ*, *icd* and *citB* is controlled by three regulatory proteins (CcpA, CcpC, and CodY) that independently sense the nutritional state of the cell by interacting with specific metabolites [reviewed in (Sonenshein, 2007)]. While CcpA and CodY are global regulatory proteins that respond to specific metabolites (fructose-1,6-bisphosphate for CcpA; GTP and branched-chain amino acids for CodY), regulation by CcpC is specific to the TCA branch genes and responds to citrate. Antagonism of CcpC-dependent repression of the *citB* and *citZ* promoters by citrate has been described in detail (Jourlin-Castelli *et al*., 2000; Kim *et al*., 2003a; Kim *et al*., 2003b). When citrate is absent, CcpC binds to sites in or near the *citB* and *citZ* promoters and blocks expression of these genes. When citrate is present, it causes a change in the interaction of CcpC with its binding sites, resulting in derepression of *citB* and *citZ*. When citrate is very abundant, CcpC activates *citB* expression, presumably reflecting a change in the interaction of CcpC with RNA polymerase (Mittal *et al*., 2012).

In addition to having enzymatic activity, the *B. subtilis* aconitase protein has a second function as an RNA-binding regulatory protein (Alén & Sonenshein, 1999; Serio *et al*., 2006). Whether aconitase is active as an enzyme or an RNA-binding protein is determined by the status of an iron-sulfur (4Fe-4S) cluster that is essential for the catalytic activity of all aconitases in nature (Beinert, 2000). The 4Fe-4S cluster interacts directly with the enzyme substrates and products (citrate, *cis*-aconitate, isocitrate), and thus is exposed to solvent. This positioning makes the cluster vulnerable to oxidation by reactive oxygen species. At low levels of oxidation, one of the four iron atoms, Fe_a, is lost, resulting in a catalytically inactive 3Fe-4S cluster (Imlay, 2006). The inactive form of the enzyme is also subject to more extensive cluster disassembly, resulting in an apoprotein that lacks the cluster entirely. The classic bifunctional aconitase, eukaryotic iron regulatory protein 1 (IRP1), is a cytosolic protein that responds to cellular iron levels by alternating between two functional states: the iron-sulfur cluster-containing aconitase enzyme and the RNA-binding apoprotein, which acts as a post transcriptional regulator (Emery-

Goodman *et al*., 1993; Haile *et al*., 1992; Kennedy *et al*., 1992). IRP1 regulates mRNA translatability or stability by binding to iron regulatory elements (IREs), stem-loop structures present in the 5' or 3' untranslated regions (UTRs) of mRNA (Beinert, 2000). IREs are found in the mRNAs of genes involved in the uptake, transport, and storage of iron (Haile, 1999). Since the discovery of IRP1, bifunctional aconitases have been described in prokaryotes, including *Escherichia coli* (Tang & Guest, 1999), *Mycobacterium tuberculosis* (Banerjee et al., 2007), and *B. subtilis* (Alén & Sonenshein 1999; Serio *et al*., 2006).

Recent work in our laboratory with an aconitase mutant (*citB5*) defective in RNA-binding has provided an unexpected twist on the question of citrate accumulation in a *citB* null mutant. The *citB5* mutant is a glutamate prototroph and exhibits high levels of aconitase activity in cell extracts (Serio *et al*., 2006), indicating that it has ample capacity to metabolize citrate. However, the *citB5* mutant also accumulates citrate in the culture fluid at levels near those generated by the *citB* null mutant strain (Serio, 2005). This result suggests that there is a connection between aconitase RNA binding activity and citrate accumulation, and thus a more complex relationship than originally assumed between the activity of aconitase and the pool of citrate. In the current work, we sought to examine the roles of the individual functions of aconitase in the maintenance of citrate levels within the cell. Mutant *citB* alleles were created in an attempt to study the two functions of aconitase separately *in vivo*. Through work on these mutants, we established that mutations in aconitase lead to overproduction of both aconitase itself and citrate synthase. In addition, we present evidence that aconitase directly regulates citrate synthase production by interacting with the *citZ* transcript. The data presented here support a new model in which both functions of aconitase contribute to the maintenance of citrate levels in *B. subtilis*.

Materials and methods

Bacterial strains and growth conditions - *E. coli* strains DH5α and JM107 were used as hosts for cloning; they were grown in L broth or on L agar plates supplemented with ampicillin (50 μg/ml) when necessary (Miller, 1972). All *B. subtilis* strains used in this work are listed in Table 8.3. Unless otherwise indicated, *B. subtilis* was grown at 37°C with aeration in DS medium [0.8% nutrient broth, 0.1% KCl, 0.025% $MgSO_4x7H_2O$, 1 mM $Ca(NO_3)_2$, 10 μM $MnCl_2$, 1 μM $FeSO_4$ (Fouet & Sonenshein, 1990)]. When necessary, DS medium was supplemented with chloramphenicol (2.5 μg/ml), tetracycline (15 μg/ml), spectinomycin (50 μg/ml) or 5-bromo-4-

chloro-3-indolyl-β-galactopyranoside (X-Gal; 80 µg/ml). TSS minimal medium [0.05 M Tris (pH 7.5), 40 µg each of $FeCl_3x6H_2O$ and trisodium citrate dihydrate per ml, 2.5 mM K_2HPO_4, 0.02% $MgSO_4x7H_2O$, 0.5% glucose (Fisher & Magasanik, 1984a)], supplemented with tryptophan (0.004%) and phenylalaline (0.004%), was utilized for the determination of glutamate auxotrophy. When necessary, glutamine (0.2%) was added. CSE minimal medium [70 mM K_2HPO_4, 30 mM KH_2PO_4, 25 mM $(NH_4)_2SO_4$, 0.5 mM $MgSO_4$, 10 mM $MnSO_4$ (Wacker *et al*., 2003)] was supplemented with ferric ammonium citrate (0.0022%), sodium succinate (0.6%), potassium glutamate (0.8%) and tryptophan (0.005%) and utilized in Northern blotting experiments.

Construction of the citB2 mutant - To create a point mutant defective in aconitase enzyme activity, cysteine residue 450, a residue integral to the 4Fe-4S cluster, was mutated to serine. To do so, the promoter region and N-terminal portion of *citB* with a decahistidine tag were amplified and mutagenized by site-directed PCR mutagenesis. The template was genomic DNA from strain AWS198 [His10-*citB*$^+$::pAWS50(*cat*)] (Serio *et al*., 2006). Primer citBF6 (5'GGGCATGCGAGAACCTCCTTAAAAGAGTTCGGTGTTATT; *Sph*I restriction site is underlined) and mutagenic primer OKP37 (5'GTTTGATGTATTTGT**AGA**GCTTGTAATCGCAGCAATGGC; mutated residues are in bold) were used to amplify the *citB* locus from 400 bp upstream to 1365 bp downstream of the start codon. Mutagenic primer OKP36 (5'GCTGCGATTACAAGC**TCT**ACAAATACATCAAACCCATACGTG; mutated residues are in bold) and primer OKP38 (5'ATACCCGGGTTGACCATCCTTGCCCACACC; *Xma*I restriction site is underlined) were used to amplify *citB* from 1333 bp to 1785 bp downstream of the start codon. The products of the two reactions were annealed and amplified using citBF6 and OKP38, yielding a final product of 2203 bp. That product was purified, digested with restriction enzymes *Sph*I and *Xma*I, and ligated to the *B. subtilis* integrative vector pJPM1 (Mueller et al., 1992), creating pKP12. After transformation of *E. coli* and verification of its structure, pKP12 was used to transform *B. subtilis* strain AWS96. Chloramphenicol resistance was used to select for integration of pKP12 at the *citB* locus by homologous recombination, creating strain KBP17 [His_{10}-*citB2*::pKP12(*cat*)]. The serial passage of KBP17 in L broth, without selection, to obtain a second crossover (and thus, an unmarked *citB2* strain) resulted in the isolation of KBP22, a strain that had retained the *citB2* allele, and lost the integrated plasmid, but acquired a suppressor mutation (*citZ340*). The *citB2* mutation was separated from *citZ340* by introducing genomic DNAs from strains KBP22 and KBP94 (*amyE*::*citBp21-lacZ tet*) simultaneously into the wild type strain AWS96. (In such experiments, 5-10% of transformants selected for one marker will have acquired a second, unlinked marker by congression.) Tetracycline-resistant

transformants were isolated on DS medium containing X-Gal and blue colonies were selected, indicative of derepressed expression of the *citB-lacZ* fusion. The resulting strain was KBP118 (*citB2 amyE*::*citBp21-lacZ tet*).

Isolation of the citZ340 mutation - Genomic DNA from strain KBP22 was introduced into strain SJB231 (*citZC*::*spc*) along with pAF23 plasmid DNA (*amyE*::*citBp23-lacZ cat*). Chloramphenicol-resistant transformants were isolated on DS medium and screened for spectinomycin sensitivity and glutamate auxotrophy. The resulting strain was KBP86 (*citZ340 amyE*::*citBp23-lacZ cat*).

Construction of the citB7 mutant - A single amino-acid substitution expected to reduce RNA binding was introduced into the *citB* gene by transformation with a PCR product. The substitution, arginine-741 to glutamate, was engineered by site-directed mutagenesis. Primers OKP71 (5'ATAGCATGCAGCGGTTGAGTTAGGGCTTAAG; *Sph*I restriction site is underlined) and mutagenic primer OKP73 (5'GATTTGGTTTTTGAT**TTC**AATGTTGGCAAATGTTCCTCTC; mutated residues are in bold) were used to amplify the *citB* locus from positions 1404 bp to 2238 bp downstream of the start codon. Mutagenic primer OKP74 (5'ACATTTGCCAACATT**GAA**ATCAAAAACCAAATCGCACCG; mutated residues are in bold) and primer OKP72 (5' ATACCCGGGATTGATTCATCAGGACTGCTTCATTTTTTCACGAAGC; *Xma*I site is underlined) were used to amplify the *citB* locus from 2206 bp downstream of the start codon to the stop codon. The products of the reactions were annealed and amplified with primers OKP71 and OKP72, yielding a final product of 1341 bp (including restriction site overhangs on the outside primers). The final product was purified and introduced into *B. subtilis* strain AWS96 by transformation along with genomic DNA from strain AF21 (*amyE*::*citBp21-lacZ cat*). Chloramphenicol-resistant transformants were selected on DS medium containing X-Gal, and blue colonies were purified. The *citB* locus was amplified by PCR and sequenced to confirm the presence of the *citB* R741E mutation. The resulting strain, KBP72 (*citB7 amyE*::*citBp21-lacZ cat*), also had an unplanned silent mutation near the 3' end of the gene. Genomic DNA from AWS173 was introduced into KBP72 by transformation to replace the *amyE* cassette, and tetracycline-resistant clones were selected, resulting in strain KBP81 (*citB7 amyE*::*citBp21-lacZ tet*).

Construction of a citB integrative vector and derivative strains - To create a marked but untagged *citB* construct for genetic manipulations in *B. subtilis*, primers citMF1 [5'GCGTCTAGAACCGTAACTTTGAAGGACGTATTCAC; *Xba*I restriction site is underlined, (Serio *et al*., 2006)] and OKP11 (5'AATAAGAGCTCGATTCATCAGGACTGCTTC; *Sac*I site) were used to amplify the C-terminal 1.2 kb of the *citB* gene. The resulting PCR product was digested with *Xba*I

and *Sac*I and ligated to pJPM1 digested with the same enzymes, producing plasmid pKP29. This plasmid was introduced into *E. coli* by transformation and the sequence was verified before introduction into *B. subtilis* strain AWS96 by single-crossover at the *citB* locus, producing KBP125 [*citB*$^{+}$::pKP29(*cat*)]. Genomic DNA from KBP125 was introduced into strain KBP94, producing strain KBP127 [*citB*$^{+}$::pKP29(*cat*) *amyE*::*citBp21-lacZ tet*). To create a marked version of the *citB2* allele, genomic DNA from KBP125 was introduced into strain KBP22, producing strain KBP126 [*citB2*::pKP29(*cat*) *citZ340*]. Genomic DNA from KBP126 was then used to transform KBP94 to chloramphenicol resistance, and transformants that retained hyper-expression of the *citB-lacZ* reporter on DS medium containing X-gal were selected. The resulting strain was KBP128 [*citB2*::pKP29(*cat*) *amyE*::*citBp21-lacZ tet*]. To create a marked version of the *citB7* allele, genomic DNA from KBP125 was introduced into strain KBP81, producing strain KBP129 [*citB7*::pKP29(*cat*) *amyE*::*citBp21-lacZ tet*]. To create isogenic strains for the analysis of the effect of a *ccpC* mutation on the phenotypes due to the *citB2* and *citB7* mutations, genomic DNA from strains KBP127, KBP128 and KBP129 was introduced into strains KBP85 (*amyE*::*citBp21-lacZ tet*) and KBP96 (*ccpC amyE*::*citBp21-lacZ tet*), producing strains KBP135, KBP136, KBP137, KBP138, KBP139 and KBP140 (see Table 8.3).

Preparation of cell extracts for enzyme assays and Western blots - *B. subtilis* cells in DS broth were collected by centrifugation, washed in TEG buffer (20 mM Tris, pH 8; 1 mM EDTA; 20% glycerol) and stored at -20°C. Thawed cells were resuspended in the same buffer supplemented with 0.1 mM phenylmethylsulfonyl fluoride (PMSF) and incubated with 0.4 mg lysozyme per ml for 30 minutes at 37°C. If necessary, the resulting lysate was gently sonicated on ice to break up genomic DNA using a Branson Sonifier (30% duty, level 2, 30 second intervals with 20 second rests, 3-4 times). Sonication was avoided, if possible, due to negative effects on aconitase enzyme activity; importantly, samples were treated identically within a single experiment. Cell extracts were clarified by centrifugation at 16,000 × *g* for 10 - 15 minutes at 4°C. Clarified extracts were kept on ice and assayed immediately for aconitase and citrate synthase activities. Protein concentrations of the samples were determined by the Bradford assay using the Bio-Rad reagent and bovine serum albumin (BSA) as a standard.

Aconitase activity assay - Aconitase enzyme activity was determined by established methods (Dingman & Sonenshein, 1987; Kennedy *et al*., 1983). One unit of activity is equivalent to 1 nmol *cis*-aconitate produced per minute, and units are expressed per milligram of protein (U/mg).

Citrate synthase activity assay - Citrate synthase activity was determined using previously described methods with slight modifications (Fortnagel & Freese, 1968; Jin, 1995; Srere *et al*., 1963). Briefly, 10 µl of cell extract or purified protein was mixed with 0.1 mM 5,5'-dithiobis(2-nitrobenzoic acid) (DTNB) and 0.3 mM acetyl CoA in TEG buffer (see above). All steps were carried out at room temperature. After a 3 minute pre-incubation, the absorbance at 412 nm (A_{412}) was measured to obtain a background reading before oxaloacetate was added to 1 mM. Samples were incubated for 10 minutes and the A_{412} was measured to detect the formation of the TNB^{2-} ion. The corrected value (Riddles *et al*., 1983) for the TNB^{2-} ion extinction coefficient (e = 14.15 ml cm^{-1} μmol^{-1}) was utilized, and citrate synthase specific activity was expressed as micromoles of TNB^{2-} produced (i.e., CoA released) per minute per milligram of protein (µmol/min/mg).

Determination of extracellular citrate concentrations - To determine the extracellular concentration of citrate in broth cultures, *B. subtilis* cells grown in DS medium were removed by centrifugation. The culture fluid was stored on ice and analyzed using a citric acid detection kit (R-Biopharm) according to the manufacturer's instructions.

β-galactosidase activity assays - For β-galactosidase activity assays, samples (0.5 - 1 ml) were removed from *B. subtilis* DS broth cultures during growth after determining the absorbance at 600 nm (A_{600}) of the culture at that time point. Cells were pelleted by centrifugation and pellets were frozen on dry ice. Cells were permeabilized and assayed as described previously (Belitsky *et al*., 1995). β-galactosidase activity (Miller Units) was calculated as described previously (Miller, 1972); however, a correction factor of 1.25 was used to account for the contribution of the sodium carbonate to the final reaction volume.

Western blot analysis of cell extracts - Preparation of cell extracts for Western blot analysis of aconitase, citrate synthase, and isocitrate dehydrogenase levels is described above. When comparing extracts, equivalent amounts of protein (~0.5 µg) were subjected to SDS-10% polyacrylamide gel electrophoresis (PAGE) before transfer to an Immobilon polyvinylidene difluoride (PVDF) membrane (Millipore). Reconstituted non-fat dry milk (5%) was used as a blocking agent and washes were performed in Tris-buffered saline (pH 8). Polyclonal antibodies raised in rabbits to *B. subtilis* aconitase (Serio, 2005), citrate synthase (Jin & Sonenshein, 1996), isocitrate dehydrogenase (K. Matsuno and A. L. Sonenshein, unpublished data), and CodY (Ratnayake-Lecamwasam *et al*., 2001) were used. Anti-rabbit IgG secondary antibodies conjugated to horseradish peroxidase (Upstate Biotechnology, Inc.) were used, and blots were

developed using the ECL Plus western blotting kit (GE Healthcare), respectively. Quantification of blots was performed using ImagQuant TL software (GE Healthcare).

Northern blotting analysis - For all Northern blot experiments, cells were grown in CSE minimal medium and harvested in exponential phase (OD_{600} = 0.5). Total RNA and Northern blot analysis were carried out as described previously (Ludwig *et al*., 2001). Digoxigenin-(DIG-) labeled RNA probes were obtained by *in vitro* transcription with T7 RNA polymerase (Roche Diagnostics) using PCR-generated DNA fragments as templates. The primer pair FM167 (5´GCGACACGCGGTCTTGAAGGG) and FM168 (5´CTAATACGACTCACTATAGGGAGAGGCGGATCAGACGGTTGTTGTC; T7 promoter sequence underlined) was used to amplify the *citZ* open reading frame (ORF) from positions 7 to 1057 bp. The primer pair FM174 (5'CAGTCTCTAACGGAGTATTAAACGTACC) and FM175 (5'CTAATACGACTCACTATAGGGAGAGCCGCTTCGTTCCATCCTAAATGC; T7 promoter sequence underlined) was used to amplify the *icd* ORF from positions 23 to 1137 bp, and primer pair FM176 (5'CGGAGCAGGTTTTACCGGAGCT) and FM177 (5'CTAATACGACTCACTATAGGGAGAGATTCAACTGATTTATTCAGCTGCGCTC) was used to amplify the *mdh* ORF from positions 33 to 909 bp. *In vitro* RNA labeling, hybridization and signal detection were carried out according to the manufacturer's instructions (Roche Diagnostics). The sizes of the transcripts were estimated based on transcripts of the *gapA* operon (Ludwig *et al*., 2001). RNA stability was analyzed as described previously (Meinken *et al*., 2003). Briefly, rifampicin (100 mg ml^{-1}) was added to cultures growing logarithmically in CSE minimal medium and samples were taken at time points after drug addition. Quantification was performed using the Image J software v1.42 (Abramoff *et al*., 2004).

Purification of wild-type, C450S, and R741E Aconitase proteins - Untagged wild-type, C450S, and R741E aconitase (Acn) proteins were purified from *B. subtilis* using methods based on those described by Dingman *et al.* (Dingman & Sonenshein, 1987). For each strain (KBP94, KBP22, KBP81), two independent cultures were prepared and harvested by centrifugation at 4°C (4,400 × *g*; JA-10 rotor) at the end of the exponential growth phase (OD_{600} ~ 0.8-1.0). While the volume of the cultures ranged from 500 ml to 2 l, in each case the amount of cell extract equivalent to a 500 ml culture was used as the input for a single preparation. Cell pellets were washed twice with ice-cold 20 mM Tris-citrate (TC) buffer (20 mM Tris, 20 mM citrate, pH adjusted with NaOH to 7.35), and stored at -80°C. Pellets were thawed and resuspended in ice-cold 20 mM TC buffer supplemented with 1 mM PMSF before being subjected to two passages through a French pressure cell (15,000 lb/in^2). The resulting lysate was sonicated (50% duty,

level 5, 30 seconds intervals with 20 seconds rests, 3 times) on ice to fragment genomic DNA. The sonicated lysate was clarified by centrifugation at 4°C (20,000 × *g*; JA-20 rotor); the soluble fraction was precipitated with ammonium sulfate on ice in a two-step process. First, ammonium sulfate was added to 40% of saturation and the sample centrifuged as described above. The supernatant fluid was then adjusted with ammonium sulfate to give 85% of saturation and subjected to centrifugation as before. The pellet was resuspended in 20 mM TC buffer, concentrated to 1 ml if necessary using a spin column (Millipore), and subjected to gel filtration chromatography on a Superose 12 column (10/300 GL, 24 ml bed volume; GE Healthcare) equilibrated with 20 mM TC buffer. Fractions containing aconitase were identified by aconitase activity assay or by SDS PAGE/Coomassie blue analysis (for the C450S mutant). The Superose 12 fractions containing aconitase were pooled (but not concentrated), giving a total volume of ~1 ml, and subjected to anion exchange chromatography using a MonoQ column (5/50 GL, 1 ml bed volume; GE Healthcare) prepared by sequential washing with 20 mM and 100 mM TC buffer (pH 7.35) followed by equilibration with 20 mM TC buffer. Protein was eluted with a linear gradient of 20 - 50 mM TC buffer (pH 7.35); aconitase eluted very early in the gradient. Fractions containing aconitase were identified by the aconitase enzyme activity assay (or SDS-PAGE analysis for the C450S mutant), pooled, and concentrated via a spin column to ~0.5 ml (Millipore). The MonoQ column concentrate was loaded onto a Superdex 200 gel filtration column (10/300 GL, 24 ml bed volume, GE Healthcare) equilibrated with 2X Storage Buffer (20 mM Tris, 70 mM KCl). Protein was eluted with the same buffer; eluted fractions containing aconitase were identified by SDS PAGE analysis with Coomassie blue. Fractions containing aconitase were pooled prior to concentration via a spin column (Millipore). Pure aconitase was diluted two-fold with 100% glycerol (final concentrations: 10 mM Tris, 35 mM KCl, 50% glycerol) and was stored at -20°C. Alternatively, wild-type aconitase for gel shift assays was purified with a cleavable C-terminal hexahistidine tag. To do so, the *citB* gene was amplified by PCR using the primers OFM3 (5'AAAGAGCTCTGATCTGAAGGGGGATTTTG; *Sac*I site underlined) and OFM4 (5'AAATCTAGATCAGTGATGGTGATGGTGATGGCCCTGAAAATACAGGTTTTCGGACTGCTTCATTTTTTACG; *Xba*I site underlined). The PCR product was digested with *Sac*I and *Xba*I, and the resulting fragment was ligated to the expression vector pBAD30 (Guzman *et al*., 1995); the resulting plasmid was pFM1. *E. coli* R1279 (Schnetz *et al*., 1996) was used as host for the overexpression of recombinant aconitase. Expression was induced by the addition of 0.2% arabinose to exponentially growing cultures (OD_{600} = 0.6). Cells were lysed by two passes at 18,000 psi through an HTU DIGI-F-Press (G. Heinemann, Germany). After lysis the crude extract was

centrifuged at 30,000 x *g* for 60 min and then passed over a Ni^{+}-NTA column (IBA, Göttingen, Germany). The protein was eluted with an imidazole gradient. After elution the fractions were screened for the presence of His_6-Acn by SDS-PAGE and subsequent staining with Coomassie blue. To remove the hexahistidine tag, the His_6-Acn-containing fractions were adjusted to 1 mM DTT and treated with AcTEV™ Protease (Invitrogen) according to the manufacturer's instructions. After removal of the protease beads and free His_6 tag by Ni^{+}-NTA chromatography, the untagged, purified aconitase was concentrated using a VIVASPIN 500 concentrator (Sartorius Stedim, Göttingen, Germany). For all aconitase preparations, the protein concentration was determined by the Bradford method as described above.

Gel mobility shift assays - To create RNA targets for gel mobility shift assays, the *citZ* leader region and *hag* transcript were amplified by PCR to generate templates for *in vitro* run-off transcription. Primers FM169 (5´CTAATACGACTCACTATA***G***GGAGAT**A**GGCTTAAACTTAAATAAGCTTATAAAAATTTG; T7 promoter is underlined, T7 transcriptional start site is italicized in bold, *citZ* transcriptional start site is in bold) and FM170 (5´CATATATAACATCTCCTTTTCAATAAATTTCC; the complement of the *citZ* start codon is underlined) were used to amplify a ~200 bp region of the *B. subtilis* chromosome extending from just upstream of the *citZ* transcriptional start site to the start codon of *citZ*. In addition, primers CD53 (5´CTAATACGACTCACTATAGGGAGATCCGATATTAATGATGTAGCCGGG; T7 promoter is underlined) and CD54 (5´CTCCATGTTCTTTTGGCTCGC) were used to amplify a 190 bp 5' region of the *hag* locus from 106 bp upstream to 84 bp downstream of the start codon. *In vitro* transcription reactions were performed using T7 RNA polymerase (Roche Diagnostics). The integrity of the RNA transcripts was analyzed by denaturing agarose gel electrophoresis (Ludwig *et al*., 2001). Binding of aconitase to the *citZ* and *hag* RNAs was assayed by gel retardation experiments as described previously with minor modifications (Schilling *et al*., 2006). Briefly, the RNA was incubated for 2 min at 95°C and placed on ice for 5 min. Purified aconitase was added to the RNA and the reactions were incubated for 10 min on ice in TAE buffer in the presence of 300 mM NaCl. Glycerol was added to a final concentration of 10% (w/v); the reactions were then subjected to electrophoresis in 8% polyacrylamide gels in Tris-acetate buffer and visualized with ethidium bromide.

Filter binding assays - To create an RNA target for filter binding assays, the *citZ* leader region was amplified by PCR to generate a template for *in vitro* run-off transcription. Primers OKP98 (5'TAATACGACTCACTATA***G***G**A**GGCTTAAACTTAAATAAGCTT; T7 promoter is underlined, T7 transcriptional start site is italicized in bold, *citZ* transcriptional start site is in bold) and

OKP99 (5'CATATATAACATCTCCTTTTC; the complement of the *citZ* start codon is underlined) were utilized to amplify a ~200 bp region of the *B. subtilis* chromosome extending from the *citZ* transcriptional start site (+1) to the start codon of *citZ*. Transcription reactions were performed using T7 RNA polymerase (Stratagene) in the presence of [α-^{32}P] UTP (Perkin-Elmer) to produce internally radiolabeled RNA. Radioactive RNA transcripts were purified by phenol-chloroform extraction, precipitated with isopropanol and sodium acetate to remove unincorporated nucleotides, and resuspended in DEPC-treated deionized water supplemented with RNaseOut (Invitrogen) prior to storage at -20°C in small aliquots to avoid freeze-thaw damage. To assay aconitase binding to *citZ*, labeled RNA was briefly heated to 80°C and then allowed to cool slowly to ambient temperature. Cooled RNA was supplemented with RNaseOut and added to reactions containing different concentrations of aconitase in buffer (10 mM Tris pH 7.5, 35 mM KCl, 20% glycerol, 0.5 mM dipyridyl, 5 mM β-mercaptoethanol). Reactions were allowed to equilibrate for 30 minutes at room temperature before filtration through nitrocellulose discs (0.45 µm HAWP, Millipore; pre-soaked in reaction buffer) using a multi-sample filtration apparatus and the in-house vacuum line. Filters were washed twice with 0.5 ml reaction buffer, removed and placed in scintillation fluid. A mock reaction was added directly to scintillation fluid to obtain a measure of the total radioactivity of the RNA.

Results

Construction of an enzymatically inactive mutant form of aconitase (C450S) - To determine the specific contribution of the enzymatic activity of aconitase to the maintenance of citrate levels within the cell, we sought to create an enzymatically dead mutant of aconitase that retained RNA-binding activity. One of the cluster-ligating cysteine residues (C450) was mutated to serine by PCR-mutagenesis; we will refer to the C450S allele as *citB2*. To create the *citB2* mutation, a 5' region of the *citB* gene containing the C450S mutation and an N-terminal decahistidine (His_{10}) tag sequence were amplified. This construct was ligated to the *B. subtilis* integrative vector pJPM1 [*cat*, (Mueller *et al*., 1992)] and the resulting plasmid, pKP12, was introduced by single crossover at the *citB* locus by selection for chloramphenicol resistance. The resulting transformants were a mixed population of glutamate auxotrophs and prototrophs. One of the glutamate auxotrophs was purified, producing a merodiploid strain [KBP17; His_{10}-*citB2*::pKP12(*cat*)], in which the mutant allele was associated with the promoter. The glutamate

auxotrophy presumably indicates that the C450S mutation abrogates aconitase enzymatic activity. Indeed, purified His_{10}-AcnC450S protein is not an active enzyme (data not shown).

To allow a second crossover event and thereby obtain an unmarked *citB2* strain, the His_{10}-*citB2*::pKP12(*cat*) strain was passaged in rich medium without selection, plated for single colonies, and screened for glutamate auxotrophy and sensitivity to chloramphenicol. Such a segregant was isolated, but sequencing of the *citZ* locus from the resulting strain (KBP22) revealed an additional mutation in the major citrate synthase gene (*citZ340*). This mutation, H340Y, produces a stable CitZ protein (as determined by Western blotting) that is inactive in enzyme assays (data not shown). The appearance of citrate synthase mutations in aconitase null mutant populations has been reported for several organisms including *E. coli* (Gruer *et al*., 1997a), *Corynebacterium glutamicum* (Baumgart *et al*., 2011), *Sinorhizobium meliloti* (Koziol *et al*., 2009), and *Vibrio fischeri* (E. Stabb, personal communication). Overproduction of citrate is apparently deleterious to bacteria.

To separate the *citB2* mutation from the *citZ340* mutation, KBP22 (*citB2 citZ340*) genomic DNA and DNA containing a *citBp-lacZ tet* construct at the nonessential *amyE* locus (KBP94) were introduced together into a wild-type strain by transformation. Tetracycline resistant colonies were screened for the acquisition by congression of the *citB-lacZ* hyperexpression phenotype [expected based on results from *citB* null cells (Kim *et al*., 2003)]; the resulting strain was *citB2 amyE*::*citBp21-lacZ tet* (KBP118). KBP118 cannot grow on minimal medium without glutamate supplementation, indicating that it is a glutamate auxotroph. Sequencing of KBP118 genomic DNA confirmed the presence of the *citB2* mutation. In addition, sequencing of the *citZ* and *citA* genes indicated that KBP118 carries the wild-type versions of both citrate synthase genes; therefore, the glutamate auxotrophy is due solely to the *citB2* mutation.

Construction of an RNA-binding mutant of aconitase (R741E) - We previously described a *B. subtilis citB* mutant strain that produces an RNA-binding-defective aconitase protein (Serio *et al*., 2006). However, this mutant (*citB5*) has five amino acid substitutions, making it difficult to discern which of these residues are important for RNA-binding. In addition, the need to retain all five mutations during strain passaging makes genetic manipulation cumbersome. To alleviate these concerns, we sought a single point mutation that would mimic the *citB5* phenotype. Given the great similarity between *B. subtilis* aconitase and mammalian IRP1 protein, we consulted the crystal structure of IRP1 in complex with its IRE target (Walden *et al*., 2006). Based on this structure, only one of the five residues mutated in the *citB5* strain, Arg-741, has an IRP1

counterpart (Arg-728) in close proximity to the RNA. To determine if this residue was solely responsible for the *citB5* phenotype, we constructed an R741E point mutant (*citB7*) by site-directed PCR mutagenesis. A linear PCR product containing the 1.3kb C-terminal portion of the *citB* gene, including the R741E-encoding point mutation, was generated and introduced into wild-type *B. subtilis* (AWS96) by congression along with genomic DNA of strain AF21 (*amyE*::*citBp21-lacZ cat*). Chloramphenicol-resistant transformants were selected and screened for colonies that overexpressed the *citBp21-lacZ* fusion, a phenotype expected based on results obtained for the *citB5* strain (A.W. Serio and K.B. Pechter, unpublished data). The sequence of the *citB* locus in strain KBP72 (*citB7 amyE*::*citBp21-lacZ cat*) confirmed the presence of the R741E mutation, but also revealed an unplanned silent mutation due to a single nucleotide change near the 3' end of the gene. To create an isogenic strain for some experiments below, genomic DNA containing the *amyE*::*citBp21-lacZ tet* fusion (AWS173) was introduced into KBP72 by transformation and tetracycline-resistant colonies were selected. The resulting strain, KBP81 (*citB7 amyE*::*citBp21-lacZ tet*), was a glutamate prototroph, indicating that it possesses an active aconitase enzyme.

Aconitase activity in cell extracts - Aconitase activity in crude extracts of the wild-type KBP94), *citB* null (AWS174), *citB2* (KBP118), and *citB7* (KBP81) strains was compared. As expected, the *citB* null strain had very low levels of activity throughout growth (Figure 5.1A). The *citB2* strain exhibited low levels of aconitase activity for the majority of the experiment; this was expected based on the strain's glutamate auxotrophy. There was, however, a small increase in aconitase activity in the *citB2* strain above the background at the 5 h time point; we attribute this to the increased presence of suppressor and/or reversion mutations in the population (see below).

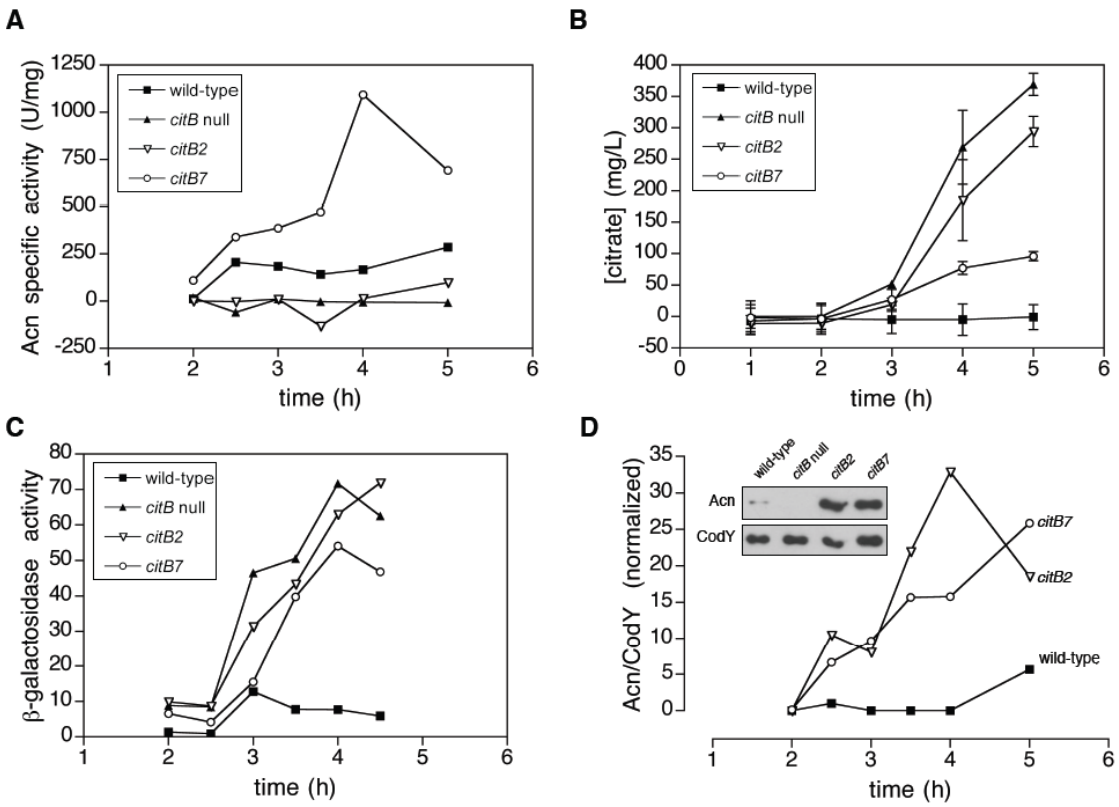

Fig. 5.1. Analysis of aconitase enzyme activity and expression levels in *citB* mutant strains. (A.) Cell extracts were prepared from *B. subtilis* strains grown in DSM and analyzed for aconitase specific activity. A representative experiment of two is shown. (B.) The concentration of citrate in the culture supernatant during growth in DSM was determined. The mean and standard deviation of two biological replicates is shown. (C.) The expression of a *citB-lacZ* fusion during growth in DSM was determined. Samples were taken at the indicated time-points and β-galactosidase activity was measured. A single experiment is shown; all strains were assayed in multiple experiments and gave similar results. (D.) Cell extracts were prepared from strains grown in DSM and analyzed by Western blot using antibodies specific to Acn and CodY (a loading control). Bands were quantitated and values are presented as a ratio of Acn relative to CodY, normalized to the ratio of the *citB*$^{+}$ strain expression level at 2.5 h. A representative experiment of two is shown; an immunoblot of a single time point (2.5 h) from that experiment is shown in the inset. The strains used were wild-type (KBP94), *citB* null (AWS174), *citB2* (KBP118), and *citB7* (KBP81).

We were surprised to find that the *citB7* strain showed very high levels of aconitase activity in cell extracts. In this strain, aconitase activity reached a peak of over 1000 U/mg at the 4 h time-point, a level more than six-fold higher than that seen in the wild-type cell extract (167 U/mg).

citB2 and citB7 mutants accumulate citrate - To know how the aconitase activity levels in the *citB2* and *citB7* mutants affect the citrate levels in these cells, we examined citrate accumulation in the *citB2* and *citB7* mutant strains. Based on the existing metabolic roadblock

model, we anticipated that any strain expressing an inactive aconitase enzyme (e.g., the *citB2* mutant) would accumulate citrate to high levels, while a strain expressing a functional enzyme (e.g., the *citB7* mutant) would not.

To assay the *citB2* and *citB7* strains for citrate accumulation in the culture fluid, the relevant strains were grown in broth cultures, samples were taken during growth, and the culture supernatant was analyzed using a citric acid assay kit (R-Biopharm). As expected, the *citB* null and *citB2* strains accumulated citrate; surprisingly, the *citB7* mutant also accumulated more citrate than did wild-type cells, albeit not to the same level as the *citB2* mutant (Figure 5.1B). Because all of these strains are derivatives of JH642, the accumulation of citrate in the culture supernatant may be exacerbated by a mutation in that strain that reduces citrate import (Srivatsan *et al*., 2008).

citB2 and citB7 mutants overexpress citB-lacZ and aconitase protein - To further explore this citrate accumulation phenotype, we monitored an expected side-effect of citrate accumulation, i.e., increased expression from the *citB* promoter (Kennedy *et al*., 1992). The β-galactosidase activities of wild type, *citB* null, *citB2* and *citB7* strains carrying a *citB-lacZ* fusion at the *amyE* locus were assayed during growth in broth cultures. As shown in Figure 5.1C, the wild-type strain induced *citB* expression at the 3 h time point, after which expression dropped but remained higher than the original basal level. As seen previously (Kim *et al*., 2003), the *citB* null strain induced *citB-lacZ* to levels far beyond those seen in the wild-type; the *citB2* strain exhibited a pattern of expression very similar to that of the null mutant. Surprisingly, the *citB7* strain also overexpressed *citB-lacZ*. Although β-galactosidase activity in the *citB7* strain did not reach the same level of Miller Units as in the *citB* null, the pattern of expression was very similar. In other experiments the *citB5* strain also showed increased expression of a *citB-lacZ* fusion (A.W. Serio and K. B. Pechter, unpublished data).

To determine if hyperexpression from the *citB* promoter leads to elevated aconitase protein levels in the *citB2* and *citB7* strains, cell extracts of the relevant strains were prepared from samples taken during growth in broth cultures. Equivalent amounts of total protein were analyzed by immunoblotting with polyclonal antibodies raised against aconitase and CodY (Ratnayake-Lecamwasam *et al*., 2001; Serio *et al*., 2006). Protein bands were quantified using ImageQuant TL software. For each sample, the amount of aconitase protein was normalized to that of CodY, used as a loading control. To allow comparison across samples, the ratio of Acn:CodY for each sample was normalized to the ratio at the 2.5 h time-point. Both the *citB2* and *citB7* strains overexpressed aconitase protein (Figure 5.1D). This result provides an

explanation for the result presented in Figure 5.1A; *citB7* cells have very high levels of aconitase activity in cell extracts due to the hyperaccumulation of aconitase protein in this strain.

The accumulation of citrate in the *citB7* strain was perplexing, however. Since the *citB7* strain is a glutamate prototroph, it must have a TCA branch of the citric acid cycle that is functional enough to produce adequate 2-ketoglutarate to serve as a substrate for glutamate biosynthesis. In fact, given that glutamate is the cell's most abundant anion, with an *in vivo* concentration of ~100-200 mM (Fisher & Magasanik, 1984b), the rate of 2-ketoglutarate synthesis must be high to maintain those levels. Indeed, we showed above that *citB7* cells have increased aconitase activity *in vivo*. Why then would a strain overexpressing a functional aconitase protein accumulate citrate? To be certain that the R741E mutation does not have an effect on enzyme activity, we purified the protein and studied it *in vitro*. In addition, to confirm that the glutamate auxotrophy in the *citB2* strain results from an inactive aconitase protein, we purified and studied the C450S aconitase protein as well.

Specific activities of C450S and R741E Acn proteins - To determine how the C450S and R741E mutations affect the specific activity of aconitase, the wild-type and mutant aconitase proteins were purified from *B. subtilis* using classical biochemical methods updated for use with Fast Pressure Liquid Chromatography (FPLC). (In unpublished work, we have found that polyhistidine tags on aconitase can lead to inappropriate phenotypes *in vivo*.) Strains KBP94 (*citB*$^{+}$) and KBP81 (*citB7*) were used to purify the wild-type and R741E proteins, respectively. However, all attempts to obtain a large (500 ml) culture of the KBP118 (*citB2*) strain resulted in a significant portion of the population acquiring suppressor or revertant mutations. (When KBP118 cultures were sampled and plated hourly between 2 and 5 hours after inoculation, the proportion of suppressors/revertants increased from approximately 0.1% to 10% of the population over time.) To circumvent this issue, the C450S protein was purified from strain KBP22 (*citB2 citZ340*); the presence of the inactivating H340Y citrate synthase mutation (*citZ340*) prevents the accumulation of citrate, the condition we assume is responsible for the selection of suppressor mutations.

The aconitase specific activities of two preparations of each of the three proteins (AcnWT, AcnC450S, AcnR741E) were determined (Figure 5.2). The proteins were assayed both with and without prior activation by incubation with reduced iron and sulfur. [Because the proteins were purified aerobically, the iron-sulfur clusters undergo some oxidative damage and can be partially reactivated by incubation in a ferrous ammonium sulfate ($Fe(NH_4)_2(SO_4)_2$) buffer with a strong reducing agent (Kennedy *et al*., 1983)]. As expected, the C450S mutation abolished

essentially all enzyme activity; a barely detectable level of activity was seen after incubation with Fe and S. Surprisingly, the R741E mutation also caused a defect in specific activity, but not nearly as severe as the C450S mutation. This result raised the possibility that citrate accumulation in *citB7* cells was due to a partial enzymatic defect. However, our assays in crude extracts indicated that the *citB7* mutant exhibits higher-than-normal aconitase enzyme activity and protein levels *in vivo* (see above), suggesting that overexpression of aconitase in *citB7* cells more than compensates for the reduced activity of individual enzyme molecules.

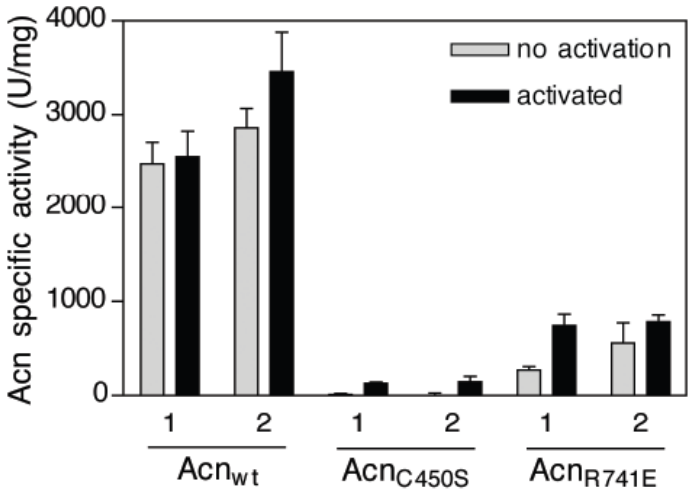

Fig. 5.2. Specific activity of purified aconitase proteins. Wild-type, C450S and R741E mutant aconitase proteins were purified from *B. subtilis* by a four-step purification scheme. Two preparations of each protein were purified from independent cultures, producing six total preparations. The concentrations of the purified proteins were determined by the Bradford assay (Bio-Rad). The specific activities of the purified proteins were determined before and after activation by incubation with exogenous Fe and S. The individual preparations are presented separately. Values shown are the mean and standard deviation of two technical replicates.

However, there was still no explanation for why *citB7* cells, which contain a vast excess of aconitase activity (i.e., the capacity to convert citrate to isocitrate) compared to wild-type cells, would accumulate so much citrate. To examine this phenomenon further, we considered the possibility that the accumulation of citrate in *citB* mutant strains was not due solely to the lack of citrate catabolism, but rather to hyperactive citrate synthesis as well.

Increased CS activity in cell extracts of citB mutants - Citrate synthase (CS) catalyzes the condensation of oxaloacetate and acetyl-CoA to citrate, and is the only TCA branch enzyme that forms a carbon-carbon bond (Wiegand & Remington, 1986). The reaction is irreversible, and in *B. subtilis,* which lacks citrate lyase, aconitase is the only enzyme capable of citrate catabolism.

Therefore, maintaining a balance between citrate synthase and aconitase enzyme activities is essential to preventing a build-up of citrate *in vivo*.

To determine if increased CS activity is involved in the overaccumulation of citrate in the *citB* mutant strains, extracts of wild-type (KBP94), *citB* null (AWS174), *citB2* (KBP118) and *citB7* (KBP81) strains were tested for CS enzyme activity. All of the strains exhibited an initial spike in CS activity at the 2.5-3.0 h time period (Figure 5.3A). This is likely caused by an initial flux of carbon into the TCA cycle; leaky expression of *citZ* provides basal CS activity, and once the substrates become available, citrate is produced and CcpC is inactivated, resulting in derepression of *citZ*. In wild-type cells, citrate is quickly catabolized; when sources of the substrates oxaloacetate and acetyl CoA are consumed, the citrate pool disappears and repression by CcpC is re-established. The three mutant strains began to diverge from the wild-type after 2.5 h; the *citB* null and *citB2* mutants did so the most dramatically. This is likely due to the lack of aconitase enzyme activity in these cells; the high citrate levels maintained in these mutants ensure that CcpC-dependent repression of *citZ* cannot be reinstated. The *citB7* mutant, however, has ample aconitase activity *in vivo*; nonetheless, CS activity in the *citB7* strain increased after 2.5 h to a level well above that seen in wild-type cells.

Increased CS protein levels in the cell extracts of citB mutants - To determine if increased synthesis of CS protein was responsible for the increased CS enzymatic activity found in *citB* mutant cells, the cell extracts described above were analyzed by quantitative Western blotting using antibodies to CS and CodY. The immunoblots were quantified using ImageQuant TL (GE Healthcare) and CS levels were normalized to the CodY loading control, and the CS:CodY ratios were normalized to the wild-type sample at 2.5 h. As with specific activity levels, CS protein levels of all strains increased between 2 and 2.5 hours of growth (Figure 5.3B). However, the *citB* null, *citB2* and *citB7* strains had higher CS levels than wild-type at time points after 2.5 hours.

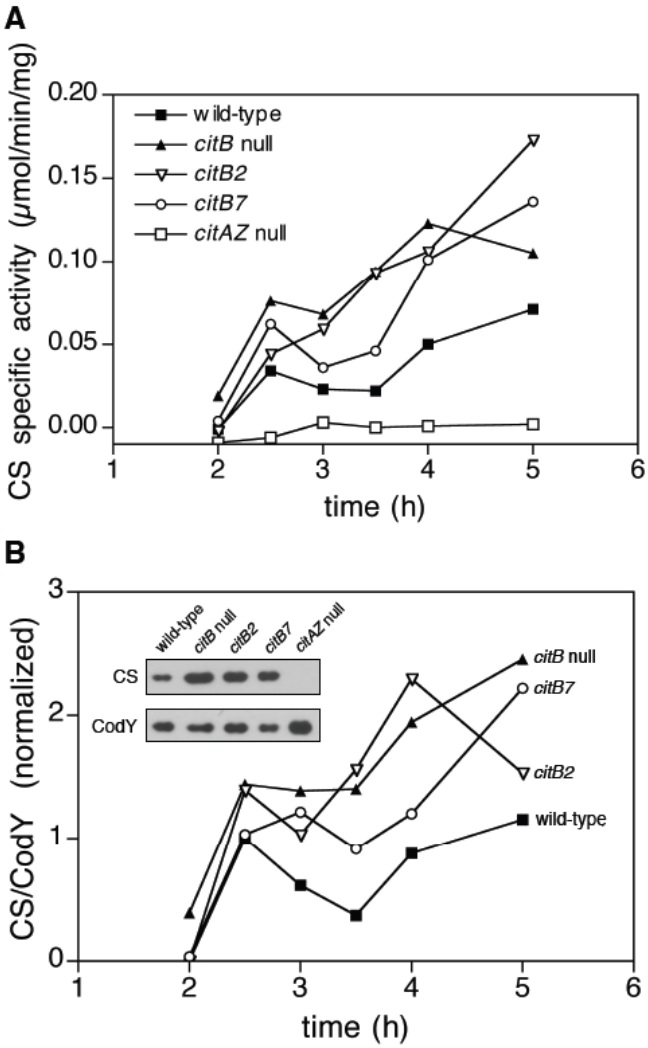

Fig. 5.3. *citB* mutant strains exhibit high levels of citrate synthase activity and protein levels in cell extracts. Strains were grown in DSM, cells were harvested by centrifugation at the indicated time points and crude cell extracts were generated. Separately, cell extracts were examined to determine (A.) the specific activity of citrate synthase, and (B.) the amount of CS protein. Cell extracts (0.25 - 0.5 µg) were analyzed by Western blot using antibodies specific to CS and CodY (a loading control). Bands were quantitated and values are presented as a ratio of CS relative to CodY, normalized to the ratio of the wild-type strain expression level at 2.5 h. A representative experiment of two is shown. An immunoblot of a single time point (3 h) in a representative experiment is inset. For (A.) and (B.), the following strains were used: wild-type (KBP94), *citB* null (AWS174), *citB2* (KBP118), *citB7* (KBP81), and SJB67 (*citAZ* null).

citZ transcript levels are increased in the aconitase null mutant strain - To determine if increases in CS protein levels and enzyme activity are due to higher-than normal levels of *citZ* transcription, we used Northern blots to analyze the steady-state levels of *citZ* mRNA. Given the complex nature of the *citZ* locus, it was necessary to examine all transcripts that include the *citZ* coding sequence. The *citZ* gene is the first gene of an operon that includes the genes for

isocitrate dehydrogenase (*icd*) and malate dehydrogenase (*mdh*). Three promoters (P1, P2, and P3) contribute to the synthesis of at least four different transcripts, as described in Figure 5.4A. The extent to which RNA processing also contributes to the diversity of *citZ* operon transcripts is not known. Total RNA from wild-type and *citB* null cells was analyzed using probes specific to *citZ*, *icd*, and *mdh* (Figure 5.4B).

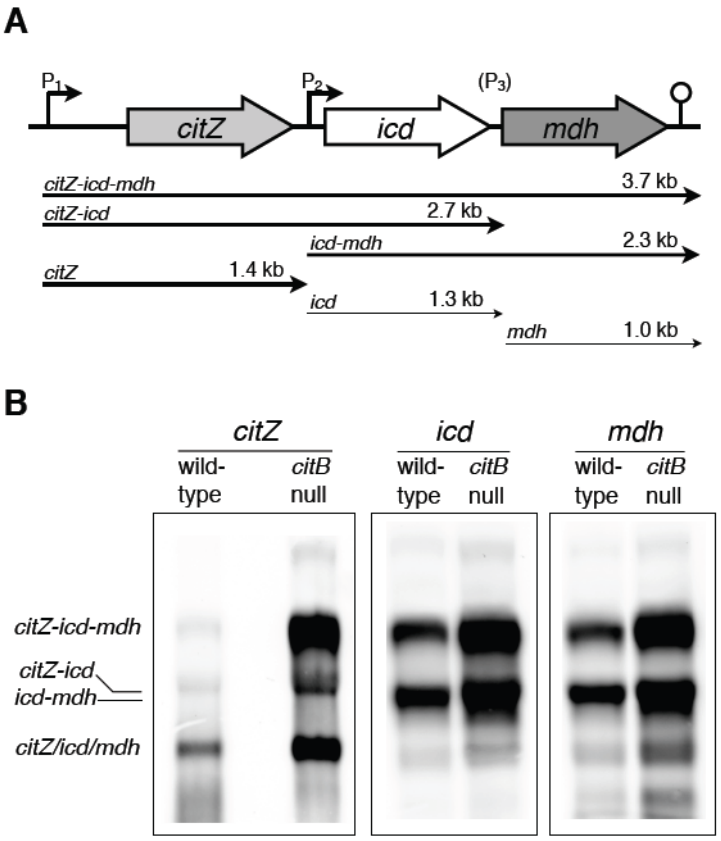

Fig. 5.4. *citZ* locus transcript levels in the *citB* null mutant. (A.) Overview of the *citZ* locus. The citrate synthase II (*citZ*), isocitrate dehydrogenase (*icd*) and malate dehydrogenase (*mdh*) genes are transcribed by promoters P_1, P_2, and P_3 (putative) to produce mono- and polycistronic messages. In addition, post-transcriptional processing of the full *citZ-icd-mdh* transcript likely contributes to the monocistronic transcript pools. Transcript lengths are indicated. (B.) Northern blot analysis of *citZ* locus transcripts in the wild-type and *citB* null mutant. RNA was isolated from wild-type (168) and *citB* null (GP1441) strains grown in CSE minimal medium and analyzed by Northern blot using probes specific for the *citZ*, *icd*, and *mdh* sense RNAs.

Transcripts detected by the *citZ*-specific probe, i.e., the *citZ-icd-mdh*, *citZ-icd* and *citZ* transcripts, were much more abundant in the *citB* null mutant than in wild-type cells. The *icd*- and *mdh*-specific probes also detected a higher level of *citZ-icd-mdh* and *citZ-icd* transcripts in the *citB* null strain. In addition, we also saw an increase in the *icd-mdh*, *icd*, and *mdh* transcripts, which do not contain *citZ*. It is possible that post-transcriptional RNA processing of the P_1-driven message is responsible for this effect. Importantly, a control transcript, the *gapA* mRNA, was

unaffected by the *citB* null mutation (data not shown), demonstrating that the effect on the *citZ* transcripts is specific.

Overexpression of citZ in an aconitase null mutant is not suppressed by a ccpC mutation - To clarify the basis for the higher *citZ* transcript level in the *citB* null mutant throughout growth, a previously described *citZ-lacZ* transcriptional fusion was utilized (Jin & Sonenshein, 1994). This construct contains a 1.3 kb fragment that includes the *citZ* promoter, a 5' leader region of 195 bp, and the first 30 codons of the *citZ* gene, and is integrated by homologous recombination at the *citZ* locus. The fusion was introduced into wild-type (AWS96) and *citB* null (MAB160) strains, producing strains KBP44 and KBP45, respectively. The production of β-galactosidase was assayed during growth in broth cultures. The *citB* null mutation caused *citZ-lacZ* levels to rise 5-fold over wild type after 5 hours of growth (Figure 5.5A); this result matches well with that obtained by Northern blotting, described above. However, given that CcpC is a repressor of *citZ*, and increased citrate levels (such as those found in the *citB* null) cause CcpC to dissociate from the *citZ* promoter (Jourlin-Castelli *et al*., 2000), it was necessary to determine if the rise in *citZ-lacZ* levels in the *citB* null mutant was merely due to alleviation of CcpC repression. To do so, a previously described *ccpC::ble* null mutation (Kim *et al*., 2006) was introduced to KBP44 and KBP45, producing strains KBP48 and KBP49. Similar to results reported previously (Jourlin-Castelli *et al*., 2000), *citZ-lacZ* expression increased two-fold in the *ccpC* null mutant (Figure 5.5B). However, the *ccpC* mutation did not suppress the *citB* phenotype; in fact, *citZ-lacZ* expression levels in the *citB* null mutant were higher than in the *ccpC* null mutant strain. Moreover, the two mutations had an additive effect; in a *citB ccpC* double null strain, *citZ-lacZ* expression rose to a level approximately five-fold higher than in the *ccpC* null mutant alone, and approximately ten-fold higher than in the wild-type. To determine how the increased expression of *citZ* affects CS protein levels, cell extracts from wild-type (KBP26), *citB* null (KBP51), *ccpC* null (KBP52) and *citB ccpC* double mutant (KBP54) strains were analyzed using the quantitative Western blot described above (Figure 5.5B). Citrate synthase protein levels correlated well with the β-galactosidase activity results described here; overexpression could be seen in both *citB* null and *ccpC* null strains, and the *citB ccpC* double mutant increased the levels of CS protein still further. Similar results were seen for the *citB2* and *citB7* strains; introduction of *citB2* or *citB7* mutations into a *ccpC* null strain resulted in heightened CS protein levels beyond those conferred by the *ccpC* null mutation alone (data not shown). These results indicate that aconitase exerts a regulatory effect on CS synthesis that is independent of CcpC.

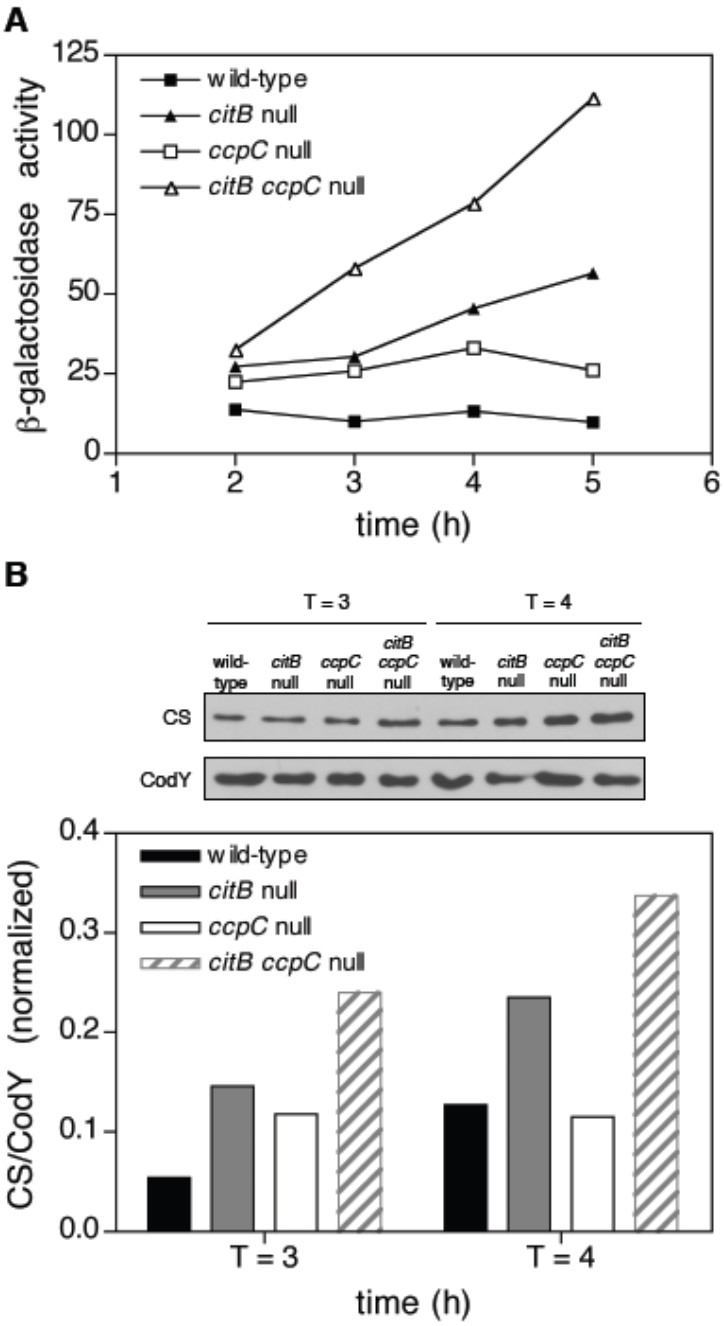

Fig. 5.5. The overexpression of citrate synthase in *citB* mutant strains is not suppressed by a *ccpC* null mutation. (A.) Expression of *citZ-lacZ* was determined in wild-type (KBP44), *citB* null (KBP45), *ccpC* null (KBP48), and *ccpC citB* null (KBP49) cells; β-galactosidase activity was measured at the indicated time-points during growth in DSM. (B.) Levels of CS protein in cell extracts were determined in wild-type (KBP26), *citB* null (KBP51), *ccpC* null (KBP52) and *ccpC citB* null (KBP54) cells. Cell extracts were generated after 3 and 4 hours of growth in DSM. Extracts were analyzed by Western blot using polyclonal antibodies raised to CS II and CodY (loading control). The bands were quantitated and values are presented as a ratio of CS relative to CodY, normalized to the ratio of the wild-type strain expression level at time 3 h. The immunoblot and quantification for a representative experiment of two are shown.

In recent work (Mittal *et al*., 2012), we described the conversion of CcpC from a repressor of *citB* gene expression to an activator when citrate accumulates. Due to the CcpC binding site architecture at the *citZ* locus, we hypothesized that CcpC could only act as a negative regulator of *citZ*. That is, one of the CcpC binding sites overlaps with the promoter -10 region and the other is located downstream of the transcriptional start site (Jourlin-Castelli *et al*., 2000). Importantly, if CcpC were able to act as a positive regulator of *citZ* in high citrate, the increase in *citZ-lacZ* expression seen in the *citB* mutant would be suppressed by the addition of the *ccpC* mutation. Therefore, the results shown in Figure 5.5A confirm that CcpC is not a positive regulator of *citZ*.

The stability of the citZ message is increased in an aconitase null mutant strain – The canonical IRP1 bifunctional aconitase model holds that binding within the 5' end of RNA targets leads to decreased transcript stability, caused by the 599 blockage of ribosome loading (Beinert, 2000). To test the stability of *citZ* mRNA, we utilized a Northern blot-based assay. Wild-type and *citB* null cells were treated with rifampicin to block RNA synthesis and total RNA was isolated from samples at specific time points following drug treatment. The RNA was then analyzed by Northern blot using a probe specific to the *citZ* RNA, as described above. While in wild-type cells the major *citZ-icd-mdh* transcript began decreasing in intensity after 2 min, with an estimated half-life of 3 min, the same transcript in the *citB* mutant exhibited the first drop in intensity after 6 min, with an estimated half-life of 11 min. (Figure 5.6). The increased steady-state concentration of *citZ* mRNA in *citB* mutant cells may be explained by its increased stability, but we have not ruled out other potential contributing factors.

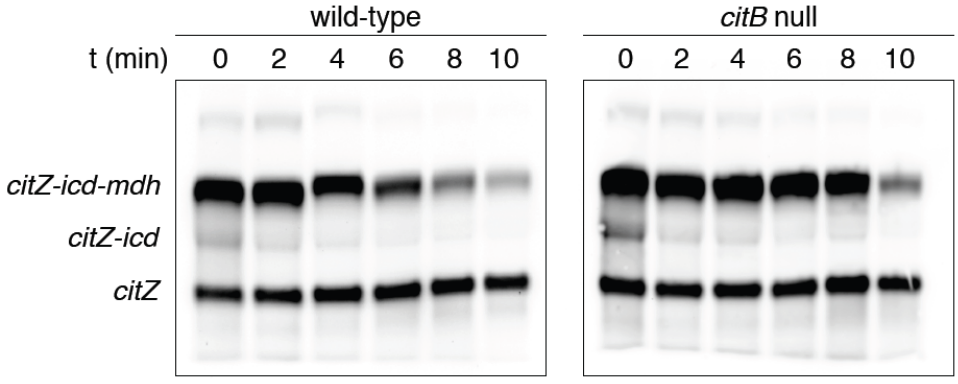

Fig. 5.6. The *citZ* transcript is stabilized by a *citB* null mutation. Wild-type (168) and *citB* null (GP1441) cells were grown in CSE minimal medium. Rifampicin (f.c. 100 mg/ml) was added to logarithmically growing cultures and samples were taken at the indicated time-points after treatment. RNA was isolated and analyzed by Northern blot using a probe specific to the *citZ* sense strand. The *citB* null RNA blot was exposed for a shorter time period than the wild type to accomodate the differences in RNA levels between the strains.

Aconitase directly interacts with the citZ 5' leader RNA in vitro - Given the greater abundance of *citZ* mRNA in *citB* mutant cells and the ability of *B. subtilis* aconitase to bind to certain mRNAs (Alén & Sonenshein, 1999; Serio *et al*., 2006), we considered the possibility that aconitase directly regulates *citZ* expression at the RNA level. We hypothesized that aconitase might regulate the translation or stability of the *citZ* message by binding to the 195-n 5' untranslated leader region of *citZ* mRNA.

We first compared the binding of aconitase to the *citZ* 5' leader region and to a 5' region of the *hag* gene (a negative control) by a gel shift assay. The *citZ* leader RNA (195 b) and the *hag* RNA (190 b) were synthesized by *in vitro* using PCR products that included a phage T7 late promoter upstream of the template DNA. Increasing concentrations of purified Acn (0.25 – 4.5 µM) were incubated with a constant concentration of probe (250 nM) before analysis by polyacrylamide gel electrophoresis. A greater than 50% shift of *citZ* 5' leader RNA was evident between 0.75 and 1.5 µM Acn; for the *hag* RNA, the highest concentration of Acn (4.5 µM) did not result in a complete shift (Figure 5.7).

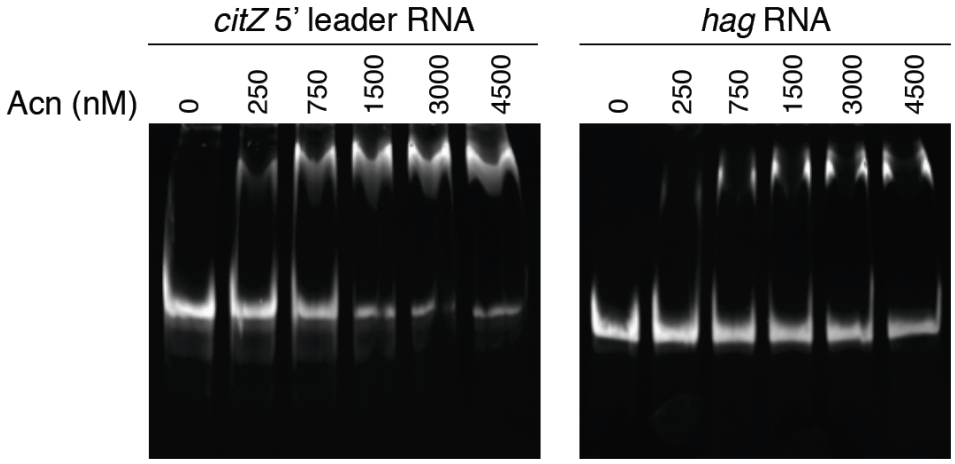

Fig. 5.7. Aconitase binds specifically to the *citZ* 5' leader region *in vitro*. Wild-type aconitase purified from *E. coli* (His_6-Acn, histidine tag cleaved with TEV protease) was mixed in increasing concentrations with *in vitro* transcribed *citZ* 5' leader RNA (250 nM). The *hag* RNA was used as a negative control. Reactions were analyzed by polyacrylamide gel electrophoresis and visualized by staining with ethidium bromide.

C450S and R741E proteins cannot bind to citZ RNA in vitro - To discover whether the accumulation of CS in the *citB2* and *citB7* strains was explainable by differences in binding to the *citZ* mRNA, we tested binding of the wild-type and mutant aconitase proteins to the *citZ* mRNA 5' leader region using a filter binding assay. Increasing concentrations of purified aconitase (in the nanomolar range) were incubated with a constant, low concentration of radiolabelled probe

(83 pM) in buffer containing 0.5 mM dipyridyl, an iron chelator that is used to increase the fraction of aconitase molecules in the RNA-binding form (Alén & Sonenshein, 1999). Whereas two independent preparations of wild-type aconitase both bound to the *citZ* leader RNA, they had different RNA-binding activities (Figure 5.8). As shown above, the enzyme activities of the two preparations were also different, but inversely so (Figure 5.2). That is, wild type preparation #1 was a better RNA-binding protein but a less active enzyme than was wild type preparation #2. The two preparations were presumably at different equilibria between the two forms of aconitase. Importantly, none of the C450S or R741E aconitase preparations bound to the *citZ* 5' leader RNA.

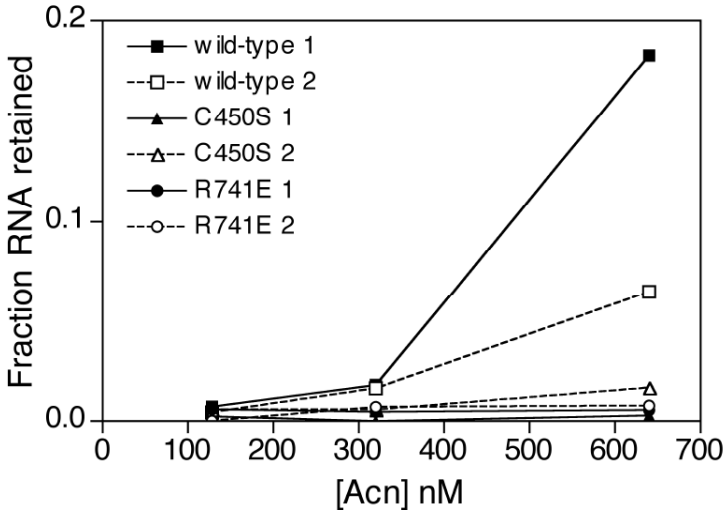

Fig. 5.8. Differential binding of wild-type and mutant aconitase proteins to the *citZ* 5' leader RNA *in vitro*. Each of six Acn protein preparations (described in Fig. 2) were mixed separately at the indicated concentrations with radiolabelled *citZ* 5' leader RNA synthesized *in vitro* (83 pM). Reactions were allowed to equilibrate in buffer containing RNAse inhibitor (RNAseOut, Invitrogen), dipyridyl (0.5 mM), and β-mercaptoethanol (5 mM) prior to passage through nitrocellulose membranes. RNA retained on each membrane was detected by scintillation counting, and the fraction RNA retained was calculated, after background subtraction, as a percentage of the input RNA. The data shown are from a single experiment; preparations wild-type 2, C450S 1, and R741E 1 were assayed in other experiments and gave similar results.

Discussion

We describe here the contributions of the two functions of *B. subtilis* aconitase to the accumulation of citrate in *B. subtilis* and, ultimately, to the regulation of the TCA branch enzymes. We found that citrate accumulates in two different aconitase mutants - in a *citB2* strain, which hyperexpresses enzymatically inactive aconitase, and in a *citB7* strain, which

hyperexpresses enzymatically active aconitase. The unexpected and puzzling nature of this last result prompted us to look for a novel explanation unrelated to aconitase enzyme activity. In fact, we found that the *citZ* transcript, CS protein, and CS activity levels are significantly increased in *citB* mutants. Our data indicate that wild-type aconitase, but neither the C450S nor the R741E mutant, binds to a region of *citZ* RNA containing the untranslated, 195-n 5' leader region *in vitro*. In addition, we found that the stability of the major *citZ* transcript is increased in the *citB* null mutant compared to wild-type, suggesting that aconitase regulates *citZ* at the post-transcriptional level.

By integrating these new data with previous studies, a more complete model for regulation of the TCA branch of the Krebs cycle can be proposed. When rapidly metabolizable carbon sources are available (e.g., glucose), the *citZ* gene is repressed by CcpA and both the *citZ* and *citB* genes are repressed by CcpC. (Neither CcpA nor CcpC is by itself able to repress *citZ* completely, but the combined effects of the two repressors give very strong repression.) When glucose is exhausted, repression by CcpA is relieved, allowing partial derepression of *citZ*. Citrate begins to accumulate, leading to complete derepression of *citZ* and at least partial derepression of *citB*. The aconitase produced, in concert with isocitrate dehydrogenase, metabolizes citrate to 2-ketoglutarate. To prevent the accumulation of excessive levels of citrate, aconitase protein binds near the 5' end of the *citZ* mRNA, decreasing its stability, and thereby limiting the concentration of citrate synthase in the cell.

As a possible rationale for this latter mode of regulation, we propose that the key factor is the relationship of citrate to iron in the cell. Citrate is both co-transported with iron and a chelator of divalent cations, including iron. If the intracellular citrate level becomes excessive, iron will be sequestered away from iron-containing proteins, including aconitase. Since excess citrate greatly stimulates aconitase synthesis via the positive regulatory effect of CcpC (Mittal *et al.*, 2012), the cell will gain the ability to metabolize citrate at a higher rate. If so much iron has been sequestered that aconitase loses enzymatic activity, the cell will acquire a high concentration of enzymatically inactive but RNA-binding-competent aconitase molecules. These aconitase proteins can bind to the *citZ* mRNA and reduce the rate of citrate accumulation by restricting the synthesis of citrate synthase protein. As shown here, the lack of aconitase enzyme activity and the lack of aconitase RNA binding activity both contribute to hyperaccumulation of citrate. These two roles of aconitase explain the fact that the *citB7* mutant accumulates citrate to abnormal levels despite having higher-than-normal aconitase enzyme activity *in vivo*.

In constructing this model, we have ignored the potential contribution of the minor *B. subtilis* citrate synthase, CitA (or CS-I) (Jin & Sonenshein, 1994). CitA contributes only a small amount of CS activity to *B. subtilis* cells due to substitution of the active site aspartate-307 by glutamate. Whereas *citZ* null strains are glutamate auxotrophs, *citA* null mutants have little observable phenotype (Jin & Sonenshein, 1994). The regulation of *citA* remains poorly understood, but it is unlikely that CitA contributes a great deal to cellular physiology under the growth conditions used; cell extracts from *citZ* null mutants have very little residual citrate synthase signal when analyzed by immunoblot with anti-CitZ antibodies that cross-react with CitA (Jin & Sonenshein, 1996).

A recent paper suggests another potential level of complexity for the aconitase-CS regulation story. Schmalisch *et al*. (Schmalisch *et al*., 2010) discovered a small RNA with strong complementarity to the *citZ* 5' leader region. The small RNA, whose synthesis is regulated by the motility sigma factor, σ^D, is suspected to act as an antisense RNA for *citZ*, but the effect of the RNA and its mechanism of action have not been elucidated. Given the sequence complementarity between the *citZ* leader and the small RNA, it is possible that aconitase binds to this small RNA in addition to (or instead of) the *citZ* transcript.

Although we hoped to isolate aconitase mutants that were selectively deficient in either enzymatic activity or RNA binding, both of the mutants we have reported here are at least partially defective in both activities. The C450S Acn protein is stable and produced in high amounts, but is neither an enzyme nor an RNA-binding protein. The basis for the RNA-binding defect in the C450S mutant is unclear. The IRP2 protein, a homolog of IRP1 that lacks aconitase enzymatic activity, is subject to regulation via oxidation of cysteine residues that lie close to the IRE-binding site (Zumbrennenn *et al*., 2009). It is possible that, in the absence of the iron-sulfur cluster, the two other cluster-ligating cysteine residues in the C450S mutant form a disulfide bond that prevents RNA binding. Similarly, the R741E Acn protein, designed to be defective in RNA binding, also exhibits a partial defect in enzymatic activity. While it is not as severe a defect as that of the C450S Acn protein, it is still surprising given the expectation that the arginine-741 residue is not involved in enzyme activity. Several arginine residues contribute to enzyme activity in IRP1 (Philpott *et al*., 1994), but the homolog of Arg-741 in IRP1 (Arg-728) is not one of them. However, a study of presumed non-enzymatic residues of IRP1 revealed that mutations of some residues resulted in decreased enzyme activity. The authors saw higher K_m and V_{max} values for the enzyme activity of certain RNA-binding point mutants (Kaldy *et al*., 1999), although mutations of Arg-728 were not specifically tested. Interestingly, mutating a neighboring residue,

Arg-732, to Glu resulted in a 9-fold increase in the K_m (Kaldy *et al*., 1999). These data, together with our results, suggest that the alteration of residues near the RNA binding pocket of aconitase can have unexpected effects on enzymatic activity.

While this work was in progress, Gao *et al.* (Gao *et al*., 2010) reported that a strain with aconitase substitutions R741E and Q744E exhibited higher-than-normal levels of *citB-lacZ* expression, aconitase protein, and aconitase activity in crude cell extracts. While the authors did not purify this protein to test its RNA binding activity *in vitro*, their results are consistent with the results we report here with the *citB7* mutant (R741E) and our work with the *citB5* strain that carries R741E, Q744E and three additional mutations [(Serio, 2005); A.W. Serio and K.B. Pechter, unpublished work].

While knowledge about the regulatory roles of bacterial aconitase proteins is limited, Tang *et al*. (Tang & Guest, 1999) have shown that the two aconitase proteins of *E. coli*, AcnA and AcnB, both bind to the 3' UTRs of their own transcripts and that this binding increases production of AcnA and AcnB proteins in an *in vitro* transcription-translation assay. Aconitase levels were shown to increase in response to oxidative stress, despite loss of aconitase activity, suggesting that the apo-Acn proteins activate this autoregulatory loop (Tang & Guest, 1999). In addition, the role of aconitase in two pathogenic bacteria has been explored. Deletion of the *Staphylococcus aureus* aconitase gene resulted in increased survival in stationary phase and reduced levels of virulence factors (Somerville *et al*., 2002), while in *Xanthomonas campestris* pv. *vesicatoria*, mutations in *acnB* were found to result in decreased proliferation on pepper plant hosts (Kirchberg *et al*., 2012). In each of these cases, the mechanism of regulation is unknown, but it is conceivable that aconitase is acting as an RNA-binding regulator of virulence.

In a broader sense, careful regulation of citrate synthase, aconitase, and citrate levels is likely to be vital in all organisms that lack a citrate lyase enzyme. For *B. subtilis* and other such organisms, once citrate is produced, aconitase is the only option for citrate removal. Other organisms that share this metabolic inflexibility are likely to have similarly layered regulatory mechanisms for preventing a potential citrate catastrophe.

Acknowledgments

The authors thank C. Kumamoto, J. Mecsas, B. Schaffhausen, C. Squires, B. Belitsky, K. O'Day-Kerstein, and C. Majerczyk for helpful discussions, D. Dingman for sharing his aconitase purification protocol, R. Isberg, A. Camilli, and K. Heldwein for the use of their FPLC equipment,

A. Hempstead, W. Amyot, and J. Pitts for sharing their FPLC expertise, and J. Busse and C. Diethmaier for their help with gel shift experiments. Research reported in this publication was supported by the National Institute of General Medical Sciences of the National Institutes of Health under award number R01GM036718 to A. L.S. and by the German Federal Ministry of Education and Research SYSMO network (PtJ-BIO/0315784B) to J. S.. F. M. was supported by Göttingen International. The content is solely the responsibility of the authors and does not necessarily represent the official views of the National Institutes of Health.

6. Discussion

6.1. The TCA cycle metabolon of *B. subtilis*

The TCA cycle is an essential hub in the metabolism of *Bacillus subtilis* and enables the bacterium to adapt to various environmental conditions by a complex interplay of transcriptional regulation and post-translational protein modification (see introduction & below). Especially in competition with other organisms an efficient metabolism including an efficiently operating TCA cycle is of vital importance.

In this work protein-protein interactions between several enzymes of the TCA cycle were identified by the use of two independent approaches (Herzberg *et al*., 2007; Karimova *et al*., 1998). Previously, global interactome studies have demonstrated that about 70% of the cellular proteins interact with at least one protein and that proteins are active in complexes rather than in an isolated way (Gavin *et al*., 2006; Krogan *et al*., 2006; Kühner *et al*., 2009). Especially the formation of protein dimers or multimers is crucial for the proper catalytic activity of many proteins and is in good agreement with the bacterial two-hybrid analysis done for the enzymes of the TCA cycle. The majority of the analyzed enzymes showed self-interactions, thus they form at least a dimeric structure (see chapter 2). Moreover, already well-established enzyme complexes like the 2-oxoglutarate dehydrogenase complex or the complex of the succinyl-CoA syntethase were found by combining these two approaches. Beside the identification of known complexes and the formation of multimers a number of still unknown interactions between the enzymes of the TCA cycle were identified. Interestingly, protein-protein interactions between several enzymes which catalyze sequential reactions in the TCA cycle were detected. For example interactions between CitG, Mdh and CitZ which catalyze three consecutive steps in the cycle were found (see chapter 2).

The interaction between proteins which catalyze sequential reactions seems to be a common feature especially for enzymes involved in metabolic pathways and was already demonstrated by several other studies. Interactions between enzymes of the central carbon metabolism (glycolysis and TCA cycle) were identified in global interactome studies as well as in numerous studies, which were focused just on a set of selected proteins. Complexes of glycolytic enzymes for example were found in *E. coli* and *B. subtilis* and in eukaryotic cells (Campanella *et al*., 2005; Commichau *et. al*., 2009; Mowbray & Moses, 1976). Also in *B. subtilis*

interactions between some TCA cycle enzymes were shown several decades ago (Barnes & Weitzman, 1986).

In this work a more detailed picture of the interactions between the TCA cycle enzymes of *B. subtilis* could be established and the formation of a so-called metabolon was identified (see chapter 2, Fig. 2.4). A metabolon is defined as a complex of enzymes which catalyze sequential reactions in a metabolic pathway and it is supposed that the intermediates of enzymes forming a metabolon can directly be transferred from enzyme to enzyme (Robinson & Srere, 1985). As a result the intermediates escape from free diffusion through the entire cell and the efficiency of the pathway is enhanced (substrate channeling, see below). Thus, the assembly of the TCA cycle enzymes in a metabolon might further enhance the efficiency of this pathway, leading to high metabolic fluxes and enhanced growth rates.

The core of the model for the TCA cycle metabolon is formed by the enzymes citrate synthase, isocitrate dehydrogenase and malate dehydrogenase (see chapter 2, Fig. 2.4). The interaction between these proteins is further supported by the genomic clustering of their genes in one operon (*citZ mdh icd* operon). The conserved clustering in one operon often indicates possible interaction (Dandekar, 1998). Indeed, the clustering of these genes in one operon is conserved in all bacilli and complexes between malate dehydrogenase and citrate synthase were also found in several other organisms like *S. cerevisiae* or *Pseudomonas aeruginosa* (Mitchell, 1996, Grandier-Vazeille *et al*., 2001).

The enzymes of the core (CitZ, Icd and Mdh) further interact with several other sequential enzymes of the TCA cycle and are also connected via protein-protein interactions with glycolysis/gluconeogenesis or nitrogen metabolism (see chapter 2). Since the TCA cycle is highly connected in a network of other metabolic pathways, especially the interaction with proteins of other metabolic pathways might be of great importance for the control of metabolic fluxes. Interestingly, the results of this work demonstrate a rather dynamic composition of the TCA cycle metabolon. The interaction between Mdh and PckA, which connects the TCA cycle with glycolysis/gluconeogenesis, takes place only under gluconeogenic conditions but not under glycolytic conditions.

Proteins which interact with other proteins and consequently form complexes can be divided into two groups: proteins which interact with several other proteins at the same time and proteins whose interaction differ depending on the specific metabolic condition (Han *et al*., 2004). Especially the metabolic conditions seem to have a great impact on complex formation of metabolic enzymes (Graham *et al*., 2007; Islam *et al*., 2007). Similarly like in *B. subtilis* for the

interaction between Mdh and PckA it was shown for the enzymes of glycolysis in plants that these enzymes form a complex only under conditions of enhanced respiration at the membrane of mitochondria. Otherwise the enzymes are equally distributed in the cytosol of the cell (Graham *et al*., 2007). Nevertheless, because of a dynamic composition or the fragility of metabolic complexes it is often difficult to detect such complexes and especially global approaches are prone to produce artefacts (Williamson & Sutcliffe, 2010). Furthermore, the identification of interactions between proteins which have more than one function can be challenging. Implausible interactions might tempt to stop further analysis. The glycolytic enzyme enolase for example was found in several organisms to be a part of the RNA degradation machinery (Carpousis, 2007; Kang *et al*., 2010; Lehnik-Habrink *et al*., 2010). It is hypothesized that this interaction connects RNA degradation with the metabolic state of the cell. However, the precise mechanisms are still unknown and thus the role of enolase in RNA degradation remains a matter of debate.

Substrate channeling

The interaction of sequential enzymes of the TCA cycle of *B. subtilis* leads to the assumption that intermediates of these enzymes are directly transferred from one active site to the next via substrate channeling. However, it is still intensively discussed if the efficiency of a reaction is improved by substrate channeling or if free diffusion is sufficient for most reactions. Nevertheless, the conditions in a cell (*in vivo*) cannot be compared with the conditions in a test tube (*in vitro*) because of the high complexity of a cell (Fulton, 1982). The extremely high concentration of proteins and metabolites (macromolecular crowding) strongly influences all cellular reactions (Johansson *et al*., 2000; Zimmerman & Minton, 1993). By substrate channeling the intracellular concentrations of labile or toxic intermediates are kept low and disadvantageous or undesired reactions are prevented by a fast turnover (Huang *et al*., 2001). Moreover, a crosstalk between different metabolic pathways might be stopped.

For the TCA cycle metabolon it seems very likely that substrates of sequential reactions are directly transferred from one enzyme to the next. Interestingly, a current *in silico* study demonstrated that glycolytic fluxes are enhanced by the formation of an enzyme complex, indicating that substrate channeling is an important mechanism for an efficient metabolism (Amar *et al*., 2008). On the one hand the flux trough the TCA cycle might be enhanced by substrate channeling and on the other hand the controlled transfer of substrates might regulate

this metabolic intersection. The intermediate oxaloacetate for example can be used by three different pathways: it is used by CitZ for the first reaction of the TCA cycle, it is used by PckA for gluconeogenesis and it is used by aspartate transaminase (AspB) for the biosynthesis of amino acids. The results of this work indicate that under gluconeogenic conditions the interaction between Mdh and PckA is directly controlled by the metabolic flux ensuring a high gluconeogenic flux by substrate channeling between these two enzymes.

In other recent studies the importance of interactions between sequential enzymes and thus for substrate channeling was already demonstrated for the catabolic pathway for branched-chain amino acids and the purine biosynthesis ("purinosome") in eukaryotes. These enzymes only interact under certain metabolic conditions and their activity is controlled by the interaction (An *et al*., 2010; Islam *et al*., 2007). Furthermore, it was demonstrated that the formation of the "purinosome" is controlled by kinase-dependent phosphorylation of the enzymes (An *et al*., 2010). The mechanisms which control the assembly of Mdh and PckA are still unknown. However, the interaction might also be controlled by allosteric regulation or by protein modification.

Localization of TCA cycle enzymes

In comparison to eukaryotic cells bacteria do not possess cellular compartments which are enclosed by a membrane (organelles). The organelles of eukaryotic cells separate specific metabolic processes from the rest of the cell and thus enhance the efficiency of these reactions. The TCA cycle of eukaryotic cells for example is located in the mitochondria, photosynthesis takes place in chloroplasts, and so on. Nevertheless, a bacterial cell is not a simple reaction vessel without any spatial organization. Even in bacterial cells many processes are localized at specific areas of the cell and thus a subcellular compartmentalization is formed. The localization of proteins or protein complexes is dependent on the signals encoded within the amino acid sequence. All cells possess three classes of proteins: Membrane proteins, membrane-associated proteins and cytosolic proteins. Membrane proteins (for example structural proteins, transporters, proteins involved in signal transduction, etc.) are directly embedded into the membrane. Membrane-associated proteins are bound at the membrane via the specific membrane potentials (composition of fatty acids) or through the interaction with membrane proteins. The correct localization of these two classes of proteins is mediated by diffusion and capture (Shapiro *et al*., 2009). Especially membrane-associated proteins can be transiently

localized to the membrane and thus can continuously change between a cytosolic and membrane-associated state. The response regulators of two-component systems for example are cytosolic proteins. However, during signal transduction the response regulators are phosphorylated by their cognate membrane bound sensor kinases and move to the membrane. The PTS components (EI and HPr) dynamically switch between different locations inside of the cell to fulfill their different functions in transport and regulation. Also the enzymes of the TCA cycle of *B. subtilis* can be divided into these classes. The succinate dehydrogenase complex (SdhCAB) is a membrane protein and a general component of the reparatory chain. A recent membrane proteome study revealed that several other proteins of the TCA cycle (Icd, OdhB, SdhB and Mdh) are membrane-associated (Hahne *et al*., 2008). For the remaining enzymes of the cycle it is assumed that they are cytosolic proteins.

The localization pattern of the TCA cycle enzymes once more support the model of physical interactions between several enzymes of the cycle. The metabolon might be associated to the membrane via an interaction to succinate dehydrogenase. Thus, the complex might be stabilized by membrane anchoring and the efficiency of the TCA cycle might be enhanced by higher local substrate concentrations. Likewise, the localization study reflects the rather transient state of the TCA cycle metabolon. For example only two proteins of the core of the metabolon (Icd and Mdh) were found to be membrane associated proteins whereas CitZ was found in the cytosol. Thus, either the method reached the boundaries of correct detection or the assembly or the composition of the metabolon is rather fluctuating. However, it still remains a scientific challenge to determine the exact localization of a protein inside of a prokaryotic cell. Studies to determine the localization of a protein are often complicated by localization artifacts (Landgraf *et al*., 2012; Margolin, 2012; Swulius & Jensen, 2012).

6.2. Carbon catabolite repression in *B. subtilis*: A hierarchy of carbon sources

In their natural habitat bacteria are often exposed to a mixture of different carbon sources that can be used for growth. As the metabolic capacities of a cell are limited most bacteria prefer a specific carbon source that allows rapid growth and consequently enables the bacteria to gain an advantage in the competition with other bacteria.

In the majority of bacteria glucose is the preferred carbon source and represses the co-utilization of alternative carbon sources (see introduction). Also in *B. subtilis* glucose was considered to be the preferred carbon source. However, it was recently shown that *B. subtilis* in

addition prefers malate and can metabolize malate even in parallel with glucose (Kleijn *et al*., 2010). The genes involved in malate uptake and utilization are no targets of glucose-dependent carbon catabolite repression. Moreover, malate represses the utilization of other carbon sources and allows a maximal specific growth rate similar to that obtained with glucose (Kleijn *et al*., 2010). For *B. subtilis* it was supposed that the cells first metabolize PTS carbohydrates, then non-PTS carbohydrate and finally organic acids (Brückner & Titgemeyer, 2002). Thus, malate represents an exception in comparison to other organic acids. However, the mechanism of malate-mediated CCR remained unclear. Because of suspected low fructose 1,6-bisphosphate concentrations an independent mechanism for malate-mediated CCR was assumed (Kleijn *et al*., 2010).

In this work the involvement of the CcpA/HPrK pathway in malate-mediated carbon catabolite repression was demonstrated (see chapter 3). In *B. subtilis*, the major regulator of CcpA-mediated carbon catabolite repression is the HPr kinase/phosphorylase (HPrK/P) whose activity is regulated by the concentrations of FBP, ATP, and P_i (Jault *et al*., 2000). FBP is an allosteric activator of the homo-oligomeric enzyme HPrK/P and the intracellular concentration of FBP is critical for kinase activity. The phosphorylation of HPr by HPr kinase already occurs at low ATP levels (25 µM). Intracellular ATP levels were described to be rather constant in *B. subtilis* (Ludwig *et al*., 2002). In this work ATP levels high enough for HPr kinase activation (higher than 40 µM) were detected under all tested experimental conditions (see chapter 3). Below concentrations of 1 mM FBP there is almost no kinase activity of HPrK detectable whereas its activity already reaches a plateau at a concentration of about 5 mM FBP (Jault *et al*., 2000). Thus, the transition between these FBP levels can be essential for CcpA-mediated CCR. Here, low FBP concentrations (2.3 mM) were detected in CSE minimal medium that do not cause catabolite repression and on the other hand high FBP concentrations (12.7 mM) were detected in CSE minimal medium with glucose which leads to strong catabolite repression. These results are in good agreement with previous observations in *B. subtilis* (Singh *et al*., 2008). In malate grown cells an intermediate FBP concentration (5.4 mM) was found and strong catabolite repression was detected. A FBP concentration as found in malate grown cells is sufficient for proper HPr kinase activity and enables CcpA-mediated CCR to be activated. Thus, HPr is phosphorylated at Ser46 by the HPr kinase and interacts with CcpA. As a result, CcpA is competent for DNA binding and controls the expression of its target genes. Furthermore, in this work it was demonstrated that the absence of HPrK/P or CcpA resulted in the loss of catabolite repression during growth in minimal medium with glucose and with malate (see chapter 3). In

conclusion, the analyzed metabolite concentrations as well as the mutant screen demonstrate the involvement of the CcpA/HPrK pathway in malate-mediated carbon catabolite repression.

In *B. subtilis* it was recently shown that different repressing carbon sources result in FBP concentrations between 4 and 14 mM (Singh *et al*., 2008). However, in this study it was also demonstrated that the strength of repression can differ. The different repressing carbon sources can be ordered in a hierarchy from strong to weak repression. The level of CcpA-mediated CCR components remains constant, whereas the level of CcpA/Hpr complex (Ser46 phosphorylated HPr) varies during growth with different repressing carbon sources (Singh *et al*., 2008). Strongly repressing carbon sources lead to the Ser46 phosphorylation of most HPr molecules and thus to high levels of CcpA/Hpr complex and strong CCR. In contrast, weakly repressing carbon sources lead only to a minor fraction of Ser46 phosphorylated HPr. Thus, focused on a specific gene and analyzing different carbon sources the strength of CCR in *B. subtilis* is dependent on the level of CcpA/Hpr complex (Singh *et al*., 2008). However, CCR strength is also dependent on the gene specific *cre* sequence and the affinity of CcpA for the particular *cre* sequence. The *cre* boxes in *B. subtilis* are low-conserved pseudo-palindromes with the consensus sequence WTGNNARCGNWWWCAW (W: A or T; R: A or G; N: any base) (Miwa *et al*., 2000; Fujita, 2009). In *B. subtilis* about 50 *cre* sites were found by experimental approaches and about 100 *cre* sites by sequence similarities to the consensus sequence (Fujita, 2009). Especially the location of the *cre* site in the promoter region and the similarity to the consensus sequence is essential for the affinity and the strength of CcpA-dependent regulation (Marciniak *et al*., 2012).

Interestingly, the strength of CCR or the level of CcpA/Hpr complex is not only dependent of the levels of FBP and ATP. Repressing carbon sources which cause strong CCR can either lead to high FBP levels of up to 14 mM or low FBP levels of about 4 mM that are still sufficient for proper HPrK activity (higher than 3-4 mM) (see chapter 3; Singh *et al*., 2008). Weakly repressing carbon sources as well can exhibit high FBP levels. Therefore, other substrate-dependent metabolites might also trigger HPr kinase activity and the formation of the CcpA/Hpr complex.

Most of the carbohydrates that cause strong CCR (glucose, fructose, mannitol, salicin, and sucrose) are substrates of the PTS (Singh *et al*., 2008). These carbohydrates are all taken up by specific EIIs, that rely on HPr(His-P)-dependent phosphorylation. Malate is not taken up by the PTS system but by a specific symporter (see introduction). Especially in comparison with another organic acid like succinate, which is a non-repressing carbon source, two questions arise: Why is the FBP level in malate grown cells sufficient for HPrK activity and how does malate

cause strong CCR? *B. subtilis* exhibits similar growth rates with malate to that observed for glucose (Kleijn *et al*., 2010). In contrast, *B. subtilis* shows much lower growth rates grown with succinate as the sole carbon source.

Instead of ubiquinone Gram-positive bacteria like *B. subtilis* make use of the more electronegative menaquinone in their respiratory chain which is a poor electron acceptor from succinate (Schirawski & Unden, 1998; Lemma *et al*., 1990). Therefore, the oxidation of succinate to fumarate by the succinate dehydrogenase (respiratory complex II) is an endergonic reaction and might be responsible for the difference in hierarchy between malate and succinate. In *B. subtilis* it was already shown that CCR can be abolished by a metabolic block. A deletion of glucose-6-phosphate isomerase or phosphofructokinase leads to the deregulation of CCR in glucose grown cells as they cannot form enough FBP (Nihashi & Fujita, 1984). Thus, it is very likely that the endergonic reaction of succinate dehydrogenase is the reason for the inability of *B. subtilis* to form higher FBP levels with succinate. With malate a high gluconeogenic flux might contribute to the formation of FBP levels high enough for HPr kinase activation.

Hierarchical utilization of carbon sources in other bacteria

In bacteria the hierarchical utilization of carbon sources is a widespread phenomenon. In most Firmicutes CCR is achieved by the CcpA/HPrK pathway (Titgemeyer & Hillen, 2002), whereas other groups of bacteria have evolved their own mechanism of CCR. However, only in the model organisms *B. subtilis* and *E. coli* the regulatory mechanism has been extensively analyzed. In *E. coli* a large number of carbohydrates additionally to glucose exert CCR (Bettenbrock *et al*., 2007). Nevertheless, the hierarchy of repressing carbon sources in *E. coli* is controlled by the phosphorylation state of $EIIA^{Glc}$ (Hogema *et al*., 1998). Moreover, in contrast to *B. subtilis* in *E. coli* the transport of carbohydrate via the PTS is essential for CCR (Deutscher *et al*., 2006). A deletion of the enzyme I of *E. coli* leads to a permanent repression of secondary catabolic genes (Postma *et al*., 1993). Because of the deletion of EI there is no phosphate transfer to $EIIA^{Glc}$. Consequently the adenylate cyclase cannot be activated, no cAMP is formed and no cAMP-CRP complex is formed which activates the expression of catabolic genes.

The mechanisms of CCR in *B. subtilis* and *E. coli* are achieved in completely different ways; nonetheless their hierarchical utilization of carbon sources is similar as both prefer glucose as carbon source.

In contrast to the mechanisms in *E. coil* and *B. subtilis*, in some organisms the hierarchical order is inverted and they prefer other carbon sources than glucose (reverse carbon catabolite repression). The Gram-negative bacterium *Pseudomonas aeruginosa* for example prefers organic acids and amino acids instead of glucose (Collier *et al*., 1996). Interestingly, in *Pseudomonas* the PTS system is not essential for CCR (Rojo, 2010). In *Pseudomonas* only fructose is transported into the cell through a PTS system, whereas all other sugars are transported via PTS-independent systems (Velázquez *et al*., 2007). Another example is *Rhizobium meliloti* which prefers succinate over glucose (Ucker & Signer, 1978). The Gram-positive bacterium *Streptococcus thermophilus* prefers lactose over glucose (van den Bogaard *et al*., 2000). Regardless of whether glucose or another carbon source is the preferred carbon source, the hierarchical utilization reflects the adaptation of bacteria to their particular ecological niches. The preferred usage of a certain carbon source enables bacteria to achieve best fitness in a changing environment.

In bacteria, the co-utilization of two carbon sources like in *B. subtilis* (glucose and malate) is rather unusual. However, other exceptions were found which do not show diauxic growth in the presence of two carbon sources. The Gram-positive bacterium *C. glutamicum* for example is able to co-metabolize glucose and fructose, glucose and lactate, and glucose and pyruvate, whereas *C. glutamicum* exhibits diauxic growth on a mixture of glucose and glutamate (Cocaign *et al*., 1993; Dominguez *et al*., 1997; Krämer *et al*., 1990). *Leuconostoc oenos* co-metabolizes glucose with citrate or fructose (Salou *et al*., 1994). Just like *B. subtilis Enterococcus faecalis* is able to metabolize malate in parallel to glucose (Mortera *et al*., 2012). Interestingly, CCR in *E. faecalis* is accomplished by the CcpA/HPrK pathway and glucose represses the genes involved in malate utilization. However, *E. faecalis* possesses in addition to the CcpA/HPrK pathway different regulatory systems to control the parallel assimilation of both carbon sources (Mortera *et al*., 2012). Also in eukaryotic organisms a simultaneous utilization of carbon sources was shown. In yeast (*Candida shehatae*) the simultaneous fermentation of glucose with xylose under anaerobic conditions was found (Kastner & Roberts, 1990). As xylan is one of the most frequent polysaccharides in nature (a major component of plants) that ability of *C. shehatae* is very interesting for biotechnology.

6.3. Malate metabolism in *B. subtilis*

B. subtilis equally prefers a glycolytic (glucose) and a gluconeogenic (malate) carbon source that can be used in parallel and that both allow fast growth (see above). In the soil (the natural habitat of *B. subtilis*) malate is commonly available as a free intermediate, whereas the majority of glucose must first be liberated from various polymers (see introduction). Thus, the preference of *B. subtilis* also for malate is not surprising.

B. subtilis possesses a complex genetic equipment for the uptake and utilization of malate. Several transporters are described to be involved in malate uptake, whereas the MaeN symporter seems to be the only essential malate transporter in *B. subtilis* (see introduction). Once malate is taken up, it enters the carbon metabolism of *B. subtilis* at the phosphoenolpyruvate-pyruvate-oxaloacetate node that connects glycolysis/gluconeogenesis with the TCA cycle. Most bacteria possess a similar setup of enzymes that catalyze glycolysis/gluconeogenesis or the TCA cycle. However, the connection via the phosphoenolpyruvate-pyruvate-oxaloacetate node is often carried out by completely different reactions (Sauer & Eikmanns, 2005). In *B. subtilis* malate can be used by five malate dehydrogenases, either by the TCA cycle enzyme Mdh or by four decarboxylating malate dehydrogenases (malic enzymes). *B. subtilis* encodes one NADP-dependent malic enzyme (YtsJ) and three NAD-dependent malic enzymes (MaeA, MalS and MleA) (Lerondel *et al*., 2006). However, less is known about the exact role of the malic enzymes in malate metabolism of *B. subtilis* and the existence of four paralogous isoforms in one species is rather uncommon (Lerondel *et al*., 2006).

In this study the role of Mdh, the malic enzymes and PckA in malate metabolism of *B. subtilis* was analyzed. Deletion mutants of the NAD-dependent malic enzymes do not show any growth defect grown in minimal medium with malate or glucose as a single carbon source. Only the deletion of the NADP-dependent malic enzyme YtsJ leads to a reduced growth in minimal medium with malate (see chapter 4; also described previously in Lerondel *et al*., 2006). In contrast, Mdh and PckA are essential for growth in a minimal medium with malate as a single carbon source and their function cannot be complemented by the malic enzymes. Oxaloacetate which is formed by Mdh is an important intermediate of the TCA cycle and serves as a substrate for three different enzymes (AspB, CitZ and PckA). Therefore, it can be assumed that the reaction of the malic enzymes and the anaplerotic reaction of PycA are not sufficient to complement the loss of Mdh. Furthermore, PckA is the only connection to gluconeogenesis in *B.*

subtilis as *B. subtilis* does not encode a PEP synthase and as the reaction of pyruvate kinase (Pyk) is irreversible. *E. coli* for example encodes a PEP synthetase (PepA). Therefore, only a *pckA pepA* double mutant is not able to use malate as a single carbon source (Hanson & Juni, 1974). Similarly to *B. subtilis,* Mdh is essential for malate utilization in *E. coli*, whereas the two malic enzymes of *E. coli* (MaeB and SfcA) are also not essential (van der Rest *et al*., 2000). SfcA and MaeB of *E. coli* are NAD- and NADP-dependent malic enzymes, respectively. Like YtsJ in *B. subtilis*, MaeB is an important source of NADPH during gluconeogenic growth (Bologna *et al*., 2007; Wang *et al*., 2011). Under gluconeogenic growth conditions in *B. subtilis* (malate as a single carbon source) 40-50% of NADPH is formed by YtsJ, whereas under glycolytic growth conditions the majority of NADPH is produced by the pentose phosphate pathway and only very small amounts are produced by YtsJ (Kleijn *et al*., 2010). Moreover, under gluconeogenic conditions about one-third of the produced NADPH is needed for gluconeogenesis, whereas all NADPH can be used for biomass formation under glycolytic conditions (Kleijn *et al*., 2010). In conclusion, YtsJ is an important NADPH source in malate grown cells.

As the expression of two NAD-dependent malic enzymes (MaeA and MalS) is specifically induced in the presence of malate by the two-component system MalKR, but the single and also the double mutants show no growth defect under inducing growth conditions (malate as a single carbon source) (Doan *et al*., 2003; Tanaka *et al*., 2003; see chapter 4), it is surprising why these enzymes are specifically induced. To further elucidate the role of the NAD-dependent malic enzymes in malate metabolism the contribution of the enzymes to the ATP pool of the cells was analyzed (see chapter 4). In the wild type of *B. subtilis* the intracellular ATP levels remains constant under different growth conditions (Ludwig *et al*., 2002). To keep the intracellular ATP levels constant key enzymes of glycolysis (e. g. phosphofructokinase) and the TCA cycle (e. g. citrate synthase) are inhibited by high ATP concentrations and activated by high AMP concentrations (Byrnes *et al*., 1994; Flechtner & Hanson, 1963; Johnson & Hanson, 1974).

Interestingly, in the *maeA* mutant the ATP level was reduced by about 10% and in a triple mutant (*maeA*, *malS* and *mleA*) even by about 20%. Thus, these results indicate that the NAD-dependent malic enzymes (especially MaeA and MalS) contribute to the ATP pool of the cells by providing NADH. Also in the *ytsJ* mutant the ATP level was reduced by about 20%. Recently it was shown, that malic enzyme mutants exhibit enhanced fluxes through the pentose phosphate pathway (Lerondel *et al*., 2006). As YtsJ provides about 40-50% of NADPH during gluconeogenic growth, a higher flux through the pentose phosphate pathway might partially

compensate the deletion. However, higher fluxes through gluconeogenesis require ATP and might explain the low ATP levels in an *ytsJ* mutant.

6.4. The regulation of the TCA cycle

In comparison with eukaryotes the control of the TCA cycle in prokaryotes is much more complex. In eukaryotic cells the TCA cycle is located in the matrix of the mitochondria and is primarily allosterically controlled. In contrast, in prokaryotes the pathway is located in the cytoplasm and is also highly controlled at the level of gene expression. In various bacteria the adaptability to changing environmental conditions and their broad metabolic abilities are based on the TCA cycle. Thus, a strict control of the pathway is much more important.

In *B. subtilis* the regulation of the TCA cycle is mainly exerted on the first enzymes of the cycle (CitZ and CitB). Depending on the various nutritional supplies the expression of the corresponding genes is controlled by a complex interplay of several transcription factors (see introduction). In this work a novel post-transcriptional control of citrate synthase by the TCA cycle enzyme aconitase was identified that extends the already complex model of transcriptional control. In an aconitase mutant the *citZ* mRNA was found to be stabilized and gel-shift experiments revealed a direct binding of aconitase to the *citZ* 5'UTR (see chapter 5). These results indicate that CitZ levels can be fine-tuned by aconitase under specific metabolic conditions, leading to improved control of citrate production (see below).

Like in *B. subtilis* also in other bacteria especially the entrance into the TCA cycle is highly regulated. The entrance into the TCA cycle in *E. coli* is catalyzed like in *B. subtilis* by citrate synthase (GltA), aconitase (AcnA and AcnB) and isocitrate dehydrogenase (Icd). However, *E. coli* possesses two aconitase proteins. AcnB is the major enzyme whereas AcnA is a stationary-phase enzyme which is induced by iron limitation and oxidative stress (Cunningham *et al*., 1997; Jordan *et al*., 1999). Like in *B. subtilis* the expression of GltA, AcnA and AcnB is controlled by carbon catabolite repression and the expression is activated by CRP (cAMP receptor protein) (Gosset *et al*., 2004). Furthermore, the expression of *acnA* and *acnB* is extensively controlled by several transcription factors. The expression of *acnA* is induced by FruR, Fur and SoxRS and is repressed by ArcA and Fnr. The expression of *acnB* is repressed by ArcA, FruR and Fis (Cunningham *et al*., 1997). As *E. coli* is able to use acetate as a sole carbon source and can bypass a section of the TCA cycle by the use of the glyoxylate cycle, additional control is necessary. The expression of glyoxylate cycle genes is strictly regulated and the switch between

TCA cycle and glyoxylate cycle is controlled by post-translational modification (phosphorylation) of isocitrate dehydrogenase (Cozzone & El-Mansi, 2005). In the Gram-positive soil bacterium *Corynebacterium glutamicum* the control of the TCA cycle is exerted on the expression of aconitase that is controlled by three separate transcription factors. The aconitase gene is repressed by AcnR (aconitase repressor), triggered by a yet unknown signal, and aconitase and also SdhCAB are repressed by RipA under iron limitation. Furthermore, the expression of aconitase is induced by RamA (regulator of acetate metabolism A) in the presence of acetate (Bott, 2007). Like in *E. coli* the control of the glyoxylate cycle requires further control.

Until now a post-transcriptional control of citrate synthase by the iron regulatory protein aconitase like in *B. subtilis* has not been found in other bacteria. However, in *E. coli* it was shown that aconitase increase the mRNA stability of its own gene product (Tang *et al*., 2002). As aconitase is active as a trigger enzyme in many organisms, TCA cycle control at the post-transcriptional level might be plausible also for other bacteria (Commichau & Stülke, 2008).

The aconitase: An iron regulatory protein

Iron is an essential trace element for the majority of living organisms, since it is an important cofactor in many biological functions. However, high iron levels are toxic and lead to the formation of highly reactive free radicals which can damage the DNA and other components of the cell by oxidative stress. Consequently, the maintenance of cellular iron homeostasis is crucial.

Already 20 years ago it was shown that the TCA cycle enzyme aconitase is involved in the regulation of iron homeostasis (Rouault *et al.*, 1988; Rouault *et al.*, 1991). During sufficient iron supply the protein is active in the TCA cycle and catalyzes the isomerization of citrate to isocitrate (see introduction). However, during iron-starvation the enzyme loses its enzymatic activity and serves as iron regulatory protein (IRP). Under these conditions, the IRP can bind to specific mRNA stem-loop structures, so-called iron responsive elements (IREs) at the 5’ or 3’ UTR. The binding of the IRP to the mRNA leads either to translational repression or to the stabilization or destabilization of the bound mRNA. Thus, the IRP modulates the expression of genes involved in iron metabolism at the post-transcriptional level (Volz, 2008). Interestingly, IRPs contain no established RNA binding motifs and does not share sequence similarities with known RNA-binding proteins (Wallander *et al*., 2006; Wang & Pantopoulos, 2011).

The catalytic function of aconitase and the switch between enzyme and IRP activities is dependent on the presence of an iron-sulfur (4Fe-4S) cluster which is covalently-bound to the protein by three cysteine residues. The cysteine residues directly interact with the iron atoms in the cluster and during enzymatic reaction the substrate is coordinated to a specific iron atom of the iron-sulfur cluster (Beinert *et al*., 1996). Under iron limiting conditions or under oxidative stress the iron-sulphur cluster is destroyed, catalytic activity is lost and the apo-protein is able to bind to specific mRNAs (Volz, 2008).

Iron regulatory proteins were first discovered in eukaryotic cells, but the dual role of aconitase was also shown in several prokaryotes (Alén & Sonenshein, 1999; Banerjee *et al*., 2007; Tang & Guest, 1999). Most eukaryotic cells possess two classes of aconitases: cytoplasmatic (c-aconitase) and mitochondrial aconitase (m-aconitase). M-aconitase is active as aconitase in the TCA cycle whereas c-aconitase is either active as cytosolic enzyme or as IRP. The aconitases of prokaryotes are highly similar to the eukaryotic IRPs (Gruer *et al*., 1997b). *B. subtilis* possesses a single aconitase protein which is encoded by the *citB* gene in a monocistronic operon (Dingman & Sonenshein, 1987). The aconitase of *B. subtilis* is homologous to the bifunctional eukaryotic IRP-1 protein and as well is functional as iron regulatory protein (Alén & Sonenshein, 1999). In this study the additional function of CitB in the control of the TCA cycle branch was demonstrated (see below). Especially in bacteria the regulatory role of the aconitase is not only limited to iron metabolism. An IRP-mediated regulatory control of the TCA cycle like in *B. subtilis* was also found in *E. coli*. Both aconitase proteins of *E. coli* (AcnA and AcnB) are RNA binding proteins. In the IRP-state they are involved in the oxidative stress response and mediate their own expression by a positive autoregulatory switch (Tang & Guest, 1999; Tang *et al*., 2002).

In *B. subtilis* CitB is also associated to sporulation, an iron-dependent process (Craig *et al*., 1997; Serio *et al*., 2006). In *Salmonella enterica* aconitase is involved in motility control by destabilizing the *ftsH* transcript (Tang *et al*., 2004). In several pathogenic bacteria aconitase is linked with toxin production and pathogenicity (Somerville *et al*., 2002; Somerville *et al*., 1999). However, it is unknown if the link is mediated by the IRP activity of aconitase.

A model for TCA cycle branch control in *B. subtilis*

In the presence of a preferred carbon source like glucose or malate the expression of the *citZ* gene is repressed by CcpA (Blencke *et al*., 2006; Miwa *et al*., 2000). In addition, *citZ* and *citB*

are repressed by CcpC in the presence of a preferred carbon and a good nitrogen source (Kim *et al*., 2002; Jourlin-Castelli *et al*., 2000). When the intracellular pools of GTP and branched-chain amino acids are high *citB* is further repressed by CodY (Ratnayake-Lecamwasam *et al*., 2001; Shivers & Sonenshein, 2004). Thus, under conditions of good nutritional supply the interplay of these three transcription factors leads to a strong repression of the TCA cycle branch at the transcriptional level. In the absence of a preferred carbon source the repression of *citZ* by CcpA is relieved. The weaker repression results in the production of small amounts of citrate. Citrate inactivates CcpC and leads to the expression of *citZ* and *citB* (see Fig. 6.1).

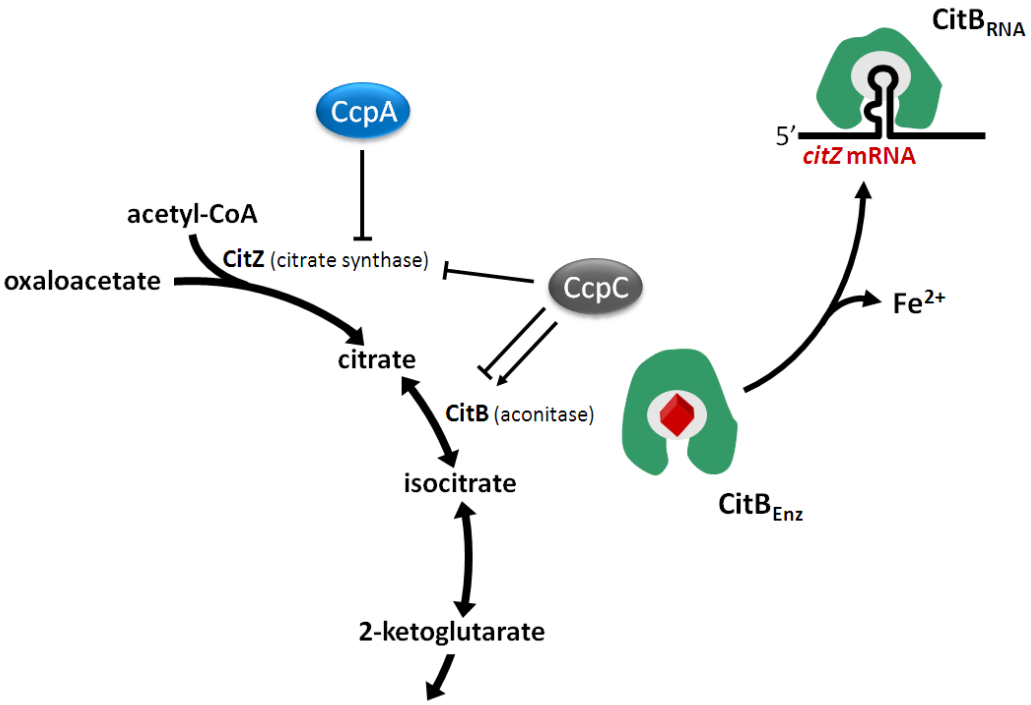

Fig. 6.1. A model for TCA cycle branch control in *B. subtilis*. In the presence of a preferred carbon source *citZ* is repressed at the transcriptional level by CcpA. In addition, *citZ* and *citB* are both repressed by CcpC in the presence of a preferred carbon and a good nitrogen source. In the absence of a preferred carbon source the repression by CcpA and CcpC is abolished. Furthermore, high intracellular citrate levels trigger CcpC to become a positive regulator of *citB*, which leads to a higher expression level of *citB*. Under iron limiting conditions CitB switches from enzymatic form to the IRP-state and binds to the 5'UTR of *citZ* mRNA. The binding of CitB leads to a decreased stability of *citZ* mRNA and lower levels of CitZ protein inside of the cell.

Beside maintenance of cellular iron homeostasis the control of intracellular citrate levels is very important. This TCA cycle intermediate can be used as carbon source, is necessary for the synthesis of fatty acids and sterols and is involved in transport of divalent metal ions. However, high citrate concentrations are toxic for the cell. Citrate is able to chelate divalent cations like

Ca^{2+}, Fe^{2+} and Zn^{2+} and is so involved in homeostasis of metal ions (Tong & Rouault, 2007). At high intracellular citrate levels, iron will be sequestered away from iron-containing proteins (including aconitase). Consequently, CitB switches from the enzymatic form to the RNA-binding form. In the IRP-state CitB interacts with the *citZ* mRNA at the post-transcriptional level and decreases the *citZ* mRNA stability. The decreased *citZ* mRNA levels lead to lower amounts of CitZ protein and a reduced production of citrate in the cell (see Fig. 6.1). Moreover, under these conditions (high citrate levels) CcpC switches its mode of activity and becomes a transcriptional activator that stimulates *citB* expression (Mittal *et al*., 2012). As a consequence the high citrate levels are further reduced by the activity of a larger amount of aconitase. Thus, in *B. subtilis* the level of citrate in the cell is tightly controlled by regulating the enzyme that produces citrate (CitZ) and by the bifunctional enzyme CitB which serves as a sensor for citrate and also utilizes citrate.

The complex regulation of the TCA cycle branch in *B. subtilis* demonstrates the great importance of an efficient control of this central pathway in carbon metabolism. However, the here postulated model for TCA cycle branch control might be still incomplete. Recently a sigma D-dependent antisense RNA with a high level of complementarity to the *citZ* 3´UTR was found in *B. subtilis* (Schmalisch *et al.,* 2010). The antisense RNA might also control the translation of *citZ* mRNA by binding of the mRNA or the antisense might be bound by CitB.

The enzymes of the TCA cycle branch and other enzymes of the whole TCA cycle are allosterically regulated or subject to post-translational modification. The enzyme activity of CitZ for example is controlled by ATP and AMP (see above) and is additionally feedback regulated by citrate (Johnson & Hanson, 1974). CitZ, Icd, Mdh, SucC, SucD and SdhA were found to be phosphorylated in *B. subtilis* (Elsholz *et al*., 2012; Eymann *et al*., 2007, Macek *et al.*, 2007). The post-translational modification might influence the protein activity, the protein stability or protein interactions (Stülke, 2010b). Icd and Mdh for example are found to be phosphorylated at an arginine residue by the protein arginine kinase McsB (Elsholz *et al*., 2012). An arginine phosphorylation is a very labile protein modification and might be important for fast modulation of Icd and Mdh activity. However, in *B. subtilis* not much is known about the extent or the importance of the phosphorylation of the TCA cycle enzymes.

Outlook

This work was focused on the TCA cycle of *B. subtilis*. On the one hand protein-protein interactions between the enzymes of the cycle were identified and on the other hand its regulation was analyzed.

The TCA cycle metabolon was found to be a rather dynamic complex, so it would be an interesting project to elucidate the regulatory network that triggers the formation of the metabolon and the influence of metabolic fluxes onto the whole metabolon. Allosteric regulation or protein modification of the single enzymes might be conceivable. Furthermore, it would be fascinating to study the exact localization pattern of the enzymes that might be influenced by different metabolic conditions. To identify the structure of the metabolon and to give a proof for enhanced metabolic fluxes mediated by substrate channeling would be a final aim.

Similarly the analysis of malate-mediated carbon catabolite repression and of TCA cycle branch control in *B. subtilis* left some open questions. To identify the additional trigger that controls the strength of malate-mediated CCR and so controls the hierarchy of carbon sources might be an interesting task in a future study. Moreover, the novel model for TCA cycle branch control established in this work might be still incomplete. Previously a small non-coding RNA was found that possesses high similarity to the *citZ* 5'UTR (Schmalisch *et al.,* 2010). To analyze the role of this small RNA in TCA cycle branch control would be another interesting project.

7. References

Abramoff, M. D., Magelhaes, P. J. & Ram, S. J. (2004). Image processing with ImageJ. *Biophotonics Int.* **11**, 36-42.

Alén, C. & Sonenshein, A. L. (1999). *Bacillus subtilis* aconitase is an RNA-binding protein. *Proc. Natl. Acad. Sci. U S A* **96**, 10412-10417.

Amar, P., Legent, G., Thellier, M., Ripoll, C., Bernot, G., Nyström, T., Saier, M. H. & Norris, V. (2008). A stochastic automaton shows how enzyme assemblies may contribute to metabolic efficiency. *BMC Syst. Biol.* **2**, 27.

An, S., Kumar, R., Sheets, E. D. & Benkovic, S. J. (2008). Reversible compartimentalization of de novo purine biosynthetic complexes in living cells. *Science*. **320**, 103-106.

An, S., Kyoung, M., Allen, J. J., Shokat, K. M. & Benkovic, S. J. (2010). Dynamic regulation of a metabolic multi-enzyme complex by protein kinase CK2. *J. Biol. Chem.* **285**, 11093-11099.

Anagnostopoulos, C. & Spizizen, J. (1961). Requirements for transformation in *Bacillus subtilis*. *J. Bacteriol.* **81**,741-746.

Asai, K., Baik, S. H., Kasahara, Y., Moriya, S. & Ogasawara, N. (2000). Regulation of the transport system for C_4-dicarboxylic acids in *Bacillus subtilis*. *Microbiology* **146**, 263-271.

Bacher, A., Eberhardt, S., Fischer, M., Kis, K. & Richter, G. (2000). Biosynthesis of vitamin B_2 (riboflavin). *Annu. Rev. Nutr*. **20**, 153-167.

Bais, H. P., Weir, T. L., Perry, L. G., Gilroy S. & Vivanco J. M. (2006). The role of root exudates in rhizosphere interactions with plants and other organisms. *Annu. Rev. Plant Biol.* **57**, 233-266.

Banerjee, S., Nandyala, A. K., Raviprasad, P., Ahmed, N. & Hasnain, S. E. (2007). Iron-dependent RNA-binding activity of *Mycobacterium tuberculosis* aconitase. *J. Bacteriol*. **189**, 4046-4052.

Barbe, V., Cruveiller, S., Kunst, F., Lenoble, P., Meurice, G. & other authors (2009). From a consortium sequence to a unified sequence: the *Bacillus subtilis* 168 reference genome a decade later. *Microbiology* **155**, 1758-1775.

Barnes, S. J. & Weitzman, P. D. (1986). Organization of citric acid cycle enzymes into a multienzyme cluster. *FEBS Lett*. *201*, 267-270.

Baumgart, M., Mustafi, N., Krug, A. & Bott, M. (2011). Deletion of the aconitase gene in *Corynebacterium glutamicum* causes strong selection pressure for secondary mutations inactivating citrate synthase. *J. Bacteriol*. **193**, 6864-6873.

Beinert, H., Kennedy, M. C. & Stout, C. D. (1996). Aconitase as iron-sulfur protein, enzyme, and iron-regulatory protein. *Chem. Rev*. **96**, 2335-2374.

Beinert, H. (2000). Iron-sulfur proteins: ancient structures, still full of surprises. *J. Biol. Inorg. Chem.* **5**, 2-15.

Belitsky, B. R., Janssen, P. J. & Sonenshein, A. L. (1995). Sites required for GltC-dependent regulation of *Bacillus subtilis* glutamate synthase expression. *J. Bacteriol*. **177**, 5686-5695.

Belitsky, B. R., Gustafsson, M. C., Sonenshein, A. L. & Von Wachenfeldt, C. (1997). An lrp-like gene of *Bacillus subtilis* involved in branched-chain amino acid transport. *J. Bacteriol*. **179**, 5448-5457.

Belitsky, B. R. & Sonenshein, A. L. (1998). Role and regulation of *Bacillus subtilis* glutamate dehydrogenase genes. *J. Bacteriol*. **180**, 6298-6305.

Belitsky, B. R. & Sonenshein, A. L. (2004). Modulation of activity of *Bacillus subtilis* regulatory proteins GltC and TnrA by glutamate dehydrogenase. *J. Bacteriol*. **186**, 3399-3407.

Bennett, B. D., Kimball, E. H., Gao, M., Osterhout, R., Van Dien, S. J. & Rabinowitz, J. D.(2009). Absolute metabolite concentrations and implied enzyme active site occupancy in *Escherichia coli*. *Nat. Chem. Biol*. **5**, 593-599.

Benson, A. K. & Haldenwang, W. G. (1993). Regulation of σ^B levels and activity in *Bacillus subtilis*. *J. Bacteriol.* **175**, 2347-2356.

Bettenbrock, K., Sauter, T., Jahreis, K., Kremling, A., Lengeler, J. W. & Gilles, E. D. (2007). Correlation between growth rates, $EIIA^{Crr}$ phosphorylation, and intracellular cyclic AMP levels in *Escherichia coli* K-12. *J. Bacteriol*. **189**, 6891-6900.

Blencke, H.-M., Homuth, G., Ludwig, H., Mäder, U., Hecker, M. & Stülke, J. (2003). Transcriptional profiling of gene expression in response to glucose in *Bacillus subtilis*: regulation of the central metabolic pathways. *Metab. Eng.* **5**, 133-149.

Blencke, H.-M., Reif, I., Commichau, F. M., Detsch, C., Wacker, I., Ludwig, H. & Stülke, J. (2006). Regulation of *citB* expression in *Bacillus subtilis*: integration of multiple metabolic signals in the citrate pool and by the general nitrogen regulatory system. *Arch. Microbiol*. **185**, 136-146.

Bologna, F. P., Andreo, C. S. & Drincovich, M. F. (2007). *Escherichia coli* malic enzymes: two isoforms with substantial differences in kinetic properties, metabolic regulation, and structure. *J. Bacteriol*. **189**, 5937-5946.

Botella, E., Fogg, M., Jules, M., Piersma, S., Doherty, G. & other authors (2010). pBaSysBioII: an integrative plasmid generating *gfp* transcriptional fusions for high-throughput analysis of gene expression in *Bacillus subtilis*. *Microbiology* **156**, 1600-1608.

Bott, M. (2007). Offering surprises: TCA cycle regulation in *Corynebacterium glutamicum*. *Trends Microbiol.* **15**, 417-425.

Braun, P., Tasan, M., Dreze, M., Barrios-Rodiles, M., Lemmens, I. & other authors (2009). An experimentally derived confidence score for binary protein-protein interactions. *Nat. Methods*. **6**, 91-97.

Brehm, S. P., Staal, S. P. & Hoch, J. A. (1973). Phenotypes of pleiotropic-negative sporulation mutants of *Bacillus subtilis*. *J. Bacteriol*. **115**, 1063-1070.

Brückner, R. & Titgemeyer, F. (2002). Carbon catabolite repression in bacteria: choice of the carbon source and autoregulatory limitation of sugar utilization. *FEMS Microbiol. Lett*. **9**, 141-148.

Buchanan, B. B. & Arnon, D. I. (1990). A reverse KREBS cycle in photosynthesis: consensus at last. *Photosynth. Res*. **24**, 47-53.

Buescher, J. M., Liebermeister, W., Jules, M., Uhr, M., Muntel, J. & other authors (2012). Global network reorganization during dynamic adaptations of *Bacillus subtilis* metabolism. *Science* **335**, 1099-1103.

Burkholder, P. R. & Giles, N. H. Jr. (1947). Induced biochemical mutations in *Bacillus subtilis*. *Am. J. Bot*. **34**, 345-348.

Byrnes, M., Zhu, X., Younathan, E. S. & Chang, S. H. (1994). Kinetic characteristics of phosphofructokinase from *Bacillus stearothermophilus*: MgATP nonallosterically inhibits the enzyme. *Biochemistry* **33**, 3424-3431.

Campanella, M. E., Chu, H. & Low, P. S. (2005). Assembly and regulation of a glycolytic enzyme complex on the human erythrocyte membrane. *Proc. Natl. Acad. Sci. U S A* **102**, 2402-2407.

Carpousis, A. J. (2007). The RNA degradosome of *Escherichia coli*: an mRNA-degrading machine assembled on RNase E. *Annu. Rev. Microbiol.* **61**, 71-87.

Chen, Y., Cao, S., Chai, Y., Clardy, J., Kolter, R., Guo, J. H. & Losick, R. (2012). A *Bacillus subtilis* sensor kinase involved in triggering biofilm formation on the roots of tomato plants. *Mol. Microbiol.* **85**, 418-430.

Choi, S. K., & Saier, M. H., Jr (2005). Regulation of *sigL* expression by the catabolite control protein CcpA involves roadblock mechanism in *Bacillus subtilis*: potential connection between carbon and nitrogen metabolism. *J. Bacteriol*. **187**, 6856-6861.

Claessen, D., Emmins, R., Hamoen, L. W., Daniel, R. A., Errington, J. & Edwards, D. H. (2008). Control of the cell elongation-division cycle by shuttling of PBP1 protein in *Bacillus subtilis*. *Mol. Microbiol*. **68**, 1029-1046.

Cocaign, M., Monnet, C. & Lindley, N. D. (1993). Batch kinetics of *Corynebacterium glutamicum* during growth on various carbon substrates: use of substrate mixtures to localise metabolic bottlenecks. *Appl. Microbiol. Biotechnol*. **40**, 526-530.

Collier, D. N., Hager, P. W. & Phibbs, P. V., Jr. (1996). Catabolite repression control in the *Pseudomonads*. *Res. Microbiol*. **147**, 551-561.

Commichau, F. M., Forchhammer, K. & Stülke, J. (2006). Regulatory links between carbon and nitrogen metabolism. *Curr. Opin. Microbiol.* **9**, 167-172.

Commichau, F. M., Wacker, I., Schleider, J., Blencke, H.-M., Reif, I., Tripal, P. & Stülke, J. (2007a). Characterization of *B. subtilis* mutants with carbon-source independent glutamate biosynthesis. *J. Mol. Microbiol. Biotechnol*. **12**, 106-113.

Commichau, F. M., Herzberg, C., Tripal, P., Valerius, O. & Stülke, J. (2007b). A regulatory protein-protein interaction governs glutamate biosynthesis in *Bacillus subtilis*: the glutamate dehydrogenase RocG moonlights in controlling the transcription factor GltC. *Mol. Microbiol.* **65**, 642-654.

Commichau, F. M., Gunka, K., Landmann, J. J. & Stülke, J. (2008). Glutamate metabolism in *Bacillus subtilis*: gene expression and enzyme activities evolved to avoid futile cycles and to allow rapid responses to perturbations of the system. *J. Bacteriol.* **190**, 3557-3564.

Commichau, F. M. & Stülke, J. (2008). Trigger enzymes: bifunctional proteins active in metabolism and in controlling gene expression. *Mol. Microbiol*. **67**, 692-702.

Commichau, F. M., Rothe, F. M., Herzberg, C., Wagner, E., Hellwig, D., Lehnik-Habrink, M., Hammer, E., Völker, U. & Stülke, J. (2009). Novel activities of glycolytic enzymes in *Bacillus subtilis*: interactions with essential proteins involved in mRNA processing. *Mol. Cell Proteomics* **8**, 1350-1360.

Cozzone, A. J. & El-Mansi, M. (2005). Control of isocitrate dehydrogenase catalytic activity by protein phosphorylation in *Escherichia coli*. *J. Mol. Microbiol. Biotechnol.* **9**, 132-146.

Craig, L. C., Gregory, J. D. & Barry G. T. (1949). Purity studies on polypeptide antibiotics; bacitracin. *J. Clin. Invest*. **28**, 1014-1017.

Craig, J. E., Ford, M. J., Blaydon, D. C. & Sonenshein, A. L. (1997). A null mutation in the *Bacillus subtilis* aconitase gene causes a block in Spo0A-phosphate-dependent gene expression. *J. Bacteriol*. **179**, 7351-7359.

Crasnier, M. (1996). Cyclic AMP and catabolite repression. *Res. Microbiol.* **147**, 479-482.

Cunningham, L., Gruer, M. J. & Guest, J. R. (1997). Transcriptional regulation of the aconitase genes (*acnA* and *acnB*) of *Escherichia coli*. *Microbiology* **143**, 3795-3805.

Dandekar, T., Snel, B., Huynen, M. & Bork, P. (1998). Conservation of gene order: a fingerprint of proteins that physically interact. *Trends Biochem. Sci.* **23**, 324-328.

Dean, D. R., Hoch, J. A. & Aronson, A. I. (1977). Alteration of the *Bacillus subtilis* glutamine synthetase results in overproduction of the enzyme. *J. Bacteriol*. **131**, 981-987.

Deng, Y., Zhu, Y., Wang, P., Zhu, L., Zheng, J., Li, R., Ruan, L., Peng, D. & Sun, M. (2011). Complete genome sequence of *Bacillus subtilis* BSn5, an endophytic bacterium of *Amorphophallus konjac* with antimicrobial activity for the plant pathogen *Erwinia carotovora* subsp. *carotovora. J. Bacteriol.* **193**, 2070-2071.

Deutscher, J., Kessler, U., Alpert, C. A. & Hengstenberg, W. (1984). Bacterial phosphoenolpyruvate-dependent phosphotransferase system: P-Ser-HPr and its possible regulatory function? *Biochemistry* **23**, 4455-4460.

Deutscher, J., Reizer, J., Fischer, C., Galinier, A., Saier, M. H., Jr. & Steinmetz M. (1994). Loss of protein kinase-catalyzed phosphorylation of HPr, a phosphocarrier protein of the phosphotransferase system, by mutation of the *ptsH* gene confers catabolite repression resistance to several catabolic genes of *Bacillus subtilis*. *J. Bacteriol.* **176**, 3336-3344.

Deutscher, J., Küster, E., Bergstedt, U., Charrier, V. & Hillen, W. (1995). Protein kinase dependent HPr/CcpA interaction links glycolytic activity to carbon catabolite repression in Gram-positive bacteria. *Mol. Microbiol.* **15**, 1049-1053.

Deutscher, J., Francke, C. & Postma, P. W. (2006). How phosphotransferase system-related protein phosphorylation regulates carbohydrate metabolism in bacteria. *Microbiol. Mol. Biol. Rev.* **70**, 939-1031.

Deutscher, J. (2008). The mechanisms of carbon catabolite repression in bacteria. *Curr. Opin. Microbiol.* **11**, 87-93.

Diethmaier, C., Pietack, N., Gunka, K., Wrede, C., Lehnik-Habrink, M., Herzberg, C., Hübner, S. & Stülke, J. (2011). A novel factor controlling bistability in *Bacillus subtilis*: the YmdB protein affects flagellin expression and biofilm formation*. J. Bacteriol*. **193**, 5997-6007.

Dimroth, P. & Schink, B. (1998). Energy conservation in the decarboxylation of dicarboxylic acids by fermenting bacteria. *Arch. Microbiol*. **170**, 69-77.

Dingman, D. W. & Sonenshein, A. L. (1987). Purification of aconitase from *Bacillus subtilis* and correlation of its N-terminal amino acid sequence with the sequence of the *citB* gene. *J. Bacteriol*. **169**, 3062-3067.

Doan, T. & Aymerich, S. (2003). Regulation of the central glycolytic genes in *Bacillus subtilis*: binding of the repressor CggR to its single DNA target sequence is modulated by fructose-1,6-bisphosphate. *Mol. Microbiol*. **47**, 1709-1721.

Doan, T., Servant, P., Tojo, S., Yamaguchi, H., Lerondel, G., Yoshida, K., Fujita, Y. & Aymerich S. (2003). The *Bacillus subtilis ywkA* gene encodes a malic enzyme and its transcription is activated by the YufL/YufM two-component system in response to malate. *Microbiology* **149**, 2331-2343.

Dominguez, H., Cocaign-Bousquet, M. & Lindley, N. D. (1997). Simultaneous consumption of glucose and fructose from sugar mixtures during batch growth of *Corynebacterium glutamicum. Appl. Microbiol. Biotechnol*. **47**, 600-603.

Dunn, M. F., Niks, D., Ngo, H., Barends, T. R. & Schlichting, I. (2008). Tryptophan synthase: the workings of a channeling nanomachine. *Trends Biochem. Sci*. **33**, 254-264.

Elsholz, A. K., Turgay, K., Michalik, S., Hessling, B., Gronau, K. & other authors (2012). Global impact of protein arginine phosphorylation on the physiology of *Bacillus subtilis*. *Proc. Natl. Acad. Sci. U S A* **109**, 7451-7456.

Emery-Goodman, A., Hirling, H., Scarpellino, L., Henderson, B. & Kühn, L. C. (1993). Iron regulatory factor expressed from recombinant baculovirus: conversion between the RNA-binding apoprotein and Fe-S cluster containing aconitase. *Nucleic Acids Res*. **21**, 1457-1461.

Evans, M. C., Buchanan, B. B. & Arnon, D. I. (1996). A new ferredoxin-dependent carbon reduction cycle in a photosynthetic bacterium. *Proc. Natl. Acad. Sci. U S A* **55**, 928-934.

Eymann, C., Becher, D., Bernhardt, J., Gronau, K., Klutzny, A. & Hecker, M. (2007). Dynamics of protein phosphorylation on Ser/Thr/Tyr in *Bacillus subtilis*. *Proteomics* **7**, 3509-3526.

Fillinger, S., Boschi-Muller, S., Azza, S., Dervyn, E., Branlant, G. & Aymerich, S. (2000). Two glyceraldehyde-3-phosphate dehydrogenase with opposite physiological roles in a nonphotosynthetic bacterium. *J. Biol. Chem.* **275**, 14031-14037.

Fisher, S. H. & Magasanik, B. (1984a). Synthesis of oxaloacetate in *Bacillus subtilis* mutants lacking the 2-ketoglutarate dehydrogenase enzyme complex. *J. Bacteriol*. **158**, 55-62.

Fisher, S. H. & Magasanik, B. (1984b). 2-Ketoglutarate and the regulation of aconitase and histidase formation in *Bacillus subtilis*. *J. Bacteriol*. **158**, 379-382.

Flechtner, V. R. & Hanson, R. S. (1969). Coarse and fine control of citrate synthase from *Bacillus subtilis*. *Biochim. Biophys. Acta*. **184**, 252-262.

Fortnagel, P., & Freese, E. (1968). Analysis of sporulation mutants II. Mutants blocked in the citric acid cycle. *J. Bacteriol*. **95**, 1431-1438.

Fouet, A. & Sonenshein, A. L. (1990). A target for carbon source-dependent negative regulation of the *citB* promoter of *Bacillus subtilis*. *J. Bacteriol*. **172**, 835-844.

Fujita, Y. & Freese, E. (1979). Purification and properties of fructose-1,6-bisphosphatase of *Bacillus subtilis. J. Biol. Chem.* **254**, 5340-5349.

Fujita, Y. (2009). Carbon catabolite control of the metabolic network in *Bacillus subtilis*. *Biosci. Biotechnol. Biochem.* **73**, 245-259.

Fulton, A. B. (1982). How crowded is the cytoplasm? *Cell* **30**, 345-347.

Gaballa, A., Antelmann, H., Aguilar, C., Khakh, S. K., Song, K. B., Smaldone, G. T. & Helmann, J. D. (2008). The *Bacillus subtilis* iron-sparing response is mediated by a Fur-regulated small RNA and three small, basic proteins. *Proc. Natl. Acad. Sci. U S A* **105**, 11927-11932.

Galinier, A., Haiech, J., Kilhoffer, M. C., Jaquinod, M., Stülke, J., Deutscher, J. & Martin-Verstraete, I. (1997). The *Bacillus subtilis crh* gene encodes a HPr-like protein involved in carbon catabolite repression. *Proc. Natl. Acad. Sci. U S A* **94**, 8439-8444.

Galinier, A., Kravanja, M., Engelmann, R., Hengstenberg, W., Kilhoffer, M. C., Deutscher, J. & Haiech, J. (1998). New protein kinase and protein phosphatase families mediate signal transduction in bacterial catabolite repression. *Proc. Natl. Acad. Sci. U S A* **95**, 1823-1828.

Galinier, A., Deutscher, J. & Martin-Verstraete, I. (1999). Phosphorylation of either Crh or HPr mediates binding of CcpA to the *Bacillus subtilis xyn cre* and catabolite repression of the xyn operon. *J. Mol. Biol.* **286**, 307-314.

Gao, W., Dai, S., Liu, Q., Xu, Y., Bai, Y. & Qiao, M. (2010). Effect of site-directed mutagenesis of *citB* on the expression and activity of *Bacillus subtilis* aconitase. *Mikrobiologiia* **79**, 774-778.

Gavin, A. C., Aloy, P., Grandi, P., Krause, R., Boesche, M. & other authors (2006). Proteome survey reveals modularity of the yeast cell machinery. *Nature* **440**, 631-636.

Gest, H. & Mandelstam, J. (1987). Longevity of microorganisms in natural environments. *Microbiol. Sci*. **4**, 69-71.

Görke, B., Fraysse, L. & Galinier, A. (2004). Drastic differences in Crh and HPr synthesis levels reflect their different impacts on catabolite repression in *Bacillus subtilis*. *J. Bacteriol.* **186**, 2992-2995.

Görke, B. & Stülke, J. (2008). Carbon catabolite repression in bacteria: many ways to make the most out of nutrients. *Nat. Rev. Microbiol.* **6**, 613-624.

Gosset, G., Zhang, Z., Nayyar, S., Cuevas, W. A. & Saier, M. H. Jr. (2004). Transcriptome analysis of Crp-dependent catabolite control of gene expression in *Escherichia coli*. *J. Bacteriol*. **186**, 3516-3524.

Graham, J. W., Williams, T. C., Morgan, M., Fernie, A. R., Ratcliffe, R. G. & Sweetlove, L. J. (2007). Glycolytic enzymes associate dynamically with mitochondria in response to respiratory demand and support substrate channeling. *Plant Cell* **19**, 3723-3738.

Grandier-Vazeille, X., Bathany, K., Chaignepain, S., Camougrand, N., Manon, S. & Schmitter, J. M. (2001). Yeast mitochondrial dehydrogenases are associated in a supramolecular complex. *Biochemistry* **40**, 9758-9769.

Groeneveld, M., Weme, R. G., Duurkens, R. H. & Slotboom, D. J. (2010). Biochemical characterization of the C_4-dicarboxylate transporter DctA from *Bacillus subtilis*. *J. Bacteriol.* **192**, 2900-2907.

Gruer, M. J., Bradbury, A. J. & Guest, J. R. (1997a). Construction and properties of aconitase mutants of *Escherichia coli*. *Microbiology* **143**, 1837-1846.

Gruer, M. J., Artymiuk, P. J. & Guest, J. R. (1997b). The aconitase family: three structural variations on a common theme. *Trends Biochem. Sci.* **22**, 3-6.

Grundy, F. J., Waters, D. A., Allen, S. H. & Henkin, T. M. (1993). Regulation of the *Bacillus subtilis* acetate kinase gene by CcpA. *J. Bacteriol.* **175**, 7348-7355.

Guérout-Fleury, A. M., Shazand, K., Frandsen, N. & Stragier, P. (1995). Antibiotic resistance cassettes for *Bacillus subtilis*. *Gene* **167**, 335-336.

Gunka, K. & Commichau, F. M. (2012). Control of glutamate homeostasis in *Bacillus subtilis*: a complex interplay between ammonium assimilation, glutamate biosynthesis and degradation. *Mol. Microbiol*. **85**, 213-224.

Gunka, K., Tholen, S., Gerwig, J., Herzberg, C., Stülke, J. & Commichau, F. M. (2012). A high-frequency mutation in *Bacillus subtilis*: requirements for the decryptification of the *gudB* glutamate dehydrogenase gene. *J. Bacteriol*. **1036**, 1036-1044.

Guzman, L. M., Belin, D., Carson, M. J. & Beckwith, J. (1995). Tight regulation, modulation, and high-level expression by vectors containing the arabinose P_{BAD} promoter. *J. Bacteriol*. **177**, 4121-4130.

Hahne, H., Wolff, S., Hecker, M. & Becher, D. (2008). From complementarity to comprehensiveness - targeting the membrane proteome of growing *Bacillus subtilis* by divergent approaches. *Proteomics* **8**, 4123-4136.

Haile, D. J., Rouault, T. A., Harford, J. B., Kennedy, M. C., Blondin, G. A., Beinert, H. & Klausner, R. D. (1992). Cellular regulation of the iron-responsive element binding protein: disassembly of the cubane iron-sulfer clustur results in high-affinity RNA binding. *Proc. Natl. Acad. Sci. U S A* **89**, 11735-11739.

Haile, D. J. (1999). Regulation of genes of iron metabolism by the iron-response proteins. *Am. J. Med. Sci*. **318**, 230-240.

Han, J. D., Bertin, N., Hao, T., Goldberg, D. S., Berriz, G. F. & other authors (2004). Evidence for dynamically organized modularity in the yeast protein-protein interaction network. *Nature* **430**, 88-93.

Hansen, E. J. & Juni, E. (1974). Two routes for synthesis of phosphoenolpyruvate from C_4-dicarboxylic acids in *Escherichia coli*. *Biochem. Biophys. Res. Commun.* **59**, 1204-1210.

Hanson, K. G., Steinhauer, K., Reizer, J., Hillen, W., & Stülke, J. (2002). HPr kinase/phosphatase of *Bacillus subtilis*: expression of the gene and effects of mutations on enzyme activity, growth and carbon catabolite repression. *Microbiology* **148**, 1805-1811.

Harwood, C. R. & Cutting, S. M. (1990). Chemically defined growth media and supplements, p. 548. *In* C. R. Harwood and S. M. Cutting (ed.), Molecular biological methods for *Bacillus*. *Wiley, Chichester, United Kingdom.*

Henkin, T. M., Grundy, F. J., Nicholson, W. L. & Chambliss, G. H. (1991). Catabolite repression of α-amylase gene expression in *Bacillus subtilis* involves a trans-acting gene product homologous to the *Escherichia coli lacI* and *galR* repressors. *Mol. Microbiol*. **5**, 575-584.

Hederstedt, L. & Rutberg, L. (1983). Orientation of succinate dehydrogenase and cytochrome b_{558} in the *Bacillus subtilis* cytoplasmic membrane. *J. Bacteriol*. **153**, 57-65.

Herzberg, C., Weidinger, L. A., Dörrbecker, B., Hübner, S., Stülke, J. & Commichau, F. M. (2007). SPINE: a method for the rapid detection and analysis of protein-protein interactions in vivo. *Proteomics* **7**, 4032-4035.

Hogema, B. M., Arents, J. C., Bader, R., Eijkemans, K., Yoshida, H., Takahashi, H., Aiba, H. & Postma, P. W. (1998). Inducer exclusion in *Escherichia coli* by non-PTS substrates: the role of the PEP to pyruvate ratio in determining the phosphorylation state of enzyme IIA^{Glc}. *Mol. Microbiol.* **30**, 487-498.

Hu, P., Janga, S. C., Babu, M., Díaz-Mejía, J. J., Butland, G., Yang, W., Pogoutse, O. & other authors (2009). Global functional atlas of *Escherichia coli* encompassing previously uncharacterized proteins. *PLoS Biol.* **7**, e96.

Huang, X., Holden, H. M. & Raushel, F. M. (2001). Channeling of substrates and intermediates in enzyme-catalyzed reactions. *Annu. Rev. Biochem*. **70**, 149-180.

Imlay, J. A. (2006). Iron-sulphur clusters and the problem with oxygen. *Mol. Microbiol*. **59**, 1073-1082.

Islam, M. M., Wallin, R., Wynn, R. M., Conway, M., Fujii, H., Mobley, J. A., Chuang, D. T. & Hutson, S. M. (2007). A novel branched-chain aminoa cid metabolon. Protein-protein interactions in a supramolecular complex. *J. Biol. Chem.* **282**, 11893-11903.

Janausch, I. G., Zientz, E., Tran, Q. H., Kröger, A. & Unden, G.(2002). C_4-dicarboxylate carriers and sensors in bacteria. *Biochim. Biophys. Acta*. **1553**, 39-56.

Jault, J. M., Fieulaine, S., Nessler, S., Gonzalo, P., Di Pietro, A., Deutscher, J. & Galinier A. (2000). The HPr kinase from *Bacillus subtilis* is a homooligomeric enzyme which exhibits strong positive cooperativity for nucleotide and fructose 1,6-bisphosphate binding. *J. Biol. Chem.* **275**, 1773-1780.

Jin, S. & Sonenshein, A. L. (1994a). Identification of two distinct *Bacillus subtilis* citrate synthase genes. *J. Bacteriol*. **176**, 4669-4679.

Jin, S. & Sonenshein, A. L. (1994b). Transcriptional regulation of *Bacillus subtilis* citrate synthase genes. *J. Bacteriol*. **176**, 4680-4690.

Jin, S. (1995). PhD Thesis. Tufts University, Boston, MA.

Jin, S. & Sonenshein, A. L. (1996). Characterization of the major citrate synthase of *Bacillus subtilis*. *J. Bacteriol.* **178**, 3658-3660.

Jin, S., Levin, P., Matsuno, K., Grossman, A. D. & Sonenshein, A. L. (1997). Deletion of the *Bacillus subtilis* isocitrate dehydrogenase gene causes a block at stage I of sporulation. *J. Bacteriol*. **179**, 4725-4732.

Johansson, H. O., Brooks, D. E. & Haynes, C. A. (2000). Macromolecular crowding and its consequences. *Int. Rev. Cytol.* **192**, 155-170.

Johnson, D. E. & Hanson, R. S. (1974). Bacterial citrate synthases: purification, molecular weight and kinetic mechanism. *Biochim. Biophys. Acta*. **350**, 336-353.

Jones, B. E., Dossonnet, V., Küster, E., Hillen, W., Deutscher, J. & Klevit, R. E. (1997). Binding of the catabolite repressor protein CcpA to its DNA target is regulated by phosphorylation of its corepressor HPr. *J. Biol. Chem.* **272**, 26530-26535.

Jordan, P. A., Tang, Y., Bradbury, A. J., Thomson, A. J. & Guest, J. R. (1999). Biochemical and spectroscopic characterization of *Escherichia coli* aconitases (AcnA and AcnB). *Biochem. J*. **344**, 739-746.

Jourlin-Castelli, C., Mani, N., Nakano, M. M. & Sonenshein, A. L. (2000). CcpC, a novel regulator of the LysR family required for glucose repression of the *citB* gene in *Bacillus subtilis*. *J. Mol. Biol.* **295**, 865-878.

Kaldy, P., Menotti, E., Moret, R. & Kühn, L. C. (1999). Identification of RNA-binding surfaces in iron regulatory protein-1. *Embo J*. **18**, 6073-6083.

Kang, S. O., Caparon, M. G. & Cho, K. H. (2010). Virulence gene regulation by CvfA, a putative RNase: the CvfA-enolase complex in *Streptococcus pyogenes* links nutritional stress, growth phase control, and virulence gene expression. *Infect. Immun.* **78**, 2754-2767.

Karimova, G., Pidoux, J., Ullmann, A. & Ladant, D. (1998). A bacterial two-hybrid system based on a reconstituted signal transduction pathway. *Proc. Natl. Acad. Sci. U S A* **95**, 5752-5756.

Karimova, G., Dautin, N. & Ladant, D. (2005). Interaction network among *Escherichia coli* membrane proteins involved in cell division as revealed by bacterial two-hybrid analysis. *J. Bacteriol*. **187**, 2233-2243.

Kastner, J. R. & Roberts, R. S. (1990). Simultaneous fermentation of D-xylose and glucose by *Candida shehatae*. *Biotechnol. Lett*. **12**, 57-60.

Kennedy, M. C., Emptage, M. H., Dreyer J.-L. & Beinert, H. (1983). The role of iron in the activation-inactivation of aconitase. *J. Biol. Chem*. **258**, 11098-11105.

Kennedy, M. C., Mende-Mueller, L., Blondin, G. A. & Beinert, H. (1992). Purification and characterization of cytosolic aconitase from beef liver and its relationship to the iron responsive element binding protein. *Proc. Natl. Acad. Sci. U S A* **89**, 11730-11734.

Kim, H. J., Roux, A. & Sonenshein, A. L. (2002). Direct and indirect roles of CcpA in regulation of *Bacillus subtilis* Krebs cycle genes. *Mol. Microbiol*. **45**, 179-190.

Kim, H. J., Kim, S. I., Ratnayake-Lecamwasam, M., Tachikawa, K., Sonenshein, A. L. & Strauch, M. (2003a). Complex regulation of the *Bacillus subtilis* aconitase gene. *J. Bacteriol*. **185**, 1672-1680.

Kim, S. I., Jourlin-Castelli, C., Wellington, S. R. & Sonenshein, A. L. (2003b). Mechanism of repression by *Bacillus subtilis* CcpC, a LysR family regulator. *J. Mol. Biol*. **334**, 609-624.

Kim, H. J., Mittal, M. & Sonenshein, A. L. (2006). CcpC-dependent regulation of *citB* and lmo0847 in *Listeria monocytogenes*. *J. Bacteriol*. **188**, 179-190.

Kirchberg, J., Büttner, D., Thiemer, B. & Sawers, R. (2012). Aconitase B is required for optimal growth of *Xanthomonas campestris* pv. *vesicatoria* in pepper plants. *PLoS One* **7**, 34941.

Kleijn, R. J., Buescher, J. M., Le Chat, L., Jules, M., Ayerich, S. & Sauer, U. (2010). Metabolic fluxes during strong carbon catabolite repression by malate in *Bacillus subtilis*. *J. Biol. Chem.* **285**, 1587-1596.

Koebmann, B. J., Westerhoff, H. V., Snoep, J. L., Nilsson, D. D. & Jensen, P. R. (2002). The glycolytic flux in *Escherichia coli* is controlled by the demand for ATP. *J. Bacteriol.* **184**, 3909-3916.

Koziol, U., Hannibal, L., Rodríguez, M. C., Fabiano, E., Kahn, M. L. & Noya, F. (2009). Deletion of citrate synthase restores growth of *Sinorhizobium meliloti* 1021 aconitase mutants. *J. Bacteriol*. **191**, 7581-7586.

Krämer, R., Lambert, C., Hoischen, C. & Ebbighausen, H. (1990). Uptake of glutamate in *Corynebacterium glutamicum*. 1. Kinetic properties and regulation by internal pH and potassium. *Eur. J. Biochem*. **194**, 929-935.

Krogan, N. J., Cagney, G., Yu, H., Zhong, G., Guo, X. & other authors (2006). Global landscape of protein complexes in the yeast *Saccharomyces cerevisiae*. *Nature* **440**, 637-643.

Krom, B. P., Aardema, R. & Lolkema, J. S. (2001). *Bacillus subtilis* YxkJ is a secondary transporter of the 2-hydroxycarboxylate transporter family that transports L-malate and citrate. *J. Bacteriol.* **183**, 5862-5869.

Kühner, S., van Noort, V., Betts, M. J., Leo-Macias, A., Batisse, C. & other authors (2009). Proteome organization in a genome-reduced bacterium. *Science* **326**, 1235-1240.

Kunst, F. & Rapoport, G. (1995). Salt stress is an environmental signal affecting degradative enzyme synthesis in *Bacillus subtilis*. *J. Bacteriol.* **177**, 2403-2407.

Lammers, C. R., Flórez, L. A., Schmeisky, A. G., Roppel, S. F., Mäder, U., Hamoen, L. & Stülke, J. (2010). Connecting parts with processes: SubtiWiki and SubtiPathways integrate gene and pathway annotation for *Bacillus subtilis*. *Microbiology* **156**, 849-859.

Landgraf, D., Okumus, B., Chien, P., Baker, T. A. & Paulsson, J. (2012). Segregation of molecules at cell division reveals native protein localization. *Nat. Methods* **9**, 480-482.

Landmann, J. J., Busse, R. A., Latz, J. H., Singh, K. D., Stülke, J. & Görke, B. (2011). Crh, the paralogue of the phosphocarrier protein HPr, controls the methylglyoxal bypass of glycolysis in *Bacillus subtilis*. *Mol. Microbiol*. **82**, 770-787.

Landmann, J. J., Werner, S., Hillen, W., Stülke, J. & Görke, B. (2012). Carbon source control of the phosphorylation state of the *Bacillus subtilis* carbon-flux regulator Crh in vivo. *FEMS Microbiol. Lett*. **327**, 47-53.

Lehnik-Habrink, M., Pförtner, H., Rempeters, L., Pietack, N., Herzberg, C. & Stülke, J. (2010). The RNA degradosome in *Bacillus subtilis*: identification of CshA as the major RNA helicase in the multiprotein complex. *Mol. Microbiol.* **77**, 958-971.

Lehnik-Habrink, M., Newman, J., Rothe, F. M., Solovyova, A. S., Rodrigues, C., Herzberg, C., Commichau, F. M., Lewis, R. J. & Stülke, J. (2011). RNase Y in *Bacillus subtilis*: a natively disordered protein that is the functional equivalent of RNase E from *Escherichia coli*. *J. Bacteriol.* **193**, 5431-5441.

Lemma, E., Unden, G. & Kröger, A. (1990). Menaquinone is an obligatory component of the chain catalyzing succinate respiration in *Bacillus subtilis*. *Arch. Microbiol.* **155**, 62-67.

Lerondel, G., Doan, T., Zamboni, N., Sauer, U. & Aymerich, S. (2006). YtsJ has the major physiological role of the four paralogous malic enzyme isoforms in *Bacillus subtilis*. *J. Bacteriol.* **188**, 4727-4736.

Licht, A., Preis, S. & Brantl, S. (2005). Implication of CcpN in the regulation of a novel untranslated RNA (SR1) in *Bacillus subtilis*. *Mol. Microbiol*. **58**, 189-206.

Lindner, C., Stülke, J. & Hecker, M. (1994). Regulation of xylanolytic enzymes in *Bacillus subtilis*. *Microbiology* **140**, 753-757.

Lindner, C., Hecker, M., Le Coq, D. & Deutscher, J. (2002). *Bacillus subtilis* mutant LicT antiterminators exhibiting enzyme I- and HPr-independent antitermination affect catabolite repression of the *bglPH* operon. *J. Bacteriol.* **184**, 4819-4828.

Ludwig, H., Homuth, G., Schmalisch, M., Dyka, F. M., Hecker, M. & Stülke, J. (2001). Transcription of glycolytic genes and operons in *Bacillus subtilis*: evidence for the presence of multiple levels of control of the gapA operon. *Mol. Microbiol.* **41**, 409-422.

Ludwig, H., Meinken, C., Matin, A. & Stülke, J. (2002a). Insufficient expression of the *ilv-leu* operon encoding enzymes of branched-chain amino acid biosynthesis limits growth of a *Bacillus subtilis ccpA* mutant. *J. Bacteriol.* **184**, 5174-5178.

Ludwig, H., Rebhan, N., Blencke, H. M., Merzbacher, M. & Stülke, J. (2002b). Control of the glycolytic *gapA* operon by the catabolite control protein A in *Bacillus subtilis*: a novel mechanism of CcpA-mediated regulation. *Mol. Microbiol.* **45**, 543-553.

Macek, B., Mijakovic, I., Olsen, J. V., Gnad, F., Kumar, C., Jensen, P. R. & Mann, M. (2007). The serine/threonine/tyrosine phosphoproteome of the model bacterium *Bacillus subtilis*. Mol. Cell. *Proteomics* **6**, 697-707.

Manolukas, J. T., Barile, M. F., Chandler, D. K. & Pollack J. D. (1988). Presence of anaplerotic reactions and transamination, and the absence of the tricarboxylic acid cycle in mollicutes. *J. Gen. Microbiol*. **134**, 791-800.

Marciniak, B. C., Pabijaniak, M., de Jong, A., Dühring, R., Seidel, G., Hillen, W. & Kuipers, O. P. (2012). High- and low-affinity *cre* boxes for CcpA binding in *Bacillus subtilis* revealed by genome-wide analysis. *BMC Genomics* **13**, 401.

Margolin W. (2012). The Price of Tags in Protein Localization Studies. *J. Bacteriol.* in press.

Matsuno, K., Blais, T., Serio, A. W., Conway, T., Henkin, T. M. & Sonenshein, A. L. (1999). Metabolic imbalance and sporulation in an isocitrate dehydrogenase mutant of *Bacillus subtilis*. *J. Bacteriol.* **181**, 3382-3391.

Meinken, C., Blencke, H. M., Ludwig, H. & Stülke, J. (2003). Expression of the glycolytic *gapA* operon in *Bacillus subtilis*: differential syntheses of proteins encoded by the operon. *Microbiology* **149**, 751-761.

Menon, A. L., Poole, F. L., Cvetkovic, A., Trauger, S. A., Kalisiak, E. & other authors (2009). Novel multiprotein complexes identified in the hyperthermophilic archaeon *Pyrococcus furiosus* by non-denaturing fractionation of the native proteome. *Mol. Cell. Proteomics* **8**, 735-751.

Merzbacher, M., Detsch, C., Hillen, W. & Stülke, J. (2004). *Mycoplasma pneumoniae* HPr kinase/phosphorylase. *Eur. J. Biochem.* **271**, 367-374.

Meyer, F. M., Gerwig, J., Hammer, E., Herzberg, C., Commichau, F. M., Völker, U. & Stülke J. (2011a). Physical interactions between tricarboxylic acid cycle enzymes in *Bacillus subtilis*: evidence for a metabolon. *Metab. Eng.* **13**, 18-27.

Meyer, F. M., Jules, M., Mehne, F. M., Le Coq, D., Landmann, J. J., Görke, B., Aymerich, S. & Stülke, J. (2011b). Malate-mediated carbon catabolite repression in *Bacillus subtilis* involves the HPrK/CcpA pathway. *J. Bacteriol.* **193**, 6939-6949.

Meyer, F. M. & Stülke, J. (2012). Malate metabolism in *Bacillus subtilis*: Distinct roles for three classes of malate-oxidizing enzymes. *FEMS Microbiol. Lett*. *in press*.

Mijakovic, I., Poncet, S., Galinier, A., Monedero, V., Fieulaine, S. & other authors (2002). Pyrophosphate-producing protein dephosphorylation by HPr kinase/phosphorylase: a relic of early life? Proc. *Natl. Acad. Sci. U S A* **99**, 13442-13447.

Miller, J. (1972). Experiments in molecular genetics. Cold Spring Harbor Laboratory, Cold Spring Harbor, NY.

Mitchell, C. G. (1996). Identification of a multienzyme complex of the tricarboxylic acid cycle enzymes containing citrate synthase isozymes from *Pseudomonas aeruginosa*. *Biochem. J.* **313**, 769-774.

Mittal, M., Pechter, K. B., Picossi, S., Kim, H. J., Kerstein, K. O. & Sonenshein, A. L. (2012). Dual role of CcpC protein in regulation of aconitase gene expression in *Listeria monocytogenes* and *Bacillus subtilis*. *Microbiology*, *in press*.

Miwa, Y., Nakata, A., Ogiwara, A., Yamamoto, M. & Fujita, Y. (2000). Evaluation and characterization of catabolite-responsive elements (*cre*) of *Bacillus subtilis*. *Nucleic Acids Res*. **28**, 1206-1210.

Monedero, V., Poncet, S., Mijakovic, I., Fieulaine, S., Dossonnet, V., Martin-Verstraete, I., Nessler, S. & Deutscher, J. (2001). Mutations lowering the phosphatase activity of HPr kinase/phosphatase switch off carbon metabolism. *EMBO J.* **20**, 3928-3937.

Monod, J. (1942). Recherches sur la croissance des cultures bactériennes. *Thesis, Hermann et Cie, Paris*

Mortera, P., Espariz, M., Suárez, C., Repizo, G., Deutscher, J., Alarcón, S., Blancato, V. & Magni, C. (2012). Fine-tuned transcriptional regulation of malate operons in *Enterococcus faecalis*. *Appl. Environ. Microbiol.* **78**, 1936-1945.

Mowbray, J. & Moses, V. (1976). The tentative identification in *Escherichia coli* of a multienzyme complex with glycolytic activity. *Eur. J. Biochem.* **66**, 25-36.

Mueller, J., Bukusoglu, G. & Sonenshein, A. L. (1992). Transcriptional regulation of *Bacillus subtilis* glucose starvation-inducible genes: control of *gsiA* by the ComP-ComA signal transduction system. *J. Bacteriol*. **174**, 4361-4373.

Nakano, M. M., Zuber, P. & Sonenshein, A. L. (1998). Anaerobic regulation of *Bacillus subtilis* Krebs cycle genes. *J. Bacteriol.* **180**, 3304-3311.

Nessler, S., Fieulaine, S., Poncet, S., Galinier, A., Deutscher, J. & Janin, J. (2003). HPr kinase/phosphorylase, the sensor enzyme of catabolite repression in gram-positive bacteria: structural aspects of the enzyme and the complex with its protein substrate. *J. Bacteriol.* **185**, 4003-4010.

Nicolas, P., Mäder, U., Dervyn, E., Rochat, T., Leduc, A. & other authors (2012). Condition-dependent transcriptome reveals high-level regulatory architecture in *Bacillus subtilis*. *Science* **335**, 1103-1106.

Nihashi, J. & Fujita, Y. (1984). Catabolite repression of inositol dehydrogenase and gluconate kinase syntheses in *Bacillus subtilis*. *Biochim. Biophys. Acta.* **798**, 88-95.

Philpott, C., Klausner, R. D. & Rouault, T. A. (1994). The bifunctional iron-responsive element binding protein/cytosolic aconitase: The role of active-site residues in ligand binding and regulation. *Proc. Natl. Acad. Sci. U S A* **91**, 7321-7325.

Pierce, J. A., Robertson, C. R. & Leighton T. J. (1992). Physiological and genetic strategies for enhanced subtilisin production by *Bacillus subtilis*. *Biotechnol. Prog*. **8**, 211-218.

Piggot, P. J. & Hilbert, D. W. (2004). Sporulation of *Bacillus subtilis*. *Curr. Opin. Microbiol*. **7**, 579-586.

Poolman, B., Molenaar, D., Smid, E. J., Ubbink, T., Abee, T., Renault, P. P. & Konings, W. N. (1991). Malolactic fermentation: electrogenic malate uptake and malate/lactate antiport generate metabolic energy. *J. Bacteriol*. **173**, 6030-6037.

Postma, P. W., Lengeler, J. W. & Jacobson, G. R. (1993). Phosphoenolpyruvate:carbohydrate phosphotransferase systems of bacteria. *Microbiol. Rev*. **57**, 543-94.

Presecan-Siedel, E., Galinier, A., Longin, R., Deutscher, J., Danchin, A., Glaser, P. & Martin-Verstraete, I. (1999). The catabolite regulation of the *pta* gene as part of carbon flow pathways in *Bacillus subtilis*. *J. Bacteriol.* **181**, 6889-6897.

Ratnayake-Lecamwasam, M., Serror, P., Wong, K. W. & Sonenshein, A. L. (2001). *Bacillus subtilis* CodY represses early-stationary-phase genes by sensing GTP levels. *Genes Dev*. **15**, 1093-1103.

Reizer, J., Bergstedt, U., Galinier, A., Küster, E., Saier, M. H., Jr, Hillen, W., Steinmetz, M. & Deutscher, J. (1996). Catabolite repression resistance of gnt operon expression in *Bacillus subtilis* conferred by mutation of His-15, the site of phosphoenolpyruvate-dependent phosphorylation of the phosphocarrier protein HPr. *J. Bacteriol*. **178**, 5480-5486.

Reizer, J., Hoischen, C., Titgemeyer, F., Rivolta, C., Rabus, R., Stülke, J., Karamata, D., Saier, M. H., Jr & Hillen, W. (1998). A novel protein kinase that controls carbon catabolite repression in bacteria. *Mol. Microbiol.* **27**, 1157-1169.

Riddles, P., Blakeley, R. & Zerner, B. (1983). Reassessment of Ellman's Reagent. *Methods in Enzymology* **91**, 49-60.

Robinson Jr., J.B. & Srere, P. A. (1985). Organization of Krebs tricarboxylic acid cycle enzymes in mitochondria. *J. Biol. Chem.* **260**, 10800-10805.

Rojo, F. (2010). Carbon catabolite repression in *Pseudomonas*: optimizing metabolic versatility and interactions with the environment. *FEMS Microbiol. Rev*. **34**, 658-684.

Ronen, M., Rosenberg, R., Shraiman, B. I. & Alon, U. (2002). Assigning numbers to the arrows: parameterizing a gene regulation network by using accurate expression kinetics. *Proc. Natl. Acad. Sci. U S A* **99**, 10555-10560.

Rouault, T. A., Hentze, M. W., Caughman, S. W., Harford, J. B. & Klausner, R. D. (1988). Binding of a cytosolic protein to the iron-responsive element of human ferritin messenger RNA. *Science* **241**, 1207-1210.

Rouault, T. A., Stout, C. D., Kaptain, S., Harford, J. B. & Klausner, R. D. (1991). Structural relationship between an iron-regulated RNA-binding protein (IRE-BP) and aconitase: functional implications. *Cell* **64**, 881-883.

Rudrappa, T., Czymmek, K. J., Paré, P. W. & Bais, H. P. (2008). Root-secreted malic acid recruits beneficial soil bacteria. *Plant Physiol.* **148**, 1547-1556.

Saier, M. H., Jr. (1989). Protein phosphorylation and allosteric control of inducer exclusion and catabolite repression by the bacterial phosphoenolpyruvate: sugar phosphotransferase system. *Microbiol. Rev.* **53**, 109-120.

Salou, P., Loubiere, P. & Pareilleux, A. (1994). Growth and energetics of *Leuconostoc oenos* during cometabolism of glucose with citrate or fructose. *Appl. Environ. Microbiol.* **60**, 1459-1466.

Sambrook, J., Fritsch, E. F. & Maniatis, T. (1989). Molecular Cloning: A Laboratory Manual, 2. Edition, Cold Spring Harbor Laboratory Press, Cold Spring Harbor, New York.

Sambrook, J. & Russell, D. (2001). Molecular cloning: a laboratory manual. Cold Spring Harbor Laboratory Press, Cold Spring Harbor, NY.

Sauer, U., Hatzimanikatis, V., Bailey, J. E., Hochuli, M., Szyperski, T. & Wüthrich K. (1997). Metabolic fluxes in riboflavin-producing *Bacillus subtilis*. *Nat. Biotechnol.* **15**, 448-452.

Sauer, U. & Eikmanns, B. J. (2005). The PEP-pyruvate-oxaloacetate node as the switch point for carbon flux distribution in bacteria. *FEMS Microbiol. Rev*. **29**, 765-794.

Schilling, O., Herzberg, C., Hertrich, T., Vörsmann, H., Jessen, D., Hübner, S., Titgemeyer, F. & Stülke, J. (2006). Keeping signals straight in transcription regulation: specificity determinants for the interaction of a family of conserved bacterial RNA-protein couples. *Nucleic Acids Res*. **34**, 6102-6115.

Schilling, O., Frick, O., Herzberg, C., Ehrenreich, A., Heinzle, E., Wittmann, C. & Stülke, J. (2007). Transcriptional and metabolic responses of *Bacillus subtilis* to the availability of organic acids: transcription regulation is important but not sufficient to account for metabolic adaptation. *Appl. Environ. Microbiol.* **73**, 499-507.

Schirawski, J. & Unden, G. (1998). Menaquinone-dependent succinate dehydrogenase of bacteria catalyzes reversed electron transport driven by the proton potential. *Eur. J. Biochem*. **257**, 210-215.

Schirmer, F., Ehrt, S. & Hillen, W. (1997). Expression, inducer spectrum, domain structure, and function of MopR, the regulator of phenol degradation in *Acinetobacter calcoaceticus* NCIB8250. *J. Bacteriol*. **179**, 1329-1336.

Schmalisch, M., Maiques, E., Nikolov, L., Camp, A. H., Chevreux, B., Muffler, A., Rodriguez, S., Perkins, J. & Losick, R. (2010). Small genes under sporulation control in the *Bacillus subtilis* genome. *J. Bacteriol*. **192**, 5402-5412.

Schnetz, K., Stülke, J., Gertz, S., Krüger, S., Krieg, M., Hecker, M. & Rak, B. (1996). LicT, a *Bacillus subtilis* transcriptional antiterminator protein of the BglG family. *J. Bacteriol*. **178**, 1971-1979.

Schreier, H. J., Brown, S. W., Hirschi, K. D., Nomellini, J. F. & Sonenshein, A. L. (1989). Regulation of *Bacillus subtilis* glutamine synthetase gene expression by the product of the *glnR* gene. *J. Mol. Biol*. **210**, 51-63.

Schumacher, M. A., Seidel, G., Hillen, W. & Brennan, R. G. (2007). Structural mechanism for the fine-tuning of CcpA function by the small molecule effectors glucose 6‑phosphate and fructose 1,6-bisphosphate. *J. Mol. Biol*. **368**, 1042-1050.

Seidel, G., Diel, M., Fuchsbauer, N. & Hillen, W. (2005) Quantitative interdependence of coeffectors, CcpA and *cre* in carbon catabolite regulation of *Bacillus subtilis*. *FEBS J*. **272**, 2566-2577.

Serio, A. W. (2005). PhD Thesis. Tufts University, Boston.

Serio, A. W., Pechter, K. B. & Sonenshein, A. L. (2006). *Bacillus subtilis* aconitase is required for efficient late-sporulation gene expression. *J. Bacteriol*. **188**, 6396-6405.

Serio, A. W. & Sonenshein, A. L. (2006). Expression of yeast mitochondrial aconitase in *Bacillus subtilis*. *J. Bacteriol*. **188**, 6406-6410.

Servant, P., Le Coq, D. & Aymerich, S. (2005). CcpN (YqzB), a novel regulator for CcpA independent catabolite repression of *Bacillus subtilis* gluconeogenic genes. *Mol. Microbiol.* **55**, 1435-1451.

Shapiro, L., McAdams, H. H. & Losick, R. (2009). Why and how bacteria localize proteins. *Science* **326**, 1225-1228.

Shivers, R. P. & Sonenshein, A. L. (2004). Activation of the *Bacillus subtilis* global regulator CodY by direct interaction with branched-chain amino acids. *Mol. Microbiol*. **53**, 599-611.

Singh, K. D., Schmalisch, M. H., Stülke, J. & Görke, B. (2008). Carbon catabolite repression in *Bacillus subtilis*: quantitative analysis of repression exerted by different carbon sources. *J. Bacteriol.* **190**, 7275-7284.

Somerville, G., Mikoryak, C. A. & Reitzer, L. (1999). Physiological characterization of *Pseudomonas aeruginosa* during exotoxin A synthesis: glutamate, iron limitation, and aconitase activity. *J. Bacteriol*. **181**, 1072-1078.

Somerville, G. A., Chaussee, M. S., Morgan, C. I., Fitzgerald, J. R., Dorward, D. W., Reitzer, L. J. & Musser, J. M. (2002). *Staphylococcus aureus* aconitase inactivation unexpectedly inhibits post-exponential-phase growth and enhances stationary-phase survival. *Infect Immun*. **70**, 6373-6382.

Sonenshein, A.L. (2007). Control of key metabolic intersections in *Bacillus subtilis*. *Nat. Rev. Microbiol.* **5**, 917-927.

Srere, P., Brazil, H. & Gonen, L. (1963). The citrate condensing enzyme of pigeon breast muscle and moth flight muscle. *Acta Chemica Scandinavica* **17**, 129-134.

Srere, P. A. (1987). Complexes of sequential metabolic enzymes. *Annu. Rev. Biochem.* **56**, 89-124.

Srivatsan, A., Han, Y., Peng, J., Tehranchi, A., Gibbs, R., Wang, J. & Chen, R. (2008). High-precision, whole-genome sequencing of laboratory strains facilitates genetic studies. *PloS Genetics* **4**, e1000139.

Steinmetz, M. & Richter, R. (1994). Easy cloning of mini-Tn10 insertions from the *Bacillus subtilis* chromosome. *J. Bacteriol.* **176**, 1761-1763.

Stülke, J. & Hillen, W. (2000). Regulation of carbon metabolism in *Bacillus* species. *Annu. Rev. Microbiol.*, 849-880.

Stülke, J. (2010a). Interactions between glycolytic enzymes of *Mycoplasma pneumoniae*. J*. Mol. Microbiol. Biotechnol.* **19**, 134-139.

Stülke, J. (2010b). More than just activity control: phosphorylation may control all aspects of a protein's properties. *Mol. Microbiol.* **77**, 273-275.

Swulius, M. T. & Jensen, G. J. (2012). The helical MreB cytoskeleton in *E. coli* MC1000/pLE7 is an artifact of the N-terminal YFP tag. *J. Bacteriol. in press*.

Tanaka, K., Kobayashi, K. & Ogasawara, N. (2003). The *Bacillus subtilis* YufLM-two-component system regulates the expression of the malate transporters MaeN (YufR) and YflS, and is essential for the utilization of malate in minimal medium. *Microbiology* **149**, 2317-2329.

Tang, Y. & Guest, J. R. (1999). Direct evidence for mRNA binding and post-transcriptional regulation by *Escherichia coli* aconitases. *Microbiology* **145**, 3069-3079.

Tang, Y., Quail, M. A., Artymiuk, P. J., Guest, J. R. & Green, J. (2002). *Escherichia coli* aconitases and oxidative stress: post-transcriptional regulation of *sodA* expression. *Microbiology* **148**, 1027-1037.

Tang, Y., Guest, J. R., Artymiuk, P. J., Read, R. C. & Green, J. (2004). Post-transcriptional regulation of bacterial motility by aconitase proteins. *Mol. Microbiol.* **51**, 1817-1826.

Tännler, S., Fischer, E., Le Coq, D., Doan, T., Jamet, E., Sauer, U. & Aymerich, S. (2008). CcpN controls carbon fluxes in *Bacillus subtilis*. *J. Bacteriol.* **190**, 6178-6187.

Titgemeyer, F. & Hillen, W. (2002). Global control of sugar metabolism: a gram-positive solution. *Antonie Van Leeuwenhoek* **82**, 59-71.

Tong, W. H. & Rouault, T. A. (2007). Metabolic regulation of citrate and iron by aconitases: role of iron-sulfur cluster biogenesis. *Biometals*. **20**, 549-564.

Trivett, T. L. & E. A. Meyer. (1971). Citrate cycle and related metabolism of *Listeria monocytogenes*. *J. Bacteriol*. **107**, 770-779.

Ucker, D. S., Signer, E. R. (1978). Catabolite-repression-like phenomenon in *Rhizobium meliloti*. *J. Bacteriol.* **136**, 1197-1200.

van den Bogaard, P. T., Kleerebezem, M., Kuipers, O. P., de Vos, W. M. (2000). Control of lactose transport, β-galactosidase activity, and glycolysis by CcpA in *Streptococcus thermophilus*: evidence for carbon catabolite repression by a non-phosphoenolpyruvate-dependent phosphotransferase system sugar. *J. Bacteriol.* **182**, 5982-5989.

van der Rest, M. E., Frank, C. & Molenaar, D. (2000). Functions of the membrane-associated and cytoplasmic malate dehydrogenases in the citric acid cycle of *Escherichia coli*. *J. Bacteriol*. **182**, 6892-6899.

Velázquez, F., Pflüger, K., Cases, I., De Eugenio, L. I. & de Lorenzo, V. (2007). The phosphotransferase system formed by PtsP, PtsO, and PtsN proteins controls production of polyhydroxyalkanoates in *Pseudomonas putida*. *J. Bacteriol.* **189**, 4529-4533.

Voelker, U., Voelker, A., Maul, B., Hecker, M., Dufour, A. & Haldenwang, W. G. (1995). Separate mechanisms activate σ^B of *Bacillus subtilis* in response to environmental and metabolic stresses. *J. Bacteriol.* **177**, 3771-3780.

Volz, K. (2008). The functional duality of iron regulatory protein 1. *Curr. Opin. Struct. Biol*. **18**, 106-111.

Wach, A. (1996). PCR-synthesis of marker cassettes with long flanking homology regions for gene disruptions in *S. cerevisiae*. *Yeast* **12**, 259-265.

Wacker, I., Ludwig, H., Reif, I., Blencke, H.-M., Detsch, C. & Stülke, J. (2003). The regulatory link between carbon and nitrogen metabolism in *Bacillus subtilis*: regulation of the *gltAB* operon by the catabolite control protein CcpA. *Microbiology* **149**, 3001-3009.

Walden, W. E., Selezneva, A. I., Dupuy, J., Volbeda, A., Fontecilla-Camps, J. C., Theil, E. C. & Volz, K. (2006). Structure of dual function iron regulatory protein I complexed with ferritin IRE-RNA. *Science* **314**, 1903-1908.

Wallander, M. L., Leibold, E. A. & Eisenstein, R. S. (2006). Molecular control of vertebrate iron homeostasis by iron regulatory proteins. *Biochim. Biophys. Acta*. **1763**, 668-689.

Wang, B., Wang, P., Zheng, E., Chen, X., Zhao, H., Song, P., Su, R., Li, X. & Zhu, G. (2011). Biochemical properties and physiological roles of NADP-dependent malic enzyme in *Escherichia coli*. *J. Microbiol*. **49**, 797-802.

Wang, J. & Pantopoulos, K. (2011). Regulation of cellular iron metabolism. *Biochem. J*. **434**, 365-381.

Warner, J. B. & Lolkema, J. S. (2003). CcpA-dependent carbon catabolite repression in bacteria. *Microbiol. Mol. Biol. Rev.* **67**, 475-490.

Wei, Y., Guffanti, A. A., Ito, M. & Krulwich, T. A. (2000). *Bacillus subtilis* YqkI is a novel malic/Na^+-lactate antiporter that enhances growth on malate at low proton motive force. *J. Biol. Chem.* **275**, 30287-30292.

Weisskopf, L., Le Bayona, R.-C., Kohlera, F., Pagec, V., Jossia, M., Gobata, J.-M., Martinoiab, E. & Aragnoa, M. (2008). Spatio-temporal dynamics of bacterial communities associated with two plant species differing in organic acid secretion: a one-year microcosm study on lupin and wheat. *Soil Biol. Biochem.* **40**, 1772-1780.

Wiegand, G. & Remington, S. (1986). Citrate synthase: structure, control, and mechanism. *Ann. Rev. Biophys. Biophys. Chem*. **15**, 97-117.

Williamson, M. P. & Sutcliffe, M. J. (2010). Protein-protein interactions. *Biochem. Soc. Trans.* **38**, 875-878.

Yamamoto, H., Murata, M. & Sekiguchi, J. (2000). The CitST two-component system regulates the expression of the Mg-citrate transporter in *Bacillus subtilis*. *Mol. Microbiol.* **37**, 898-912.

Yanofsky, C. & Rachmeler, M. (1958). The exclusion of free indole as an intermediate in the biosynthesis of tryptophan in *Neurospora crassa*. *Biochim. Biophys. Acta*. **28**, 640-641.

Zalieckas, J. M., Wray, L. V. & Fischer, S. (1999). *trans*-acting factors affecting carbon catabolite repression of the *hut* operon in *Bacillus subtilis*. *J. Bacteriol.* **181**, 2883-2888.

Zaslaver, A., Bren, A., Ronen, M., Itzkovitz, S., Kikoin, I., Shavit, S., Liebermeister, W., Surette, M. G. & Alon, U. (2006). A comprehensive library of fluorescent transcriptional reporters for *Escherichia coli*. *Nat. Methods* **3**, 623-628.

Zeigler, D. R., Prágai, Z., Rodriguez, S., Chevreux, B., Muffler, A., Albert, T., Bai, R., Wyss, M. & Perkins, J, B. (2008). The origins of 168, W23, and other *Bacillus subtilis* legacy strains. *J. Bacteriol*. **190**, 6983-6995.

Zimmerman, S. B. & Minton, A. P. (1993). Macromolecular crowding: biochemical, biophysical, and physiological consequences. *Annu. Rev. Biophys. Biomol. Struct.* **22**, 27-65.

Zumbrennen, K. B., Wallander, M. L., Romney, S. J. & Leibold, E. A. (2009). Cysteine oxidation regulates the RNA-binding activity of iron regulatory protein 2. *Mol. Cell Biol*. **29**, 2219-2229.

8. Appendix

8.1. Oligonucleotides

Oligonucleotides were purchased from either Sigma Aldrich (Munich, Germany) or Eurofins MWG Operon (Ebersber, Germany). Underlined are restriction site and T7 Polymerase recognition sites.

Name	Sequence (5´ → 3´)	Description
CD53	5´CTAATACGACTCACTATAGGGAGATCCGATATTAATGATGTAG CCGGG	Riboprobe *hag* for
CD54	5´CTCCATGTTCTTTTGGCTCGC	Riboprobe *hag* rev
FM1	5´AAAGGATCCATGGGGAAACCAACTGGATTTATGGAGATC	*gltB* in pGP380 for (*Bam*HI)
FM2	5´AAAGTCGACTCATTACGGAAGAACTGAACTCCCCATCAAATAT C	*gltB* in pGP380 rev (*Sal*I)
FM3	5´AAAGGATCCATGACAGCGACACGCGGTCTTGAAG	*citZ* in pGP380 for (*Bam*HI)
FM4	5´AAAGTCGACTCATTAGGCTCTTTCTTCAATCGGAACGAATTTTT G	*citZ* in pGP380 rev (*Sal*I)
FM5	5´AAAGGATCCGTGGCACAAGGTGAAAAAATTACAGTCTC	*icd* in pGP380 for (*Bam*HI)
FM6	5´AAAGTCGACTCATTAGTCCATGTTTTTGATCAGTTCTTCTCCGA AC	*icd* in pGP380 rev (*Sal*I)
FM7	5´AAAGGATCCATGGCGGAAATTAAGGTACCTGAATTAGC	*odhB* in pGP380 for (*Bam*HI)
FM8	5´AAAGTCGACTCATTATCCTTCTAATAAAAGCTGTTCAGGATCTT CC	*odhB* in pGP380 rev (*Sal*I)
FM9	5´AAAGGATCCATGGAATACAGAATTGAACGAGACACCATGG	*citG* in pGP380 for (*Bam*HI)
FM10	5´AAAGTCGACTCATTACGCCTTTGGTTTTACCATGTCTTCCG	*citG* in pGP380 rev (*Sal*I)
FM11	5´AAAGGATCCATGGGAAATACTCGTAAAAAAGTTTCTGTTATCG G	*mdh* in pGP380 for (*Bam*HI)
FM12	5´AAAGTCGACTCATTAGGATAATACTTTCATGACATTTTTGACAG ATTCAACTG	*mdh* in pGP380 rev (*Sal*I)
FM20	5´AAATCTAGAGATGACAGCGACACGCGGTCTTGAAG	*citZ* BACTH for (*Xba*I)
FM21	5´TTTGGTACCCGGGCTCTTTCTTCAATCGGAACGAATTTTTGTTT G	*citZ* BACTH rev (*Kpn*I)
FM22	5´AAATCTAGAGATGGCACAAGGTGAAAAAATTACAGTCTC	*icd* BACTH for (*Xba*I)
FM23	5´TTTGGTACCCGGTCCATGTTTTTGATCAGTTCTTCTCCGAACTCT	*icd* BACTH rev (*Kpn*I)
FM24	5´AAATCTAGAGATGGAATACAGAATTGAACGAGACACCATGG	*citG* BACTH for (*Xba*I)
FM25	5´TTTGGTACCCGCGCCTTTGGTTTTACCATGTCTTCCGGGC	*citG* BACTH rev (*Kpn*I)
FM26	5´AAATCTAGAGATGGGAAATACTCGTAAAAAAGTTTCTGTTATC GG	*mdh* BACTH for (*Xba*I)
FM27	5´TTTGGTACCCGGGATAATACTTTCATGACATTTTTGACAGATTC AACTG	*mdh* BACTH rev (*Kpn*I)
FM28	5´AAATCTAGAGATGGGGAAACCAACTGGATTTATGGAGATC	*gltB* BACTH for (*Xba*I)
FM29	5´TTTGGTACCCGCGGAAGAACTGAACTCCCCATCAAATATC	*gltB* BACTH rev (*Kpn*I)
FM30	5´AAATCTAGAGATGGCAAACGAGCAAAAAACTGCAGCAAAAG	*citB* BACTH for (*Xba*I)
FM31	5´TTTGGTACCCGGGACTGCTTCATTTTTTCACGAAGCACCATT	*citB* BACTH rev (*Kpn*I)
FM35	5´AAATCTAGAGATGGCGGAAATTAAGGTACCTGAATTAGC	*odhB* BACTH for (*Xba*I)
FM36	5´TTTGAATTCGATCCTTCTAATAAAAGCTGTTCAGGATCTTCCAG	*odhB* BACTH rev (*EcoR*I)
FM37	5´TTTGAATTCTTATCCTTCTAATAAAAGCTGTTCAGGATCTTCC	*odhB* BACTH rev in pKT25 (*EcoR*I)
FM38	5´AAATCTAGAGATGGTAGTAGGAGATTTCCCTATTGAAACAGAT A	*pdhD* BACTH for (*Xba*I)
FM39	5´TTTGGTACCCGTTTTACGATGTGAATCGGACTTCCGATTGC	*pdhD* BACTH rev (*Kpn*I)
FM41	5´AAATCTAGAGATGAGTGAACAAAAAACCATACGATTTATTATC ACACG	*sdhB* BACTH for (*Xba*I)
FM42	5´TTTGGTACCCGTACTCTGTCGCTTCCGAAGAAATTGCG	*sdhB* BACTH rev (*Kpn*I)
FM43	5´AAATCTAGAGATGAACTCAGTTGATTTGACCGCTGATTTACAA G	*pckA* BACTH for (*Xba*I)

FM44	5´TTTGGTACCCGTACGAGAGGGCCGCCTGCCT	*pckA* BACTH rev (*Kpn*I)
FM46	5´AAATCTAGAGATGTTTCAAAATAGTATGAAACAACGAATGAATTGGGAAG	*odhA* BACTH for (*Xba*I)
FM47	5´TTTGGTACCCGGTTTTTGCGAGTCAAGCTATCAGATACAATACG	*odhA* BACTH rev (*Kpn*I)
FM51	5´AAATCTAGAGATGACGTACAATCAAATGCCAAAAGCTCAAGG	*gltA* BACTH for (*Xba*I)
FM52	5´TTTGGTACCCGCTGTACTACCGCTTGTTTTTGTCCCG	*gltA* BACTH rev(*Kpn*I)
FM53	5´AAATCTAGAGATGAATATCCATGAGTACCAGGGAAAAGAAGTC	*sucC* BACTH for (*Xba*I)
FM54	5´TTTGGTACCCGAACTAAGGATACGATTTTCTGCGCGCC	*sucC* BACTH rev (*Kpn*I)
FM55	5´AAATCTAGAGATGGCGCAAATGACAATGATTCAAGCAATCAC	*pdhB* BACTH for (*Xba*I)
FM56	5´TTTGGTACCCGAAATTCAAGCACTTTTCTTGCTGTTTCAAGAACG	*pdhB* BACTH rev (*Kpn*I)
FM58	5´AAATCTAGAGATGAGTGTTTTCATTAATAAAGATACAAGAGTTATTGTGCA	*sucD* BACTH for (*Xba*I)
FM59	5´TTTGGTACCCGATGCGTTTTACAAGTTTCGAACAAGTTCTTCTCT	*sucD* BACTH rev (*Kpn*I)
FM60	5´AAATCTAGAGATGAGTCAATCAAGCATTATCGTAGTCGGC	*sdhA* BACTH for (*Xba*I)
FM61	5´TTTGGTACCCGTTTCGCCACCTTCTTCTTCGAGTAATCC	*sdhA* BACTH rev (*Kpn*I)
FM63	5´AAATCTAGAGATGTCTGGGAACAGAGAGTTTTATTTTCGAAGAT	*sdhC* BACTH for (*Xba*I)
FM64	5´TTTGGTACCCGAACAAATGCAAAAATCGCTTTTAAGCCTACGTATG	*sdhC* BACTH rev (*Kpn*I)
FM65	5´AAATCTAGAGATGGCTGCAAAAACGAAAAAAGCTATCGTTGAC	*pdhA* BACTH for (*Xba*I)
FM66	5´TTTGGTACCCGCTTCGACTCCTTCTGTGTATAAATTTCAAATTGC	*pdhA* BACTH rev (*Kpn*I)
FM67	5´AAATCTAGAGGTGGCATTTGAATTTAAACTTCCAGATATCGGG	*pdhC* BACTH for (*Xba*I)
FM68	5´TTTGGTACCCGCGCCTCCATTAAAATTAATTGTGGATCGTTCAG	*pdhC* BACTH rev (*Kpn*I)
FM69	5´TTTCAATTGTTTGTAAATCGATGCCGCCTAGC	*gltA* BACTH rev (*Mfe*I)
FM70	5´CCGGCTCGTATGTTGTGTGGAAT	Sequencing primer P25-N for
FM71	5´AAATCTAGAATGAACTCAGTTGATTTGACCGCTGATTTACA	*pckA* in pGP380 for (*Xba*I)
FM72	5´AAACTGCAGTCATTATACGAGAGGGCCGCCTGCC	*pckA* in pGP380 rev (*Pst*I)
FM73	5´AAAGTCGACGTGGATGAAGATACACGCGAAGCCAA	*pckA* in pGP1331 for (*Sal*I)
FM74	5´AAAGCATGCTACGAGAGGGCCGCCTGCCT	*pckA* in pGP1331 rev (*Sph*I)
FM75	5´AAAGGATCCAGGAAATCGTGAAATATTCTCCTGACTCTATTATTG	*mdh* in pGP1331 for (*Bam*HI)
FM76	5´AAAGTCGACGGATAATACTTTCATGACATTTTTGACAGATTCAACTGAT	*mdh* in pGP1331 rev (*Sal*I)
FM77	5´CAGACGGCACTCATTCCGAAACG	Sequencing primer *pckA*
FM78	5´CGTGTAATCGGCCAGGCAGGTGTGCTTGATAC	Mutagenesis *mdh* Ser-149-Ala
FM79	5´CGTGTAATCGGCCAGGACGGTGTGCTTGATACG	Mutagenesis *mdh* Ser-149-Asp
FM80	5´AAAGGATCCGCGACATTGTGATGTGCGATTCCAAAG	*ytsJ* in pGP1331 for (*Bam*HI)
FM81	5´AAAGTCGACTTCACCAATAATCGTAAGTTTTCTTGTTTTTTCTGCG	*ytsJ* in pGP1331 rev (*Sal*I)
FM82	5´AAAGGATCCCCACGCGCTGACAAGCCATGAC	*citG* in pGP1331 for (*Bam*HI)
FM83	5´AAAGTCGACCGCCTTTGGTTTTACCATGTCTTCCG	*citG* in pGP1331 rev (*Sal*I)
FM84	5´AAAGGATCCATGTCATTAAGAGAAGAAGCATTACACCTGCATA	*ytsJ* in pGP380 for (*Bam*HI)
FM85	5´AAAGTCGACTCATTATTCACCAATAATCGTAAGTTTTCTTGTTTTTTCTGCG	*ytsJ* in pGP380 rev (*Sal*I)
FM86	5´CTGCCTTAAGAGCATCGCATGAGGTA	LFH-PCR *sucC* (up-fragment for)
FM87	5´GGCAATCGGCGCAAGGGACG	Sequencing primer *sucC*
FM88	5´CCTATCACCTCAAATGGTTCGCTGCACTTTACCTTCAGGAACAGATACCCC	LFH-PCR *sucC* (up-fragment rev)
FM89	5´CCGAGCGCCTACGAGGAATTTGTATCGTCCTTAGTGAATCAGGATTAAACATTACATCTGC	LFH-PCR *sucC* (down-fragment for)
FM90	5´CTCCTTTTGTTAGAAAAAGCAGGAACAGCC	LFH-PCR *sucC* (down-fragment rev)
FM91	5´GACATAGACGGATCGGCTTTCCACC	Sequencing primer *sucC*
FM92	5´AAAGAATTCGGGGTTTCATCCGTACGGAAGAGG	*glpF* promoter region in pAC5 for

FM93	5´AAAGGATCCATGGCAACACCCAATCCCCATCCAAATA	*glpF* promoter region in pAC5 rev
FM94	5´CAGAATGACCAGCAGCACAAAGGCAT	LFH-PCR *mleA* (up-fragment for)
FM95	5´CGCGCAGAGTTCCAACTATAATTATTATAAACTG	Sequencing primer *mleA*
FM96	5´CCTATCACCTCAAATGGTTCGCTGCTCAGCCGCTTGATTCAAAAGTCCATC	LFH-PCR *mleA* (up-fragment rev)
FM97	5´CCGAGCGCCTACGAGGAATTTGTATCGGATGGCCGTAGCCACCCTTCC	LFH-PCR *mleA* (down-fragment for)
FM98	5´CATTGCCATGATCGCAATTGGAGAGG	LFH-PCR *mleA* (down-fragment rev)
FM99	5´TGGAATTTATTCACCCAAGTATCTTTTTACTGGC	Sequencing primer *mleA*
FM100	5´AAAGTCGACATGAACTCAGTTGATTTGACCGCTGATTTACAAG	*pckA* in pWH844 for (*Sal*I)
FM101	5´AAACTGCAGTTATACGAGAGGGCCGCCTGCC	*pckA* in pWH844 rev (*Pst*I)
FM102	5´AAAGAGCTCGATGAACTCAGTTGATTTGACCGCTGATTTACAAG	*pckA* in pGP172 for (*Sac*I)
FM103	5´AAAGGTACCTTATACGAGAGGGCCGCCTGCC	*pckA* in pGP172 rev (*Kpn*I)
FM104	5´AAAGAGCTCGATGGGAAATACTCGTAAAAAAGTTTCTGTTATCGG	*mdh* in pGP172 for (*Sac*I)
FM105	5´AAAGGATCCTCATTAGGATAATACTTTCATGACATTTTTGACAGATTCAACTG	*mdh* in pGP172 rev (*Bam*HI)
FM106	5´AAAGGATCCCGCCTGCCGGAAAGTATTTGCAAGAA	*citB* in pGP1331 for (*Bam*HI)
FM107	5´AAAGTCGACGGACTGCTTCATTTTTTCACGAAGCACC	*citB* in pGP1331 rev (*Sal*I)
FM108	5´GGCATATGCGCTGGCTGGAACG	LFH-PCR *citB* (up-fragment for)
FM109	5´CTTCTGATTACGTCTGTCCTTTCCGG	Sequencing primer *citB*
FM110	5´CCGAGCGCCTACGAGGAATTTGTATCGGCGGATACACTCGGCTTAACGGG	LFH-PCR *citB* (down-fragment for)
FM111	5´CAACAGATAGGTTTCTCAAAAGGAGGGG	LFH-PCR *citB* (down-fragment rev)
FM112	5´GGCCGCTGTCCTGAAGTATCATGC	Sequencing primer *citB*
FM113	5´AAAGAGCTCGATGACAGCGACACGCGGTCTTGAAG	*citZ* in pGP172 for (*Sac*I)
FM114	5´AAAGGATCCTCATTAGGCTCTTTCTTCAATCGGAACGAATTTTTG	*citZ* in pGP172 rev (*Bam*HI)
FM115	5´AAAGAGCTCGATGTCAAAACAACAAATCGGCGTTATCGGAC	*gndA* in pGP172 for (*Sac*I)
FM116	5´AAAGGATCCTTACTTCATCCATTCAGTATGGAAGATGCC	*gndA* in pGP172 rev (*Bam*HI)
FM117	5´AAATCTAGAGATGTTATTCTTTGTTGATACAGCCAATATCGATG	*ywjH* BACTH for (*Xba*I)
FM118	5´TTTGGTACCCGTTTGTTCCAGTCTGCCAGGAATTGTTCG	*ywjH* BACTH rev (*Kpn*I)
FM119	5´AAAGGATCCCTTTGTGCGCGGACAATATCATGCTG	*zwf* in pGP1331 for (*Bam*HI)
FM120	5´AAAGCATGCTATGTTCCACCAGTGTAAGCCGTCTTTC	*zwf* in pGP1331 rev (*Sph*I)
FM121	5´AAAGGATCCCACACAGGAAAAGGGCCGCACG	*ykgB* in pGP1331 for (*Bam*HI)
FM122	5´AAAGCATGCTACTTGATGTAAAAACTTTACACAAACCGGGTAAG	*ykgB* in pGP1331 rev (*Sph*I)
FM123	5´AAAGGATCCGACAAGCCAAAGCGCACTTGACTTAG	*gndA* in pGP1331 for (*Bam*HI)
FM124	5´AAAGTCGACCTTCATCCATTCAGTATGGAAGATGCCTTC	*gndA* in pGP1331 rev (*Sal*I)
FM125	5´AAAGGATCCCGAAATGAAATCAAAGAGTTAATGGACGAATTGC	*ywlF* in pGP1331 for (*Bam*HI)
FM126	5´AAAGTCGACCAGGTTTTTCTCTTCATAATCGGAGATTTTTCC	*ywlF* in pGP1331 rev (*Sal*I)
FM127	5´AAAGGATCCGGCGGAGCCGATTGTATTCATATTGATG	*rpe* in pGP1331 for (*Bam*HI)
FM128	5´AAAGTCGACTTTACTTCCTCTGATTTCAGAAATTGCTTTTTTGCG	*rpe* in pGP1331 rev (*Sal*I)
FM129	5´AAAGGATCCGTGAAGACGGTCCGACGCACG	*tkt* in pGP1331 for (*Bam*HI)
FM130	5´AAAGTCGACCTTATTGATTAATGCCTTAACTCGATTCACTACG	*tkt* in pGP1331 rev (*Sal*I)
FM131	5´AAAGGATCCGAAGCGAATGAATTAGGAATTCTCGCCG	*ywjH* in pGP1331 for (*Bam*HI)
FM132	5´AAAGTCGACTTTGTTCCAGTCTGCCAGGAATTGTTCG	*ywjH* in pGP1331 rev (*Sal*I)
FM133	5´GAGAAGGATGATATTTTAATTGACGGCGG	Sequencing primer *gndA*
FM134	5´GCGTTTCCGGCGGAGAAGAAGG	LFH-PCR *gndA* (up-fragment for)
FM135	5´CCGAGCGCCTACGAGGAATTTGTATCGGCAGTTGCCCAAGGTGTGCCG	LFH-PCR *gndA* (down-fragment for)
FM136	5´CCCTTCTTGCAATGGAGCCGCC	LFH-PCR *gndA* (down-fragment rev)

FM137	5´CACTAGGCGTTGAAGACCGCGC	Sequencing primer *gndA*
FM138	5´CGACTGCCTTGCACCTGCATTAGG	Sequencing primer *ywjH*
FM139	5´CCGCTAGTTCTTCACGGCGGTAC	LFH-PCR *ywjH* (up-fragment for)
FM140	5´CCGAGCGCCTACGAGGAATTTGTATCGGGGGCTCATATCGGCACAATGCC	LFH-PCR *ywjH* (down-fragment for)
FM141	5´GATCTCAGGCTCCTTGGCAGCG	LFH-PCR *ywjH* (down-fragment rev)
FM142	5´GTGCAGTTCCTTCACGCCGTCG	Sequencing primer *ywjH*
FM143	5´AAAGGATCCGACATGACGGCTGTCATGAATCTCAG	*odhB* in pGP1331 for (*Bam*HI)
FM144	5´AAAGTCGACTCCTTCTAATAAAAGCTGTTCAGGATCTTCC	*odhB* in pGP1331 rev (*Sal*I)
FM145	5´AAAGGATCCGGTGAAGGTCAAACGCTTCATGGAAG	*sucD* in pGP1331 for (*Bam*HI)
FM146	5´AAAGTCGACATGCGTTTTACAAGTTTCGAACAAGTTCTTCTC	*sucD* in pGP1331 rev (*Sal*I)
FM147	5´AAAGGATCCGAGAAGACAACCCCTGTCACATGGG	*sdhB* in pGP1331 for (*Bam*HI)
FM148	5´AAAGTCGACTACTCTGTCGCTTCCGAAGAAATTGCG	*sdhB* in pGP1331 rev (*Sal*I)
FM149	5´AAAGGATCCCAGTAGGACGCCGTCCAAACACTG	*pdhD* in pGP1331 for (*Bam*HI)
FM150	5´AAAGTCGACTTTTACGATGTGAATCGGACTTCCGATTGC	*pdhD* in pGP1331 rev (*Sal*I)
FM151	5´AAAGGTACCGATGTCAAAACAACAAATCGGCGTTATCGGAC	*gndA* BACTH for (*Kpn*I)
FM152	5´AAAGAATTCCGCTTCATCCATTCAGTATGGAAGATGCCTTC	*gndA* BACTH rev (*Eco*RI)
FM153	5´AAAGAATTCTTACTTCATCCATTCAGTATGGAAGATGCC	*gndA* BACTH rev in pKT25 (*Eco*RI)
FM154	5´AAATCTAGACAGAAAATTTCTTAATCAGGGAGGCTTTTTGAAAATG	*ywjH* in pET3c for (*Xba*I)
FM155	5´AAAGGATCCTTATTTGTTCCAGTCTGCCAGGAATTGTTCG	*ywjH* in pET3c rev (*Bam*HI)
FM156	5´AAACATATGTCAAAACAACAAATCGGCGTTATCGGAC	*gndA* in pET3c for (*Nde*I)
FM157	5´AAAGGATCCTTACTTCATCCATTCAGTATGGAAGATGCC	*gndA* in pET3c rev (*Bam*HI)
FM158	5´CGAGGCGACGCACGGAACG	Sequencing primer *mdh*
FM159	5´GCATTTAGGATGGAACGAAGCGGCTGA	LFH-PCR *mdh* (up-fragment for)
FM160	5´CCGAGCGCCTACGAGGAATTTGTATCGCGGCTATGAAGGCATCTACCTTGGTG	LFH-PCR *mdh* (down-fragment for)
FM161	5´CGCGAAGATGGCTGATGTGCACATC	LFH-PCR *mdh* (down-fragment rev)
FM162	5´CGAATACAGAAAAAAGGCGCACACGG	Sequencing primer *mdh*
FM163	5´AAAGAGCTCGATGGCAAACGAGCAAAAAACTGCAGCAAAAG	*citB* in pGP172 for (*Sac*I)
FM164	5´AAAGGATCCTCATCAGGACTGCTTCATTTTTTCACGAAGCAC	*citB* in pGP172 rev (*Bam*HI)
FM165	5'AAAGAGCTCTGATCTGAAGGGGGATTTTGGAGAATGG	*citB* in pGP574 for (*Sac*I)
FM166	5´AAAGGATCCGGACTGCTTCATTTTTTCACGAAGCACC	*citB* in pGP574 rev (*Bam*HI)
FM167	5´GCGACACGCGGTCTTGAAGGG	Riboprobe *citZ* for
FM168	5´CTAATACGACTCACTATAGGGAGAGGCGGATCAGACGGTTGTTGTC	Riboprobe *citZ* rev
FM169	5´CTAATACGACTCACTATAGGGAGATAGGCTTAAACTTAAATAAGCTTATAAAAATTTG	5´UTR *citZ* for
FM170	5´CATATATAACATCTCCTTTTCAATAAATTTCC	5´UTR *citZ* rev
FM171	5´CTAATACGACTCACTATAGGGAGAGGAGATTGCAAGCGAGCTATTTATCAGTG	3´UTR *gerE* for
FM172	5´TTGTCCATCCCTCACTCAAGGATCTC	3´UTR *gerE* rev
FM173	5´AAAGAATTCAAAGGAGGAAACAATCATGGGAAATACTCGTAAAAAAGTTTCTGTTATCGG	*mdh* in pBP7 for (*Eco*RI)
FM174	5´CAGTCTCTAACGGAGTATTAAACGTACC	Riboprobe *icd* for
FM175	5´CTAATACGACTCACTATAGGGAGAGCCGCTTCGTTCCATCCTAAATGC	Riboprobe *icd* rev
FM176	5´CGGAGCAGGTTTTACCGGAGCT	Riboprobe *mdh* for
FM177	5´CTAATACGACTCACTATAGGGAGAGATTCAACTGATTTATTCAGCTGCGCTC	Riboprobe *mdh* rev
FM178	5´CTAATACGACTCACTATAGGGAGACACCATGGTGACCATATGGACGG	IRE *qoxD* for
FM179	5´GTTTGCCGTTAACGTCATTGTCGCTC	IRE *qoxD* rev
FM180	5´GAAAGCCTATGATCCTAGCACATGGG	Sequencing primer *yflS*
FM181	5´GTCATGGTGGATATCCCTGCAAACAC	LFH-PCR *yflS* (up-fragment for)

FM182	5´CCTATCACCTCAAATGGTTCGCTGGATTAGTCCCACAGCGACAGTAATAAGC	LFH-PCR *yflS* (up-fragment rev)
FM183	5´CCGAGCGCCTACGAGGAATTTGTATCGGGTCCATCGGATTTATCCTGTCGATTG	LFH-PCR *yflS* (down-fragment for)
FM184	5´CACTTGATCGTTGACGCTTACTTCCTG	LFH-PCR *yflS* (up-fragment rev)
FM185	5´CAATGTGTCGATCAGCTTCTTCAGCTC	Sequencing primer *yflS*
FM186	5´GTGTGCTTGATACGGCAGCATTCAGAACATTTGTGGC	Mutagenesis *mdh* Arg-156-Ala
FM187	5´GTGTGCTTGATACGGCAGACTTCAGAACATTTGTGGCAG	Mutagenesis *mdh* Arg-156-Asp
FX15	5´AAAGGATCCGCGGAATTTAAGCGTTCTCCAGTGCC	*ccpA* in pGP1389 for
FX16	5´AAAGTCGACTGACTTGGTTGACTTTCTAAGCTCTATACGG	*ccpA* in pGP1389 rev
oFM3	5´AAAGAGCTCTGATCTGAAGGGGGATTTTG	*citB* in pBAD30 for
oFM4	5´AAATCTAGATCAGTGATGGTGATGGTGATGGCCCTGAAAATACAGGTTTTCGGACTGCTTCATTTTTTCACG	*citB* in pBAD30/ pBB544 rev
oFM5	5´AAAGTCGACCGGAAAAGATACGCCTGC	*citB´* in pBB544 for

8.2. Plasmids

Name	Relevant characteristics	Restriction sites	Reference
pBAD30	Arabinose-inducible expression of proteins in *E. coli*		Guzman *et al*., 1995
pBB544	Derivative of pBluescript SK(2) (Stratagene, Inc.) containing a neomycin resistance marker		Belitsky *et al.,* 1997
pBP7	Expression of proteins in *B. subtilis* by the *gudB*-promoter*;* integration into the *amyE*		Gunka & Commichau, Göttingen
pBP14	Expression of proteins carrying a N-terminal CFP fusion in *B. subtilis;* integration into the amyE		Gunka & Commichau, Göttingen
pET3c	Expression of proteins in *E. coli*		Novagen, Germany
pFM1	pBAD30-*citB*	*Sac*I / *Xba*I	Pechter *et al*., *in revision*
pFM2	pBB544-´*citB*	*Sac*I / *Xba*I	Pechter *et al*., *in revision*
pGP172	Expression of proteins with N-terminal Strep-tag fusion in *E. coli*		Merzbacher *et al*., 2004
pGP380	Expression of proteins with N-terminal Strep-tag fusion in *B. subtilis*		Herzberg *et al.*, 2007
pGP466	pUT18-*odhB*	*Xba*I / *Eco*RI	Meyer *et al.*, 2011a
pGP467	pUT18c-*odhB*	*Xba*I / *Eco*RI	Meyer *et al.*, 2011a
pGP468	pKT25-*odhB*	*Xba*I / *Eco*RI	Meyer *et al.*, 2011a
pGP469	p25-N-*odhB*	*Xba*I / *Eco*RI	Meyer *et al.*, 2011a
pGP470	pUT18-*pdhD*	*Xba*I / *Kpn*I	Meyer *et al.*, 2011a
pGP471	pUT18c-*pdhD*	*Xba*I / *Kpn*I	Meyer *et al.*, 2011a
pGP472	pKT25-*pdhD*	*Xba*I / *Kpn*I	Meyer *et al.*, 2011a
pGP473	p25-N-*pdhD*	*Xba*I / *Kpn*I	Meyer *et al.*, 2011a
pGP474	pUT18-*sdhB*	*Xba*I / *Kpn*I	Meyer *et al.*, 2011a
pGP475	pUT18c-*sdhB*	*Xba*I / *Kpn*I	Meyer *et al.*, 2011a
pGP476	pKT25-*sdhB*	*Xba*I / *Kpn*I	Meyer *et al.*, 2011a
pGP477	p25-N-*sdhB*	*Xba*I / *Kpn*I	Meyer *et al.*, 2011a
pGP478	pUT18-*pckA*	*Xba*I / *Kpn*I	Meyer *et al.*, 2011a
pGP479	pUT18c-*pckA*	*Xba*I / *Kpn*I	Meyer *et al.*, 2011a
pGP480	pKT25-*pckA*	*Xba*I / *Kpn*I	Meyer *et al.*, 2011a
pGP481	p25-N-*pckA*	*Xba*I / *Kpn*I	Meyer *et al.*, 2011a
pGP482	pUT18-*odhA*	*Xba*I / *Kpn*I	Meyer *et al.*, 2011a
pGP483	pUT18c-*odhA*	*Xba*I / *Kpn*I	Meyer *et al.*, 2011a
pGP484	pKT25-*odhA*	*Xba*I / *Kpn*I	Meyer *et al.*, 2011a
pGP485	pKT25-*odhA*	*Xba*I / *Kpn*I	Meyer *et al.*, 2011a

pGP486	pUT18-*gltA*	*Xba*I / *Kpn*I	Meyer *et al.*, 2011a
pGP487	pUT18c-*gltA*	*Xba*I / *Kpn*I	Meyer *et al.*, 2011a
pGP488	pKT25-*gltA*	*Xba*I / *Kpn*I	Meyer *et al.*, 2011a
pGP489	pKT25-*gltA*	*Xba*I / *Kpn*I	Meyer *et al.*, 2011a
pGP490	pUT18-*sucC*	*Xba*I / *Kpn*I	Meyer *et al.*, 2011a
pGP491	pUT18c-*sucC*	*Xba*I / *Kpn*I	Meyer *et al.*, 2011a
pGP492	pKT25-*sucC*	*Xba*I / *Kpn*I	Meyer *et al.*, 2011a
pGP493	p25-N-*sucC*	*Xba*I / *Kpn*I	Meyer *et al.*, 2011a
pGP494	pUT18-*pdhB*	*Xba*I / *Kpn*I	Meyer *et al.*, 2011a
pGP495	pUT18c-*pdhB*	*Xba*I / *Kpn*I	Meyer *et al.*, 2011a
pGP496	pKT25-*pdhB*	*Xba*I / *Kpn*I	Meyer *et al.*, 2011a
pGP497	p25-N-*pdhB*	*Xba*I / *Kpn*I	Meyer *et al.*, 2011a
pGP882	origin of pUC19, *bla* resistance gene, and regions flanking the *B. subtilis lacA* gene		Diethmaier *et al.*, 2011
pGP884	pGP882 containing a *aphA3* resistance gene, the *xylA* promoter and the *xylR* repressor gene		Diethmaier *et al.*, 2011
pGP888	pGP884 containing C-YFP. Allows overexpression of genes by the P_{xyl}-promoter, integrates into *lacA* site		Diethmaier *et al.*, 2011
pGP1119	pGP380-*gltB*	*Bam*HI / *Sal*I	Meyer *et al.*, 2011a
pGP1120	pGP380-*citZ*	*Bam*HI / *Sal*I	Meyer *et al.*, 2011a
pGP1121	pGP380-*icd*	*Bam*HI / *Sal*I	Meyer *et al.*, 2011a
pGP1122	pGP380-*citG*	*Bam*HI / *Sal*I	Meyer *et al.*, 2011a
pGP1123	pGP380-*mdh*	*Bam*HI / *Sal*I	Meyer *et al.*, 2011a
pGP1125	pUT18-*citZ*	*Xba*I / *Kpn*I	Meyer *et al.*, 2011a
pGP1126	pUT18c-*citZ*	*Xba*I / *Kpn*I	Meyer *et al.*, 2011a
pGP1127	pKT25-*citZ*	*Xba*I / *Kpn*I	Meyer *et al.*, 2011a
pGP1128	p25-N-*citZ*	*Xba*I / *Kpn*I	Meyer *et al.*, 2011a
pGP1129	pUT18-*icd*	*Xba*I / *Kpn*I	Meyer *et al.*, 2011a
pGP1130	pUT18c-*icd*	*Xba*I / *Kpn*I	Meyer *et al.*, 2011a
pGP1131	pKT25-*icd*	*Xba*I / *Kpn*I	Meyer *et al.*, 2011a
pGP1132	p25-N-*icd*	*Xba*I / *Kpn*I	Meyer *et al.*, 2011a
pGP1133	pUT18-*citG*	*Xba*I / *Kpn*I	Meyer *et al.*, 2011a
pGP1134	pUT18c-*citG*	*Xba*I / *Kpn*I	Meyer *et al.*, 2011a
pGP1135	pKT25-*citG*	*Xba*I / *Kpn*I	Meyer *et al.*, 2011a
pGP1136	p25-N-*citG*	*Xba*I / *Kpn*I	Meyer *et al.*, 2011a
pGP1137	pUT18-*mdh*	*Xba*I / *Kpn*I	Meyer *et al.*, 2011a
pGP1138	pUT18c-*mdh*	*Xba*I / *Kpn*I	Meyer *et al.*, 2011a
pGP1139	pKT25-*mdh*	*Xba*I / *Kpn*I	Meyer *et al.*, 2011a
pGP1140	p25-N-*mdh*	*Xba*I / *Kpn*I	Meyer *et al.*, 2011a
pGP1141	pUT18-*gltB*	*Xba*I / *Kpn*I	Meyer *et al.*, 2011a
pGP1142	pUT18c-*gltB*	*Xba*I / *Kpn*I	Meyer *et al.*, 2011a
pGP1143	pKT25-*gltB*	*Xba*I / *Kpn*I	Meyer *et al.*, 2011a
pGP1144	p25-N-*gltB*	*Xba*I / *Kpn*I	Meyer *et al.*, 2011a
pGP1145	pGP380-*odhB*	*Bam*HI / *Sal*I	Meyer *et al.*, 2011a
pGP1146	pUT18-*citB*	*Xba*I / *Kpn*I	Meyer *et al.*, 2011a
pGP1147	pUT18c-*citB*	*Xba*I / *Kpn*I	Meyer *et al.*, 2011a
pGP1148	pKT25-*citB*	*Xba*I / *Kpn*I	Meyer *et al.*, 2011a
pGP1149	p25-N-*citB*	*Xba*I / *Kpn*I	Meyer *et al.*, 2011a
pGP1331	pUS19-3xFLAG	*Hind*III	Lehnik-Habrink *et al.*, 2010
pGP1389	pUS19-StrepTag	*Pst*I / *Hind*III	Lehnik-Habrink *et al.*, 2011
pGP1519	pUT18-*pdhC*	*Xba*I / *Kpn*I	Meyer *et al.*, 2011a
pGP1520	pUT18c-*pdhC*	*Xba*I / *Kpn*I	Meyer *et al.*, 2011a

pGP1521	pKT25-*pdhC*	*Xba*I / *Kpn*I	Meyer *et al.*, 2011a
pGP1522	p25-N-*pdhC*	*Xba*I / *Kpn*I	Meyer *et al.*, 2011a
pGP1523	pUT18-*sucD*	*Xba*I / *Kpn*I	Meyer *et al.*, 2011a
pGP1524	pUT18c-*sucD*	*Xba*I / *Kpn*I	Meyer *et al.*, 2011a
pGP1525	pKT25-*sucD*	*Xba*I / *Kpn*I	Meyer *et al.*, 2011a
pGP1526	p25-N-*sucD*	*Xba*I / *Kpn*I	Meyer *et al.*, 2011a
pGP1527	pUT18-*sdhA*	*Xba*I / *Kpn*I	Meyer *et al.*, 2011a
pGP1528	pUT18c-*sdhA*	*Xba*I / *Kpn*I	Meyer *et al.*, 2011a
pGP1529	pKT25-*sdhA*	*Xba*I / *Kpn*I	Meyer *et al.*, 2011a
pGP1530	p25-N-*sdhA*	*Xba*I / *Kpn*I	Meyer *et al.*, 2011a
pGP1531	pUT18-*sdhC*	*Xba*I / *Kpn*I	Meyer *et al.*, 2011a
pGP1532	pUT18c-*sdhC*	*Xba*I / *Kpn*I	Meyer *et al.*, 2011a
pGP1533	pKT25-*sdhC*	*Xba*I / *Kpn*I	Meyer *et al.*, 2011a
pGP1534	p25-N-*sdhC*	*Xba*I / *Kpn*I	Meyer *et al.*, 2011a
pGP1535	pUT18-*pdhA*	*Xba*I / *Kpn*I	Meyer *et al.*, 2011a
pGP1536	pUT18c-*pdhA*	*Xba*I / *Kpn*I	Meyer *et al.*, 2011a
pGP1537	pKT25-*pdhA*	*Xba*I / *Kpn*I	Meyer *et al.*, 2011a
pGP1538	p25-N-*pdhA*	*Xba*I / *Kpn*I	Meyer *et al.*, 2011a
pGP1751	pGP1331-*pckA*	*Sal*I / *Sph*I	Meyer *et al.*, 2011a
pGP1752	pGP1331-*mdh*	*Bam*HI / *Sal*I	Meyer *et al.*, 2011a
pGP1753	pGP380-*pckA*	*Xba*I / *Pst*I	Meyer *et al.*, 2011a
pGP1754	pGP380-*mdh* (S149A)	*Bam*HI / *Sal*I	This study
pGP1755	pWH844-*mdh* (S149A)	*Bam*HI / *Pst*I	This study
pGP1756	pGP380-*mdh* (S149D)	*Bam*HI / *Sal*I	This study
pGP1757	pWH844-*mdh* (S149D)	*Bam*HI / *Pst*I	This study
pGP1758	pGP1331-*ytsJ*	*Bam*HI / *Sal*I	Meyer *et al.*, 2011a
pGP1759	pGP1331-*citG*	*Bam*HI / *Sal*I	This study
pGP1760	pGP380-*ytsJ*	*Bam*HI / *Sal*I	This study
pGP1761	pWH844-*citZ*	*BamH*I / *Sal*I	This study
pGP1762	pWH844-*pckA*	*Sal*I / *Pst*I	This study
pGP1763	pGP172-*pckA*	*Sac*I / *Kpn*I	This study
pGP1764	pGP172-*mdh*	*Sac*I / *Bam*HI	This study
pGP1765	pGP172-*mdh* (S149A)	*Sac*I / *Bam*HI	This study
pGP1766	pGP172-*mdh* (S149D)	*Sac*I / *Bam*HI	This study
pGP1767	pUT18-*mdh* (S149A)	*Kpn*I / *Xba*I	This study
pGP1768	pUT18c-*mdh* (S149A)	*Kpn*I / *Xba*I	This study
pGP1769	pKT25-*mdh* (S149A)	*Kpn*I /*Xba*I	This study
pGP1770	p25-N-*mdh* (S149A)	*Kpn*I / *Xba*I	This study
pGP1771	pUT18-*mdh* (S149D)	*Kpn*I / *Xba*I	This study
pGP1772	pUT18c-*mdh* (S149D)	*Kpn*I / *Xba*I	This study
pGP1773	pKT25-*mdh* (S149D)	*Kpn*I / *Xba*I	This study
pGP1774	p25-N-*mdh* (S149D)	*Kpn*I / *Xba*I	This study
pGP1775	pGP1331-*citB*	*Bam*HI / *Sal*I	This study
pGP1776	pGP172-*citZ*	*Sac*I / *Bam*HI	This study
pGP1777	pGP172-*gndA*	*Sac*I / *Bam*HI	This study
pGP1778	pUT18-*ywjH*	*Kpn*I / *Xba*I	This study
pGP1779	pUT18c-*ywjH*	*Kpn*I / *Xba*I	This study
pGP1780	pKT25-*ywjH*	*Kpn*I / *Xba*I	This study
pGP1781	p25-N-*ywjH*	*Kpn*I / *Xba*I	This study
pGP1782	pGP1331-*zwf*	*Bam*HI / *Sph*I	This study
pGP1783	pGP1331-*ykgB*	*Bam*HI / *Sph*I	This study
pGP1784	pGP1331-*gndA*	*Bam*HI / *Sal*I	This study
pGP1785	pGP1331-*ywlF*	*Bam*HI / *Sal*I	This study
pGP1786	pGP1331-*rpe*	*Bam*HI / *Sal*I	This study
pGP1787	pGP1331-*tkt*	*Bam*HI / *Sal*I	This study
pGP1788	pGP1331-*ywjH*	*Bam*HI / *Sal*I	This study
pGP1789	pGP1389-*gndA*	*Bam*HI / *Sal*I	This study

pGP1790	pGP1389-*ywjH*	*Bam*HI / *Sal*I	This study
pGP1791	pGP1331-*odhB*	*Bam*HI / *Sal*I	This study
pGP1792	pGP1331-*sucD*	*Bam*HI / *Sal*I	This study
pGP1793	pGP1331-*sdhB*	*Bam*HI / *Sal*I	This study
pGP1794	pGP1331-*pdhD*	*Bam*HI / *Sal*I	This study
pGP1795	pUT18-*gndA*	*Kpn*I / *Xba*I	This study
pGP1796	pUT18c-*gndA*	*Kpn*I / *Xba*I	This study
pGP1797	pKT25-*gndA*	*Kpn*I / *Xba*I	This study
pGP1798	p25-N-*gndA*	*Kpn*I / *Xba*I	This study
pGP1799	pGP1870-*pckA*	*Sal*I / *Sph*I	This study
pGP1800	pGP1870-*mdh*	*Bam*HI / *Sal*I	This study
pGP1801	pGP1870-*ytsJ*	*Bam*HI / *Sal*I	This study
pGP1802	pGP1870-*citG*	*Bam*HI / *Sal*I	This study
pGP1803	pGP1870-*citB*	*Bam*HI / *Sal*I	This study
pGP1804	pGP1389-*mdh*	*Bam*HI / *Sal*I	This study
pGP1805	pGP1870-*sucD*	*Bam*HI / *Sal*I	This study
pGP1806	pGP1870-*sdhB*	*Bam*HI / *Sal*I	This study
pGP1807	pGP1389-*citB*	*Bam*HI / *Sal*I	This study
pGP1808	pET3c-*ywjH*	*Xba*I / *Bam*HI	This study
pGP1809	pET3c-*gndA*	*Ndh*I / *Bam*HI	This study
pGP1810	pGP172-*citB*	*Sac*I / *Bam*HI	This study
pGP1812	pGP888-*mdh*	*Xba*I / *Bam*HI	This study
pGP1813	pGP888-*mdh* (S149D)	*Xba*I / *Bam*HI	This study
pGP1814	pBP7-*mdh*	*Eco*RI / *Bam*HI	This study
pGP1815	pBP7-*mdh* (S149D)	*Eco*RI / *Bam*HI	This study
pGP1816	pBP14-*mdh*	*Eco*RI / *Bam*HI	This study
pGP1817	pBP14-*mdh* (S149A)	*Eco*RI / *Bam*HI	This study
pGP1818	pBP14-*mdh* (S149D)	*Eco*RI / *Bam*HI	This study
pGP1819	pGP1871-*mdh*	*Sal*I / *Sph*I	This study
pGP1820	pGP1871-*pckA*	*Bam*HI / *Sal*I	This study
pGP1821	pGP380-*mdh* (R156A)	*Bam*HI / *Sal*I	This study
pGP1822	pGP380-*mdh* (R156D)	*Bam*HI / *Sal*I	This study
pGP1870	pUS19-*gfp*	*Hind*III	D. Tödter, bachelor thesis
pGP1871	pUS19-y*fp*	*Hind*III	D. Tödter, bachelor thesis
pGP1952	pGP1389-*ccpA*	*Bam*HI / *Sal*I	Meyer *et al*., 2011b
pKT25	P_{lac}-*cyaA*-mcs *kan*		Karimova *et al.*, 1998
pKT25::zip	P_{lac}-*cyaA-zip kan*		Karimova *et al.*, 1998
pUS19			Benson & Haldenwang,1993
pUT18	P_{lac}-mcs-*cyaA bla*		Karimova *et al.*, 1998
pUT18c	P_{lac}-*cyaA*-mcs *bla*		Karimova *et al.*, 1998
pUT18c::zip	P_{lac}-*cyaA-zip bla*		Karimova *et al.*, 1998
pWH844	Expression of proteins carrying a His tag at their N-terminus in *E. coli*		Schirmer *et al.*, 1997
p25-N	P_{lac}-mcs-*cyaA kan*		Claessen *et al.,* 2008

8.3. Strains

B. subtilis strains used in this study

Strain	Genotype	Reference / Construction
168	*trpC2*	Laboratory collection
AF21	*ΔamyE::Φ(citBp21-lacZ cat)*	Fouet & Sonenshein, 1990
AWS96	*trpC2 pheA1*	Serio *et al*., 2006
AWS173	*citA::neo citZ517 ΔamyE::Φ(citBp21-lacZ tet)*	Serio, Ph.D. thesis

AWS174	*trpC2 pheA1 ΩcitB::spc ΔamyE::Φ(citBp21-lacZ tet)*	Serio, Ph.D. thesis
AWS198	*trpC2 pheA1 His10-citB+::pAWS50(cat)*	Serio *et al*., 2006
BAE048	*trpC2 ΔywlE*::*kan*	Ulf Gerth, Greifswald
BBA0028	P_{gntR}-*gfpmut3/spc*	Meyer *et al.*, 2011b
BBA0118	P_{fruR}-*gfpmut3/spc*	Meyer *et al.*, 2011b
BBA0121	P_{glpF}-*gfpmut3/spc*	Meyer *et al.*, 2011b
BBA0223	P_{bglP}-*gfpmut3/spc*	Meyer *et al.*, 2011b
BBA0359	P_{sacP}-*gfpmut3/spc*	Meyer *et al.*, 2011b
BEK89	*trpC2 ΔmcsB*::*kan*	Ulf Gerth, Greifswald
BDO01	*trpC2 ΔywlE*::*tet*	Elsholz *et al.*, 2012
BSB168	Wild type	Botella *et al*., 2010
CJB8	*ccpC::spc*	Jourlin-Castelli *et al*., 2000
DB104	*his nprR2 ΔaprE3 nprE18 ccpN::cat*	Sabine Brantl, Jena
GM1038	*sacA321* Δ(*sacR-B*)$_{23}$ *ccpA*::Tn*917*Δ(*erm lacZ*)::*phleo*	Meyer *et al.*, 2011b
GM1222	*trpC2 pheA1* Δ*(bgaX) amyE*::*(gntRK'-lacZ) ptsH1 cat*	Deutscher *et al*., 1994
GM2705	*trpC2* Δ*pckA*::*neo*	Tännler *et al.*, 2008
GM2907	*ccpA*::Tn*917*Δ*(erm lacZ)*::*phleo*	Meyer *et al.*, 2011b
GM2924	*crh*::*aphA3*	Meyer *et al.*, 2011b
GM2933	*ptsH1 cat*	Meyer *et al.*, 2011b
GM3001	P_{araA}-*gfpmut3/spc*	Meyer *et al.*, 2011b
GM3002	$P_{gntRcre2}$-*gfpmut3/spc*	Meyer *et al.*, 2011b
GM3003	$P_{sacPΔRAT\text{-}term}$-*gfpmut3/spc*	Meyer *et al.*, 2011b
GM3004	$P_{glpFΔterm}$-*gfpmut3/spc*	Meyer *et al.*, 2011b
GM3005	*fruA-gfpmut3/spc*	Meyer *et al.*, 2011b
GM3007	$P_{bglPΔRAT\text{-}term}$-*gfpmut3/spc*	Meyer *et al.*, 2011b
GM3008	P_{araE}-*gfpmut3/spc*	Meyer *et al.*, 2011b
GM3013	P_{araA}-*gfpmut3/spc ccpA*::Tn*917*Δ(*erm lacZ*)::*phleo*	Meyer *et al.*, 2011b
GM3014	$P_{gntRcre2}$-*gfpmut3/spc ccpA*::Tn*917*Δ(*erm lacZ*)::*phleo*	Meyer *et al.*, 2011b
GM3015	$P_{sacPΔRAT\text{-}term}$-*gfpmut3 ccpA*::Tn*917*Δ(*erm lacZ*)::*phleo*	Meyer *et al.*, 2011b
GM3016	$P_{glpFΔterm}$-*gfpmut3/spc ccpA*::Tn*917*Δ(*erm lacZ*)::*phleo*	Meyer *et al.*, 2011b
GM3017	*fruA-gfpmut3/spc ccpA*::Tn*917*Δ(*erm lacZ*)::*phleo*	Meyer *et al.*, 2011b
GM3019	$P_{bglPΔRAT\text{-}term}$-*gfpmut3/spc ccpA*::Tn*917*Δ(*erm lacZ*)::*phleo*	Meyer *et al.*, 2011b
GM3020	P_{araE}-*gfpmut3/spc ccpA*::Tn*917*Δ(*erm lacZ*)::*phleo*	Meyer *et al.*, 2011b
GM3022	P_{glpF}-*gfpmut3/spc ccpA*::Tn*917*Δ(*erm lacZ*)::*phleo*	Meyer *et al.*, 2011b
GM3023	P_{bglP}-*gfpmut3/spc ccpA*::Tn*917*Δ(*erm lacZ*)::*phleo*	Meyer *et al.*, 2011b
GM3024	P_{sacP}-*gfpmut3/spc ccpA*::Tn*917*Δ(*erm lacZ*)::*phleo*	Meyer *et al.*, 2011b
GM3027	P_{fruR}-*gfpmut3/spc ccpA*::Tn*917*Δ(*erm lacZ*)::*phleo*	Meyer *et al.*, 2011b
GM3029	$P_{gntRcre2}$-*gfpmut3/spc crh*::*aphA3*	Meyer *et al.*, 2011b
GM3031	P_{bglP}-*gfpmut3/spc crh*::*aphA3*	Meyer *et al.*, 2011b
GM3033	$P_{bglPΔRAT\text{-}term}$-*gfpmut3/spc crh*::*aphA3*	Meyer *et al.*, 2011b
GM3037	$P_{gntRcre2}$-*gfpmut3/spc ptsH1 cat*	Meyer *et al.*, 2011b
GM3039	P_{bglP}-*gfpmut3/spc ptsH1cat*	Meyer *et al.*, 2011b
GM3043	$P_{bglPΔRAT\text{-}term}$-*gfpmut3/spc ptsH1 cat*	Meyer *et al.*, 2011b
GM3057	P_{glpF_term}-*gfpmut3/spc crh*::*aphA3*	Meyer *et al.*, 2011b
GM3059	*fruA-gfpmut3/spc crh*::*aphA3*	Meyer *et al.*, 2011b
GM3061	P_{fruR}-*gfpmut3/spc crh*::*aphA3*	Meyer *et al.*, 2011b
GM3063	P_{araE}-*gfpmut3/spc crh*::*aphA3*	Meyer *et al.*, 2011b
GM3065	P_{araA}-*gfpmut3/spc crh*::*aphA3*	Meyer *et al.*, 2011b
GM3067	$P_{sacPΔRAT\text{-}term}$-*gfpmut3 crh*::*aphA3*	Meyer *et al.*, 2011b
GM3069	$P_{glpFΔterm}$-*gfpmut3/spc ptsH1 cat*	Meyer *et al.*, 2011b
GM3071	*fruA-gfpmut3/spc ptsH1 cat*	Meyer *et al.*, 2011b
GM3073	P_{fruR}-*gfpmut3/spc ptsH1 cat*	Meyer *et al.*, 2011b
GM3075	P_{araE}-*gfpmut3/spc ptsH1 cat*	Meyer *et al.*, 2011b
GM3077	P_{araA}-*gfpmut3/spc ptsH1 cat*	Meyer *et al.*, 2011b
GM3079	$P_{sacPΔRAT\text{-}term}$-*gfpmut3 ptsH1 cat*	Meyer *et al.*, 2011b
GP205	*trpC2 amyE*::(*gltA-lacZ cat*)	Blencke *et al*., 2006

GP270	*trpC2 xylR*::*ermC*	Singh *et al*., 2008
GP284	*trpC2 xylR*::*ermC ptsH1*	Singh *et al*., 2008
GP287	*trpC2 xylR*::*ermC ptsH1 crh*::*spc*	Singh *et al*., 2008
GP289	*trpC2 xylR*::*ermC hprK*::*aphA3*	Singh *et al*., 2008
GP297	*trpC2 xylR*::*ermC crh*::*spc*	Singh *et al*., 2008
GP342	*trpC2* amyE::(*gltA-lacZ aphA3*)	Wacker *et al*., 2003
GP717	*trpC2* Δ*gudB*::*cat rocG*::*Tn10 spc amyE*::(*gltA-lacZ aphA3*) *gltB1*	Commichau *et al*., 2008
GP718	*trpC2* Δ*citG*::*spc amyE*::(*gltA-lacZ aphA3*)	Meyer *et al.*, 2011a
GP719	*trpC2* Δ*mdh*::*spc amyE*::*(gltA-lacZ aphA3)*	Meyer *et al.*, 2011a
GP853	*trpC2 xylR*::*ermC ccpA*::*spc*	Singh *et al*., 2008
GP1128	*trpC2* Δ*ccpN*::*cat*	DB104 → 168
GP1129	*trpC2 pckA*-3xFLAG-tag *spc*	Meyer *et al.*, 2011a
GP1130	*trpC2 mdh*-3xFLAG-tag *spc*	Meyer *et al.*, 2011a
GP1131	*trpC2 ytsJ*-3xFLAG-tag *spc*	Meyer *et al.*, 2011a
GP1132	*trpC2 citG*-3xFLAG-tag *spc*	pGP1759 → 168
GP1133	*trpC2* Δ*ccpN*::*cat pckA*-3xFLAG-tag *spc*	pGP1751 → GP1128
GP1134	*trpC2* Δ*sucC*::*cat*	LFH-PCR product → 168
GP1135	*trpC2* Δ*pckA*::*neo mdh*-3xFLAG-tag *spc*	pGP1752 → GM2705
GP1136	*trpC2* Δ*mleA*::*cat*	Meyer & Stülke, 2012
GP1137	*trpC2* Δ*maeA*::*kan* Δ*xylR*::*ery*	GTD102 → GP270
GP1138	*trpC2* Δ*malS*::*spc* Δ*xylR*::*ery*	GTD110 → GP270
GP1139	*trpC2* Δ*ytsJ*::*spc* Δ*xylR*::*ery*	GP612 → GP270
GP1140	*trpC2* Δ*mleA*::*cat* Δ*xylR*::*ery*	GP1136 → GP270
GP1141	*trpC2* Δ*maeA*::*kan*	Meyer & Stülke, 2012
GP1142	*trpC2* Δ*malS*::*spc*	Meyer & Stülke, 2012
GP1143	*trpC2* Δ*ytsJ*::*spc*	Meyer & Stülke, 2012
GP1144	*trpC2 citB*-3xFLAG-tag *spc*	pGP1775 → 168
GP1145	*trpC2 citB*-3xFLAG-tag *kan*	LFH-PCR produkt → 168
GP1146	*trpC2* Δ*ccpA*::*spc* Δ*xylR*::*ery* Δ*maeA*::*kan*	GTD102 → GP853
GP1147	*trpC2* Δ*pckA*::*neo*	Meyer & Stülke, 2012
GP1150	*trpC2* Δ*md*::*spc*	Meyer & Stülke, 2012
GP1303	*trpC2 ccpA*-Strep *spc*	Meyer *et al*., 2011b
GP1401	*trpC2 zwf*-3xFLAG-tag *spc*	pGP1782 → 168
GP1402	*trpC2 ykgB*-3xFLAG-tag *spc*	pGP1783 → 168
GP1403	*trpC2 gndA*-3xFLAG-tag *spc*	pGP1784 → 168
GP1404	*trpC2 ywlF*-3xFLAG-tag *spc*	pGP1785 → 168
GP1405	*trpC2 rpe*-3xFLAG-tag *spc*	pGP1786 → 168
GP1406	*trpC2 tkt*-3xFLAG-tag *spc*	pGP1787 → 168
GP1407	*trpC2 ywjH*-3xFLAG-tag *spc*	pGP1788 → 168
GP1408	*trpC2 gndA*-Strep-tag *spc*	pGP1789 → 168
GP1409	*trpC2 ywjH*-Strep-tag *spc*	pGP1790 → 168
GP1410	*trpC2 gndA*-Strep-tag *cat*	LFH-PCR product → 168
GP1411	*trpC2 ywjH*-Strep-tag *cat*	LFH-PCR product → 168
GP1412	*trpC2 ywjH*-Strep-tag *cat zwf*-3xFLAG-tag *spc*	GP1401 → GP1411
GP1413	*trpC2 ywjH*-Strep-tag *cat ykgB*-3xFLAG-tag *spc*	GP1402 → GP1411
GP1414	*trpC2 ywjH*-Strep-tag *cat gndA*-3xFLAG-tag *spc*	GP1403 → GP1411
GP1415	*trpC2 ywjH*-Strep-tag *cat ywlF*-3xFLAG-tag *spc*	GP1404 → GP1411
GP1416	*trpC2 ywjH*-Strep-tag *cat rpe*-3xFLAG-tag *spc*	GP1405 → GP1411
GP1417	*trpC2 ywjH*-Strep-tag *cat tkt*-3xFLAG-tag *spc*	GP1406 → GP1411
GP1418	*trpC2 gndA*-Strep-tag *cat zwf*-3xFLAG-tag *spc*	GP1401 → GP1410
GP1419	*trpC2 gndA*-Strep-tag *cat ykgB*-3xFLAG-tag *spc*	GP1402 → GP1410
GP1420	*trpC2 gndA*-Strep-tag *cat ywjH*-3xFLAG-tag *spc*	GP1407 → GP1410
GP1421	*trpC2 gndA*-Strep-tag *cat ywlF*-3xFLAG-tag *spc*	GP1404 → GP1411
GP1422	*trpC2 gndA*-Strep-tag *cat rpe*-3xFLAG-tag *spc*	GP1405 → GP1411
GP1423	*trpC2 gndA*-Strep-tag *cat tkt*-3xFLAG-tag *spc*	GP1406 → GP1410
GP1424	*trpC2 odhB*-3xFLAG-tag *spc*	pGP1791 → 168

GP1425	*trpC2 sucD*-3xFLAG-tag *spc*	pGP1792 → 168
GP1426	*trpC2 sdhB*-3xFLAG-tag *spc*	pGP1793 → 168
GP1427	*trpC2 pdhD*-3xFLAG-tag *spc*	pGP1794 → 168
GP1428	*trpC2 ywjH*-Strep-tag *cat ytsJ*-3xFLAG-tag *spc*	pGP1758 → GP1411
GP1429	*trpC2 mdh-yfp*::*spc*	pGP1819 → 168
GP1430	*trpC2 pckA-gfp spc*	pGP1799 → 168
GP1431	*trpC2 mdh-gfp spc*	pGP1800 → 168
GP1432	*trpC2 ytsJ-gfp spc*	pGP1801 → 168
GP1433	*trpC2 citG-gfp spc*	pGP1802 → 168
GP1434	*trpC2 citB-gfp spc*	pGP1803 → 168
GP1435	*trpC2 sucD-gfp spc*	pGP1805 → 168
GP1436	*trpC2 sdhB-gfp spc*	pGP1806 → 168
GP1438	*trpC2 mdh*-Strep *spc*	pGP1804 → 168
GP1439	*trpC2 citB*-Strep *spc*	pGP1807 → 168
GP1440	*trpC2 mdh*-Strep *cat*	LFH-PCR product → 168
GP1441	*trpC2* Δ*citB*::*spc*	Pechter *et al*., *in revision*
GP1442	*trpC2* Δ*ccpC*::*aphA3*	pGP702 → 168
GP1444	*trpC2 mdh*-Strep::*cat pckA*-3xFLAG-tag *spc*	pGP1753 → GP1440
GP1446	*trpC2* Δ*maeA*::*kan* Δ*malS*::*spc*	Meyer & Stülke, 2012
GP1448	*trpC2* Δ*mleA*::*cat* Δ*malS*::*spc* Δ*maeA*::*kan*	Meyer & Stülke, 2012
GP1449	*trpC2* Δ*maeN*::*Tn917(erm)*	1A642 → 168
GP1450	*trpC2* Δ*yflS*::*cat*	LFH-PCR product → 168
GP1451	*trpC2 lacA*::(*mdh aphA3*)	pGP1812 → 168
GP1452	*trpC2 lacA*::(*mdh* (S149D) *aphA3*)	pGP1813 → 168
GP1453	*trpC2 amyE*::(*mdh cat*)	p1814 → 168
GP1454	*trpC2 amyE*::(*mdh* (S149D) *cat*)	p1815 → 168
GP1455	*trpC2* ∆*mdh*::*spc amyE*::(*mdh cat*)	GP719 → GP1453
GP1456	*trpC2* ∆*mdh*::*spc amyE*::(*mdh* (S149D) *cat*)	GP719 → GP1454
GP1457	*trpC2 ΔmcsB*::*kan*	BEK89 → 168
GP1458	*trpC2 ΔywlE*::*kan*	BAE048 → 168
GP1459	*trpC2 ΔywlE*::*tet*	BDO01 → 168
GP1460	*trpC2 ΔmleN*::*spc*	VK3 → 168
GP1461	*trpC2* Δ*yflS*::*cat* Δ*maeN*::*Tn917(erm)*	GP1450 → GP1449
GP1462	*trpC2 amyE::*(*cfp-mdh cat)*	pGP1816 → 168
GP1463	*trpC2 amyE*::(*cfp-mdh cat)* ∆*mdh*::*spc*	pGP1816 → GP719
GTD102	*maeA*::*kan*	Doan *et al*., 2003
GTD110	Δ*malS*::*spc*	Doan *et al*., 2003
HKB186	*ΔamyE::Φ(citBp21-lacZ cat) ΔccpC::ble*	Kim *et al*., 2006
JH642	*trpC2 pheA1*	Brehm *et al*., 1973
KBP17	*trpC2 pheA1* His10-*citB2::*pKP12(*cat*)	Pechter *et al*., *in revision*
KBP22	*trpC2 pheA1 citB2 citZ340*	Pechter *et al*., *in revision*
KBP26	*trpC2 pheA1 ΔamyE::Φ(citBp21-lacZ cat)*	Pechter *et al*., *in revision*
KBP44	*trpC2 pheA1 citZ::Φ(citZ'-lacZ cat)*	Pechter *et al*., *in revision*
KBP45	*trpC2 pheA1 ΩcitB::spc citZ::Φ(citZ'-lacZ cat)*	Pechter *et al*., *in revision*
KBP48	*trpC2 pheA1 citZ::Φ(citZ'-lacZ cat) ΔccpC::ble*	Pechter *et al*., *in revision*
KBP49	*trpC2 pheA1 ΩcitB::spc citZ::Φ(citZ'-lacZ cat) ΔccpC::ble*	Pechter *et al*., *in revision*
KBP51	*trpC2 pheA1 ΩcitB::spc ΔamyE::Φ(citBp21-lacZ cat)*	Pechter *et al*., *in revision*
KBP52	*trpC2 pheA1 ΔamyE::Φ(citBp21-lacZ cat) ΔccpC::ble*	Pechter *et al*., *in revision*
KBP54	*trpC2 pheA1 ΩcitB::spc ΔamyE::Φ(citBp21-lacZ cat) ΔccpC::ble*	Pechter *et al*., *in revision*
KBP72	*trpC2 pheA1 citB7 ΔamyE::Φ(citBp21-lacZ cat)*	Pechter *et al*., *in revision*
KBP81	*trpC2 pheA1 citB7 ΔamyE::Φ(citBp21-lacZ tet)*	Pechter *et al*., *in revision*
KBP85	*trpC2 pheA1 ΔamyE::Φ(citBp21-lacZ tet)*	Pechter *et al*., *in revision*
KBP86	*trpC2 pheA1 citZ340 ΔamyE::Φ(citBp23-lacZ cat)*	Pechter *et al*., *in revision*
KBP94	*trpC2 pheA1 ΔamyE::Φ(citBp21-lacZ tet)*	Pechter *et al*., *in revision*
KBP96	*trpC2 pheA1 ccpC::spc ΔamyE::Φ(citBp21-lacZ tet)*	Pechter *et al*., *in revision*

KBP118	*trpC2 pheA1 citB2 ΔamyE::Φ(citBp21-lacZ tet)*	Pechter *et al*., *in revision*
KBP125	*trpC2 pheA1 citB+::*pKP29*(cat)*	Pechter *et al*., *in revision*
KBP126	*trpC2 pheA1 citB2::*pKP29*(cat) citZ340*	Pechter *et al*., *in revision*
KBP127	*trpC2 pheA1 citB+::*pKP29*(cat) ΔamyE::Φ(citBp21-lacZ tet)*	Pechter *et al*., *in revision*
KBP128	*trpC2 pheA1 citB2::*pKP29*(cat) ΔamyE::Φ(citBp21-lacZ tet)*	Pechter *et al*., *in revision*
KBP129	*trpC2 pheA1 citB7::*pKP29*(cat) ΔamyE::Φ(citBp21-lacZ tet)*	Pechter *et al*., *in revision*
KBP135	*trpC2 pheA1 citB+::*pKP29*(cat) ΔamyE::Φ(citBp21-lacZ tet)*	Pechter *et al*., *in revision*
KBP136	*trpC2 pheA1 citB2::*pKP29*(cat) ΔamyE::Φ(citBp21-lacZ tet)*	Pechter *et al*., *in revision*
KBP137	*trpC2 pheA1 citB7::*pKP29*(cat) ΔamyE::Φ(citBp21-lacZ tet)*	Pechter *et al*., *in revision*
KBP138	*trpC2 pheA1 citB+::*pKP29*(cat) ccpC::spc ΔamyE::Φ(citBp21-lacZ tet)*	Pechter *et al*., *in revision*
KBP139	*trpC2 pheA1 citB2::*pKP29*(cat) ccpC::spc ΔamyE::Φ(citBp21-lacZ tet)*	Pechter *et al*., *in revision*
KBP140	*trpC2 pheA1 citB7::*pKP29*(cat) ccpC::spc ΔamyE::Φ(citBp21-lacZ tet)*	Pechter *et al*., *in revision*
LS1003	*trpC2 pheA1 citZ::Φ(citZ'-lacZ cat)*	Jin & Sonenshein, 1994
MAB160	*trpC2 pheA1 ΩcitB::spc*	Craig *et al*., 1997
SJB66	*trpC2 pheA1 ΔcitZ471*	Jin & Sonenshein, 1994
SJB67	*trpC2 pheA1 ΔcitA::neo ΔcitZ471*	Jin & Sonenshein, 1994
SJB231	*trpC2 pheA1 ΔcitZC::spc*	Matsuno *et al*., 1999
QB7098	*trpC2 crh::aphA3 amyE::(PΔB levD'-'lacZ cat)*	Galinier *et al*., 1997
VK3	*trpC2 ΔmleN::spc*	Wei *et al*., 2000

E. coli strains used in this study

Strain	Genotype	Reference / Construction
BL21 (DE)	*F⁻ ompT gal dcm lon hsdS$_B$(r_{B-} m_{B-}) λ(DE3) pLysS(cm^R)*	Sambrook *et al.*, 1989
BTH101	F⁻ *cya-99 araD139 galE15 galK16 rpsL1* (Str^r) *hsdR2 mcrA1 mcrB1*	Karimova *et al.*, 2005
DH5α	*F- endA1 glnV44 thi-1 recA1 relA1 gyrA96 deoR nupG Φ80dlacZΔM15 Δ(lacZYA-argF)U169, hsdR17(r_{K-} m_{K+}), λ–*	Sambrook *et al.*, 1989
XL1-Blue	*endA1 gyrA96(nalR) thi-1 recA1 relA1 lac glnV44 F'[::Tn10 proAB$_+$ lacI^q Δ(lacZ)M15] hsdR17(r_{K-} m_{K+})*	Karimova *et al.*, 2005

8.4. Supplementary material chapter 2

Table 8.4.1. Protein report on identification of interaction partners in the SPINE experiment

Protein report on identification of interaction partners in the SPINE experiment

Peak-list generating software:
Extract-Msn in Bioworks 3.2 (Thermo)
Search Engine: Sequest
Version: v.27, rev. 11
Fragment Tolerance: 1.00 Da (Monoisotopic)
Parent Tolerance: 10 ppm (Monoisotopic)
Fixed Modifications: -
Variable Modifications: +16 on M (Oxidation), +71 on C (Propionamide)
Database: the SLRprot_18072003 database (extracted from SubtiList (genolist.pasteur.fr/SubtiList/), 4106 entries)
Digestion Enzyme: Trypsin
Max Missed Cleavages: 2
Scaffold Version: Scaffold_2_01_02
Peptide Thresholds: 90.0% minimum
Protein Thresholds: 99.0% minimum and 2 peptides minimum

[1]Bait protein
[2]cross linking by formaldehyde
[3]Proteins named multiple times (especially the bait proteins) were found in more than one gel slice.
[4]Protein identifier from SubtiList database and Subtwiki database
[5]Protein molecular weight
[6]Protein probality calculated by Protein Prophet
[7]Number of unique peptides
[8] Sequence coverage

Bait[1]	CL[2]	Protein[3,4]	Protein name	MW[5] (Da)	Protein prob.[6]	peptides[7]	SC[8]	Bait[1]	CL[2]	Protein[3,4]
CitG	(+)	Icd	isocitrate dehydrogenase	46,401.00	100.00%	24	58.20%	CitG	(+)	Icd
CitG	(-)	CitG	fumarate hydratase	50,514.70	100.00%	23	41.80%	CitG	(-)	CitG
CitG	(-)	CitG	fumarate hydratase	50,514.70	100.00%	22	39.00%	CitG	(-)	CitG
CitG	(+)	CitB	aconitate hydratase	99,317.30	100.00%	22	30.60%	CitG	(+)	CitB
CitG	(-)	CitG	fumarate hydratase	50,514.70	100.00%	18	31.00%	CitG	(-)	CitG
CitG	(-)	DnaK	class I heat-shock protein (molecular chaperone)	65,985.00	100.00%	15	24.10%	CitG	(-)	DnaK
CitG	(+)	CitG	fumarate hydratase	50,514.70	100.00%	13	31.80%	CitG	(+)	CitG
CitG	(-)	CitG	fumarate hydratase	50,514.70	100.00%	12	29.40%	CitG	(-)	CitG
CitG	(+)	CitG	fumarate hydratase	50,514.70	100.00%	11	30.70%	CitG	(+)	CitG
CitG	(-)	CitG	fumarate hydratase	50,514.70	100.00%	11	24.90%	CitG	(-)	CitG
CitG	(-)	CitG	fumarate hydratase	50,514.70	100.00%	9	15.60%	CitG	(-)	CitG
CitG	(-)	YclQ	unknown; similar to ferrichrome ABC transporter (binding protein)	34,775.00	100.00%	8	26.50%	CitG	(-)	YclQ
CitG	(-)	YqfA	resistence protein (against sublancin)	35,623.60	100.00%	8	30.20%	CitG	(-)	YqfA
CitG	(+)	SucC	succinyl-CoA synthetase (beta subunit)	41,354.40	100.00%	8	22.30%	CitG	(+)	SucC
CitG	(+)	CitZ	citrate synthase II (major)	41,712.30	100.00%	7	29.60%	CitG	(+)	CitZ
CitG	(-)	YdjI	unknown	36,064.10	100.00%	7	23.80%	CitG	(-)	YdjI
CitG	(+)	BdhA	acetoine/	37,322.70	100.00%	7	24.90%	CitG	(+)	BdhA

			butanediol dehydrogenase							
CitG	(+)	AspB	aspartate aminotransferase	43,071.10	100.00%	7	26.70%	CitG	(+)	AspB
CitG	(+)	CitG	fumarate hydratase	50,514.70	100.00%	7	18.20%	CitG	(+)	CitG
CitG	(+)	PurB	adenylosuccinate lyase	49,468.10	100.00%	6	14.60%	CitG	(+)	PurB
CitG	(+)	RpoA	RNA polymerase (alpha subunit)	34,782.20	100.00%	6	21.30%	CitG	(+)	RpoA
CitG	(+)	CitG	fumarate hydratase	50,514.70	100.00%	6	17.10%	CitG	(+)	CitG
CitG	(+)	GroEL	class I heat-shock protein (chaperonin)	57,406.30	100.00%	5	10.80%	CitG	(+)	GroEL
CitG	(+)	YtsJ	NAD-dependent malate dehydrogenase	43,649.20	100.00%	5	18.00%	CitG	(+)	YtsJ
CitG	(+)	TufA	elongation factor Tu	43,574.90	100.00%	4	14.90%	CitG	(+)	TufA
CitG	(+)	CitG	fumarate hydratase	50,514.70	100.00%	4	13.60%	CitG	(+)	CitG
CitG	(+)	PdhA	pyruvate dehydrogenase (E1 alpha subunit)	41,531.40	100.00%	4	12.40%	CitG	(+)	PdhA
CitG	(-)	RplA	ribosomal protein L1 (BL1)	24,904.40	100.00%	4	19.00%	CitG	(-)	RplA
CitG	(+)	PheT	phenylalanyl-tRNA synthetase (beta subunit)	87,928.80	100.00%	3	6.34%	CitG	(+)	PheT
CitG	(+)	CitG	fumarate hydratase	50,514.70	100.00%	3	10.80%	CitG	(+)	CitG
CitG	(+)	OxdC	oxalate decarboxylase	43,548.50	100.00%	3	10.90%	CitG	(+)	OxdC
CitG	(+)	GapA	glyceraldehyde-3-phosphate dehydrogenase	35,814.50	100.00%	3	10.40%	CitG	(+)	GapA
CitG	(+)	YxjG	unknown	43,098.50	100.00%	3	7.41%	CitG	(+)	YxjG
CitG	(+)	CitZ	citrate synthase II (major)	41,712.30	100.00%	3	9.14%	CitG	(+)	CitZ
CitG	(-)	CitG	fumarate hydratase	50,514.70	100.00%	3	6.49%	CitG	(-)	CitG
CitG	(-)	CitG	fumarate hydratase	50,514.70	100.00%	3	4.33%	CitG	(-)	CitG
CitG	(+)	YoaC	unknown; similar to xylulokinase	54,092.20	99.80%	2	6.37%	CitG	(+)	YoaC
CitG	(+)	YtkK	unknown; similar to 3-oxoacyl- acyl-carrier protein reductase	27,957.20	99.80%	2	10.60%	CitG	(+)	YtkK
CitG	(+)	SpoVK	disruption leads to the production of immature spores	36,661.10	99.60%	2	11.80%	CitG	(+)	SpoVK
CitG	(+)	YueB	unknown	119,968.90	99.80%	2	2.88%	CitG	(+)	YueB
CitG	(+)	PncB	putative nicotinate phosphoribosyltransferase	56,163.90	99.80%	2	5.10%	CitG	(+)	PncB
CitG	(-)	YvgJ	unknown	70,731.50	99.80%	2	2.92%	CitG	(-)	YvgJ
CitG	(-)	PdhB	pyruvate dehydrogenase (E1 beta subunit)	35,456.40	99.60%	2	5.23%	CitG	(-)	PdhB
CitG	(-)	PksN	polyketide synthase	609,580.70	100.00%	2	0.64%	CitG	(-)	PksN
CitG	(-)	YetO	unknown; similar to cytochrome P450 / NADPH-cytochrome P450 reductase	119,453.30	99.70%	2	3.20%	CitG	(-)	YetO
CitG	(-)	PksM	polyketide	475,746.30	100.00%	2	0.89%	CitG	(-)	PksM

CitG	(-)	Smc	synthase chromosome condensation and segregation SMC protein	135,497.20	99.90%	2	1.35%	CitG	(-)	Smc
CitG	(-)	SrfAA	surfactin synthetase / competence	402,063.70	99.80%	2	1.37%	CitG	(-)	SrfAA
CitG	(-)	YxjH	unknown	38,281.40	99.80%	2	7.35%	CitG	(-)	YxjH
CitG	(-)	YoaC	unknown; similar to xylulokinase	54,092.20	99.80%	2	6.37%	CitG	(-)	YoaC
CitG	(-)	YwqJ	unknown	66,674.50	99.60%	2	6.31%	CitG	(-)	YwqJ
CitG	(-)	GyrA	DNA gyrase (subunit A)	92,084.10	99.80%	2	4.38%	CitG	(-)	GyrA
CitG	(-)	YwbM	elemental iron uptake system (permease)	42,779.80	99.70%	2	4.68%	CitG	(-)	YwbM
CitG	(-)	MaeN	Na+/malate symporter	47,809.20	99.70%	2	3.79%	CitG	(-)	MaeN
CitG	(-)	CitZ	citrate synthase II (major)	41,712.30	99.70%	2	9.14%	CitG	(-)	CitZ
CitG	(-)	YoaC	unknown; similar to xylulokinase	54,092.20	99.70%	2	6.37%	CitG	(-)	YoaC
CitG	(-)	TagF	CDP-glycerol:polyglycerol phosphate glycero-phosphotransferase	88,050.80	99.70%	2	2.55%	CitG	(-)	TagF
CitG	(-)	Buk	probable branched-chain fatty-acid kinase (butyrate kinase)	39,747.10	99.60%	2	5.51%	CitG	(-)	Buk
CitG	(-)	YcgQ	unknown	33,190.80	99.70%	2	7.72%	CitG	(-)	YcgQ
CitG	(-)	YpuA	unknown	31,277.20	99.70%	2	8.62%	CitG	(-)	YpuA
CitG	(-)	PksL	polyketide synthase	506,300.20	99.90%	2	0.68%	CitG	(-)	PksL
CitG	(-)	SpoIIE	serine phosphatase (sigma-F activation) / asymmetric septum formation	91,954.10	99.70%	2	2.90%	CitG	(-)	SpoIIE
CitG	(-)	Bpr	bacillopeptidase F	154,562.00	99.90%	2	1.67%	CitG	(-)	Bpr
CitG	(-)	NadC	nicotinate-nucleotide pyrophosphorylase	31,375.70	99.70%	2	5.88%	CitG	(-)	NadC
CitG	(-)	PgdS	gamma-DL-glutamyl hydrolase	45,230.10	99.70%	2	9.20%	CitG	(-)	PgdS
CitG	(-)	PncB	putative nicotinate phosphoribosyltransferase	56,163.90	99.50%	2	7.14%	CitG	(-)	PncB
CitG	(-)	RocR	transcriptional activator of arginine utilization operons	52,161.40	99.70%	2	7.16%	CitG	(-)	RocR
CitG	(-)	XtmA	PBSX terminase (small subunit)	30,227.30	99.70%	2	7.55%	CitG	(-)	XtmA
CitG	(+)	CitG	fumarate hydratase	50,514.70	99.90%	2	5.63%	CitG	(+)	CitG
CitG	(+)	YqbO	unknown; similar to phage-related protein	171,017.30	99.90%	2	1.45%	CitG	(+)	YqbO
CitG	(+)	YqbO	unknown; similar to phage-related protein	171,017.30	99.90%	2	1.96%	CitG	(+)	YqbO
CitG	(+)	YkgB	unknown	38,392.10	99.80%	2	6.02%	CitG	(+)	YkgB

CitG	(+)	YceH	unknown; similar to toxic anion resistance protein	41,656.80	99.80%	2	5.51%	CitG	(+)	YceH
CitG	(+)	AckA	acetate kinase	43,120.60	99.80%	2	7.34%	CitG	(+)	AckA
CitG	(-)	YjbV	4-amino-5-hydroxymethyl-2-methylpyrimidine pyrophosphate kinase	29,106.30	99.80%	2	9.59%	CitG	(-)	YjbV
CitG	(-)	CitG	fumarate hydratase	50,514.70	99.80%	2	8.44%	CitG	(-)	CitG
CitG	(-)	DegU	two-component response regulator involved in degradative enzyme and competence regulation	25,848.10	99.80%	2	9.17%	CitG	(-)	DegU
CitG	(-)	YflB	unknown	10,007.50	99.80%	2	32.60%	CitG	(-)	YflB
CitG	(-)	PksM	polyketide synthase	475,746.30	100.00%	2	0.75%	CitG	(-)	PksM

Bait[1]	**CL**[2]	**Protein**[3,4]	**Protein name**	**MW**[5] **(Da)**	**Protein prob.**[6]	**peptides**[7]	**SC**[8]	**Bait**[1]	**CL**[2]	**Protein**[3,4]
Mdh	(+)	Mdh	malate dehydrogenase	33,626.00	100.00%	22	61.50%	Mdh	(+)	Mdh
Mdh	(+)	GuaB	inosine-monophosphate dehydrogenase	52,973.30	100.00%	21	55.30%	Mdh	(+)	GuaB
Mdh	(+)	PurH	phosphoribosylaminoimidazole carboxy formyl formyltransferase / inosine-monophosphate cyclohydrolase	55,721.90	100.00%	17	37.70%	Mdh	(+)	PurH
Mdh	(+)	FusA	elongation factor G	76,527.20	100.00%	16	25.10%	Mdh	(+)	FusA
Mdh	(+)	Mdh	malate dehydrogenase	33,626.00	100.00%	15	50.60%	Mdh	(+)	Mdh
Mdh	(+)	Mdh	malate dehydrogenase	33,626.00	100.00%	15	51.00%	Mdh	(+)	Mdh
Mdh	(+)	Mdh	malate dehydrogenase	33,626.00	100.00%	15	51.90%	Mdh	(+)	Mdh
Mdh	(+)	Icd	isocitrate dehydrogenase	46,401.00	100.00%	15	39.50%	Mdh	(+)	Icd
Mdh	(+)	Hom	homoserine dehydrogenase	47,476.40	100.00%	15	35.10%	Mdh	(+)	Hom
Mdh	(+)	Mdh	malate dehydrogenase	33,626.00	100.00%	14	53.80%	Mdh	(+)	Mdh
Mdh	(+)	Mdh	malate dehydrogenase	33,626.00	100.00%	14	52.20%	Mdh	(+)	Mdh
Mdh	(+)	Mdh	malate dehydrogenase	33,626.00	100.00%	14	54.80%	Mdh	(+)	Mdh
Mdh	(+)	Mdh	malate dehydrogenase	33,626.00	100.00%	14	54.80%	Mdh	(+)	Mdh
Mdh	(+)	ThiC	biosynthesis of the pyrimidine moiety of thiamin	65,899.90	100.00%	13	28.10%	Mdh	(+)	ThiC
Mdh	(+)	TufA	elongation factor Tu	43,574.90	100.00%	13	37.10%	Mdh	(+)	TufA
Mdh	(+)	AtpD	ATP synthase (subunit beta)	51,402.10	100.00%	13	40.60%	Mdh	(+)	AtpD
Mdh	(+)	Mdh	malate dehydrogenase	33,626.00	100.00%	13	56.10%	Mdh	(+)	Mdh
Mdh	(+)	AsnS	asparaginyl-tRNA synthetase	49,067.10	100.00%	12	31.40%	Mdh	(+)	AsnS
Mdh	(+)	Mdh	malate dehydrogenase	33,626.00	100.00%	12	51.00%	Mdh	(+)	Mdh
Mdh	(+)	Mdh	malate dehydrogenase	33,626.00	100.00%	12	49.00%	Mdh	(+)	Mdh

Mdh	(+)	PckA	phosphoenolpyruvate carboxykinase	58,283.20	100.00%	11	23.10%	Mdh	(+)	PckA
Mdh	(+)	Mdh	malate dehydrogenase	33,626.00	100.00%	11	42.90%	Mdh	(+)	Mdh
Mdh	(+)	Mdh	malate dehydrogenase	33,626.00	100.00%	11	49.00%	Mdh	(+)	Mdh
Mdh	(+)	Mdh	malate dehydrogenase	33,626.00	100.00%	11	46.20%	Mdh	(+)	Mdh
Mdh	(+)	PdxS	pyridoxal-5'-phosphate synthase	31,593.30	100.00%	11	40.50%	Mdh	(+)	PdxS
Mdh	(+)	Mdh	malate dehydrogenase	33,626.00	100.00%	10	41.70%	Mdh	(+)	Mdh
Mdh	(+)	Mdh	malate dehydrogenase	33,626.00	100.00%	10	48.40%	Mdh	(+)	Mdh
Mdh	(+)	Mdh	malate dehydrogenase	33,626.00	100.00%	10	46.80%	Mdh	(+)	Mdh
Mdh	(+)	AroA	3-deoxy-D-arabino-heptulosonate 7-phosphate synthase / chorismate mutase-isozyme 3	39,522.50	100.00%	10	31.60%	Mdh	(+)	AroA
Mdh	(+)	DapA	dihydrodipicolinate synthase	31,024.30	100.00%	10	53.80%	Mdh	(+)	DapA
Mdh	(+)	ThiG	hydroxyethylthiazole phosphate biosynthesis	27,005.20	100.00%	10	48.80%	Mdh	(+)	ThiG
Mdh	(+)	DegU	two-component response regulator involved in degradative enzyme and competence regulation	25,848.10	100.00%	10	46.30%	Mdh	(+)	DegU
Mdh	(+)	TenA	transcriptional regulator of extracellular enzyme genes	27,399.00	100.00%	10	40.70%	Mdh	(+)	TenA
Mdh	(+)	GndA	NADP-dependent phosphogluconate dehydrogenase	51,758.80	100.00%	10	26.20%	Mdh	(+)	GndA
Mdh	(+)	PckA	phosphoenolpyruvate carboxykinase	58,283.20	100.00%	9	20.70%	Mdh	(+)	PckA
Mdh	(+)	AtpA	ATP synthase (subunit alpha)	54,581.90	100.00%	9	20.30%	Mdh	(+)	AtpA
Mdh	(+)	SucC	succinyl-CoA synthetase (beta subunit)	41,354.40	100.00%	9	27.80%	Mdh	(+)	SucC
Mdh	(+)	Pgi	glucose-6-phosphate isomerase	50,510.80	100.00%	9	28.40%	Mdh	(+)	Pgi
Mdh	(+)	TufA	elongation factor Tu	43,574.90	100.00%	9	32.80%	Mdh	(+)	TufA
Mdh	(+)	Mdh	malate dehydrogenase	33,626.00	100.00%	9	40.70%	Mdh	(+)	Mdh
Mdh	(+)	FbaA	fructose-1,6-bisphosphate aldolase	30,382.30	100.00%	9	30.90%	Mdh	(+)	FbaA
Mdh	(+)	SerA	phosphoglycerate dehydrogenase	57,098.20	100.00%	8	17.90%	Mdh	(+)	SerA
Mdh	(+)	Zwf	probable glucose-6-phosphate 1-dehydrogenase	55,643.40	100.00%	8	25.80%	Mdh	(+)	Zwf
Mdh	(+)	Mdh	malate dehydrogenase	33,626.00	100.00%	8	33.30%	Mdh	(+)	Mdh
Mdh	(+)	SufC	ABC transporter (ATP-binding	29,014.30	100.00%	8	44.10%	Mdh	(+)	SufC

			protein), synthesis of Fe-S clusters							
Mdh	(+)	RpsB	ribosomal protein S2	27,950.20	100.00%	8	28.90%	Mdh	(+)	RpsB
Mdh	(+)	GuaA	GMP synthetase	57,934.60	100.00%	7	17.70%	Mdh	(+)	GuaA
Mdh	(+)	PurL	phosphoribosylformylglycinamidine synthetase II	80,273.60	100.00%	7	10.80%	Mdh	(+)	PurL
Mdh	(+)	YpwA	unknown; similar to carboxypeptidase	58,159.50	100.00%	7	16.40%	Mdh	(+)	YpwA
Mdh	(+)	LeuA	2-isopropylmalate synthase	56,894.60	100.00%	7	19.30%	Mdh	(+)	LeuA
Mdh	(+)	LutB	lactate oxidase	53,456.70	100.00%	7	16.70%	Mdh	(+)	LutB
Mdh	(+)	Ndh	NADH dehydrogenase	41,935.80	100.00%	7	22.70%	Mdh	(+)	Ndh
Mdh	(+)	Spo0M	sporulation-control gene	29,689.70	100.00%	7	27.90%	Mdh	(+)	Spo0M
Mdh	(+)	Mdh	malate dehydrogenase	33,626.00	100.00%	7	35.90%	Mdh	(+)	Mdh
Mdh	(+)	PepF	oligoendopeptidase	70,128.70	100.00%	6	13.30%	Mdh	(+)	PepF
Mdh	(+)	ArgS	arginyl-tRNA synthetase	62,707.30	100.00%	6	12.80%	Mdh	(+)	ArgS
Mdh	(+)	SufB	synthesis of Fe-S-clusters	52,712.80	100.00%	6	14.20%	Mdh	(+)	SufB
Mdh	(+)	GltB	glutamate synthase (small subunit)	54,931.00	100.00%	6	16.80%	Mdh	(+)	GltB
Mdh	(+)	IlvC	ketol-acid reductoisomerase	37,438.80	100.00%	6	25.10%	Mdh	(+)	IlvC
Mdh	(+)	Prs	phosphoribosylpyrophosphate synthetase	34,851.50	100.00%	6	24.90%	Mdh	(+)	Prs
Mdh	(+)	FabI	enoyl-acyl carrier protein reductase	27,856.50	100.00%	6	26.00%	Mdh	(+)	FabI
Mdh	(+)	GtaB	UTP-glucose-1-phosphate uridylyltransferase	33,053.30	100.00%	6	25.70%	Mdh	(+)	GtaB
Mdh	(+)	DnaK	class I heat-shock protein (molecular chaperone)	65,985.00	100.00%	5	9.66%	Mdh	(+)	DnaK
Mdh	(+)	GroEL	class I heat-shock protein (chaperonin)	57,406.30	100.00%	5	10.10%	Mdh	(+)	GroEL
Mdh	(+)	PdhC	pyruvate dehydrogenase (dihydrolipoamide acetyltransferase E2 subunit)	47,520.60	100.00%	5	13.80%	Mdh	(+)	PdhC
Mdh	(+)	SufD	synthesis of Fe-S-clusters	48,275.60	100.00%	5	10.80%	Mdh	(+)	SufD
Mdh	(+)	RnjA	RNase J1	61,500.70	100.00%	5	14.20%	Mdh	(+)	RnjA
Mdh	(+)	AccC	acetyl-CoA carboxylase (biotin carboxylase subunit)	49,560.30	100.00%	5	13.30%	Mdh	(+)	AccC
Mdh	(+)	OxdC	oxalate decarboxylase	43,548.50	100.00%	5	16.10%	Mdh	(+)	OxdC
Mdh	(+)	TufA	elongation factor Tu	43,574.90	100.00%	5	16.70%	Mdh	(+)	TufA
Mdh	(+)	TufA	elongation factor Tu	43,574.90	100.00%	5	16.90%	Mdh	(+)	TufA
Mdh	(+)	CshA	DEAD-box RNA helicase	57,262.10	100.00%	5	12.90%	Mdh	(+)	CshA
Mdh	(+)	SerS	seryl-tRNA synthetase	48,824.70	100.00%	5	14.40%	Mdh	(+)	SerS

Mdh	(+)	AhpF	alkyl hydroperoxide reductase (large subunit) / NADH dehydrogenase	54,856.40	100.00%	5	9.43%	Mdh	(+)	AhpF
Mdh	(+)	GatB	glutamyl-tRNA(Gln) amidotransferase (subunit B)	53,390.90	100.00%	5	12.60%	Mdh	(+)	GatB
Mdh	(+)	CitZ	citrate synthase II (major)	41,712.30	100.00%	5	17.70%	Mdh	(+)	CitZ
Mdh	(+)	GapA	glyceraldehyde-3-phosphate dehydrogenase	35,814.50	100.00%	5	18.20%	Mdh	(+)	GapA
Mdh	(+)	YumC	ferredoxin-NAD(P)+ oxidoreductase	36,823.20	100.00%	5	22.60%	Mdh	(+)	YumC
Mdh	(+)	Tsf	elongation factor Ts	32,336.00	100.00%	5	23.90%	Mdh	(+)	Tsf
Mdh	(+)	ThrB	homoserine kinase	33,306.70	100.00%	5	16.80%	Mdh	(+)	ThrB
Mdh	(+)	YkwC	putative beta-hydroxyacid dehydrogenase	30,694.60	100.00%	5	25.70%	Mdh	(+)	YkwC
Mdh	(+)	YwfI	unknown	29,488.30	100.00%	5	16.90%	Mdh	(+)	YwfI
Mdh	(+)	CitG	fumarate hydratase	50,514.70	100.00%	5	15.20%	Mdh	(+)	CitG
Mdh	(+)	RpsC	ribosomal protein S3 (BS3)	24,315.50	100.00%	5	22.00%	Mdh	(+)	RpsC
Mdh	(+)	CitB	aconitate hydratase	99,317.30	100.00%	4	4.40%	Mdh	(+)	CitB
Mdh	(+)	AlaS	alanyl-tRNA synthetase	97,262.10	100.00%	4	5.69%	Mdh	(+)	AlaS
Mdh	(+)	PdhD	pyruvate dehydrogenase / 2-oxoglutarate dehydrogenase (dihydrolipoamide dehydrogenase E3 subunit)	49,715.20	100.00%	4	9.36%	Mdh	(+)	PdhD
Mdh	(+)	GltX	glutamyl-tRNA synthetase	55,705.90	100.00%	4	11.00%	Mdh	(+)	GltX
Mdh	(+)	FabF	beta-ketoacyl-acyl carrier protein synthase II	43,987.60	100.00%	4	10.40%	Mdh	(+)	FabF
Mdh	(+)	BdhA	acetoine/ butanediol dehydrogenase	37,322.70	100.00%	4	16.80%	Mdh	(+)	BdhA
Mdh	(+)	AckA	acetate kinase	43,120.60	100.00%	4	15.90%	Mdh	(+)	AckA
Mdh	(+)	YcdA	unknown	39,163.60	100.00%	4	13.30%	Mdh	(+)	YcdA
Mdh	(+)	RpoA	RNA polymerase (alpha subunit)	34,782.20	100.00%	4	15.00%	Mdh	(+)	RpoA
Mdh	(+)	GltX	glutamyl-tRNA synthetase	55,705.90	100.00%	4	10.40%	Mdh	(+)	GltX
Mdh	(+)	OppA	oligopeptide ABC transporter (binding protein) (initiation of sporulation, competence development)	61,476.00	100.00%	4	9.36%	Mdh	(+)	OppA
Mdh	(+)	Hom	homoserine dehydrogenase	47,476.40	100.00%	4	10.40%	Mdh	(+)	Hom
Mdh	(+)	PncB	putative nicotinate phosphoribosyltransferase	56,163.90	100.00%	4	9.59%	Mdh	(+)	PncB
Mdh	(+)	HisC	histidinol-phosphate aminotransferase / tyrosine and	40,068.00	100.00%	4	11.10%	Mdh	(+)	HisC

			phenylalanine aminotransferase							
Mdh	(+)	PdhA	pyruvate dehydrogenase (E1 alpha subunit)	41,531.40	100.00%	4	11.90%	Mdh	(+)	PdhA
Mdh	(+)	NadC	nicotinate-nucleotide pyrophosphorylase	31,375.70	100.00%	4	15.60%	Mdh	(+)	NadC
Mdh	(+)	YqfA	resistence protein (against sublancin)	35,623.60	100.00%	4	17.50%	Mdh	(+)	YqfA
Mdh	(+)	SdhB	succinate dehydrogenase (iron-sulfur protein)	28,400.10	100.00%	4	19.00%	Mdh	(+)	SdhB
Mdh	(+)	YwfI	unknown	29,488.30	100.00%	4	12.60%	Mdh	(+)	YwfI
Mdh	(+)	RplA	ribosomal protein L1 (BL1)	24,904.40	100.00%	4	22.80%	Mdh	(+)	RplA
Mdh	(+)	Mdh	malate dehydrogenase	33,626.00	100.00%	4	14.40%	Mdh	(+)	Mdh
Mdh	(+)	YvgN	glyoxal reductase	31,645.80	100.00%	4	13.80%	Mdh	(+)	YvgN
Mdh	(+)	PyrR	transcriptional attenuation of the pyrimidine operon / uracil phosphoribosyltransferase activity	20,245.80	100.00%	4	26.00%	Mdh	(+)	PyrR
Mdh	(+)	TufA	elongation factor Tu	43,574.90	100.00%	3	10.90%	Mdh	(+)	TufA
Mdh	(+)	YwqJ	unknown	66,674.50	100.00%	3	5.48%	Mdh	(+)	YwqJ
Mdh	(+)	GndA	NADP-dependent phosphogluconate dehydrogenase	51,758.80	100.00%	3	6.61%	Mdh	(+)	GndA
Mdh	(+)	PckA	phosphoenolpyruvate carboxykinase	58,283.20	100.00%	3	9.68%	Mdh	(+)	PckA
Mdh	(+)	OpuAA	glycine betaine ABC transporter (ATP-binding protein)	46,422.00	100.00%	3	12.20%	Mdh	(+)	OpuAA
Mdh	(+)	FtsZ	cell-division initiation protein (septum formation)	40,337.30	100.00%	3	11.00%	Mdh	(+)	FtsZ
Mdh	(+)	YceH	unknown; similar to toxic anion resistance protein	41,656.80	100.00%	3	9.09%	Mdh	(+)	YceH
Mdh	(+)	PckA	phosphoenolpyruvate carboxykinase	58,283.20	100.00%	3	7.97%	Mdh	(+)	PckA
Mdh	(+)	PheS	phenylalanyl-tRNA synthetase (alpha subunit)	38,657.40	100.00%	3	10.80%	Mdh	(+)	PheS
Mdh	(+)	DnaK	class I heat-shock protein (molecular chaperone)	65,985.00	100.00%	3	5.73%	Mdh	(+)	DnaK
Mdh	(+)	ThiC	biosynthesis of the pyrimidine moiety of thiamin	65,899.90	100.00%	3	8.14%	Mdh	(+)	ThiC
Mdh	(+)	ProS	prolyl-tRNA synthetase	63,287.50	100.00%	3	5.85%	Mdh	(+)	ProS
Mdh	(+)	PnbA	para-nitrobenzyl esterase	53,969.70	100.00%	3	6.95%	Mdh	(+)	PnbA
Mdh	(+)	PurF	glutamine phosphoribosylpyrophosphate amidotransferase	51,602.10	100.00%	3	9.87%	Mdh	(+)	PurF
Mdh	(+)	TufA	elongation factor Tu	43,574.90	100.00%	3	12.40%	Mdh	(+)	TufA

Mdh	(+)	GcaD	UDP-N-acetylglucosamine pyrophosphorylase	49,435.50	100.00%	3	8.55%	Mdh	(+)	GcaD
Mdh	(+)	GatB	glutamyl-tRNA(Gln) amidotransferase (subunit B)	53,390.90	100.00%	3	6.30%	Mdh	(+)	GatB
Mdh	(+)	ClpY	two-component ATP-dependent protease [ClpQ]	52,569.20	100.00%	3	7.71%	Mdh	(+)	ClpY
Mdh	(+)	GatA	glutamyl-tRNA(Gln) amidotransferase (subunit A)	52,647.60	100.00%	3	8.87%	Mdh	(+)	GatA
Mdh	(+)	PyrAA	carbamoyl-phosphate synthetase (glutaminase subunit)	40,101.90	100.00%	3	7.97%	Mdh	(+)	PyrAA
Mdh	(+)	YugJ	unknown; similar to NADH-dependent butanol dehydrogenase	42,715.50	100.00%	3	11.10%	Mdh	(+)	YugJ
Mdh	(+)	IspG	unknown; similar to peptidoglycan acetylation	40,566.40	100.00%	3	8.75%	Mdh	(+)	IspG
Mdh	(+)	Dat	probable D-alanine aminotransferase	31,164.90	100.00%	3	10.60%	Mdh	(+)	Dat
Mdh	(+)	Pta	phosphotransacetylase	34,773.50	100.00%	3	10.80%	Mdh	(+)	Pta
Mdh	(+)	SucD	succinyl-CoA synthetase (alpha subunit)	31,363.60	100.00%	3	15.70%	Mdh	(+)	SucD
Mdh	(+)	MenB	dihydroxynapthoic acid synthetase	29,881.60	100.00%	3	14.00%	Mdh	(+)	MenB
Mdh	(+)	AccC	acetyl-CoA carboxylase (biotin carboxylase subunit)	49,560.30	100.00%	3	9.11%	Mdh	(+)	AccC
Mdh	(+)	GlmM	phosphoglucosamine mutase	48,415.70	100.00%	3	8.71%	Mdh	(+)	GlmM
Mdh	(+)	AroF	chorismate synthase	40,186.20	100.00%	3	11.90%	Mdh	(+)	AroF
Mdh	(+)	Sat	probable sulfate adenylyltransferase	42,866.10	100.00%	3	13.40%	Mdh	(+)	Sat
Mdh	(+)	AspB	aspartate aminotransferase	43,071.10	100.00%	3	10.90%	Mdh	(+)	AspB
Mdh	(+)	NadC	nicotinate-nucleotide pyrophosphorylase	31,375.70	100.00%	3	12.80%	Mdh	(+)	NadC
Mdh	(+)	YceE	unknown; similar to tellurium resistance protein	20,930.20	100.00%	3	18.80%	Mdh	(+)	YceE
Mdh	(+)	Rny	RNase Y	58,903.20	100.00%	3	4.62%	Mdh	(+)	Rny
Mdh	(+)	FusA	elongation factor G	76,527.20	99.80%	2	3.18%	Mdh	(+)	FusA
Mdh	(+)	OdhA	2-oxoglutarate dehydrogenase (E1 subunit)	105,724.10	99.80%	2	2.34%	Mdh	(+)	OdhA
Mdh	(+)	YetO	unknown; similar to cytochrome P450 / NADPH-cytochrome P450 reductase	119,453.30	99.60%	2	1.79%	Mdh	(+)	YetO

Mdh	(+)	SrfAA	surfactin synthetase / competence	402,063.70	99.90%	2	0.84%	Mdh	(+)	SrfAA
Mdh	(+)	YoaC	unknown; similar to xylulokinase	54,092.20	99.80%	2	6.37%	Mdh	(+)	YoaC
Mdh	(+)	PksL	polyketide synthase	506,300.20	99.80%	2	1.01%	Mdh	(+)	PksL
Mdh	(+)	FtsH	cell-division protein / general stress protein (class III heat-shock)	70,920.80	99.80%	2	3.61%	Mdh	(+)	FtsH
Mdh	(+)	NadC	nicotinate-nucleotide pyrophosphorylase	31,375.70	99.80%	2	5.88%	Mdh	(+)	NadC
Mdh	(+)	SbcC	DNA exonuclease	128,902.70	99.50%	2	2.65%	Mdh	(+)	SbcC
Mdh	(+)	Sul	dihydropteroate synthase	30,984.10	99.80%	2	11.60%	Mdh	(+)	Sul
Mdh	(+)	YoaC	unknown; similar to xylulokinase	54,092.20	99.80%	2	6.37%	Mdh	(+)	YoaC
Mdh	(+)	YerA	unknown; similar to adenine deaminase	66,630.20	99.80%	2	5.00%	Mdh	(+)	YerA
Mdh	(+)	YoaH	unknown; similar to methyl-accepting chemotaxis protein	58,230.70	99.80%	2	5.06%	Mdh	(+)	YoaH
Mdh	(+)	GlmS	L-glutamine-D-fructose-6-phosphate amidotransferase	65,320.20	100.00%	2	4.67%	Mdh	(+)	GlmS
Mdh	(+)	YmcB	unknown	58,153.30	99.80%	2	4.13%	Mdh	(+)	YmcB
Mdh	(+)	FusA	elongation factor G	76,527.20	99.60%	2	2.89%	Mdh	(+)	FusA
Mdh	(+)	Bpr	bacillopeptidase F	154,562.00	99.60%	2	1.19%	Mdh	(+)	Bpr
Mdh	(+)	ProA	gamma-glutamyl phosphate reductase	45,319.60	99.80%	2	5.30%	Mdh	(+)	ProA
Mdh	(+)	YlmB	amidohydrolase; thiamine salvage	47,164.10	99.80%	2	5.40%	Mdh	(+)	YlmB
Mdh	(+)	YncD	alanine racemase	43,630.90	99.80%	2	8.88%	Mdh	(+)	YncD
Mdh	(+)	SerA	phosphoglycerate dehydrogenase	57,098.20	99.80%	2	5.52%	Mdh	(+)	SerA
Mdh	(+)	YutJ	putative NADH dehydrogenase	36,890.50	99.80%	2	6.97%	Mdh	(+)	YutJ
Mdh	(+)	YoaC	unknown; similar to xylulokinase	54,092.20	99.80%	2	6.37%	Mdh	(+)	YoaC
Mdh	(+)	YpgR	unknown; similar to unknown proteins	42,550.90	99.80%	2	5.84%	Mdh	(+)	YpgR
Mdh	(+)	AspB	aspartate aminotransferase	43,071.10	99.70%	2	5.85%	Mdh	(+)	AspB
Mdh	(+)	SpsJ	spore coat polysaccharide synthesis	35,522.70	99.60%	2	9.21%	Mdh	(+)	SpsJ
Mdh	(+)	Asd	aspartate-semialdehyde dehydrogenase	37,829.10	99.80%	2	12.70%	Mdh	(+)	Asd
Mdh	(+)	MetE	cobalamin-independent methionine synthase	86,812.60	99.80%	2	5.12%	Mdh	(+)	MetE
Mdh	(+)	FusA	elongation factor G	76,527.20	99.80%	2	2.60%	Mdh	(+)	FusA
Mdh	(+)	PdhD	pyruvate dehydrogenase / 2-oxoglutarate dehydrogenase (dihydrolipoamide	49,715.20	99.80%	2	5.32%	Mdh	(+)	PdhD

			dehydrogenase E3 subunit)							
Mdh	(+)	LeuA	2-isopropylmalate synthase	56,894.60	99.80%	2	4.44%	Mdh	(+)	LeuA
Mdh	(+)	DhaS	aldehyde dehydrogenase	53,865.10	99.80%	2	6.26%	Mdh	(+)	DhaS
Mdh	(+)	CysS	cysteinyl-tRNA synthetase	53,891.20	99.80%	2	5.36%	Mdh	(+)	CysS
Mdh	(+)	Rho	transcriptional terminator Rho	48,661.50	99.80%	2	6.56%	Mdh	(+)	Rho
Mdh	(+)	YfmG	unknown	56,526.30	99.80%	2	5.34%	Mdh	(+)	YfmG
Mdh	(+)	ClpY	two-component ATP-dependent protease [ClpQ]	52,569.20	99.80%	2	6.21%	Mdh	(+)	ClpY
Mdh	(+)	Tpx	probable thiol peroxidase	18,197.70	99.70%	2	11.40%	Mdh	(+)	Tpx
Mdh	(+)	TufA	elongation factor Tu	43,574.90	99.80%	2	8.84%	Mdh	(+)	TufA
Mdh	(+)	AroA	3-deoxy-D-arabino-heptulosonate 7-phosphate synthase / chorismate mutase-isozyme 3	39,522.50	99.80%	2	4.75%	Mdh	(+)	AroA
Mdh	(+)	YqjE	unknown; similar to tripeptidase	39,639.60	99.80%	2	6.47%	Mdh	(+)	YqjE
Mdh	(+)	GapB	glyceraldehyde-3-phosphate dehydrogenase	37,458.00	99.80%	2	3.82%	Mdh	(+)	GapB
Mdh	(+)	MetI	O-succinylhomoserine lyase	41,688.50	99.80%	2	9.12%	Mdh	(+)	MetI
Mdh	(+)	YomI	unknown; similar to lytic transglycosylase	252,302.70	99.60%	2	1.58%	Mdh	(+)	YomI
Mdh	(+)	YvrO	unknown; similar to amino acid ABC transporter (ATP-binding protein)	25,461.00	99.80%	2	6.11%	Mdh	(+)	YvrO
Mdh	(+)	SerC	phosphoserine aminotransferase	40,118.60	99.80%	2	12.30%	Mdh	(+)	SerC
Mdh	(+)	TrxB	thioredoxin reductase	34,501.60	99.80%	2	6.65%	Mdh	(+)	TrxB
Mdh	(+)	Era	GTP-binding protein	34,057.70	99.80%	2	6.64%	Mdh	(+)	Era
Mdh	(+)	PspA	phage shock protein A homolog	25,124.50	99.80%	2	12.30%	Mdh	(+)	PspA
Mdh	(+)	PpsC	plipastatin synthetase	287,490.70	99.80%	2	0.94%	Mdh	(+)	PpsC
Mdh	(+)	FtsE	cell-division ATP-binding protein	25,601.80	99.80%	2	8.33%	Mdh	(+)	FtsE
Mdh	(+)	CysH	phosphoadenosine phosphosulfate	26,957.40	99.80%	2	7.30%	Mdh	(+)	CysH
Mdh	(+)	PurQ	phosphoribosylformylglycinamidine synthetase I	24,766.30	100.00%	2	9.69%	Mdh	(+)	PurQ
Mdh	(+)	TufA	elongation factor Tu	43,574.90	99.90%	2	8.84%	Mdh	(+)	TufA
Mdh	(+)	LexA	transcriptional repressor of the SOS regulon	22,831.50	99.80%	2	21.00%	Mdh	(+)	LexA
Mdh	(+)	GlnA	glutamine synthetase	50,261.70	99.80%	2	4.95%	Mdh	(+)	GlnA
Mdh	(+)	FabF	beta-ketoacyl-acyl carrier protein synthase II	43,987.60	99.80%	2	4.36%	Mdh	(+)	FabF
Mdh	(+)	MurD	UDP-N-acetylmuramoylalanyl-D-glutamate	49,633.50	99.80%	2	5.10%	Mdh	(+)	MurD

			ligase							
Mdh	(+)	MetK	S-adenosylmethionine synthetase	44,025.70	99.80%	2	6.50%	Mdh	(+)	MetK
Mdh	(+)	PurB	adenylosuccinate lyase	49,468.10	100.00%	2	4.64%	Mdh	(+)	PurB
Mdh	(+)	AroE	5-enolpyruvoylshikimate-3-phosphate synthase	45,223.50	99.80%	2	6.31%	Mdh	(+)	AroE
Mdh	(+)	TufA	elongation factor Tu	43,574.90	99.80%	2	8.33%	Mdh	(+)	TufA
Mdh	(+)	HisA	phosphoribosylformimino-5-aminoimidazole carboxamide ribotide isomerase	26,511.70	99.80%	2	13.10%	Mdh	(+)	HisA
Mdh	(+)	FabL	enoyl-acyl carrier protein reductase	27,160.60	99.80%	2	8.40%	Mdh	(+)	FabL
Mdh	(+)	YybJ	unknown; similar to ABC transporter (ATP-binding protein)	24,256.20	99.80%	2	10.60%	Mdh	(+)	YybJ

Bait[1]	**CL**[2]	**Protein**[3,4]	**Protein name**	**MW**[7] **(Da)**	**Protein prob.**[8]	**peptides**[9]	**SC**[10]	**Bait**[1]	**CL**[2]	**Protein**[3,4]
CitZ	(+)	MetE	cobalamin-independent methionine synthase	86,812.60	100.00%	36	47.00%	CitZ	(+)	MetE
CitZ	(+)	TufA	elongation factor Tu	43,574.90	100.00%	22	56.10%	CitZ	(+)	TufA
CitZ	(-)	CitZ	citrate synthase II (major)	41,712.30	100.00%	21	48.90%	CitZ	(-)	CitZ
CitZ	(-)	CitZ	citrate synthase II (major)	41,712.30	100.00%	20	50.30%	CitZ	(-)	CitZ
CitZ	(-)	CitZ	citrate synthase II (major)	41,712.30	100.00%	18	47.60%	CitZ	(-)	CitZ
CitZ	(+)	CitZ	citrate synthase II (major)	41,712.30	100.00%	17	46.50%	CitZ	(+)	CitZ
CitZ	(+)	FusA	elongation factor G	76,527.20	100.00%	16	29.80%	CitZ	(+)	FusA
CitZ	(+)	Icd	isocitrate dehydrogenase	46,401.00	100.00%	16	46.30%	CitZ	(+)	Icd
CitZ	(-)	CitZ	citrate synthase II (major)	41,712.30	100.00%	16	35.80%	CitZ	(-)	CitZ
CitZ	(+)	PurL	phosphoribosylformylglycinamidine synthetase II	80,273.60	100.00%	15	28.20%	CitZ	(+)	PurL
CitZ	(+)	CitZ	citrate synthase II (major)	41,712.30	100.00%	14	41.10%	CitZ	(+)	CitZ
CitZ	(+)	FusA	elongation factor G	76,527.20	100.00%	13	23.60%	CitZ	(+)	FusA
CitZ	(-)	YqfA	resistence protein	35,623.60	100.00%	13	48.00%	CitZ	(-)	YqfA
CitZ	(-)	CitZ	citrate synthase II (major)	41,712.30	100.00%	13	34.70%	CitZ	(-)	CitZ
CitZ	(+)	CitZ	citrate synthase II (major)	41,712.30	100.00%	12	40.10%	CitZ	(+)	CitZ
CitZ	(+)	SecA	preprotein translocase subunit (ATPase)	95,514.70	100.00%	10	13.40%	CitZ	(+)	SecA
CitZ	(+)	SrfAB	surfactin synthetase / competence	401,240.30	100.00%	10	3.40%	CitZ	(+)	SrfAB
CitZ	(-)	Tsf	elongation factor Ts	32,336.00	100.00%	10	39.90%	CitZ	(-)	Tsf
CitZ	(-)	CitZ	citrate synthase II (major)	41,712.30	100.00%	10	22.60%	CitZ	(-)	CitZ
CitZ	(-)	CitZ	citrate synthase II	41,712.30	100.00%	10	27.40%	CitZ	(-)	CitZ

			(major)							
CitZ	(-)	CitZ	citrate synthase II (major)	41,712.30	100.00%	10	21.80%	CitZ	(-)	CitZ
CitZ	(+)	PurB	adenylosuccinate lyase	49,468.10	100.00%	9	21.30%	CitZ	(+)	PurB
CitZ	(-)	FbaA	fructose-1,6-bisphosphate aldolase	30,382.30	100.00%	9	33.00%	CitZ	(-)	FbaA
CitZ	(-)	CitZ	citrate synthase II (major)	41,712.30	100.00%	9	23.10%	CitZ	(-)	CitZ
CitZ	(+)	TufA	elongation factor Tu	43,574.90	100.00%	8	25.00%	CitZ	(+)	TufA
CitZ	(-)	YxeB	hydroxamate siderophore ABC transporter	35,233.40	100.00%	8	36.70%	CitZ	(-)	YxeB
CitZ	(-)	AtpF	ATP synthase (subunit b)	19,191.10	100.00%	8	37.10%	CitZ	(-)	AtpF
CitZ	(-)	CitZ	citrate synthase II (major)	41,712.30	100.00%	8	14.20%	CitZ	(-)	CitZ
CitZ	(+)	GyrA	DNA gyrase (subunit A)	92,084.10	100.00%	7	9.62%	CitZ	(+)	GyrA
CitZ	(+)	BdhA	acetoine/ butanediol dehydrogenase	37,322.70	100.00%	7	31.50%	CitZ	(+)	BdhA
CitZ	(+)	RpoA	RNA polymerase (alpha subunit)	34,782.20	100.00%	7	25.20%	CitZ	(+)	RpoA
CitZ	(-)	RplJ	ribosomal protein L10 (BL5)	18,010.70	100.00%	7	30.70%	CitZ	(-)	RplJ
CitZ	(-)	MetQ	methionine ABC transporter	30,338.60	100.00%	6	22.30%	CitZ	(-)	MetQ
CitZ	(+)	Eno	enolase	46,564.30	100.00%	6	28.80%	CitZ	(+)	Eno
CitZ	(+)	DhbC	isochorismate synthase	43,427.80	100.00%	6	19.80%	CitZ	(+)	DhbC
CitZ	(+)	TufA	elongation factor Tu	43,574.90	100.00%	6	23.20%	CitZ	(+)	TufA
CitZ	(-)	YjlC	unknown	15,564.90	100.00%	6	51.40%	CitZ	(-)	YjlC
CitZ	(+)	MetE	cobalamin-independent methionine synthase	86,812.60	100.00%	5	8.01%	CitZ	(+)	MetE
CitZ	(+)	Pgk	phosphoglycerate kinase	42,173.30	100.00%	5	18.00%	CitZ	(+)	Pgk
CitZ	(-)	PdxS	pyridoxal-5'-phosphate synthase	31,593.30	100.00%	5	17.00%	CitZ	(-)	PdxS
CitZ	(-)	CitZ	citrate synthase II (major)	41,712.30	100.00%	5	13.20%	CitZ	(-)	CitZ
CitZ	(-)	TufA	elongation factor Tu	43,574.90	100.00%	5	18.40%	CitZ	(-)	TufA
CitZ	(+)	InfB	initiation factor IF-2	78,519.30	100.00%	4	7.40%	CitZ	(+)	InfB
CitZ	(-)	PurC	phosphoribosylaminoimidazole succinocarboxamide synthetase	27,443.50	100.00%	4	19.10%	CitZ	(-)	PurC
CitZ	(-)	YybJ	unknown; similar to ABC transporter (ATP-binding protein)	24,256.20	100.00%	4	22.00%	CitZ	(-)	YybJ
CitZ	(+)	CitZ	citrate synthase II (major)	41,712.30	100.00%	4	11.80%	CitZ	(+)	CitZ
CitZ	(+)	GndA	NADP-dependent phosphogluconate dehydrogenase	51,758.80	100.00%	4	9.81%	CitZ	(+)	GndA
CitZ	(+)	RecA	multifunctional protein involved in homologous recombination and DNA repair (LexA-autocleavage)	38,072.80	100.00%	4	13.80%	CitZ	(+)	RecA

CitZ	(+)	GapA	glyceraldehyde-3-phosphate dehydrogenase	35,814.50	100.00%	4	14.60%	CitZ	(+)	GapA
CitZ	(+)	FtsZ	cell-division initiation protein (septum formation)	40,337.30	100.00%	4	18.10%	CitZ	(+)	FtsZ
CitZ	(+)	AspB	aspartate aminotransferase	43,071.10	100.00%	4	13.00%	CitZ	(+)	AspB
CitZ	(+)	AroF	chorismate synthase	40,186.20	100.00%	4	13.60%	CitZ	(+)	AroF
CitZ	(+)	YtsJ	NAD-dependent malate dehydrogenase	43,649.20	100.00%	4	13.20%	CitZ	(+)	YtsJ
CitZ	(-)	CitZ	citrate synthase II (major)	41,712.30	100.00%	4	11.80%	CitZ	(-)	CitZ
CitZ	(-)	RpsJ	ribosomal protein S10 (BS13)	11,648.20	100.00%	4	46.10%	CitZ	(-)	RpsJ
CitZ	(-)	MetQ	methionine ABC transporter	30,338.60	100.00%	3	11.30%	CitZ	(-)	MetQ
CitZ	(-)	OpuAC	glycine betaine ABC transporter (glycine betaine-binding protein)	32,198.20	100.00%	3	11.30%	CitZ	(-)	OpuAC
CitZ	(-)	RplA	ribosomal protein L1 (BL1)	24,904.40	100.00%	3	15.90%	CitZ	(-)	RplA
CitZ	(-)	SdhB	succinate dehydrogenase (iron-sulfur protein)	28,400.10	100.00%	3	13.80%	CitZ	(-)	SdhB
CitZ	(-)	FabI	enoyl-acyl carrier protein reductase	27,856.50	100.00%	3	14.00%	CitZ	(-)	FabI
CitZ	(-)	ThiG	hydroxyethylthiazole phosphate biosynthesis	27,005.20	100.00%	3	18.00%	CitZ	(-)	ThiG
CitZ	(-)	RpsC	ribosomal protein S3 (BS3)	24,315.50	100.00%	3	14.20%	CitZ	(-)	RpsC
CitZ	(+)	PpsB	plipastatin synthetase	290,153.30	100.00%	3	2.38%	CitZ	(+)	PpsB
CitZ	(+)	PksM	polyketide synthase	475,746.30	100.00%	3	0.73%	CitZ	(+)	PksM
CitZ	(+)	Alr	D-alanine racemase	43,248.30	100.00%	3	16.50%	CitZ	(+)	Alr
CitZ	(-)	SucD	succinyl-CoA synthetase (alpha subunit)	31,363.60	100.00%	3	15.70%	CitZ	(-)	SucD
CitZ	(-)	RpsE	ribosomal protein S5	17,604.80	100.00%	3	13.30%	CitZ	(-)	RpsE
CitZ	(-)	YqbO	unknown; similar to phage-related protein	171,017.30	100.00%	3	2.71%	CitZ	(-)	YqbO
CitZ	(-)	RplK	ribosomal protein L11 (BL11)	14,899.40	100.00%	3	20.60%	CitZ	(-)	RplK
CitZ	(-)	RpsK	ribosomal protein S11 (BS11)	13,907.10	100.00%	3	22.10%	CitZ	(-)	RpsK
CitZ	(+)	YobI	unknown	140,614.20	99.50%	2	1.50%	CitZ	(+)	YobI
CitZ	(+)	PpsA	plipastatin synthetase	289,173.30	99.80%	2	0.94%	CitZ	(+)	PpsA
CitZ	(+)	SacA	sucrase-6-phosphate hydrolase	54,871.00	99.80%	2	8.33%	CitZ	(+)	SacA
CitZ	(+)	YoaC	unknown; similar to xylulokinase	54,092.20	99.80%	2	6.37%	CitZ	(+)	YoaC
CitZ	(+)	GapA	glyceraldehyde-3-phosphate dehydrogenase	35,814.50	99.80%	2	8.66%	CitZ	(+)	GapA
CitZ	(+)	FolD	methylenetetrahydrofolate dehydrogenase / methenyltetrahydrofolate	30,667.50	99.80%	2	8.83%	CitZ	(+)	FolD

			cyclohydrolase							
CitZ	(+)	Spo0F	two-component response regulator involved in the initiation of sporulation	14,210.70	99.80%	2	17.70%	CitZ	(+)	Spo0F
CitZ	(+)	CheA	two-component sensor histidine kinase chemotactic signal modulator	74,751.40	99.80%	2	3.87%	CitZ	(+)	CheA
CitZ	(+)	YxnA	general stress protein	39,340.20	99.80%	2	9.55%	CitZ	(+)	YxnA
CitZ	(+)	PrkA	serine protein kinase	72,873.60	99.80%	2	5.07%	CitZ	(+)	PrkA
CitZ	(+)	YoaC	unknown; similar to xylulokinase	54,092.20	99.80%	2	6.37%	CitZ	(+)	YoaC
CitZ	(+)	PksL	polyketide synthase	506,300.20	99.90%	2	0.46%	CitZ	(+)	PksL
CitZ	(+)	YqbO	unknown; similar to phage-related protein	171,017.30	99.90%	2	1.96%	CitZ	(+)	YqbO
CitZ	(+)	RocB	involved in arginine and ornithine utilization	64,893.50	99.80%	2	5.30%	CitZ	(+)	RocB
CitZ	(+)	GltA	glutamate synthase (large subunit)	168,842.80	99.70%	2	1.18%	CitZ	(+)	GltA
CitZ	(+)	YcgN	1-pyrroline-5-carboxylate dehydrogenase	56,470.70	99.80%	2	5.24%	CitZ	(+)	YcgN
CitZ	(+)	PurL	phosphoribosylformylglycinamidine synthetase II	80,273.60	99.80%	2	3.50%	CitZ	(+)	PurL
CitZ	(+)	PpsD	plipastatin synthetase	406,795.60	99.90%	2	1.00%	CitZ	(+)	PpsD
CitZ	(+)	UxaC	glucuronate isomerase	54,596.30	99.80%	2	5.50%	CitZ	(+)	UxaC
CitZ	(-)	OpuBC	choline ABC transporter (choline-binding protein)	34,384.30	99.80%	2	6.54%	CitZ	(-)	OpuBC
CitZ	(-)	YwfH	unknown; similar to 3-oxoacyl- acyl-carrier protein reductase	28,005.00	99.80%	2	7.34%	CitZ	(-)	YwfH
CitZ	(-)	YqfL	Modulator of CcpN activity	30,332.00	99.80%	2	11.10%	CitZ	(-)	YqfL
CitZ	(-)	YaaO	putative lysine decarboxylase	53,147.00	99.80%	2	5.21%	CitZ	(-)	YaaO
CitZ	(-)	SpoVK	disruption leads to the production of immature spores	36,661.10	99.80%	2	11.80%	CitZ	(-)	SpoVK
CitZ	(-)	YhaP	unknown	45,413.30	99.80%	2	5.25%	CitZ	(-)	YhaP
CitZ	(-)	PurQ	phosphoribosylformylglycinamidine synthetase I	24,766.30	99.70%	2	9.69%	CitZ	(-)	PurQ
CitZ	(-)	YufO	unknown; similar to ABC transporter (ATP-binding protein)	56,284.10	99.50%	2	7.06%	CitZ	(-)	YufO
CitZ	(-)	PksL	polyketide synthase	506,300.20	99.90%	2	0.66%	CitZ	(-)	PksL
CitZ	(-)	PksJ	polyketide synthase	563,012.00	99.80%	2	0.50%	CitZ	(-)	PksJ
CitZ	(-)	YmcB	unknown	58,153.30	99.80%	2	6.29%	CitZ	(-)	YmcB
CitZ	(-)	Smc	chromosome condensation and segregation SMC	135,497.20	99.50%	2	1.77%	CitZ	(-)	Smc

			protein							
CitZ	(-)	YoaC	unknown; similar to xylulokinase	54,092.20	99.80%	2	6.37%	CitZ	(-)	YoaC
CitZ	(-)	PbpD	penicillin-binding protein 4	70,610.50	99.80%	2	3.85%	CitZ	(-)	PbpD
CitZ	(-)	YomG	unknown	98,872.10	99.80%	2	3.77%	CitZ	(-)	YomG
CitZ	(-)	RpsD	ribosomal protein S4 (BS4)	22,818.10	99.80%	2	9.00%	CitZ	(-)	RpsD
CitZ	(-)	YonS	unknown	22,235.80	99.80%	2	10.80%	CitZ	(-)	YonS
CitZ	(-)	YokF	unknown; similar to micrococcal nuclease	32,985.20	99.60%	2	6.76%	CitZ	(-)	YokF
CitZ	(-)	GuaB	inosine-monophosphate dehydrogenase	52,973.30	99.90%	2	6.35%	CitZ	(-)	GuaB
CitZ	(-)	PyrR	transcriptional attenuation of the pyrimidine operon / uracil phosphoribosyltransferase activity	20,245.80	99.90%	2	13.30%	CitZ	(-)	PyrR
CitZ	(-)	SpoIVCA	site-specific DNA recombinase required for creating the sigK gene (excision of the skin element)	57,467.10	99.60%	2	7.40%	CitZ	(-)	SpoIVCA
CitZ	(-)	YwqJ	unknown	66,674.50	99.60%	2	2.66%	CitZ	(-)	YwqJ
CitZ	(-)	PbpD	penicillin-binding protein 4	70,610.50	99.80%	2	3.85%	CitZ	(-)	PbpD
CitZ	(-)	SpoVK	disruption leads to the production of immature spores	36,661.10	99.80%	2	11.80%	CitZ	(-)	SpoVK
CitZ	(-)	DivIC	cell-division initiation protein (septum formation)	14,703.60	99.80%	2	21.60%	CitZ	(-)	DivIC
CitZ	(-)	YxkC	unknown	22,938.50	99.80%	2	9.86%	CitZ	(-)	YxkC
CitZ	(+)	YyaF	unknown; similar to GTP-binding protein	40,051.00	99.90%	2	7.10%	CitZ	(+)	YyaF
CitZ	(+)	YetM	FAD-dependent monooxygenase	40,960.00	99.80%	2	11.40%	CitZ	(+)	YetM
CitZ	(+)	PksN	polyketide synthase	609,580.70	99.90%	2	0.44%	CitZ	(+)	PksN
CitZ	(+)	AddB	ATP-dependent deoxyribonuclease (subunit B)	134,619.20	99.80%	2	2.14%	CitZ	(+)	AddB
CitZ	(+)	YlnE	probably siroheme ferrochelatase	28,816.90	99.60%	2	16.10%	CitZ	(+)	YlnE
CitZ	(+)	YkgB	unknown	38,392.10	99.80%	2	4.87%	CitZ	(+)	YkgB
CitZ	(+)	MtnW	2,3-diketo-5-methylthiopentyl-1-phosphate enolase	45,032.50	99.80%	2	4.83%	CitZ	(+)	MtnW
CitZ	(+)	PpsD	plipastatin synthetase	406,795.60	99.80%	2	0.92%	CitZ	(+)	PpsD
CitZ	(+)	Asd	aspartate-semialdehyde dehydrogenase	37,829.10	99.80%	2	7.80%	CitZ	(+)	Asd
CitZ	(+)	PriA	primosomal replication factor Y	91,337.20	99.70%	2	3.60%	CitZ	(+)	PriA
CitZ	(+)	CoaX	pantothenate kinase	26,200.10	99.70%	2	8.58%	CitZ	(+)	CoaX
CitZ	(-)	PrfB	peptide chain release factor 2	42,056.20	99.80%	2	9.29%	CitZ	(-)	PrfB
CitZ	(-)	NadC	nicotinate-nucleotide	31,375.70	99.80%	2	5.88%	CitZ	(-)	NadC

			pyrophosphorylase							
CitZ	(-)	PyrK	dihydroorotate dehydrogenase (electron transfer subunit)	28,081.10	99.80%	2	16.40%	CitZ	(-)	PyrK
CitZ	(-)	HemN	coproporphyrinogen III oxidase	41,545.40	99.80%	2	10.10%	CitZ	(-)	HemN
CitZ	(-)	YqbO	unknown; similar to phage-related protein	171,017.30	99.90%	2	1.96%	CitZ	(-)	YqbO
CitZ	(-)	ArgD	N-acetylornithine aminotransferase	40,876.40	99.50%	2	7.27%	CitZ	(-)	ArgD
CitZ	(-)	XkdO	PBSX prophage	145,135.90	99.80%	2	2.78%	CitZ	(-)	XkdO
CitZ	(-)	RpoC	RNA polymerase (beta' subunit)	134,125.20	99.80%	2	2.34%	CitZ	(-)	RpoC
CitZ	(-)	YonE	unknown	57,800.00	99.70%	2	5.53%	CitZ	(-)	YonE
CitZ	(-)	SdpA	unknown	18,633.70	99.80%	2	15.20%	CitZ	(-)	SdpA
CitZ	(-)	DivIVA	cell-division initiation protein (septum placement)	19,323.60	99.80%	2	13.40%	CitZ	(-)	DivIVA
CitZ	(-)	YhcR	extracellular non-specific endonuclease	132,671.40	99.60%	2	3.04%	CitZ	(-)	YhcR
CitZ	(-)	YwpB	unknown; similar to hydroxymyristoyl-(acyl carrier protein) dehydratase	14,750.30	99.80%	2	12.90%	CitZ	(-)	YwpB
CitZ	(-)	RplM	ribosomal protein L13	16,274.50	99.80%	2	15.20%	CitZ	(-)	RplM
CitZ	(-)	TagO	teichoic acid linkage unit synthesis	39,348.00	99.80%	2	8.10%	CitZ	(-)	TagO
CitZ	(-)	Tpx	probable thiol peroxidase	18,197.70	99.80%	2	11.40%	CitZ	(-)	Tpx
CitZ	(-)	YaaO	putative lysine decarboxylase	53,147.00	99.60%	2	5.21%	CitZ	(-)	YaaO
CitZ	(-)	SpoIVA	required for proper spore cortex formation and coat assembly	55,157.70	99.80%	2	7.72%	CitZ	(-)	SpoIVA
CitZ	(-)	YtdP	unknown; similar to transcriptional regulator (AraC/XylS family)	89,531.30	99.80%	2	4.79%	CitZ	(-)	YtdP
CitZ	(-)	SrfAB	surfactin synthetase / competence	401,240.30	99.80%	2	0.73%	CitZ	(-)	SrfAB
CitZ	(-)	YflB	unknown	10,007.50	99.80%	2	32.60%	CitZ	(-)	YflB

Bait[1]	**CL[2]**	**Protein[3,4]**	**Protein name**	**MW[7] (Da)**	**Protein prob.[8]**	**peptides[9]**	**SC[10]**	**Bait[1]**	**CL[2]**	**Protein[3,4]**
Icd	(+)	Icd	isocitrate dehydrogenase	46,401.00	100.00%	36	66.40%	Icd	(+)	Icd
Icd	(+)	FusA	elongation factor G	76,527.20	100.00%	35	55.60%	Icd	(+)	FusA
Icd	(-)	Icd	isocitrate dehydrogenase	46,401.00	100.00%	31	63.80%	Icd	(-)	Icd
Icd	(-)	Icd	isocitrate dehydrogenase	46,401.00	100.00%	30	65.20%	Icd	(-)	Icd
Icd	(+)	Icd	isocitrate dehydrogenase	46,401.00	100.00%	29	63.80%	Icd	(+)	Icd
Icd	(-)	Icd	isocitrate dehydrogenase	46,401.00	100.00%	27	63.40%	Icd	(-)	Icd
Icd	(-)	Icd	isocitrate dehydrogenase	46,401.00	100.00%	22	51.50%	Icd	(-)	Icd
Icd	(+)	Icd	isocitrate	46,401.00	100.00%	16	39.70%	Icd	(+)	Icd

			dehydrogenase							
Icd	(-)	Icd	isocitrate dehydrogenase	46,401.00	100.00%	15	40.00%	Icd	(-)	Icd
Icd	(+)	SucC	succinyl-CoA synthetase (beta subunit)	41,354.40	100.00%	14	39.20%	Icd	(+)	SucC
Icd	(+)	MetE	cobalamin-independent methionine synthase	86,812.60	100.00%	13	21.50%	Icd	(+)	MetE
Icd	(-)	RpsB	ribosomal protein S2	27,950.20	100.00%	13	48.40%	Icd	(-)	RpsB
Icd	(-)	DegU	two-component response regulator involved in degradative enzyme and competence regulation	25,848.10	100.00%	13	62.90%	Icd	(-)	DegU
Icd	(+)	Icd	isocitrate dehydrogenase	46,401.00	100.00%	12	31.70%	Icd	(+)	Icd
Icd	(+)	Icd	isocitrate dehydrogenase	46,401.00	100.00%	11	28.80%	Icd	(+)	Icd
Icd	(+)	PurL	phosphoribosylformylglycinamidine synthetase II	80,273.60	100.00%	10	16.40%	Icd	(+)	PurL
Icd	(+)	TufA	elongation factor Tu	43,574.90	100.00%	8	26.30%	Icd	(+)	TufA
Icd	(+)	CitZ	citrate synthase II (major)	41,712.30	100.00%	8	27.40%	Icd	(+)	CitZ
Icd	(+)	PdhA	pyruvate dehydrogenase (E1 alpha subunit)	41,531.40	100.00%	8	22.90%	Icd	(+)	PdhA
Icd	(+)	AroA	3-deoxy-D-arabino-heptulosonate 7-phosphate synthase / chorismate mutase-isozyme 3	39,522.50	100.00%	7	16.80%	Icd	(+)	AroA
Icd	(+)	InfB	initiation factor IF-2	78,519.30	100.00%	6	7.96%	Icd	(+)	InfB
Icd	(+)	IlvC	ketol-acid reductoisomerase	37,438.80	100.00%	5	25.40%	Icd	(+)	IlvC
Icd	(+)	Ndh	NADH dehydrogenase	41,935.80	100.00%	5	16.10%	Icd	(+)	Ndh
Icd	(+)	RpoC	RNA polymerase (beta' subunit)	134,125.20	100.00%	5	5.25%	Icd	(+)	RpoC
Icd	(+)	YumC	unknown; similar to thioredoxin reductase	36,823.20	100.00%	5	22.30%	Icd	(+)	YumC
Icd	(-)	GtaB	UTP-glucose-1-phosphate uridylyltransferase	33,053.30	100.00%	5	19.20%	Icd	(-)	GtaB
Icd	(+)	Icd	isocitrate dehydrogenase	46,401.00	100.00%	4	8.75%	Icd	(+)	Icd
Icd	(+)	SecA	preprotein translocase subunit (ATPase)	95,514.70	100.00%	4	5.11%	Icd	(+)	SecA
Icd	(+)	SalA	MRP family regulator	38,620.90	100.00%	4	16.80%	Icd	(+)	SalA
Icd	(+)	TufA	elongation factor Tu	43,574.90	100.00%	3	10.90%	Icd	(+)	TufA
Icd	(+)	GapB	glyceraldehyde-3-phosphate dehydrogenase	37,458.00	100.00%	3	7.94%	Icd	(+)	GapB
Icd	(-)	NadC	nicotinate-nucleotide pyrophosphorylase	31,375.70	100.00%	3	11.40%	Icd	(-)	NadC

Icd	(-)	RpsB	ribosomal protein S2	27,950.20	100.00%	3	10.20%	Icd	(-)	RpsB
Icd	(-)	YjbV	4-amino-5-hydroxymethyl-2-methylpyrimidine pyrophosphate kinase	29,106.30	100.00%	3	17.00%	Icd	(-)	YjbV
Icd	(+)	PdhD	pyruvate dehydrogenase / 2-oxoglutarate dehydrogenase (dihydrolipoamide dehydrogenase E3 subunit)	49,715.20	99.60%	2	6.17%	Icd	(+)	PdhD
Icd	(+)	CitZ	citrate synthase II (major)	41,712.30	99.80%	2	7.53%	Icd	(+)	CitZ
Icd	(+)	YoaC	unknown; similar to xylulokinase	54,092.20	99.80%	2	7.60%	Icd	(+)	YoaC
Icd	(+)	FabF	beta-ketoacyl-acyl carrier protein synthase II	43,987.60	99.80%	2	4.36%	Icd	(+)	FabF
Icd	(+)	YqiQ	methylisocitrate lyase	33,080.40	99.60%	2	14.30%	Icd	(+)	YqiQ
Icd	(+)	Smc	chromosome condensation and segregation SMC protein	135,497.20	99.80%	2	2.53%	Icd	(+)	Smc
Icd	(+)	XkdO	PBSX prophage	145,135.90	99.60%	2	3.45%	Icd	(+)	XkdO
Icd	(+)	AroA	3-deoxy-D-arabino-heptulosonate 7-phosphate synthase / chorismate mutase-isozyme 3	39,522.50	99.90%	2	5.87%	Icd	(+)	AroA
Icd	(+)	SerC	phosphoserine aminotransferase	40,118.60	99.80%	2	8.36%	Icd	(+)	SerC
Icd	(+)	ThrC	threonine synthase	37,446.30	99.80%	2	6.82%	Icd	(+)	ThrC
Icd	(+)	ParC	subunit of DNA topoisomerase IV	91,319.80	99.80%	2	5.71%	Icd	(+)	ParC
Icd	(-)	PrsA	protein secretion (post-translocation molecular chaperone)	32,493.30	99.80%	2	10.60%	Icd	(-)	PrsA
Icd	(-)	YjhA	unknown	23,961.00	99.80%	2	10.30%	Icd	(-)	YjhA
Icd	(-)	RplA	ribosomal protein L1 (BL1)	24,904.40	99.80%	2	9.48%	Icd	(-)	RplA

Bait[1]	**CL[2]**	**Protein[3,4]**	**Protein name**	**MW[7] (Da)**	**Protein prob.[8]**	**peptides[9]**	**SC[10]**	**Bait[1]**	**CL[2]**	**Protein[3,4]**
OdhB	(+)	OdhA	2-oxoglutarate dehydrogenase (E1 subunit)	105,724.10	100.00%	33	38.20%	OdhB	(+)	OdhA
OdhB	(-)	DnaK	class I heat-shock protein (molecular chaperone)	65,985.00	100.00%	21	38.10%	OdhB	(-)	DnaK
OdhB	(-)	OdhB	2-oxoglutarate dehydrogenase (dihydrolipoamide transsuccinylase, E2 subunit)	45,970.70	100.00%	19	44.60%	OdhB	(-)	OdhB
OdhB	(+)	OdhB	2-oxoglutarate dehydrogenase (dihydrolipoamide transsuccinylase, E2 subunit)	45,970.70	100.00%	16	30.50%	OdhB	(+)	OdhB
OdhB	(-)	OdhB	2-oxoglutarate dehydrogenase	45,970.70	100.00%	15	27.30%	OdhB	(-)	OdhB

			(dihydrolipoamide transsuccinylase, E2 subunit)							
OdhB	(-)	OdhB	2-oxoglutarate dehydrogenase (dihydrolipoamide transsuccinylase, E2 subunit)	45,970.70	100.00%	14	36.90%	OdhB	(-)	OdhB
OdhB	(-)	OdhB	2-oxoglutarate dehydrogenase (dihydrolipoamide transsuccinylase, E2 subunit)	45,970.70	100.00%	14	31.70%	OdhB	(-)	OdhB
OdhB	(+)	OdhB	2-oxoglutarate dehydrogenase (dihydrolipoamide transsuccinylase, E2 subunit)	45,970.70	100.00%	12	33.30%	OdhB	(+)	OdhB
OdhB	(-)	OdhB	2-oxoglutarate dehydrogenase (dihydrolipoamide transsuccinylase, E2 subunit)	45,970.70	100.00%	12	20.90%	OdhB	(-)	OdhB
OdhB	(-)	PdhB	pyruvate dehydrogenase (E1 beta subunit)	35,456.40	100.00%	12	50.20%	OdhB	(-)	PdhB
OdhB	(-)	TufA	elongation factor Tu	43,574.90	100.00%	11	34.30%	OdhB	(-)	TufA
OdhB	(-)	DegU	two-component response regulator involved in degradative enzyme and competence regulation	25,848.10	100.00%	10	52.00%	OdhB	(-)	DegU
OdhB	(-)	OdhB	2-oxoglutarate dehydrogenase (dihydrolipoamide transsuccinylase, E2 subunit)	45,970.70	100.00%	10	17.50%	OdhB	(-)	OdhB
OdhB	(-)	RplA	ribosomal protein L1 (BL1)	24,904.40	100.00%	9	43.10%	OdhB	(-)	RplA
OdhB	(-)	RpsB	ribosomal protein S2	27,950.20	100.00%	9	30.90%	OdhB	(-)	RpsB
OdhB	(+)	CitB	aconitate hydratase	99,317.30	100.00%	8	10.70%	OdhB	(+)	CitB
OdhB	(-)	OdhB	2-oxoglutarate dehydrogenase (dihydrolipoamide transsuccinylase, E2 subunit)	45,970.70	100.00%	8	17.50%	OdhB	(-)	OdhB
OdhB	(-)	SrfAC	surfactin synthetase / competence	143,804.00	100.00%	8	8.63%	OdhB	(-)	SrfAC
OdhB	(-)	OdhA	2-oxoglutarate dehydrogenase (E1 subunit)	105,724.10	100.00%	7	6.91%	OdhB	(-)	OdhA
OdhB	(-)	PgcA	alpha-phosphoglucomutase	62,884.50	100.00%	7	11.90%	OdhB	(-)	PgcA
OdhB	(+)	PdhD	pyruvate dehydrogenase / 2-oxoglutarate dehydrogenase (dihydrolipoamide dehydrogenase E3 subunit)	49,715.20	100.00%	7	20.60%	OdhB	(+)	PdhD
OdhB	(-)	SrfAB	surfactin synthetase / competence	401,240.30	100.00%	6	1.92%	OdhB	(-)	SrfAB
OdhB	(-)	PurL	phosphoribosylfor	80,273.60	100.00%	6	10.80%	OdhB	(-)	PurL

			mylglycinamidine synthetase II							
OdhB	(-)	OdhB	2-oxoglutarate dehydrogenase (dihydrolipoamide transsuccinylase, E2 subunit)	45,970.70	100.00%	5	14.60%	OdhB	(-)	OdhB
OdhB	(-)	Pyk	pyruvate kinase	62,156.30	100.00%	5	21.50%	OdhB	(-)	Pyk
OdhB	(-)	OdhB	2-oxoglutarate dehydrogenase (dihydrolipoamide transsuccinylase, E2 subunit)	45,970.70	100.00%	5	9.59%	OdhB	(-)	OdhB
OdhB	(-)	AroA	3-deoxy-D-arabino-heptulosonate 7-phosphate synthase / chorismate mutase-isozyme 3	39,522.50	100.00%	5	13.40%	OdhB	(-)	AroA
OdhB	(-)	FusA	elongation factor G	76,527.20	100.00%	5	7.80%	OdhB	(-)	FusA
OdhB	(-)	OdhB	2-oxoglutarate dehydrogenase (dihydrolipoamide transsuccinylase, E2 subunit)	45,970.70	100.00%	4	10.30%	OdhB	(-)	OdhB
OdhB	(-)	OdhB	2-oxoglutarate dehydrogenase (dihydrolipoamide transsuccinylase, E2 subunit)	45,970.70	100.00%	4	10.80%	OdhB	(-)	OdhB
OdhB	(-)	YjbV	4-amino-5-hydroxymethyl-2-methylpyrimidine pyrophosphate kinase	29,106.30	100.00%	3	12.90%	OdhB	(-)	YjbV
OdhB	(+)	Pyk	pyruvate kinase	62,156.30	100.00%	3	14.40%	OdhB	(+)	Pyk
OdhB	(-)	SucC	succinyl-CoA synthetase (beta subunit)	41,354.40	100.00%	3	9.35%	OdhB	(-)	SucC
OdhB	(-)	IlvC	ketol-acid reductoisomerase	37,438.80	100.00%	3	14.60%	OdhB	(-)	IlvC
OdhB	(-)	Mbl	MreB-like protein	35,843.60	100.00%	3	8.71%	OdhB	(-)	Mbl
OdhB	(-)	PdxS	pyridoxal-5'-phosphate synthase	31,593.30	100.00%	3	14.30%	OdhB	(-)	PdxS
OdhB	(-)	RpsB	ribosomal protein S2	27,950.20	100.00%	3	11.40%	OdhB	(-)	RpsB
OdhB	(-)	SrfAB	surfactin synthetase / competence	401,240.30	100.00%	3	1.76%	OdhB	(-)	SrfAB
OdhB	(-)	OdhB	2-oxoglutarate dehydrogenase (dihydrolipoamide transsuccinylase, E2 subunit)	45,970.70	100.00%	3	7.19%	OdhB	(-)	OdhB
OdhB	(-)	YjhA	unknown	23,961.00	99.80%	2	10.30%	OdhB	(-)	YjhA
OdhB	(-)	YknY	ABC transporter	25,254.40	99.70%	2	11.30%	OdhB	(-)	YknY
OdhB	(-)	SucC	succinyl-CoA synthetase (beta subunit)	41,354.40	99.80%	2	6.49%	OdhB	(-)	SucC
OdhB	(-)	RnhC	ribonuclease HIII	34,053.20	99.80%	2	8.63%	OdhB	(-)	RnhC
OdhB	(-)	PdhD	pyruvate dehydrogenase / 2-oxoglutarate dehydrogenase (dihydrolipoamide dehydrogenase E3 subunit)	49,715.20	99.70%	2	7.02%	OdhB	(-)	PdhD
OdhB	(-)	SrfAA	surfactin	402,063.70	99.70%	2	1.09%	OdhB	(-)	SrfAA

			synthetase / competence							
OdhB	(+)	NarH	nitrate reductase (beta subunit)	55,455.60	99.70%	2	4.93%	OdhB	(+)	NarH
OdhB	(-)	OdhA	2-oxoglutarate dehydrogenase (E1 subunit)	105,724.10	99.40%	2	2.76%	OdhB	(-)	OdhA
OdhB	(+)	RibC	riboflavin kinase / FAD synthase	35,644.60	99.60%	2	9.18%	OdhB	(+)	RibC
OdhB	(+)	SerA	phosphoglycerate dehydrogenase	57,098.20	99.80%	2	5.52%	OdhB	(+)	SerA
OdhB	(-)	OdhB	2-oxoglutarate dehydrogenase (dihydrolipoamide transsuccinylase, E2 subunit)	45,970.70	99.80%	2	4.08%	OdhB	(-)	OdhB
OdhB	(-)	YufN	unknown; similar to lipoprotein	37,331.30	99.80%	2	5.71%	OdhB	(-)	YufN
OdhB	(-)	FbaA	fructose-1,6-bisphosphate aldolase	30,382.30	99.80%	2	7.37%	OdhB	(-)	FbaA
OdhB	(-)	NadC	nicotinate-nucleotide pyrophosphorylase	31,375.70	99.80%	2	5.88%	OdhB	(-)	NadC
OdhB	(-)	PriA	primosomal replication factor Y	91,337.20	99.80%	2	4.35%	OdhB	(-)	PriA

Bait[1]	**CL[2]**	**Protein[3,4]**	**Protein name**	**MW[7] (Da)**	**Protein prob.[8]**	**peptides[9]**	**SC[10]**	**Bait[1]**	**CL[2]**	**Protein[3,4]**
GltB	(+)	GltA	glutamate synthase (large subunit)	168,842.80	100.00%	23	18.40%	GltB	(+)	GltA
GltB	(-)	GltB	glutamate synthase (small subunit)	54,931.00	100.00%	14	33.90%	GltB	(-)	GltB
GltB	(-)	Mdh	malate dehydrogenase	33,626.00	100.00%	14	52.90%	GltB	(-)	Mdh
GltB	(-)	GltB	glutamate synthase (small subunit)	54,931.00	100.00%	14	30.40%	GltB	(-)	GltB
GltB	(-)	GltB	glutamate synthase (small subunit)	54,931.00	100.00%	13	29.40%	GltB	(-)	GltB
GltB	(-)	TufA	elongation factor Tu	43,574.90	100.00%	11	34.60%	GltB	(-)	TufA
GltB	(-)	AroA	3-deoxy-D-arabino-heptulosonate 7-phosphate synthase / chorismate mutase-isozyme 3	39,522.50	100.00%	10	28.50%	GltB	(-)	AroA
GltB	(-)	SucC	succinyl-CoA synthetase (beta subunit)	41,354.40	100.00%	9	21.80%	GltB	(-)	SucC
GltB	(-)	GltB	glutamate synthase (small subunit)	54,931.00	100.00%	8	21.10%	GltB	(-)	GltB
GltB	(-)	YqfA	resistence protein	35,623.60	100.00%	8	29.00%	GltB	(-)	YqfA
GltB	(-)	DegU	two-component response regulator involved in degradative enzyme and competence regulation	25,848.10	100.00%	8	38.00%	GltB	(-)	DegU
GltB	(+)	GroEL	class I heat-shock protein (chaperonin)	57,406.30	100.00%	7	13.20%	GltB	(+)	GroEL

GltB	(-)	Ndh	NADH dehydrogenase	41,935.80	100.00%	7	21.70%	GltB	(-)	Ndh
GltB	(+)	GltB	glutamate synthase (small subunit)	54,931.00	100.00%	6	16.80%	GltB	(+)	GltB
GltB	(-)	SucC	succinyl-CoA synthetase (beta subunit)	41,354.40	100.00%	6	16.90%	GltB	(-)	SucC
GltB	(-)	GltB	glutamate synthase (small subunit)	54,931.00	100.00%	5	13.20%	GltB	(-)	GltB
GltB	(-)	GltB	glutamate synthase (small subunit)	54,931.00	100.00%	5	14.20%	GltB	(-)	GltB
GltB	(+)	Mdh	malate dehydrogenase	33,626.00	100.00%	4	24.40%	GltB	(+)	Mdh
GltB	(+)	GltA	glutamate synthase (large subunit)	168,842.80	100.00%	4	3.03%	GltB	(+)	GltA
GltB	(+)	Icd	isocitrate dehydrogenase	46,401.00	100.00%	4	11.80%	GltB	(+)	Icd
GltB	(-)	AlbA	antilisterial bacteriocin (subtilosin) production	51,496.80	100.00%	4	7.81%	GltB	(-)	AlbA
GltB	(-)	GltB	glutamate synthase (small subunit)	54,931.00	100.00%	4	11.00%	GltB	(-)	GltB
GltB	(-)	CitZ	citrate synthase II (major)	41,712.30	100.00%	4	11.80%	GltB	(-)	CitZ
GltB	(-)	GapB	glyceraldehyde-3-phosphate dehydrogenase	37,458.00	100.00%	4	10.90%	GltB	(-)	GapB
GltB	(+)	SrfAB	surfactin synthetase / competence	401,240.30	100.00%	3	1.37%	GltB	(+)	SrfAB
GltB	(-)	YknX	ABC-type antimicrobial peptide transporter	41,689.20	100.00%	3	7.43%	GltB	(-)	YknX
GltB	(-)	YtsJ	NAD-dependent malate dehydrogenase	43,649.20	100.00%	3	18.00%	GltB	(-)	YtsJ
GltB	(-)	PdhA	pyruvate dehydrogenase (E1 alpha subunit)	41,531.40	100.00%	3	8.09%	GltB	(-)	PdhA
GltB	(-)	SalA	MRP family regulator	38,620.90	100.00%	3	11.60%	GltB	(-)	SalA
GltB	(-)	GltB	glutamate synthase (small subunit)	54,931.00	100.00%	3	10.50%	GltB	(-)	GltB
GltB	(-)	YdjI	unknown	36,064.10	100.00%	3	11.80%	GltB	(-)	YdjI
GltB	(+)	IolD	myo-inositol catabolism	64,119.00	99.80%	2	6.55%	GltB	(+)	IolD
GltB	(+)	ArtM	high affinity arginine ABC transporter	26,932.00	99.60%	2	11.20%	GltB	(+)	ArtM
GltB	(+)	BdhA	acetoine/ butanediol dehydrogenase	37,322.70	99.80%	2	12.40%	GltB	(+)	BdhA
GltB	(+)	WprA	cell wall-associated protein precursor	96,472.50	99.70%	2	2.24%	GltB	(+)	WprA
GltB	(+)	YhbB	unknown	35,815.00	99.80%	2	10.90%	GltB	(+)	YhbB
GltB	(+)	LonA	class III heat-shock ATP-dependent protease	86,592.30	99.50%	2	2.97%	GltB	(+)	LonA
GltB	(+)	CshB	DEAD-box RNA helicase	50,012.00	99.80%	2	6.62%	GltB	(+)	CshB
GltB	(+)	PbpC	penicillin-binding	74,390.90	99.90%	2	4.94%	GltB	(+)	PbpC

			protein 3							
GltB	(+)	Bpr	bacillopeptidase F	154,562.00	99.80%	2	1.88%	GltB	(+)	Bpr
GltB	(+)	YopR	unknown	37,555.00	99.80%	2	6.46%	GltB	(+)	YopR
GltB	(+)	TufA	elongation factor Tu	43,574.90	99.80%	2	8.08%	GltB	(+)	TufA
GltB	(+)	AnsB	L-aspartase	52,536.50	99.80%	2	4.42%	GltB	(+)	AnsB
GltB	(+)	NasD	assimilatory nitrite reductase (subunit)	88,415.40	99.40%	2	4.97%	GltB	(+)	NasD
GltB	(+)	TufA	elongation factor Tu	43,574.90	99.80%	2	6.31%	GltB	(+)	TufA
GltB	(+)	PksN	polyketide synthase	609,580.70	99.70%	2	0.49%	GltB	(+)	PksN
GltB	(+)	GltB	glutamate synthase (small subunit)	54,931.00	99.90%	2	3.65%	GltB	(+)	GltB
GltB	(+)	PrfB	peptide chain release factor 2	42,056.20	99.80%	2	9.29%	GltB	(+)	PrfB
GltB	(+)	AsnH	asparagine synthetase	85,834.30	99.70%	2	5.09%	GltB	(+)	AsnH
GltB	(+)	TufA	elongation factor Tu	43,574.90	99.80%	2	8.33%	GltB	(+)	TufA
GltB	(+)	YufO	unknown; similar to ABC transporter (ATP-binding protein)	56,284.10	99.60%	2	5.69%	GltB	(+)	YufO
GltB	(+)	YqbO	unknown; similar to phage-related protein	171,017.30	100.00%	2	1.96%	GltB	(+)	YqbO
GltB	(+)	YncD	alanine racemase	43,630.90	99.80%	2	8.38%	GltB	(+)	YncD
GltB	(+)	RnhC	ribonuclease HIII	34,053.20	99.80%	2	5.75%	GltB	(+)	RnhC
GltB	(+)	Obg	GTP-binding protein involved in initiation of sporulation (Spo0A activation)	47,671.40	99.50%	2	5.37%	GltB	(+)	Obg
GltB	(+)	YqxD	unknown	22,524.50	99.80%	2	15.30%	GltB	(+)	YqxD
GltB	(+)	YkaA	unknown	23,827.60	99.80%	2	12.70%	GltB	(+)	YkaA
GltB	(+)	PpsE	plipastatin synthetase	144,606.70	99.80%	2	2.74%	GltB	(+)	PpsE
GltB	(+)	PriA	primosomal replication factor Y	91,337.20	99.70%	2	3.60%	GltB	(+)	PriA
GltB	(-)	YfiJ	two-component sensor kinase	44,525.90	99.80%	2	8.75%	GltB	(-)	YfiJ
GltB	(-)	AccC	acetyl-CoA carboxylase (biotin carboxylase subunit)	49,560.30	99.80%	2	4.00%	GltB	(-)	AccC
GltB	(-)	PksJ	polyketide synthase	563,012.00	99.80%	2	0.61%	GltB	(-)	PksJ
GltB	(-)	OpuAA	glycine betaine ABC transporter (ATP-binding protein)	46,422.00	99.80%	2	5.02%	GltB	(-)	OpuAA
GltB	(-)	ProA	gamma-glutamyl phosphate reductase	45,319.60	99.90%	2	5.30%	GltB	(-)	ProA
GltB	(-)	RecA	multifunctional protein involved in homologous recombination and DNA repair (LexA-autocleavage)	38,072.80	99.80%	2	7.78%	GltB	(-)	RecA
GltB	(-)	Icd	isocitrate dehydrogenase	46,401.00	99.70%	2	5.20%	GltB	(-)	Icd
GltB	(-)	AroA	3-deoxy-D-arabino-heptulosonate 7-	39,522.50	99.90%	2	8.38%	GltB	(-)	AroA

GltB	(-)	PlsX	phosphate synthase / chorismate mutase-isozyme 3 involved in fatty acid/phospholipid synthesis	35,745.30	99.80%	2	6.31%	GltB	(-)	PlsX
GltB	(-)	YdbB	unknown	12,923.50	99.70%	2	23.00%	GltB	(-)	YdbB
GltB	(-)	MalK	two-component sensor kinase	58,913.60	99.80%	2	5.25%	GltB	(-)	MalK
GltB	(-)	PdhB	pyruvate dehydrogenase (E1 beta subunit)	35,456.40	99.80%	2	8.31%	GltB	(-)	PdhB
GltB	(-)	PfkA	6-phosphofructokinase	34,237.00	99.80%	2	9.72%	GltB	(-)	PfkA
GltB	(-)	FlgK	flagellar hook-associated protein 1 (HAP1)	54,338.40	99.80%	2	4.93%	GltB	(-)	FlgK
GltB	(-)	GltB	glutamate synthase (small subunit)	54,931.00	99.80%	2	3.45%	GltB	(-)	GltB
GltB	(-)	YjhA	unknown	23,961.00	99.80%	2	10.30%	GltB	(-)	YjhA

8.5. Supplementary material chapter 3

Table 8.5.1. Growth rates obtained for the *gfp* reporter strains grown in presence of the different carbon sources.

	Growth rates (h^{-1}) [a]									
	WT				*ΔccpA*		*ptsH1*		*Δcrh*	
Fusion	- (M9SE)[b]	+ Inducer[c]	+ Glucose	+ Malate	+ Glucose	+ Malate	+ Glucose	+ Malate	+ Glucose	+ Malate
P_{bglP}-*gfp*	0.53 ±0.05	BBA0223 0.84 ±0.08	0.88 ±0.13	0.86 ±0.04	GM3023 0.87 ±0.04	0.78 ±0.13	-	-	-	-
$P_{bglP\Delta RAT\text{-}term}$-*gfp*	0.52 ±0.02	GM3007 0.75 ±0.08	0.88 ±0.03	0.78 ±0.02	GM3019 0.81 ±0.02	0.68 ±0.02	GM3043 0.92 ±0.04	0.70 ±0.01	GM3033 0.92 ±0.02	0.75 ±0.02
P_{sacP}-*gfp*	0.58 ±0.05	BBA0359 1.01 ±0.05	0.89 ±0.10	1.03 ±0.12	GM3024 0.96 ±0.05	0.81 ±0.06	-	-	-	-
$P_{sacP\Delta RAT\text{-}term}$-*gfp*	0.57 ±0.04	GM3003 1.01 ±0.07	0.98 ±0.07	1.01 ±0.07	GM3015 0.80 ±0.04	0.73 ±0.04	GM3079 0.87 ±0.04	0.76 ±0.01	GM3067 0.97 ±0.05	0.82 ±0.01
$P_{gntRcre2}$-*gfp*	0.63 ±0.04	GM3002 0.80 ±0.10	1.04 ±0.01	0.96 ±0.01	GM3014 1.03 ±0.01	0.92 ±0.02	GM3037 0.53 ±0.02	0.44 ±0.02	GM3029 1.05 ±0.06	0.98 ±0.03
P_{glpF}-*gfp*	0.52 ±0.03	BBA0121 0.87 ±0.02	1.01 ±0.02	0.80 ±0.04	GM3022 0.40 ±0.03	0.38 ±0.01	-	-	-	-
$P_{glpF\Delta term}$-*gfp*	0.63 ±0.02	GM3004 0.68 ±0.03	0.98 ±0.03	0.87 ±0.02	GM3016 0.37 ±0.02	0.36 ±0.02	GM3069 0.86 ±0.03	0.82 ±0.03	GM3057 1.04 ±0.03	0.82 ±0.01
P_{gntR}-*gfp*	*n.d.*	BBA0028 0.56 ±0.03	0.71 ±0.01	0.76 ±0.03	-	-	-	-	-	-
fruA-gfp	0.58 ±0.02	GM3005 1.00 ±0.04	0.96 ±0.04	0.94 ±0.01	GM3017 0.76 ±0.04	0.62 ±0.02	GM3071 0.94 ±0.07	0.82 ±0.05	GM3059 0.90 ±0.05	0.93 ±0.02
P_{fruR}-*gfp*	0.61 ±0.04	BBA0118 1.02 ±0.02	1.00 ±0.06	1.02 ±0.02	GM3027 0.80 ±0.04	0.71 ±0.02	GM3073 0.92 ±0.03	0.70 ±0.03	GM3061 1.00 ±0.03	0.96 ±0.02
P_{araE}-*gfp*	0.61 ±0.08	GM3008 0.66 ±0.04	1.07 ±0.06	1.03 ±0.05	GM3020 0.85 ±0.06	0.65 ±0.02	GM3075 0.80 ±0.03	0.99 ±0.06	GM3063 0.96 ±0.04	0.95 ±0.04
P_{araA}-*gfp*	0.60 ±0.05	GM3001 0.65 ±0.09	1.04 ±0.12	1.00 ±0.08	GM3013 0.86 ±0.02	*n.d.*	GM3077 0.90 ±0.11	0.87 ±0.04	GM3065 0.95 ±0.06	0.91 ±0.03

[a] Mean values of three or more independent experiments.
[b] M9 minimal medium with succinate and glutamate (see experimental procedures).
[c] Inducer was D-gluconate for P_{gntR}-*gfp*, D-fructose for *fruA*-*gfp* and P_{fruR}-*gfp*, glycerol for P_{glpF}-*gfp*, salicin for P_{bglP}-*gfp*, sucrose for P_{sacP}-*gfp* and L-arabinose for P_{araE}-*gfp* and P_{araA}-*gfp* derivative strains.

8.6. Curriculum vitae

Personal data

Name:	Frederik Meyer
Date of birth:	11 January 1983
Place of birth:	Gehrden
Nationality:	German

School education

1989 - 1993	Grundschule, Gehrden
1993 - 1995	Orientierungsschule, Gehrden
1995 - 2003	Matthias-Claudius-Gymnasium, Gehrden

Scientific education

2003 - 2004	Study of bioengineering, Technische Universität Braunschweig
2004 - 2009	Study of biology, Georg-August-University of Göttingen
2008 - 2009	Diploma Thesis in the group of Prof. Dr. Jörg Stülke - Department of General Microbiology at the Georg-August-University Göttingen
2010 - 2013	Ph.D. Thesis in the group of Prof. Dr. Jörg Stülke - Department of General Microbiology at the Georg-August-University Göttingen